SCIENCE&ENGINEERING SYMPOSIUM

PROCEEDINGS

16-19 OCTOBER

THEME: "Advanced Technologies – Key to Capabilities at Affordable Costs"

VOL. II. PROPULSION

CO-SPONSORED BY
NAVAL MATERIAL COMMAND
AIR FORCE SYSTEMS COMMAND

- Avionics
- Propulsion
- Flight Dynamics
- Basic Research
- Material
- Armament
- Human Resources

PROCEEDINGS

OF THE

1978 SCIENCE AND ENGINEERING SYMPOSIUM

16 - 19 OCTOBER 1978

NAVAL AMPHIBIOUS BASE
CORONADO, CALIFORNIA

VOLUME II

APPROVED FOR PUBLIC RELEASE;
DISTRIBUTION UNLIMITED

SYMPOSIUM OFFICIALS

CO-SPONSORS

NAVAL MATERIAL COMMAND

AIR FORCE SYSTEMS COMMAND

HOSTS

NAVAL OCEAN SYSTEMS CENTER
WEST COAST COORDINATOR

NAVAL AMPHIBIOUS BASE
FACILITIES

CO-CHAIRMEN

WILLIAM KOVEN
Associate Technical Director
Naval Air Research and Technology
Naval Air Systems Command

DR. BERNARD KULP
Chief Scientist
Director of Science and Technology
Air Force Systems Command

DEPUTY CO-CHAIRMEN

JAMES MULQUIN
Advanced Systems Technology Planning
Naval Air Research and Technology
Naval Air Systems Command

MAJOR LARRY FEHRENBACHER
Assistant to Chief Scientist
Director of Science and Technology
Air Force Systems Command

PREFACE

The initial co-sponsored Air Force Systems Command/Naval Material Command Science and Engineering Symposium was held at the Naval Amphibious Base, Coronado on 16 - 19 October 1978. The theme of the 1978 Symposium was "Advanced Technologies - Key to Capabilities at Affordable Cost."

The objectives of this first joint Navy/Air Force Science and Engineering Symposium were to:

- Provide a forum for military and civilian laboratory scientific and technical researchers to demonstrate the spectrum and nature of 1978 achievements by their services in the areas of
  - Armament
  - Avionics
  - Basic Research
  - Flight Dynamics
  - Human Resources
  - Materials
  - Propulsion
- Recognize outstanding technical achievement in each of these areas and select the outstanding technical paper within the Navy and the Air Force for 1978
- Assist in placing the future Air Research and Development of both services in correct perspective and to promote the exchange of ideas between the Navy and Air Force Laboratories
- Stress the need for imagination, vision and overall excellence within the technology community, assuring that the air systems of the future will not only be effective but affordable.

Based upon the success of the initial joint symposium (which was heretofore an Air Force event), future symposia are planned with joint Navy/Air Force participation.

TABLE OF CONTENTS

VOLUME I

AVIONICS

R. S. VAUGHN, NADC — COL R. LOPINA, AFAL
CO-CHAIRMEN

The Airborne Electronic Terrain Map System (AETMS) 1
Capt F. Barney, USAF and Dr. L. Tamburino, AFAL

The Assessment of GaAs Passivation and Its Applications 17
Dr. F. Schuermeyer, J. Blassingame, AFAL and Dr. H. Hartnagel, Univ. of New Castle-Upon-Thames, England

Identification of Impurity Complexes in Gallium Arsenide Device Material by High Resolution Magneto-Photoluminescence 50
G. McCoy, Maj R. Almassy, USAF, D. Reynolds and C. Litton, AFAL

Microcircuit Analysis Techniques Using Field-Effect Liquid Crystals 69
D. J. Burns, RADC

Surface Acoustic Wave Frequency Synthesizer for JTIDS 85
P. H. Carr, A. J. Budreau and A. J. Slovodnik, RADC

Enhanced Measurement Capability Using a Background Suppression Scheme 110
G. A. Vanasse and E. R. Huppi, AFGL

Spectrum Estimation and Adaptive Controller for Long-Range Complex Scattering Targets 122
R. F. Ogrodnik, RADC

Spatial and Temporal Coding of GaAs Lasers for a Laser Line Scan Sensor 149
Capt R. S. Shinkle, USAF, ASD

VOLUME II

PROPULSION

AERO-PROPULSION

A. A. MARTINO, NAPC — COL G. STRAND, AFAPL
CO-CHAIRMEN

ROCKET PROPULSION

B. W. HAYES, NWC — COL W. F. MORRIS, AFRPL

CO-CHAIRMEN

Airbreathing Propulsion Functional Area Review 164
Col G. E. Strand, USAF, AFAPL

Rocket Propulsion Overview 196
Col W. F. Morris, USAF, AFRPL

Role of Turbine Engine Technology on Life Cycle Cost 212
R. F. Panella and R. G. McNally, AFAPL

VORBIX Augmentation - An Improved Performance Afterburner for Turbo Fan Engines 247
W. W. Wagner, NAPC

A Retirement for Cause Study of an Engine Turbine Disk 265
R. Hill, AFAPL, R. Reimann, AFML and L. Ogg, ASD

Payoffs of Variable Cycle Engines for Supersonic VSTOL Aircraft 296
R. T. Lazarick and P. F. Piscopo, NAPC

The Coanda/Refraction Concept for Gasturbine Engine Exhaust Noise Suppression During Ground Testing 322
D. Croce, NAEC

Expendable Design Concept 349
Lt D. C. Hall, USAF, AFAPL and H. F. Due, Teledyne CAE

The Supersonic Expendable Turbine Engine Development Program 363
T. E. Elsasser, NAPC

Unique Approach for Reducing Two Phase Flow Losses in Solid Rocket Motors 383
Lt D. C. Ferguson, USAF, AFRPL

Missile System Propulsion Cook-Off 414
R. F. Vetter, NWC

A Powerful New Tool for Solid Rocket Motor Design 428
W. S. Woltosz, AFRPL

Quantification of the Thermal Environment for Air-Launched Weapons 453
H. C. Schafer, NWC

A Study of Rocket-Propelled Stand-Off Missiles 470
Lt L. K. Slimak, USAF, AFRPL

Prediction of Rocket Motor Exhaust Plume Effects on Missile Effectiveness 496
A. C. Victor, NWC

VOLUME III

FLIGHT DYNAMICS

C. A. DeCRESCENTE, NADC COL G. CUDAHY, USAF, AFFDL
CO-CHAIRMEN

Air Force Flight Dynamics Functional Area Review 521
Col G. F. Cudahy, USAF, AFFDL

A Functional Area Review (FAR) of Navy Flight Dynamics 592
C. A. DeCrescente, NADC

Aircraft Aft-Fuselage Sonic Damping 615
G. Pigman, E. Roeser and M. Devine, NADC

Active Control Applications to Wing/Store Flutter Suppression 626
L. J. Hutsell, T. E. Noll and D. E. Cooley, AFFDL

Maximum Performance Escape System (MPES) 657
J. J. Tyburski, NADC and W. J. Stone, NWC

Status of Circulation Control Rotor and X-Wing VTOL Advanced Development Program 673
T. M. Clancy, D. G. Kirkpatrick and R. M. Williams, DTNSRDC

AFFTC Parameter Identification Experience 697
Lt D. P. Maunder, USAF, AFFTC

Developments in Flight Dynamics Technology for Navy V/STOL Aircraft 719
J. W. Clark, Jr., and C. Henderson, NADC

Cost Effective Thrust Drag Accounting 750
R. B. Sorrells, III, AEDC

Drag Prediction for Wing-Body-Nacelle Configurations 766
T. C. Tai, DTNSRDC

Numerical Solution of the Supersonic and Hypersonic Viscous Flow Around Thin Delta Wings 793
Maj G. S. Bluford, USAF and Dr. W. L. Hankey, AFFDL

Optimization of Airframe Structures: A Review and Some Recommendations 828
V. B. Venkayya, AFFDL

Use of Full Mission Simulation for Aircraft Systems Evaluation 870
K. A. Adams, AFFDL

VOLUME IV

BASIC RESEARCH

DR. E. H. WEINBERG, NAL DR. L. KRAVITZ, AFOSR
CO-CHAIRMEN

The Electronic and Electro-Optic Future of III-V Semiconductor Compounds 885
H. L. Lessoff, NRL and J. K. Kennedy, RADC

Collective Ion Acceleration and Intense Electron Beam Propagation Within an Evacuated Dielectric Tube 912
Capt R. L. Gullickson, USAF, AFOSR, R. K. Parker and J. A. Pasour, NRL

High Spatial Resolution Optical Observations Through the Earth's Atmosphere 939
Capt S. P. Worden, USAF, AFGL

High Burnout Schottky Barrier Mixer Diodes for X-Band and Millimeter Frequencies 954
A. Christou, NRL

New Energetic Plasticizers: Synthesis, Characterization and Potential Applications 968
Lt R. A. Hildreth, USAF, Lt S. L. Clift, USAF and Lt J. P. Smith, FJSRL

Improved Corrosion and Mechanical Behavior of Alloys by Means of Ion Implantation 981
J. K. Hirvonen and J. Butler, NRL

Symmetric Body Vortex Wake Characteristics in Supersonic Flow 1000
Dr. W. L. Oberkampf, Univ of Texas at Austin and Dr. D. C. Daniel, AFATL

Materials Effects in High Reflectance Coatings 1033
H. E. Bennett, NWC

Improved Substrate Materials for Surface Acoustic Wave (SAW) Devices 1058
Capt R. M. O'Connell, USAF, RADC

A Simple Prediction Method for Viscous Drag and Heating Rates 1075
T. F. Zien, NSWC

Assessing the Impact of Air Force Operations on the Stratosphere Composition 1110
C. C. Gallagher and Capt R. V. Pieri, USAF, AFGL

On the Modelling of Turbulence Near a Solid Wall 1131
K. Y. Chien, NSWC

Atmospheric Electric Hazards to Aircraft 1146
L. H. Ruhnke, NRL

Efficient Operation of a 100 Watt Transverse Flow Oxygen-Iodine Chemical Laser 1161
Maj W. E. McDermott, USAF, Capt N. R. Pchelkin, USAF,
Dr. J. Bernard and Maj R. R. Bousek, USAF, AFWL

VOLUME V

MATERIALS

F. S. WILLIAMS, NADC — COL P. O. BOUCHARD, USAF, AFML
CO-CHAIRMEN

Advanced Materials Technologies - The Key to New Capabilities at Affordable Costs 1173
Col P. O. Bouchard, USAF, AFML

Ceramics in Rolling Element Bearings 1182
C. F. Bersch, NAVAIR

Group Technology Key to Manufacturing Process Integration 1198
Capt D. Shunk, USAF, AFML

An Attempt to Predict the Effect of Moisture on Carbon Fiber Composites 1213
J. M. Augl, NSWC

Evaluation of Spectrometric Oil Analysis Techniques for Jet Engine Condition Monitoring 1252
Lt T. J. Thomton, USAF and K. J. Eisentraut, AFML

Characterization of Structural Polymers, Using Nuclear Magnetic Resonance Techniques 1287
W. B. Moniz, C. F. Poranski, Jr., A. N. Garroway and H. A. Resing, NRL

On the Variation of Fatigue Crack Opening Load with Measurement Location 1308
D. E. Macha, D. M. Corbly, J. W. Jones, AFML

Environmentally Induced Catastrophic Damage Phenomena and Control 1335
Dr. J. L. DeLuccia, NADC

Improved High Temperature Capability of Titanium Alloys by Ion Implantation/Plating 1366
S. Fujishiro, AFML and E. Eylon, Univ of Cincinnati

Measurement of the Physical Properties and Recombination Process in Bulk Silicon Materials 1384
Lt T. C. Chandler, USAF, AFML

Deuterated Synthetic Hydrocarbon Lubricant 1396
A. A. Corte, NADC

The Cordell Plot: Key to a Better Understanding of the Behavior of Fiber-Reinforced Composites 1410
T. M. Cordell, AFML

VOLUME VI

ARMAMENT

DR. J. MAYERSAK, AFATL R. M. HILLYER, NWC
CO-CHAIRMEN

Armament Technology - Functional Overview 1434
Dr. J. R. Mayersak, AFATL

The Digital Integrating Subsystem-Modularity, Flexibility and Standardization of Hardware and Software 1449
D. L. Gardner, AFATL

Bank-To-Turn (BTT) Technology 1490
R. M. McGehee, AFATL

Advances in Microwave Striplines with Applications 1507
J. A. Mosko, NWC

Considerations for the Design of Microwave Solid-State Transmitters 1543
M. Afendykiew, Jon Bumgardner and Darry Kinman, NWC

Strapdown Seeker Guidance for Air-to-Surface Tactical Weapons 1590
Capt T. R. Callen, USAF, AFATL

Optimizing the Performance of Antennas Mounted on Complex Airframes 1614
Dr. C. L. Yu, NWC

VOLUME VII

HUMAN RESOURCES

H. J. CLARK, AFHRL DR. J. HARVEY, NTEC
CO-CHAIRMEN

Human Resources Research and Development 1640
H. J. Clark, AFHRL

Human Resources in Naval Aviation 1649
Dr. J. Harvey, NTEC

LCCIM: A Model for Analyzing the Impact of Design on Weapon System Support Requirements and LCC 1683
H. A. Baran, AFHRL, A. J. Czuchry and J. C. Goclowski, Dynamics Research Corp

Pacts: Use of Individualized Automated Training Technology 1703
Dr. R. Breaux, NTEC

Increasing the Affordability of I-Level Maintenance Training Through Simulation 1711
G. G. Miller, D. R. Baum and D. I. Downing, AFHRL

Psychomotor/Perceptual Measures for the Selection of Pilot Trainees 1741
D. R. Hunter, AFHRL

Modern Maintenance Training Technology and Our National Defense Posture 1758
Dr. W. J. King and Dr. P. E. Van Hemel, NTEC

Prediction of System Performance and Cost Effectiveness Using Human Operator Modelling 1781
LCDR N. E. Lane, USN, W. Leyland, NADC and H. I. Strieb (Analytics)

An Inflight Physiological Data Acquisition and Analysis System 1804
Capt J. T. Merrifield, USAF, T. P. Waddell, D. G. Powell, USAF/SAM and E. B. Croson, PMTC

Synthetic Selection of Naval Aviators: A Novel Approach 1821
D. E. Norman, D. Wightman, NTEC and CDR L. Waldeisen, NAMRL

Modeling: The Air Force Manpower and Personnel System for Policy Analysis 1831
Capt S. B. Polk, USAF, AFHRL

Evoked Brain Potentials as Predictors of Performance: The Hemispheric Assymetry as Related to Pilot and Radar Intercept Officer Performance 1841
Dr. B. Rimland and Dr. G. W. Lewis, NPRDC

Launch Opportunity for Air-to-Ground Visually Delivered Weapons 1863
R. A. Erickson and C. J. Burge, NWC

VOLUME VIII

AVIONICS, PROPULSION, AND FLIGHT DYNAMICS (CLASSIFIED)

Functional Area Review of Avionics 1
Col R. F. Lopina, USAF, AFAL

The MADAIR System 27
J. A. Titus, NCSC

Electronically Agile Array for Long-Range Airborne Surveillance Radar 89
Dr. J. K. Smith, NADC

Automatic Ship Classification System 118
W. G. Hueber and Dr. L. A. Wilson, NWC

Reduction of False Alarm Rates in Aircraft Attack Warning Systems 144
H. L. Jaeger, NWC

Impact of Focal Plane Array Technology on Airborne Forward Looking Infrared Sensors 179
M. Hess and S. Campana, NADC

Advanced Sonobuoy Technology - ERAPS (Expendable Reliable Acoustic Path Sonobuoy) 200
J. J. Stephenosky, NADC

NAVSTAR Global Positioning System Field Test Results Aboard Air Force and Navy Test Vehicles 220
LCDR J. A. Strada, USN, SAMSO

An Overview of Soviet Propulsion Capabilities 240
W. A. Zwart, FTD

Reduced Observables - An Approach for Providing More Effective and Affordable Combat Weapon Systems 273
D. E. Fraga, AFFDL

Soviet Method of Calculating the Aerodynamic Characteristics of Wings Flying in Ground Effect 330
Lt C. R. Gallaway, USAF, FTD

VOLUME IX

MATERIALS, ARMAMENT, AND HUMAN RESOURCES (CLASSIFIED)

Soviet Materials for Aircraft Engines 362
R. F. Frontani, FTD

CCD Camera/Tracker Seeker Technology 390
G. F. Teate, NWC

Warhead Designs for Wide Area Antiarmor Cluster Munitions 404
Dr. J. C. Foster and Capt E. M. Cutler, USAF, AFATL

Active Moving Target Tracking Seeker Captive Flight Test 427
A. N. DiSalvio, AFATL

Inter-Laboratory Air-to-Air Missile Technology - An Innovative Approach 449
T. C. Aden, AFATL

Aimable Ordnance for Tactical Anti-Air and Anti-Surface Missiles 485
T. R. Zulkoski and P. H. Amundson, NWC

Manned Threat Quantification 549
Capt G. J. Valentino, USAF and Lt R. B. Kaplan, USAF, AMRL

AIRBREATHING PROPULSION FUNCTIONAL AREA REVIEW

PRESENTED BY COL GEORGE E. STRAND

COMMANDER, AIR FORCE AERO PROPULSION LABORATORY

AIR FORCE SYSTEMS COMMAND

PROPULSION SESSION CHAIRMEN:

COL GEORGE E. STRAND
AIR FORCE AERO PROPULSION LABORATORY

COL WILLIAM F. MORRIS
AIR FORCE ROCKET PROPULSION LABORATORY

ALBERT A. MARTINO
NAVAL AIR PROPULSION CENTER

BURRELL W. HAYES
NAVAL WEAPONS CENTER

Over $600 million was spent on airbreathing propulsion research and development in fiscal 1978. Of this 44 percent was provided by the Department of Defense, 14 percent by other government organizations, and the remainder by contractors' Independent Research and Development (IR&D). About six percent of this total was devoted to ramjets (up from three percent two years ago), with the remainder addressing turbine engines. The American airbreathing propulsion industry employs 76,000 people, working in facilities valued at $3 billion. Annual sales exceed $5 billion, distributed fairly evenly among U.S. military, U.S. commercial, and foreign military.

The government airbreathing propulsion community consists of over two dozen organizations, most of which are located east of the Mississippi. Those most involved in airbreathing propulsion R&D are the Air Force Aero Propulsion Laboratory and Aeronautical Systems Division (both at Wright-Patterson Air Force Base, Ohio), the Naval Air Propulsion Center (Trenton, New Jersey), the Army Mobility R&D Laboratory (Fort Eustis, Virginia), and NASA's Lewis Research Center (Cleveland, Ohio). Technology-dedicated government facilities are largely limited to those at NASA Lewis and the AFAPL. Facilities at the NAPC and AEDC are predominantly for engineering development, and include the government's only facility for freejet testing ramjet engines under conditions simulating their entire envelopes.

The major thrusts of the Air Force program in FY78 was propulsion for transonic/supersonic CTOL and STOL aircraft and for air-launched tactical and strategic cruise missiles. Over half of the Air Force's funding was devoted to technology (as opposed to engineering development). By contrast 6.4 accounted for over 80 percent of the Navy program. The Navy's technology program emphasizes V/STOL applications of turbine engines, and ramjets for both ship-and air-launched missiles. The first ramjet 6.4 program in many years was initiated to develop engines for the Navy's Firebrand target. Widespread interest in ramjets was also reflected by a new Army program studying their use in anti-armor missiles. That service's primary interest in turbine engines is helicopter propulsion, although a gas turbine is undergoing engineering development for the XM-1 tank. NASA's very extensive program to develop technology for commercial engines emphasizes fuel efficiency, quiet operation and low emissions. DARPA supported Air Force and Navy investigations of advanced materials for turbine engines and fuel efficient cruise missile engines.

Only a few companies are capable of developing and producing turbine engines of all types and sizes. In the free world these include Pratt & Whitney, General Electric, Detroit Diesel Allison, Rolls Royce, and SNECMA. The Japanese are making significant strides to develop a technology base for both military and commercial engines. The United Kingdom and Soviet Union both have operational ramjet powered systems, while several European countries are pursuing them for surface-launched cruise missiles. The U.S. is the only nation developing ramjets for air-launched systems. Current government interest has led to a significant expansion of the ramjet contractor base.

PURPOSE OF BRIEFING

PROVIDE AN OVERVIEW & STATUS
OF
AIRBREATHING PROPULSION TECHNOLOGY

BRIEFING RECIPIENTS

CHAIN OF COMMAND	FOR INFORMATION
AFWAL/CC	ASD/YZ
AFSC/DL	ASD TECH COUNCIL
AFSC/CC	ASD/CC
AIR STAFF	FTD
USAF/RD	AFLC/ALD
SAF/RD	OUSDRE
	NASA HQ
	S&E SYMPOSIUM

BRIEFING OUTLINE

NATIONAL INVESTMENT

U.S. R&D PROGRAM

- GOVERNMENT
- INDUSTRY

FOREIGN CAPABILITIES

SUMMARY

FY78 R&D FUNDING

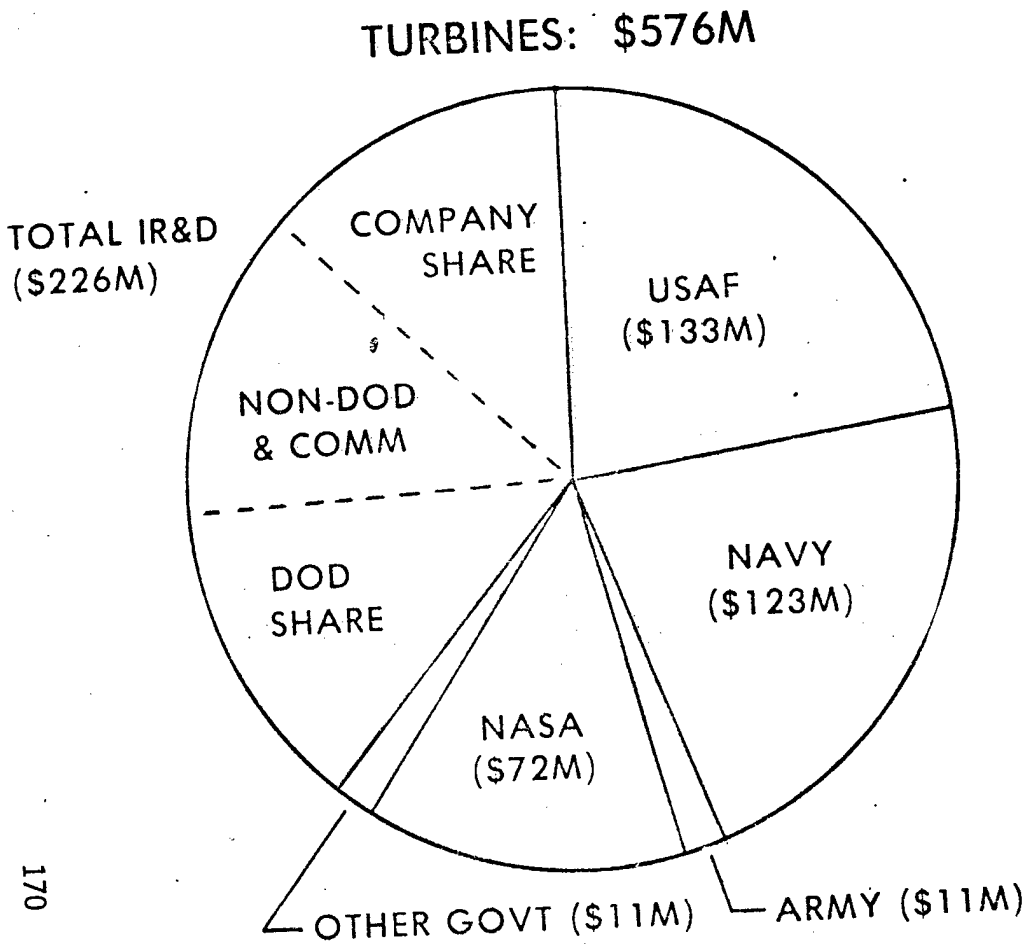

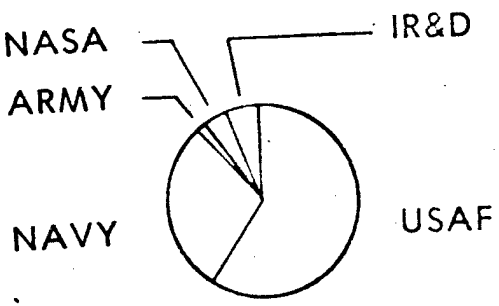

RAMJETS: $34M

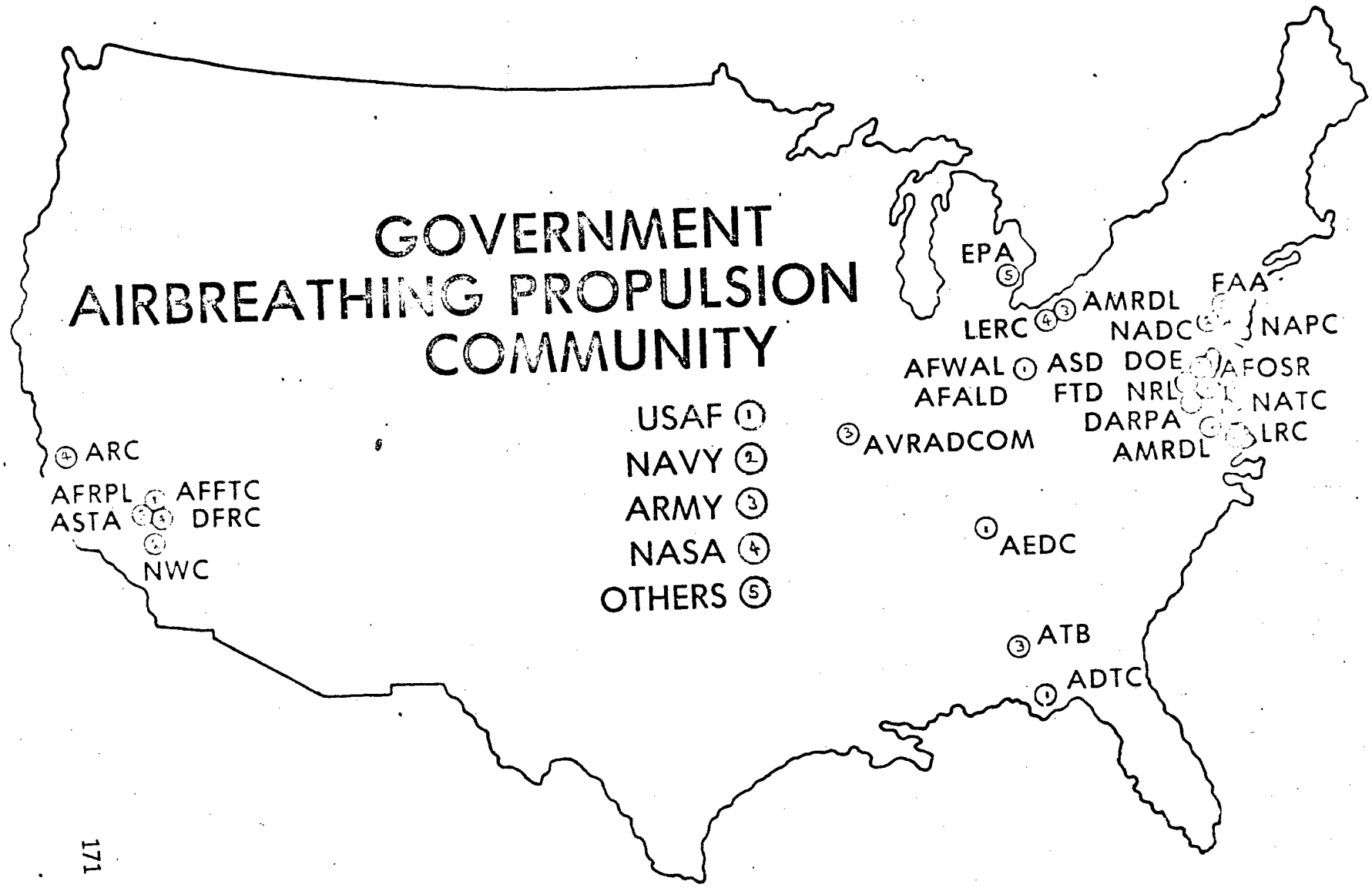
GOVERNMENT
AIRBREATHING PROPULSION
COMMUNITY
USAF (1)
NAVY (2)
ARMY (3)
NASA (4)
OTHERS (5)
EPA (5)
LERC (4) (3)
AMRDL
FAA
NADC (5)
NAPC
AFWAL (1)
ASD
DOE
AFOSR
AFALD
FTD
NRL
NATC
DARPA (4)
LRC
AMRDL
(3) AVRADCOM
(1) AEDC
(3) ATB
(1) ADTC
(4) ARC
AFRPL (1)
AFFTC
ASTA (2) (4)
DFRC
(2)
NWC

171

USAF AIRBREATHING PROPULSION

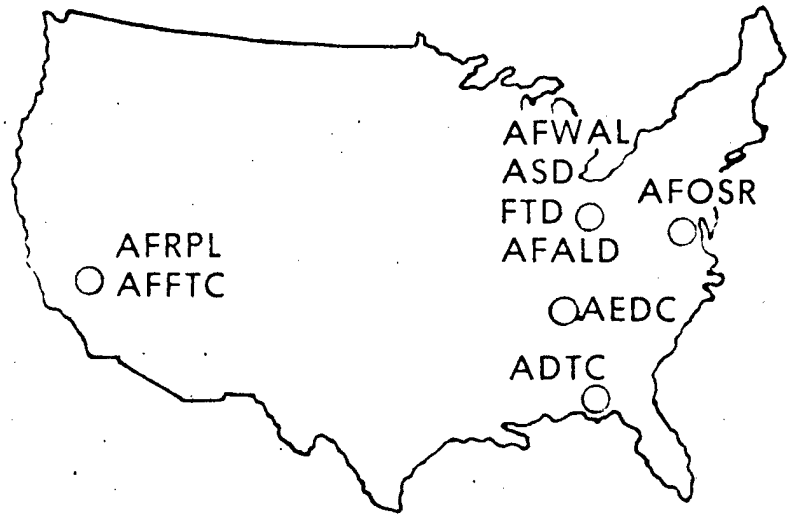

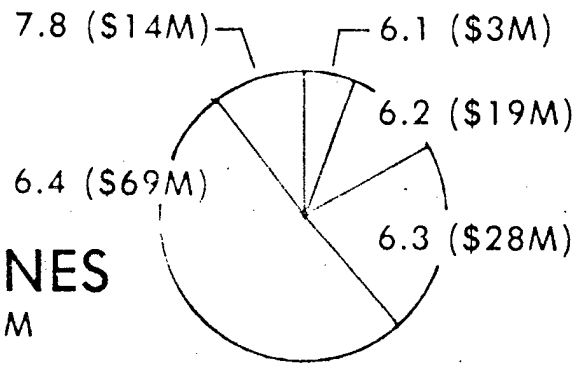

TURBINES
$133M

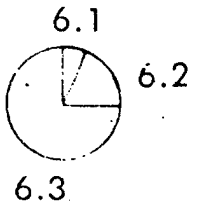

RAMJETS
$21M

RESEARCH IN AIRBREATHING PROPULSION
- SOLID MECHANICS, FLUID DYNAMICS

TURBINE ENGINE COMPONENTS
- DESIGNED FOR TRANSITION TO 6.3

GAS GENERATORS
- DESIGNED TO SERVE AS "TECH DEMO" CORES

ENGINE TECHNOLOGY DEMONSTRATORS
- VARIABLE CYCLE CONFIGURATIONS

INCREASED DURABILITY, REDUCED COST
- ACCELERATED MISSION TESTING

PROPULSION SYSTEM INTEGRATION

LIQUID FUELED RAMJETS FOR
- ASALM
- STRATEGIC PENETRATORS
- INTERCEPT AAM'S

SOLID FUELED RAMJETS FOR TACTICAL ASM'S

DUCTED ROCKETS FOR AMRAAM'S

NAVY AIRBREATHING PROPULSION

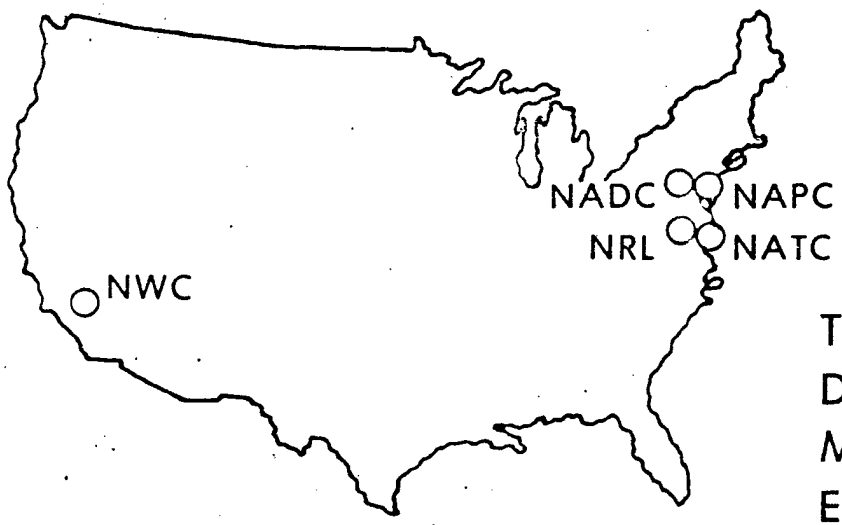

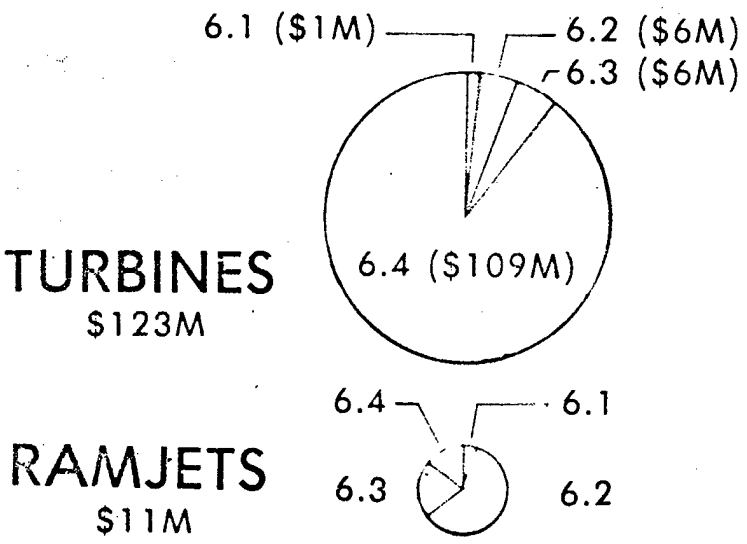

- TURBINE ENGINE COMPONENTS
- DIGITAL ELECTRONIC CONTROLS
- MATERIALS & STRUCTURES
- ENGINE TECHNOLOGY DEMONSTRATORS
- V/STOL APPLICATIONS
- SUPERSONIC EXPENDABLE ENGINES

- LIQUID FUELED RAMJETS FOR
  - LONG RANGE AAM'S
  - SHIP LAUNCHED SAM'S
  - TORPEDO TUBE CRUISE MISSILES
- SOLID FUELED RAMJETS FOR AAM's, ASM's
- SCRAM FOR SHIP LAUNCHED SAM's

ARMY AIRBREATHING PROPULSION

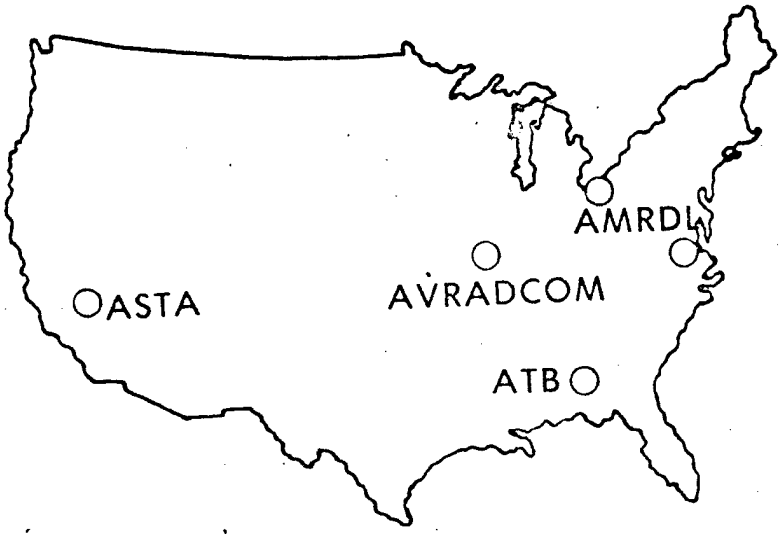

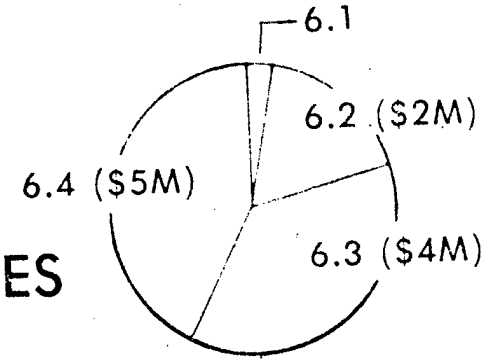

TURBINES
$11M

RAMJETS
$0.3M

○ 6.2

TURBINE ENGINE TECHNOLOGY

- SMALL ENGINE COMPONENTS
- INLET PARTICLE SEPARATORS
- MATERIALS & STRUCTURES
- POWER TRANSMISSIONS
- 800 HP TECH DEMO ENGINE

SOLID FUEL RAMJETS

- FOR ANTI-ARMOR MISSILES

174

NASA AIRBREATHING PROPULSION

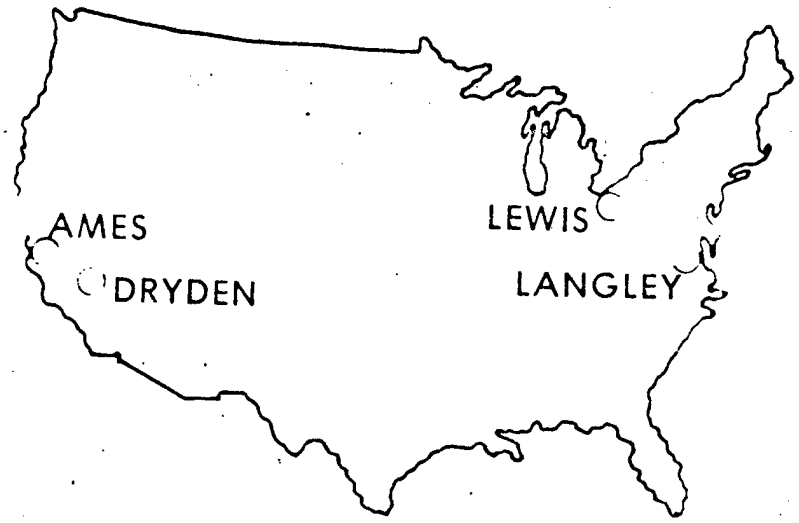

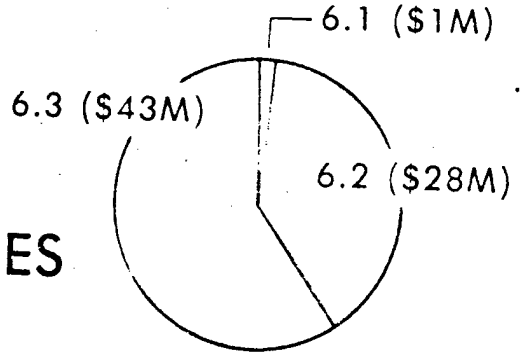

TURBINES
$72M

RAMJETS
$1M

○ 6.2

TECHNOLOGY

- EXHAUST & NOISE REDUCTION
- TURBINE ENGINE COMPONENTS
- V/STOL PROPULSION RESEARCH
- MATERIALS & STRUCTURES
- POWER TRANSMISSIONS
- FULL SCALE ENGINE RESEARCH
- INSTRUMENTATION & CONTROLS
- SUPERSONIC CRUISE AIRCRAFT RESEARCH
- PROPULSION SYSTEM INTEGRATION
- ENGINES FOR LIGHT AIRCRAFT
- HYPERSONIC SCRAMJET PROPULSION

ENGINE DEMONSTRATIONS

- QUIET CLEAN SHORT HAUL EXPERIMENTAL ENGINE
- QUIET CLEAN GENERAL AVIATION TURBOFAN
- FUEL CONSERVATIVE SUBSONIC ENGINES
- MATERIALS FOR ADVANCED TURBINE ENGINES

OTHER RELATED ACTIVITY

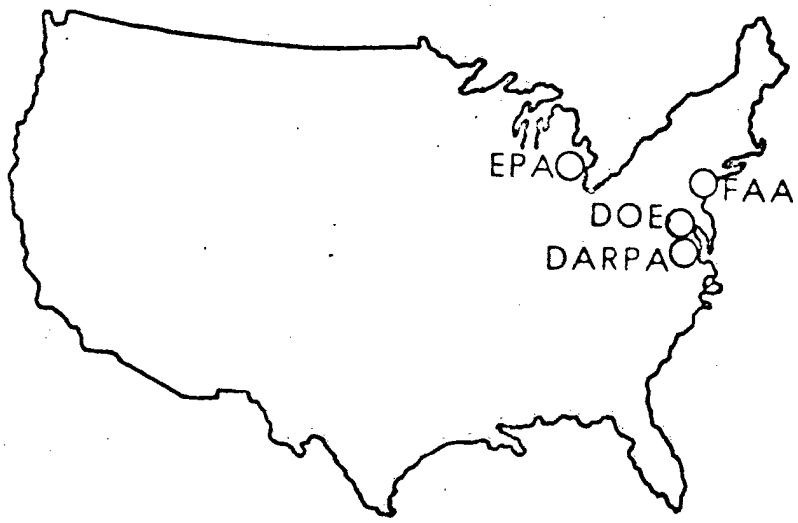

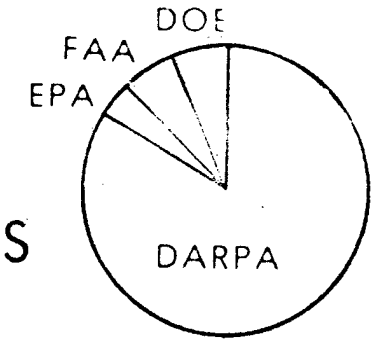

TURBINES
$11M

DEFENSE ADV RES PROJECTS AGENCY

- T76 CERAMIC HOT SECTION (NAVY
- ADV MATERIALS, MANUF PROCESSES (USAF
- FUEL EFFICIENT CRUISE MISSILE ENGINES (USAF

ENVIRONMENTAL PROTECTION AGENCY

- EMISSIONS MEASUREMENTS & STANDARDS

FEDERAL AVIATION ADMINISTRATION

- FOD SAFETY
- ENGINE CERTIFICATION CRITERIA
- EMISSIONS MEASUREMENT

DEPARTMENT OF ENERGY

- CERAMICS FOR AUTOMOTIVE GAS TURBINES

CURRENT ENGINEERING DEVELOPMENT

SPONSOR	MANUF	DESIG	APPLICATION	TYPE	CLASS
USAF	P&W	F100	F-16	ABTF	25,000LB
	G.E.	F101	~~B-1~~	ABTF	30,000LB
	WRC	F107	ALCM	TF	600LB
NAVY	WRC	F107	TOMAHAWK	TF	600LB
	ROLLS	F402	AV-8B	TF	21,000LB
	G.E.	F404	F-18	ABTF	16,000LB
		T700	SH-60B	TS	1,500HP
	GARRETT	T76	OV-10	TP	1,000HP
	MARQUARDT	MA215	FIREBRAND	LFRJ	8,000LB
ARMY	G.E.	T700	UH-60A	TS	1,500HP
	AVCO	AGT1500	XM-1TANK	TS	1,500HP

NOT SHOWN: KC-135 REENGINING (USAF), F-14 ENGINE REPLACEMENT (NAVY)

COMPONENT IMPROVEMENT PROGRAM

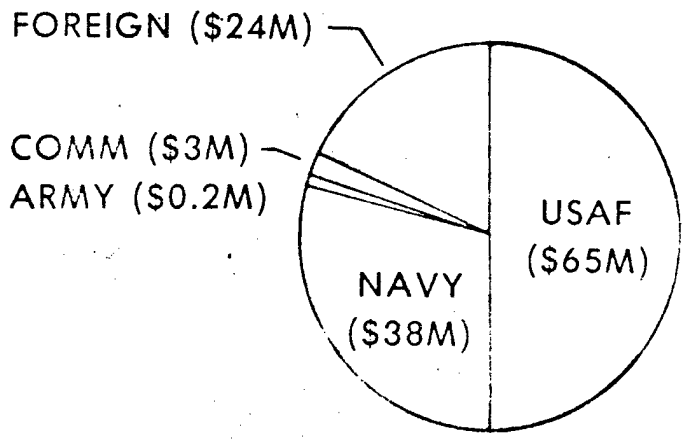

TOTAL: $130M

PURPOSE

REDUCE ENGINE LIFE CYCLE COST
& IMPROVE OPERATIONAL READINESS
USING PROVEN TECHNOLOGY

FUNDING

BUDGET LINE ITEMS (3010 MONEY)
FOR FOREIGN USERS, ACCORDING
TO ENGINE TYPE & FLEET SIZE

ENGINE MODEL DERIVATIVE PROGRAM

RECOMMENDED BY 1975 SAB/KERREBROCK PANEL

PERFORMANCE OF MOST NEW ENGINES
CAN BE INCREASED 15-20%

POST 1968 CIP DISALLOWS SUCH PERFORMANCE IMPROVEMENTS

EMDP PROVIDES ORDERLY GROWTH OR MODIFICATION
OF SELECTED ENGINES

- ASD/YZ DIRECTION
- SPECIFIC PROJECTS ASSOCIATED WITH APPROPRIATE SPO
- USE ADEQUATELY PROVEN TECHNOLOGY

6.4 PROGRAM, STARTING AT $2.9M IN FY79

POTENTIAL FUTURE USAF SYSTEMS

SYSTEM	CANDIDATE AIRFRAME	CANDIDATE ENGINE
ADV RECONNAISSANCE AIRCRAFT (RF-X)	MOD F-15 OR F-16	F100 DERIV
FOLLOW-ON INTERCEPTOR	MOD F-15	F100 DERIV
ADV TACTICAL FIGHTER	NEW	PROBABLY NEW
ADV PROPULSION FIGHTER	NEW	PROBABLY NEW
ADV FORWARD AIR CONTROLLER (FAC-X)	MOD A-7 OR A-10	NEW OR DERIV
ADV MEDIUM STOL TRANSPORT	YC-14/YC-15	NEW OR DERIV
ADV GUNSHIP (AC-X)	MOD AMST	NEW OR DERIV
AIRBORNE COMMAND CENTER (E-X)	MOD 707, WBT	EXISTING OR DERIV
ADV AIRBORNE NATIONAL COMMAND POST (E-4X)	MOD E-4	CF6,JT9D
ADV STRATEGIC TRANSPORT AIRCRAFT	NEW	NEW
VERY LARGE AIRCRAFT	NEW	NEW
PRIMARY TRAINER REPLACEMENT AIRCRAFT	NEW	NEW OR DERIV
COMPASS COPE		TF34 DERIV
ADV REMOTELY PILOTED VEHICLE (BGM-X)	NEW	NEW OR DERIV
TACTICAL EXPENDABLE DRONE SYSTEM (BGM-XX)	NEW	NEW
ADV STRATEGIC AIR LAUNCHED MISSILE	NEW	IRR

OTHER SERVICES' FUTURE SYSTEMS

NAVY/MARINES

- ADV FIGHTER/ATTACK AIRCRAFT (V/STOL B)
- INTERMEDIATE/ADVANCED TRAINER (VTX)
- LAND-BASED TANKER (KCX)
- LAND-BASED MARITIME PATROL AIRCRAFT
- AIRBORNE EARLY WARNING AIRCRAFT
- CARRIER ON—BOARD DELIVERY AIRCRAFT
- ALL-WEATHER ATTACK AIRCRAFT (VAMX)
- ATTACK/OBSERVATION HELICOPTER (AHX)
- SEA-BASED ROTARY WING ASW (HSX)
- ADV INTERCEPT AAM (WITH USAF)

ARMY

- ARMED SCOUT HELICOPTER
- LIGHT OBSERVATION HELICOPTER
- LIGHT UTILITY HELICOPTER
- HEAVY LIFT HELICOPTER
- ADV AERIAL WEAPON SYSTEM
- ADV TARGET TRAINER
- UNMANNED AIRCRAFT SYSTEM
- REMOTELY PILOTED VEHICLE

OPERATIONAL GOVERNMENT FACILITIES

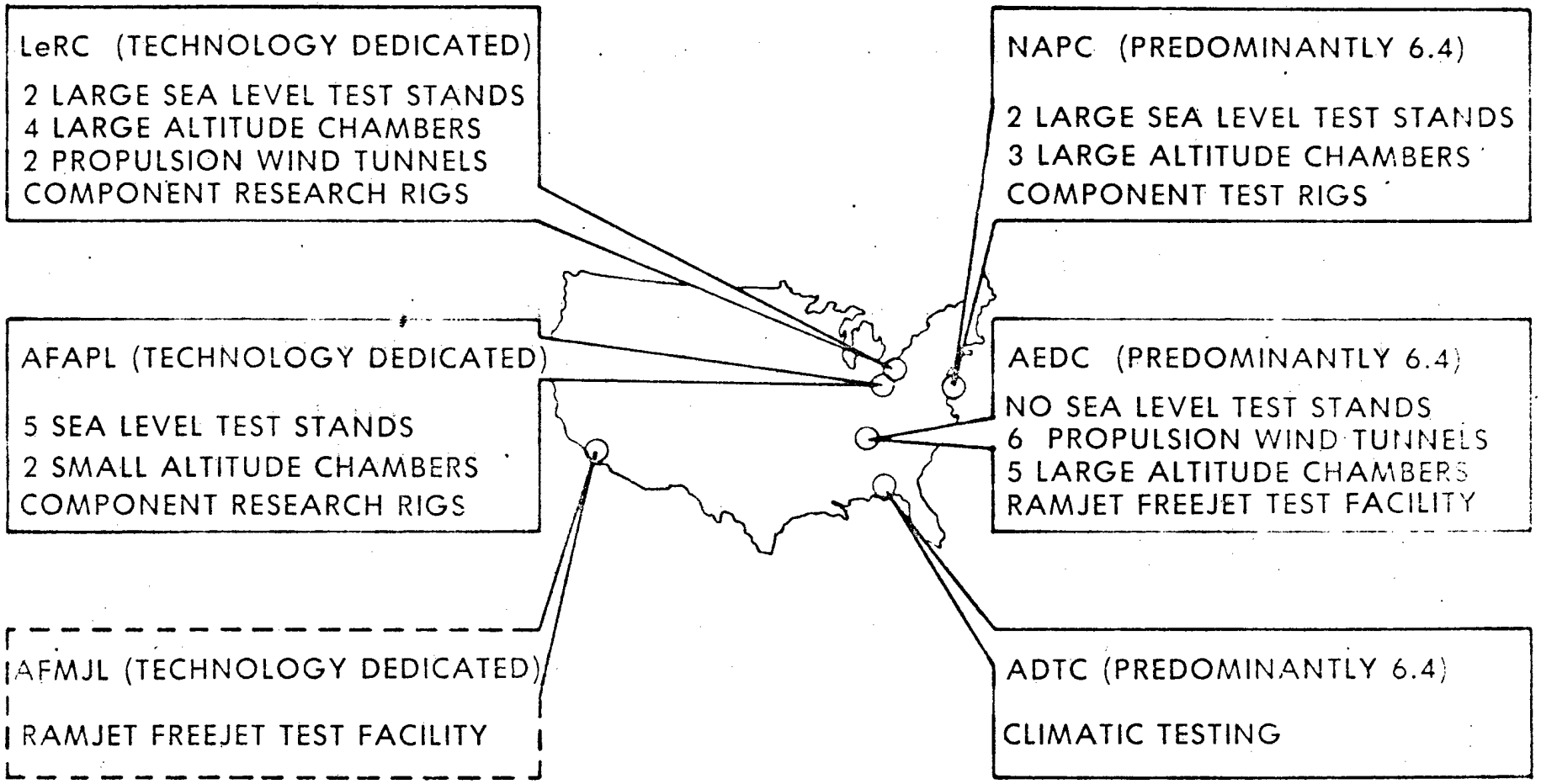

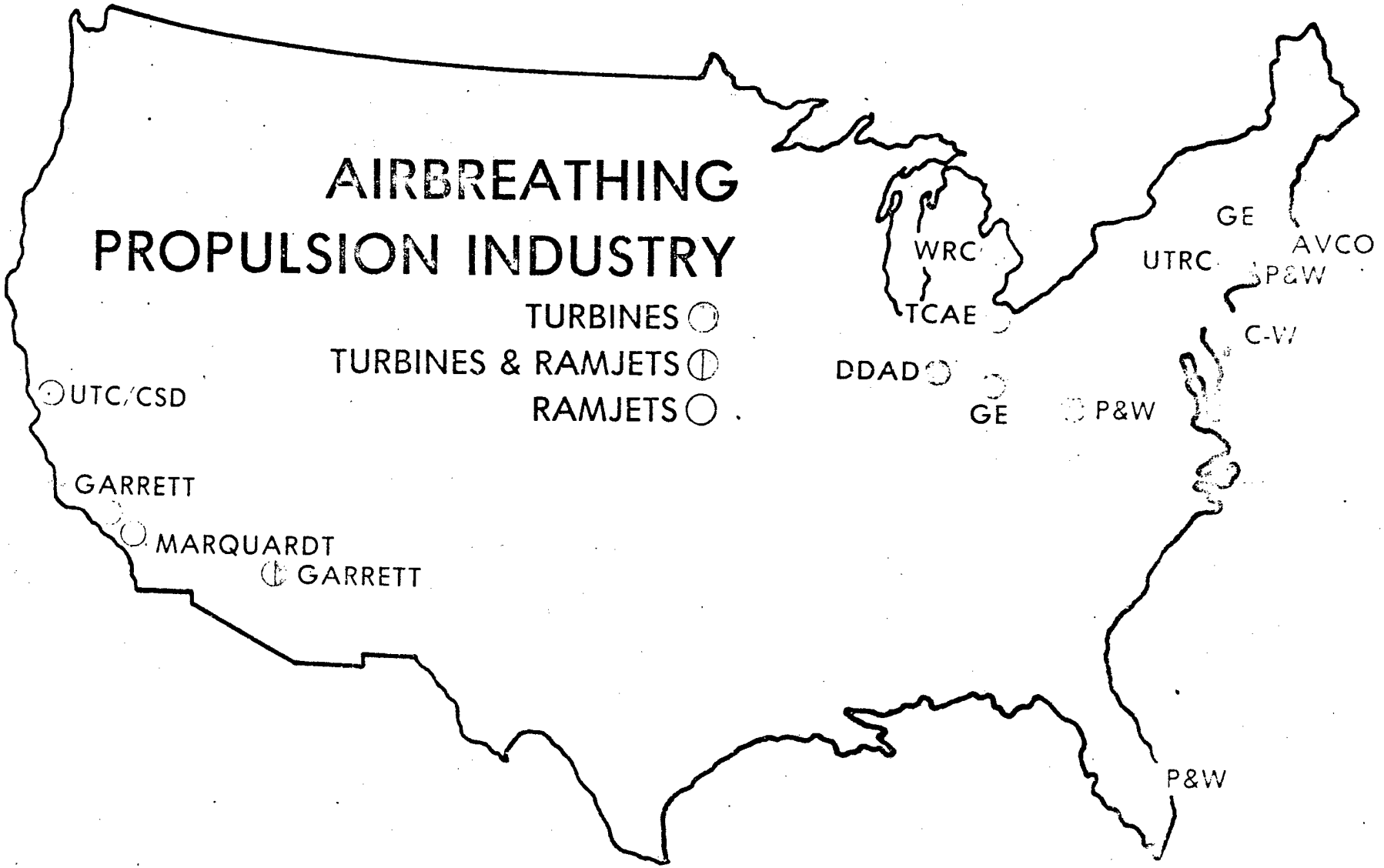
AIRBREATHING
PROPULSION INDUSTRY
TURBINES
TURBINES & RAMJETS
RAMJETS
UTC/CSD
GARRETT
MARQUARDT
GARRETT
WRC
TCAE
DDAD
GE
P&W
GE
AVCO
UTRC
P&W
C-W
P&W

INDEPENDENT RESEARCH & DEVELOPMENT

PURPOSE

PROVIDE FREEDOM & FUNDING NEEDED BY MANUFACTURER TO STAY COMPETITIVE

FUNDING

OVERHEAD CHARGE ON ALL GOVERNMENT & COMMERCIAL SALES

DIRECT COMPANY INVESTMENT

SCOPE

EXCLUDES MANUFACTURING & PRODUCTION ENGINEERING

AVERAGE PROGRAM IS 5% OF GROSS SALES

ONE-SIXTH OF $1.1 BILLION ANNUAL PROGRAM RELATED TO AIRBREATHING PROPULSION

IR&D APPLICATION

($228M IN CFY78)

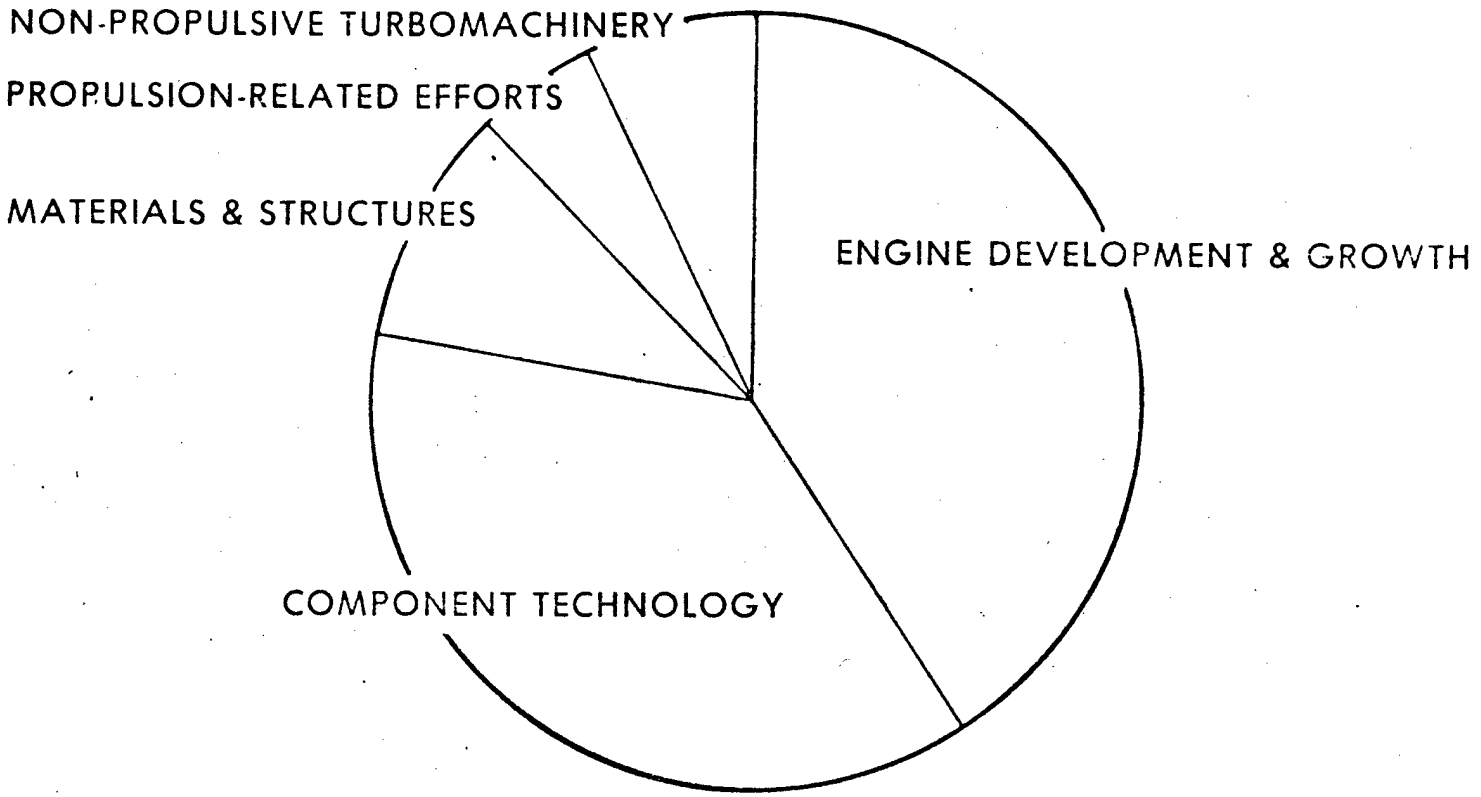

NEW COMMERCIAL DEVELOPMENTS

MANUFACTURER	DESIGNATION	APPLICATION	TYPE	CLASS
P&W	JT8D-209	DC-9-80	TF	19,000LB
	JT9D-7R	B767	HBTF	44,000LB
	JT10D-136	B757	HBTF	36,000LB
	JT15D-5	TRAINERS, GEN AV	TF	3,000LB
	PT6A-65	GEN AV	TP	1,300HP
G.E.	CF6-32	TRANSPORTS	HBTF	35,000LB
	CF6-45B2	A310	HBTF	46,000LB
	CF6-80	TRANSPORTS	HBTF	50,000LB
	CF34	TRANSPORTS	HBTF	9,000LB
	CFM56	TRANSPORTS	HBTF	22,000LB
AVCO	ALF101	TRAINERS	HBTF	1,600LB
	ALF 502L	HS146	TF	7,500LB
	LTP101	AGRI A/C	TP	800HP
GARRETT	ATF 3-6	FALCON 20G	TF	5,000LB
	TPE 331	AGRI A/C	TP	1,000HP

INDUSTRY RESOURCES

(EXCLUDING VENDORS)

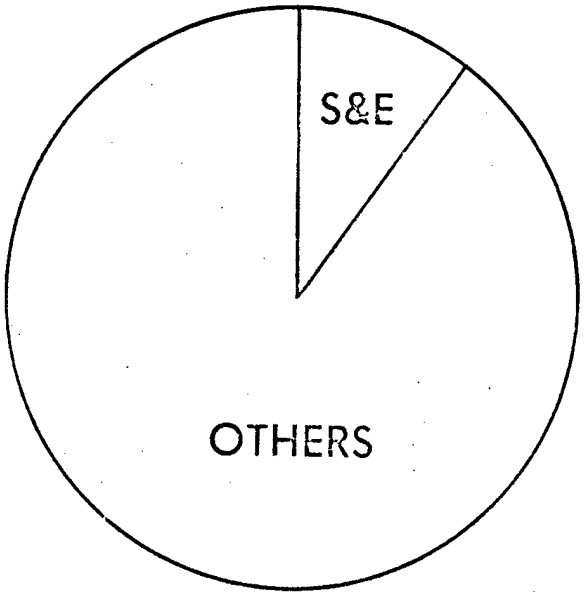

76,000 PEOPLE

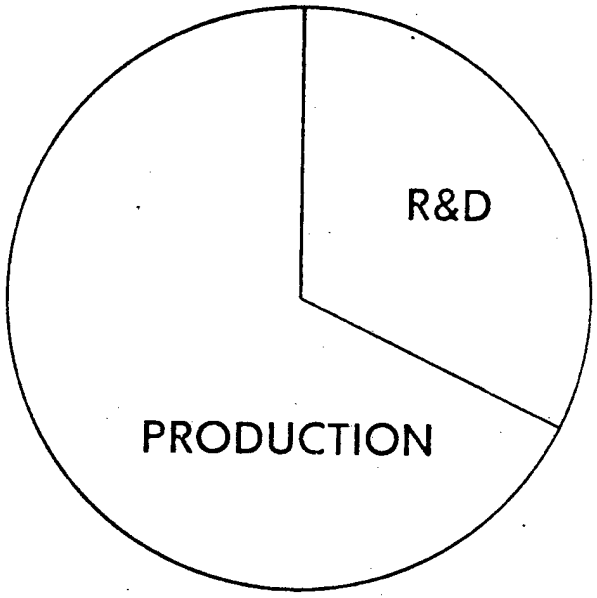

$3B IN FACILITIES

INDUSTRY SALES BASE

($5.4B IN 1978)

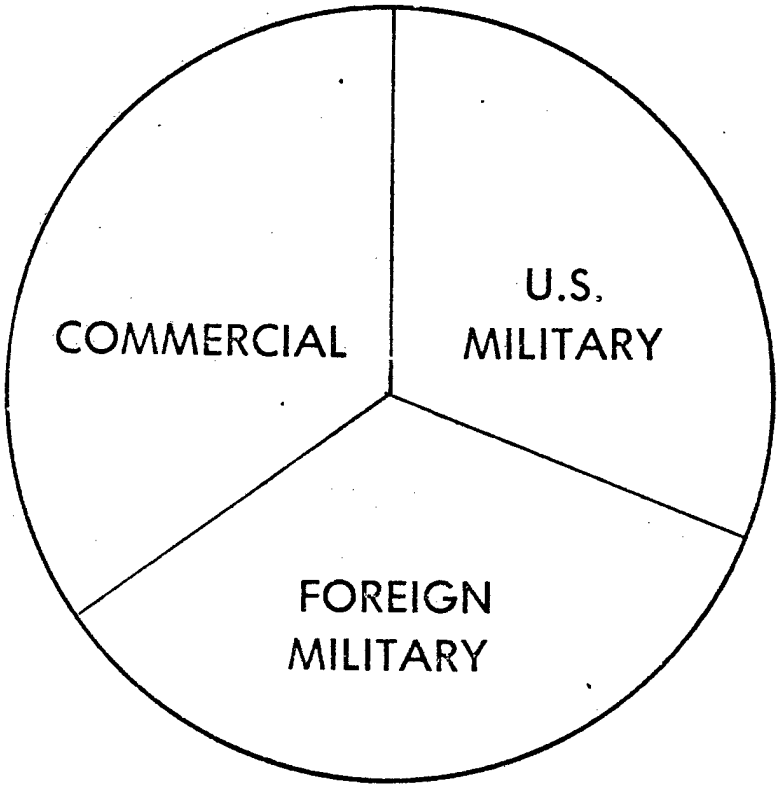

INDUSTRY STATE OF HEALTH

TURBINES RAMJETS DEAD

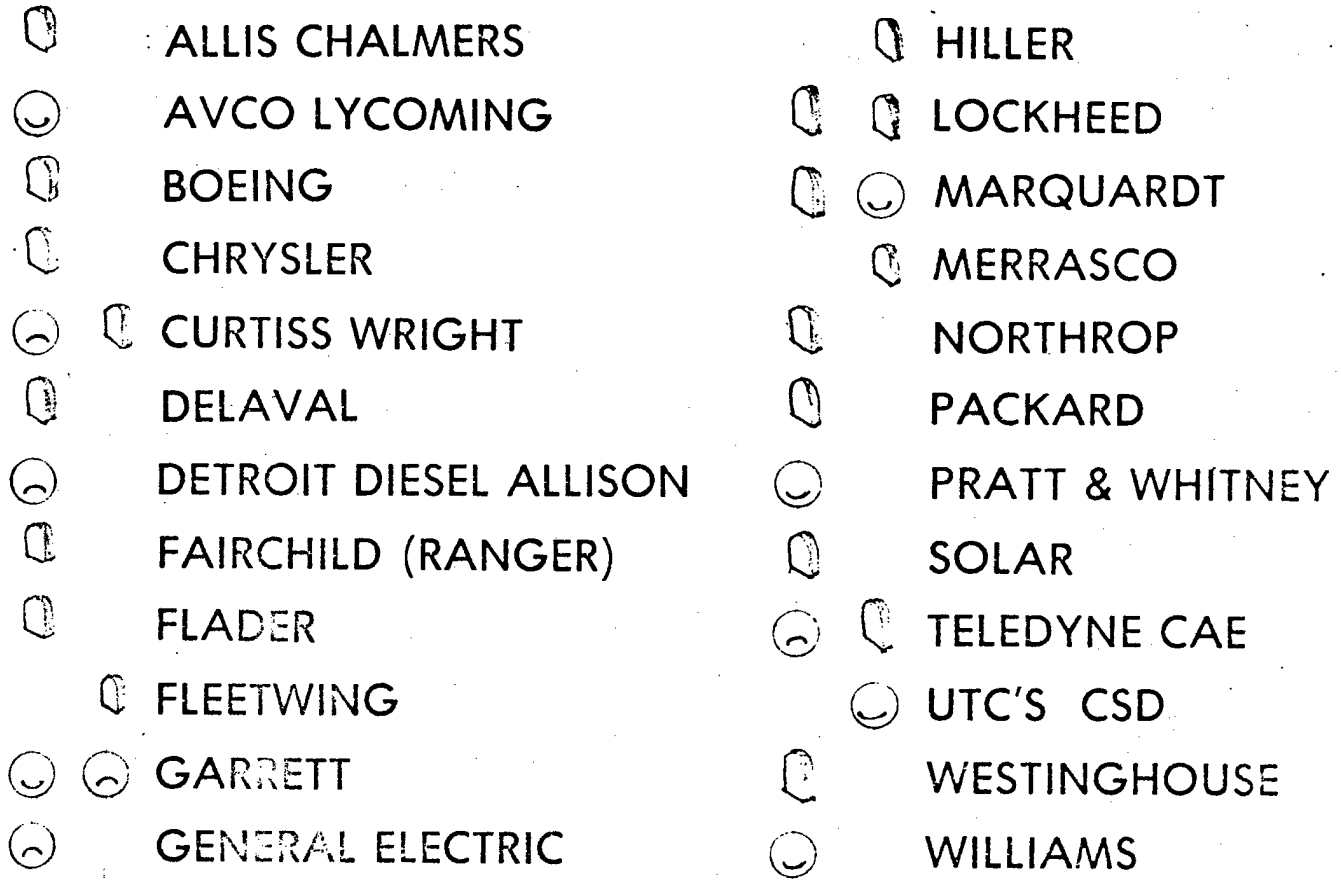

CURRENT SCORE: ☺6, ☹5, ▯18

FOREIGN CAPABILITIES

● SIGNIFICANT TURBINE ACTIVITY ○ RAMJETS ◐ BOTH

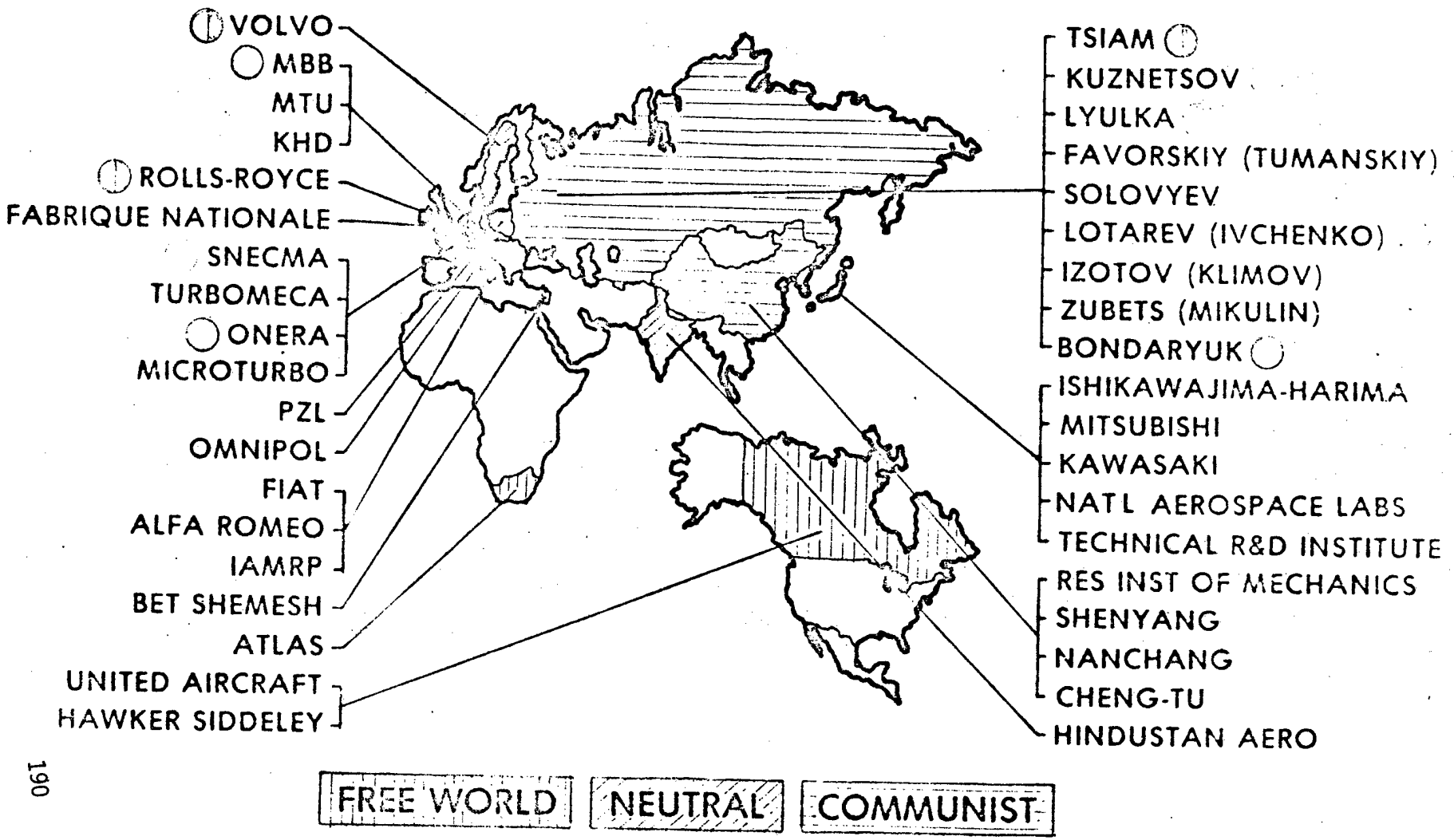

RAMJET POWERED MISSILES

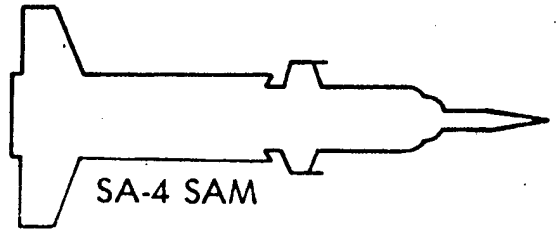
SA-4 SAM

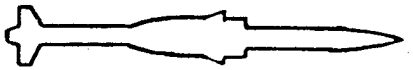
SA-6 SAM

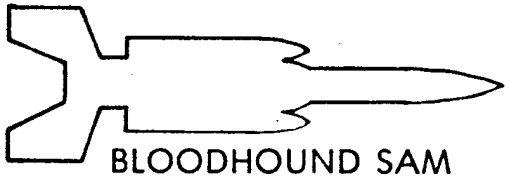
BLOODHOUND SAM


SEA DART SSM

?
SEA SKIMMER SSM

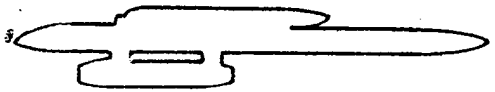
ROADRUNNER TARGET


VEGA SSM

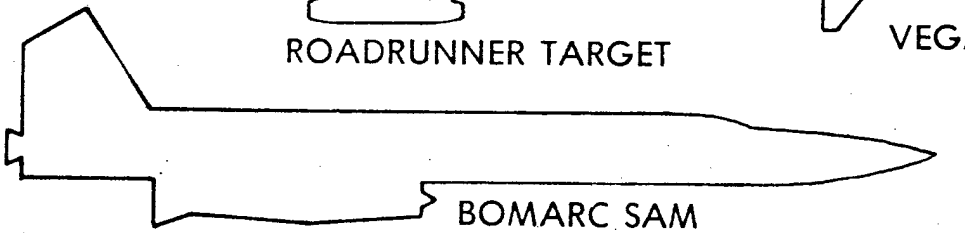
BOMARC SAM

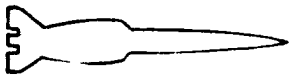
ALVRJ AGM

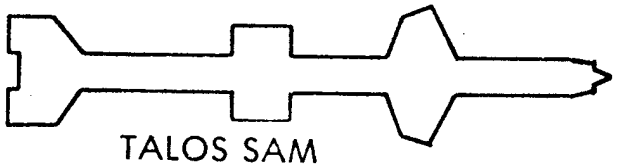
TALOS SAM

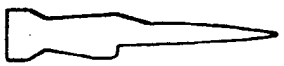
LASRM AGM

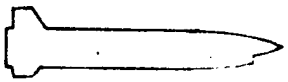
ASALM AGM

1950 1960 1970 1980

SIGNIFICANT FOREIGN ENGINES

MANUFACTURER	DESIGNATION	APPLICATION	TYPE	CLASS	STATUS	NEAREST U. S. EQUIV
ROLLS-ROYCE	RB401	GEN AV	TF	6,000 LB	DEV	ATF 3
	M45H	VFW 614	HBTF	8,000LB	PROD	TF34
	ADOUR 804	JAGUAR INT'L	ABTF	8,000LB	DEV	J85-21
	PEGASUS	HARRIER	LCTF	22,000LB	PROD	NONE
	RB211-535	TRANSPORTS	HBTF	36,000LB	DEV	CF6-32
RR/MTU/FIAT	RB199	TORNADO	ABTF	15,000 LB	DEV	F404
RR/ALFA ROMEO	RB318	GEN AV	TP	600HP	DEV	TPE 331
RR/SNECMA	OLYMPUS 593	CONCORDE	ABTF	38,000LB	PROD	J58,J93
SNECMA	M53-5	MIRAGE 2000	ABTF	20,000LB	DEV	F100
SNECMA/MTU	LARZAC 04	ALPHAJET	TF	3,000LB	PROD	TFE 731
SNECMA/G. E.	CFM 56	TRANSPORTS	HBTF	22,000LB	DEV	
MTU/FIAT/P&W	JT10D	TRANSPORTS	HBTF	36,000LB	DEV	
VOLVO	RM8B	VIGGEN	ABTF	28,000LB	PROD	TF30
NATL AEROSPACE LAB	FJR710	TRANSPORTS	HBTF	11,000LB	DEV	TF34
TECH R&D INST	XF-3	TRAINERS	TF	3,000LB	DEV	TFE 731

ENGINE EXPORTS

THE GOOD NEWS

U.S. ENGINES POWER 82% OF FREE WORLD COMMERCIAL AIRCRAFT

$800 MILLION IN U.S. ENGINES EXPORTED IN 1976

LARGE CONTRIBUTION TO POSITIVE BALANCE OF PAYMENTS

FOREIGN MILITARY SALES STILL GROWING

THE BAD NEWS

NOW EXPORTING OUR MOST ADVANCED ENGINE TECHNOLOGY

MILITARY & COMMERCIAL SUPERIORITY ENDANGERED

LONG TERM ECONOMIC IMPACT MAY BE NEGATIVE

SUMMARY

WORLD'S BEST TURBINE ENGINE TECHNOLOGY

- HAS PROVIDED WEAPON SYSTEMS SUPERIORITY, COMMERCIAL DOMINANCE
- ADDITIONAL LARGE GAINS ARE POSSIBLE
- PROGRAM WELL COORDINATED, COOPERATIVE AMONG MANY ORGANIZATIONS
- PROGRAM NEEDS CONTINUED SUPPORT, SELECTIVE EXPANSION

TURBINE ENGINE INDUSTRY HEALTH IS OF CONCERN

- BUSINESS FORECAST UNCERTAIN IN OUTYEARS
- LARGE INVESTMENTS REQUIRED, FUNDING SOURCES LIMITED
  - LIMITS COMPETITION
  - LITTLE INCENTIVE TO MODERNIZE OLD FACILITIES
  - ADVANCED TECHNOLOGY GETS LOW PRIORITY
  - FOREIGN FINANCIAL SUPPORT SOUGHT
- MILITARY & COMMERCIAL SUPERIORITY THREATENED

RAMJET TECHNOLOGY BASE WEAK BUT EXPANDING

- NEW STRATEGIC & TACTICAL APPLICATIONS
- LIMITED INDUSTRIAL/FACILITY CAPABILITY
- VERY LITLE IR&D, PRODUCTION ACTIVITY

BIOGRAPHY

Colonel George E. Strand
Commander, Air Force Aero Propulsion Laboratory

Colonel George E. Strand is the Commander of the Air Force Aero Propulsion Laboratory, Wright-Patterson Air Force Base, Ohio.

Born in Minneapolis, Minnesota, Colonel Strand entered the United States Air Force as an Aviation Cadet in June 1955. He completed his Navigator Flying Training at Harlingen Air Force Base, Texas, and was commissioned in the United States Air Force in September 1956.

His initial flying assignment was as a navigator in the 17th Air Transport Squadron, Military Air Transport Service, Charleston Air Force Base, South Carolina. In 1958 Colonel Strand was transferred to the 2157th Special Air Rescue Squadron, Ramey Air Force Base, Puerto Rico, and subsequently served in the 64th Air Rescue Squadron, Bergstrom Air Force Base, Texas, and the 48th Air Rescue Squadron, Eglin Air Force Base, Florida. Colonel Strand entered the Air Force Institute of Technology, Wright-Patterson Air Force Base, Ohio, where he received a Bachelors Degree in Aeronautical Engineering in 1964 and was selected to enter the graduate program. His graduate work was in the propulsion area and he received a Masters Degree in Aero-Mechanical Engineering in 1965.

In 1965 Colonel Strand was assigned to the Turbine Engine Division of the Air Force Aero Propulsion Laboratory, Wright-Patterson Air Force Base, Ohio, as a Development Engineer and later served as a Branch Chief in the Turbine Engine Division, with the responsibility for the turbine engine advanced development programs. In 1969 Colonel Strand was assigned to the 20th Tactical Air Support Squadron, Da Nang, Vietnam, where he served as a Forward Air Navigator. He flew over 200 combat missions and accumulated over 800 hours of flying time in OV-10 and O-2 aircraft. Upon his return from Vietnam in October 1970, he was assigned to the Pentagon to serve on the Air Staff under the Deputy Chief of Staff, Research and Development as an Aircraft Propulsion Staff Officer. In September 1974 he returned to the Air Force Systems Command to become the Chief of the Propulsion Division for the Director of Science and Technology, Headquarters Air Force Systems Command, Andrews Air Force Base, Maryland. Colonel Strand was assigned to the Air Force Aero Propulsion Laboratory as Director of the Ramjet Engine Division in September 1977. He served in that position until September 1978. At that time he was appointed Commander of the Aero Propulsion Laboratory.

Colonel Strand is a Master Navigator with over 5200 flying hours. His military decorations include the Distinguished Flying Cross, the Air Medal with twelve Oak Leaf Clusters and the Air Force Commendation Medal.

Colonel Strand is married to the former Shirley N. Simmons of Summerville, South Carolina. He and Mrs. Strand have two daughters.

ROCKET PROPULSION OVERVIEW

William F. Morris, Colonel, USAF
Commander, Air Force Rocket Propulsion Laboratory

OUTLINE (Fig 1)

Because of the emphasis on aircraft and aircraft support systems, this overview on rocket propulsion will be admittedly brief. Nonetheless, salient features of the activity in rocket propulsion are included and will provide adequate perspective on the status of the overall area. Included is information on the level of government investment, the extent of US industrial participation and a summary of on-going rocket propulsion development and technology efforts by the three military services.

ROCKET PROPULSION FUNDING (Fig 2)

Figure 2 presents a summary of funding for rocket propulsion research (6.1), exploratory development (6.2) and advanced development (6.3) for the two fiscal years, FY78 and FY79. That portion of the funds spent by the three services and NASA equivalent are shown along with the totals. These numbers indicate that the Air Force is a prime mover of rocket technology. Approximately 65 to 70 percent of the technology resources are provided by the Air Force. It is noted that the increase in total funding for the Air Force in going from FY78 to FY79 is almost entirely in the advanced development category. Funding levels for research and exploratory development remain essentially the same for the two fiscal years. The increase in Air Force advanced development funding is accounted for in a two-fold increase in FY79 funding for MX missile propulsion.

ROCKET PROPULSION ENGINEERING DEVELOPMENT FUNDING (Fig 3)

Funding for rocket propulsion engineering development in FY79 is shown. Again the funding is shown for the three services and NASA. From a funds viewpoint the major system undergoing development is the NASA Space Transportation System (Shuttle). Ninety-two percent of the $454M spent is for shuttle propulsion. The remaining funding is divided among the three services as follows: Air Force, 4.8%; Navy, 1.9%; Army, 1.3%. The major weapon systems undergoing development by the three services are shown on the figure.

ROCKET PROPULSION FUNCTIONAL AREA (Fig 4)

Figure 4 provides an overall perspective of the rocket propulsion functional area. Shown in the left column are technology objective categories as taken from the Technology Coordinating Paper for Missile and Space Vehicle Propulsion prepared by the USDR&E. Across the top of the figure are columns which represent the three services and NASA. Within these columns are coded symbols which reflect the type of effort (e.g., exploratory development, advanced development and engineering

development) each agency is working for each technology objective category. Several observations can be made: (1) Only the Air Force and Navy work Ballistic Missile propulsion. In that category, the Air Force alone works advanced development for booster and payload propulsion. The Navy primarily works engineering development; (2) all three services work the area of Air Launched Missile propulsion and tend to work closely together in this area; (3) the Army is the only agency having a mission responsibility which requires the use of shoulder fired rockets. Thus it is not surprising to see that they work this propulsion area alone; (4) only the Air Force and NASA work Space Propulsion. Although the Air Force is a major user of launch vehicles, they are not directly involved in technology or developments in that sub-category. The reason for this is clear. The next launch vehicle will be the Space Shuttle and that is a NASA responsibility. The Air Force assists, as required, in that area, but is not involved in funding new developments in that area. The sub-category of maneuvering includes both upper stages and orbital transfer stages. Both agencies are very active in these areas as well as in the sub-category of satellite propulsion.

ROCKET PROPULSION SALES (Fig 5)

Total sales for rocket propulsion have remained fairly constant over the past ten years, with a slight upturn over the past three of those ten years. This upturn is accounted for by the funding on space shuttle propulsion and the Navy Trident ballistic missile. Projected sales in FY79 show a decrease in R&D and an increase in production sales. This corresponds to a shift in Trident funding from R&D to production categories. The principal rocket propulsion companies in solid rockets are Thiokol, Hercules, Aerojet, Chemical Systems Division and Atlantic Research. Similarly, those in liquid rockets are Rocketdyne, Bell and Aerojet. There are several others, primarily in the small engine business for supporting satellite development needs. But about 90% of the total sales are accounted for by those principal companies listed. Of the principal companies, Rocketdyne in the liquid rocket area and Thiokol in the solid rocket area are the largest in terms of total sales. About 60% of the total sales is for solid rocket business; the remainder essentially for liquids. Note that these funds are unadjusted for inflation.

INDEPENDENT RESEARCH & DEVELOPMENT (Fig 6)

IR&D funding over the past ten years has varied between $16M to $21M. This is reflected in Figure 6 which shows IR&D for the principal rocket companies and is divided into the two categories, total IR&D and that portion of the total being spent for rocket propulsion. There are several fluctuations in the line representing rocket propulsion. These fluctuations tend to correspond to the anticipated award of a new weapon system. The increase in 1970 corresponds to increased effort by Rocketdyne and Pratt and Whitney prior to the SSME award. Similarly, the increase in 1972 reflects a general increase in effort prior to the Trident and Shuttle Solid Rocket Motor contract awards. The recent increase starting in 1975 and a larger increase in 1978 generally reflect the start of advanced development and full scale development of the MX missile. The industrial

trend toward spending a bigger share of the IR&D funds on rocket propulsion is encouraging. In years past, when the missile business was at a low ebb, the industry was spending a large percentage of the IR&D funds for developing new government business opportunities in the areas of high energy laser technology, environment and energy fields. This was disconcerting because of a feared erosion of the rocket propulsion technology base. Since there is no commercial market for rocket propulsion, the government must maintain a viable industry to satisfy its needs.

AIR FORCE AIR LAUNCHED MISSILE PROPULSION (Fig 7)

Rocket propulsion activities for Air Force air launched missiles are summarized in Figure 7 and are shown in the categories of development and technology. Development includes both advanced (6.3) and engineering development. The Air Force has followed a recently successful development of a reduced smoke Sidewinder, AIM-9J, with an engineering development for a reduced smoke AIM-9L. That program is progressing well. Under Air Force contract, a Boeing/Thiokol team is developing a long life motor modification of the Short Range Attack Missile (SRAM). This primarily involves a propellant change from the carboxy terminated polybutadiene (CTPB) used in the current SRAM to a hydroxyl terminated polybutadiene (HTPB), which offers improved physical and mechanical properties. Although the objective of the SRAM development program is to improve service life, an ancillary objective is to provide another contractor source for SRAM propulsion. Lockheed Propulsion Company was the contractor for the SRAM in the inventory today; but they no longer exist.

The other three programs listed under development are advanced development efforts. The Advanced Medium Range Air-Air Missile (AMRAAM) is well publicized and is a program managed by the Armament Development and Test Center at Eglin AFB, Florida. The Lightweight Missile Motor and Low Cost Missile Motor programs are managed by the Air Force Rocket Propulsion Laboratory. The objective of the former is to integrate solid rocket motor technologies that provide maximum system cost effectiveness for the next generation medium range missiles and carries through a PFRT-type demonstration. This motor uses HTPB propellant and will be reduced smoke. It will provide the AMRAAM System Program Office an optional, improved performance approach to the AMRAAM engineering development program when it begins in future years. The Low Cost Missile Motor program integrates cost reduction technologies to demonstrate overall reductions in motor cost. It is directed primarily toward the armament motor that is manufactured in lots of tens or hundreds of thousands and where a cost reduction could have a major acquisition cost impact. It uses HTPB propellant and is reduced smoke. It is being demonstrated in a nozzleless configuration which thus eliminates the cost of the nozzle. It now appears that cost reductions on the order of at least 32% are possible.

Major drivers in technology are: (1) reduced missile signature; (2) increased range and maneuverability; and (3) balanced performance and cost. Note that reduced missile signature includes UV/IR signature as well as minimum smoke rocket exhaust. Although the Air Force's responsibility for ramjet technology rests with the Aero Propulsion Laboratory, the AFRPL is involved in providing booster motors and ducted rocket gas generator propellants for the ramjets.

NAVY ROCKET PROPULSION (Fig 8)

Navy rocket propulsion development programs are being conducted on Trident, High Speed Anti-Radiation Missile (HARM) and several systems using rocket booster motors for integral rocket-ramjet applications. Representative propulsion technology for these systems is indicated in Figure 8. The major thrust for the Navy in air launched missiles over the past several years has been in ramjet technology. However, recent signs indicate increased attention is being placed on rocket propulsion for this category of application.

Several of the titles for Navy technology sound similar to those of the Air Force and Army; and the technology is similar - but not duplicative. The differences rest primarily in the different applications for this technology by the three services. Motor sizes, uses and operating conditions are sufficiently different to warrant separate but complimentary efforts. There is a lot of interchange among the three services and the programs are jointly reviewed annually by all concerned.

The major thrusts of the Navy are very similar to those of the Air Force; i.e., improved performance, reduced signature and lower costs. Emphasis is also placed on hazards definition due to the concern over shipboard use of the weapon systems. The incidence of combustion instability is greater for reduced and/or minimum smoke propellant motors. Thus more attention is being placed on this potential problem area.

ARMY ROCKET PROPULSION (Fig 9)

Army rocket propulsion engineering development, advanced development and technology activities are summarized in Figure 9. Emphasis in Army applications is clearly on reduced signature, high propellant burn rate, and low cost motor technologies. The General Support Rocket System is a major new development for the Army and will be used by the NATO forces in the 1980s. It uses HTPB propellant and will involve a transfer of that technology to our allies at that time.

SUMMARY (Fig 10)

In summary, the state-of-health of the rocket propulsion industry is good. During the period of reduced missile developments in the late 1960s - early 1970s, the rocket propulsion industry and government community were drastically reduced in size. Nonetheless it has remained a viable community and has the experienced personnel necessary to meet the current and anticipated future challenges. All signs point to an increase in attention to the needs of missile propulsion. Major drivers in air launched missile propulsion for all three services can essentially be summarized as increased performance capability, reduced signature and balanced performance and cost. The programs being conducted, or planned, by all three services are directed toward meeting these objectives and are highly complimentary. Close cooperation between all the services exists. The programs are jointly reviewed for interdependency at least annually.

trend toward spending a bigger share of the IR&D funds on rocket propulsion is encouraging. In years past, when the missile business was at a low ebb, the industry was spending a large percentage of the IR&D funds for developing new government business opportunities in the areas of high energy laser technology, environment and energy fields. This was disconcerting because of a feared erosion of the rocket propulsion technology base. Since there is no commercial market for rocket propulsion, the government must maintain a viable industry to satisfy its needs.

AIR FORCE AIR LAUNCHED MISSILE PROPULSION (Fig 7)

Rocket propulsion activities for Air Force air launched missiles are summarized in Figure 7 and are shown in the categories of development and technology. Development includes both advanced (6.3) and engineering development. The Air Force has followed a recently successful development of a reduced smoke Sidewinder, AIM-9J, with an engineering development for a reduced smoke AIM-9L. That program is progressing well. Under Air Force contract, a Boeing/Thiokol team is developing a long life motor modification of the Short Range Attack Missile (SRAM). This primarily involves a propellant change from the carboxy terminated polybutadiene (CTPB) used in the current SRAM to a hydroxyl terminated polybutadiene (HTPB), which offers improved physical and mechanical properties. Although the objective of the SRAM development program is to improve service life, an ancillary objective is to provide another contractor source for SRAM propulsion. Lockheed Propulsion Company was the contractor for the SRAM in the inventory today; but they no longer exist.

The other three programs listed under development are advanced development efforts. The Advanced Medium Range Air-Air Missile (AMRAAM) is well publicized and is a program managed by the Armament Development and Test Center at Eglin AFB, Florida. The Lightweight Missile Motor and Low Cost Missile Motor programs are managed by the Air Force Rocket Propulsion Laboratory. The objective of the former is to integrate solid rocket motor technologies that provide maximum system cost effectiveness for the next generation medium range missiles and carries through a PFRT-type demonstration. This motor uses HTPB propellant and will be reduced smoke. It will provide the AMRAAM System Program Office an optional, improved performance approach to the AMRAAM engineering development program when it begins in future years. The Low Cost Missile Motor program integrates cost reduction technologies to demonstrate overall reductions in motor cost. It is directed primarily toward the armament motor that is manufactured in lots of tens or hundreds of thousands and where a cost reduction could have a major acquisition cost impact. It uses HTPB propellant and is reduced smoke. It is being demonstrated in a nozzleless configuration which thus eliminates the cost of the nozzle. It now appears that cost reductions on the order of at least 32% are possible.

Major drivers in technology are: (1) reduced missile signature; (2) increased range and maneuverability; and (3) balanced performance and cost. Note that reduced missile signature includes UV/IR signature as well as minimum smoke rocket exhaust. Although the Air Force's responsibility for ramjet technology rests with the Aero Propulsion Laboratory, the AFRPL is involved in providing booster motors and ducted rocket gas generator propellants for the ramjets.

NAVY ROCKET PROPULSION (Fig 8)

Navy rocket propulsion development programs are being conducted on Trident, High Speed Anti-Radiation Missile (HARM) and several systems using rocket booster motors for integral rocket-ramjet applications. Representative propulsion technology for these systems is indicated in Figure 8. The major thrust for the Navy in air launched missiles over the past several years has been in ramjet technology. However, recent signs indicate increased attention is being placed on rocket propulsion for this category of application.

Several of the titles for Navy technology sound similar to those of the Air Force and Army; and the technology is similar - but not duplicative. The differences rest primarily in the different applications for this technology by the three services. Motor sizes, uses and operating conditions are sufficiently different to warrant separate but complimentary efforts. There is a lot of interchange among the three services and the programs are jointly reviewed annually by all concerned.

The major thrusts of the Navy are very similar to those of the Air Force; i.e., improved performance, reduced signature and lower costs. Emphasis is also placed on hazards definition due to the concern over shipboard use of the weapon systems. The incidence of combustion instability is greater for reduced and/or minimum smoke propellant motors. Thus more attention is being placed on this potential problem area.

ARMY ROCKET PROPULSION (Fig 9)

Army rocket propulsion engineering development, advanced development and technology activities are summarized in Figure 9. Emphasis in Army applications is clearly on reduced signature, high propellant burn rate, and low cost motor technologies. The General Support Rocket System is a major new development for the Army and will be used by the NATO forces in the 1980s. It uses HTPB propellant and will involve a transfer of that technology to our allies at that time.

SUMMARY (Fig 10)

In summary, the state-of-health of the rocket propulsion industry is good. During the period of reduced missile developments in the late 1960s - early 1970s, the rocket propulsion industry and government community were drastically reduced in size. Nonetheless it has remained a viable community and has the experienced personnel necessary to meet the current and anticipated future challenges. All signs point to an increase in attention to the needs of missile propulsion. Major drivers in air launched missile propulsion for all three services can essentially be summarized as increased performance capability, reduced signature and balanced performance and cost. The programs being conducted, or planned, by all three services are directed toward meeting these objectives and are highly complimentary. Close cooperation between all the services exists. The programs are jointly reviewed for interdependency at least annually.

ROCKET PROPULSION

BRIEFING OUTLINE

- U.S. GOVERNMENT INVESTMENT
- U.S. INDUSTRY PARTICIPATION
- DOD PROGRAM HIGHLIGHTS
- SUMMARY

200

FIGURE 1

ROCKET PROPULSION FUNDING
(6.1,6.2,6.3)*

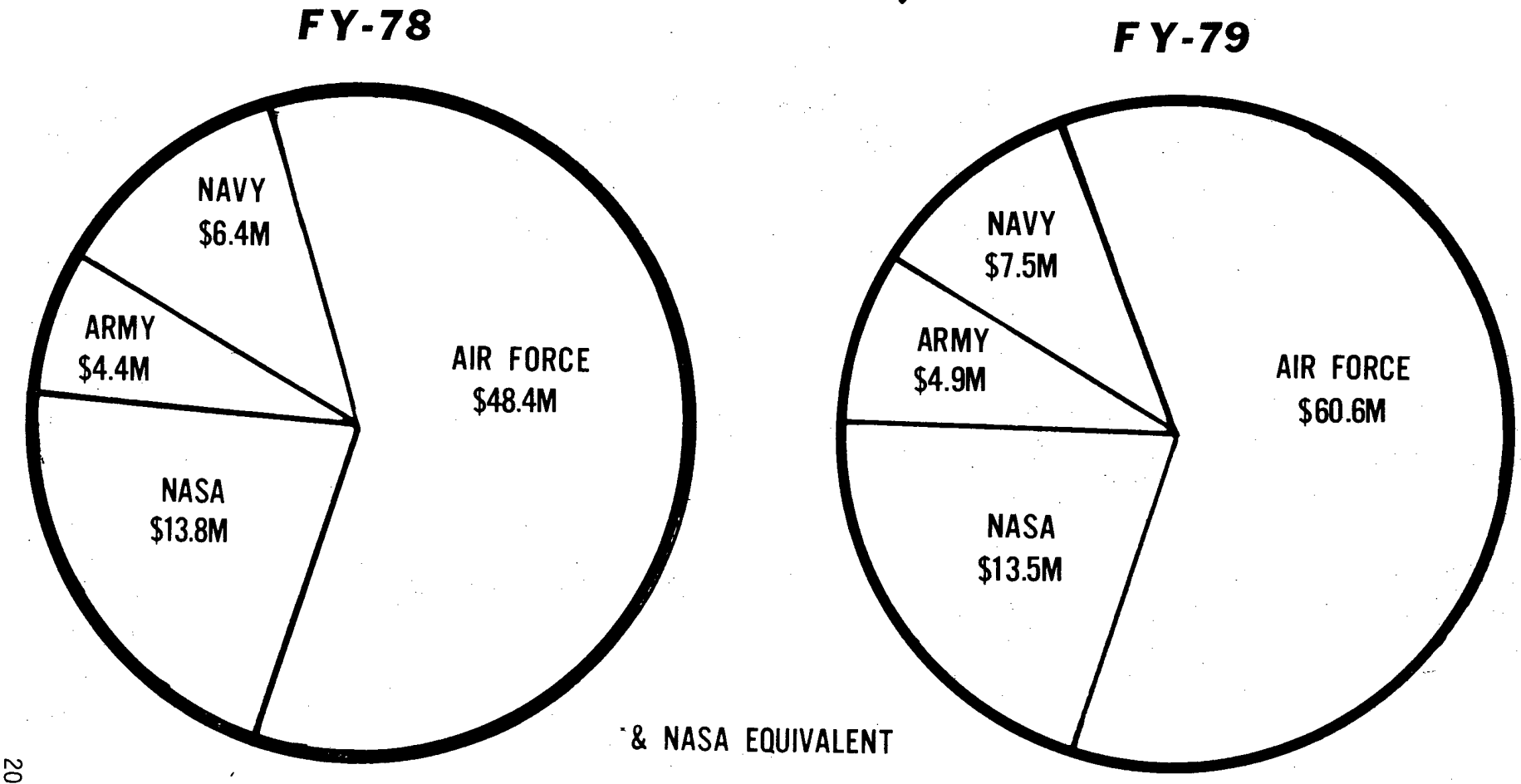

*& NASA EQUIVALENT

TOTAL: $73.0 MILLION

TOTAL $86.5 MILLION

201

201

FIGURE 2

ROCKET PROPULSION ENGINEERING DEVELOPMENT FUNDING

FY-79

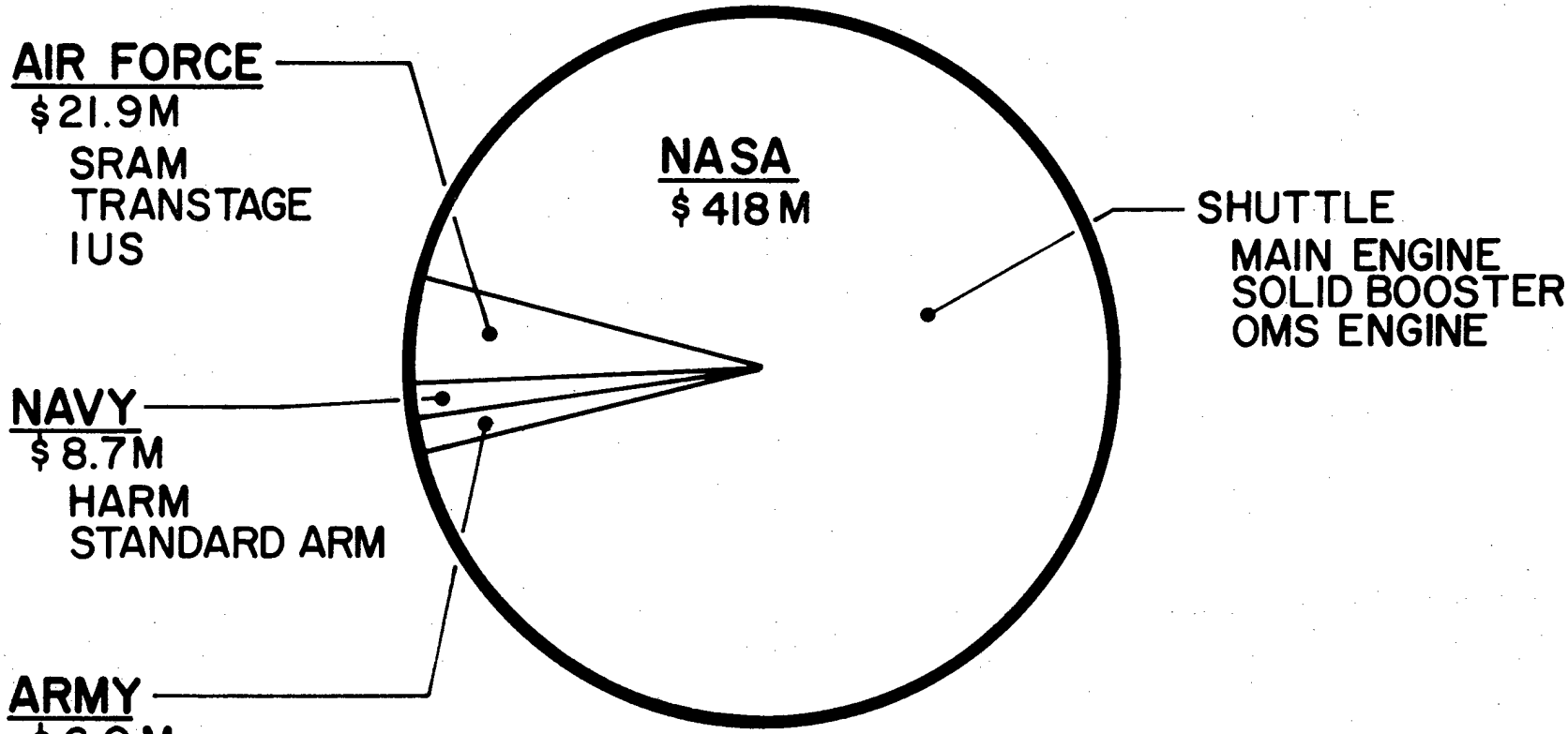

TOTAL: $454.6 MILLION

ROCKET PROPULSION FUNCTIONAL AREA

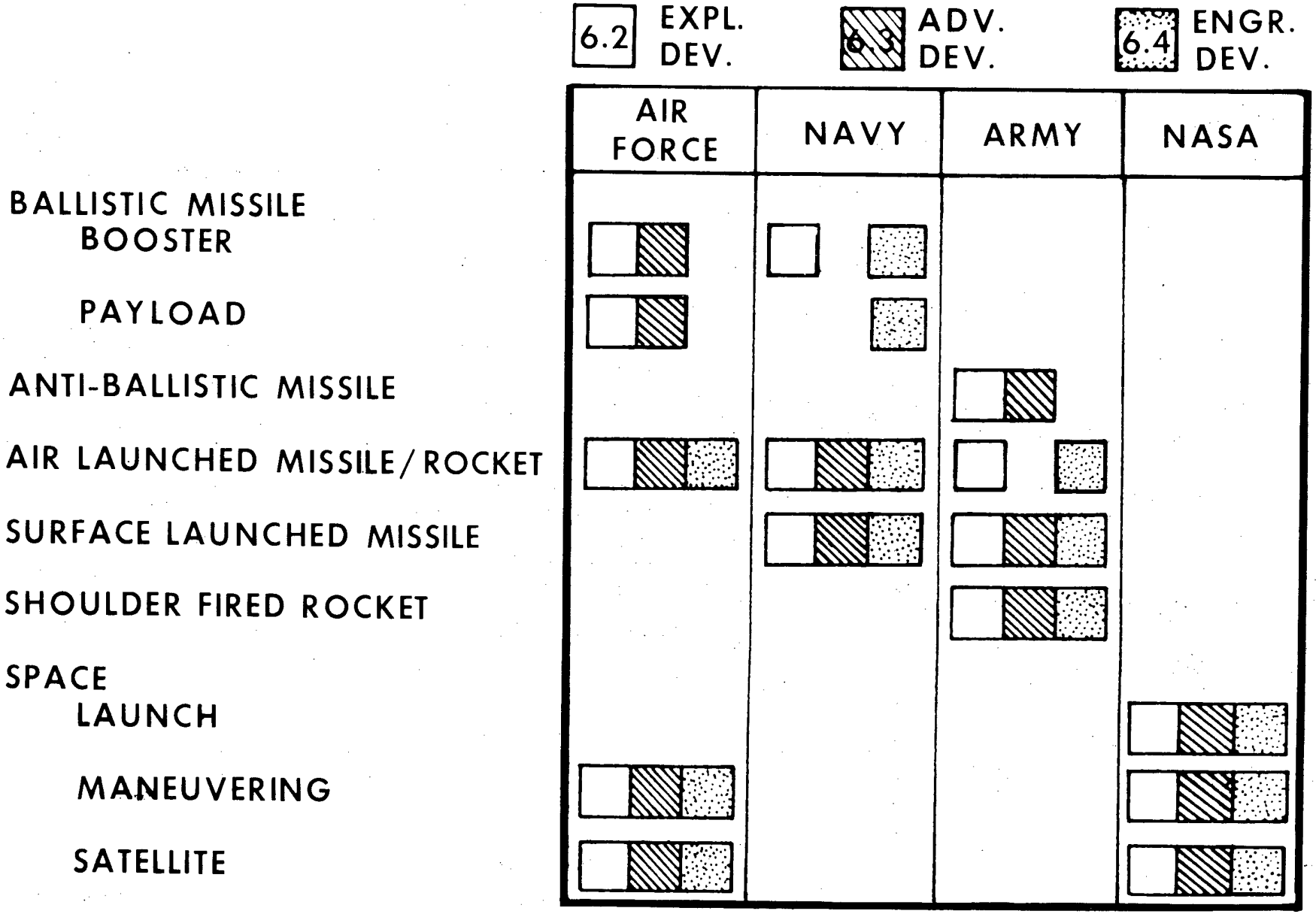

ROCKET PROPULSION SALES
OF PRINCIPAL COMPANIES

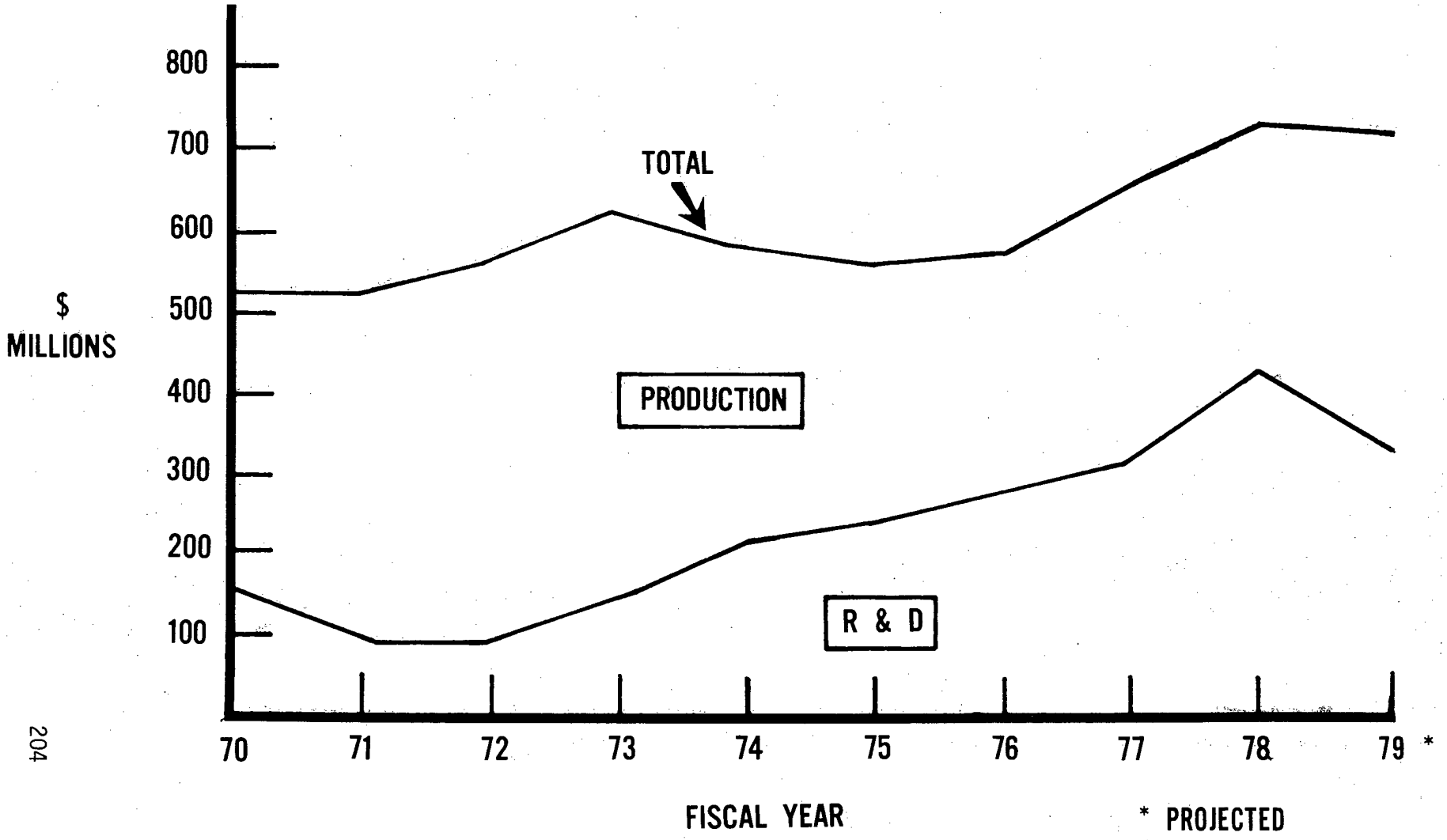

FIGURE 5

INDEPENDENT RESEARCH & DEVELOPMENT

OF PRINCIPAL ROCKET COMPANIES

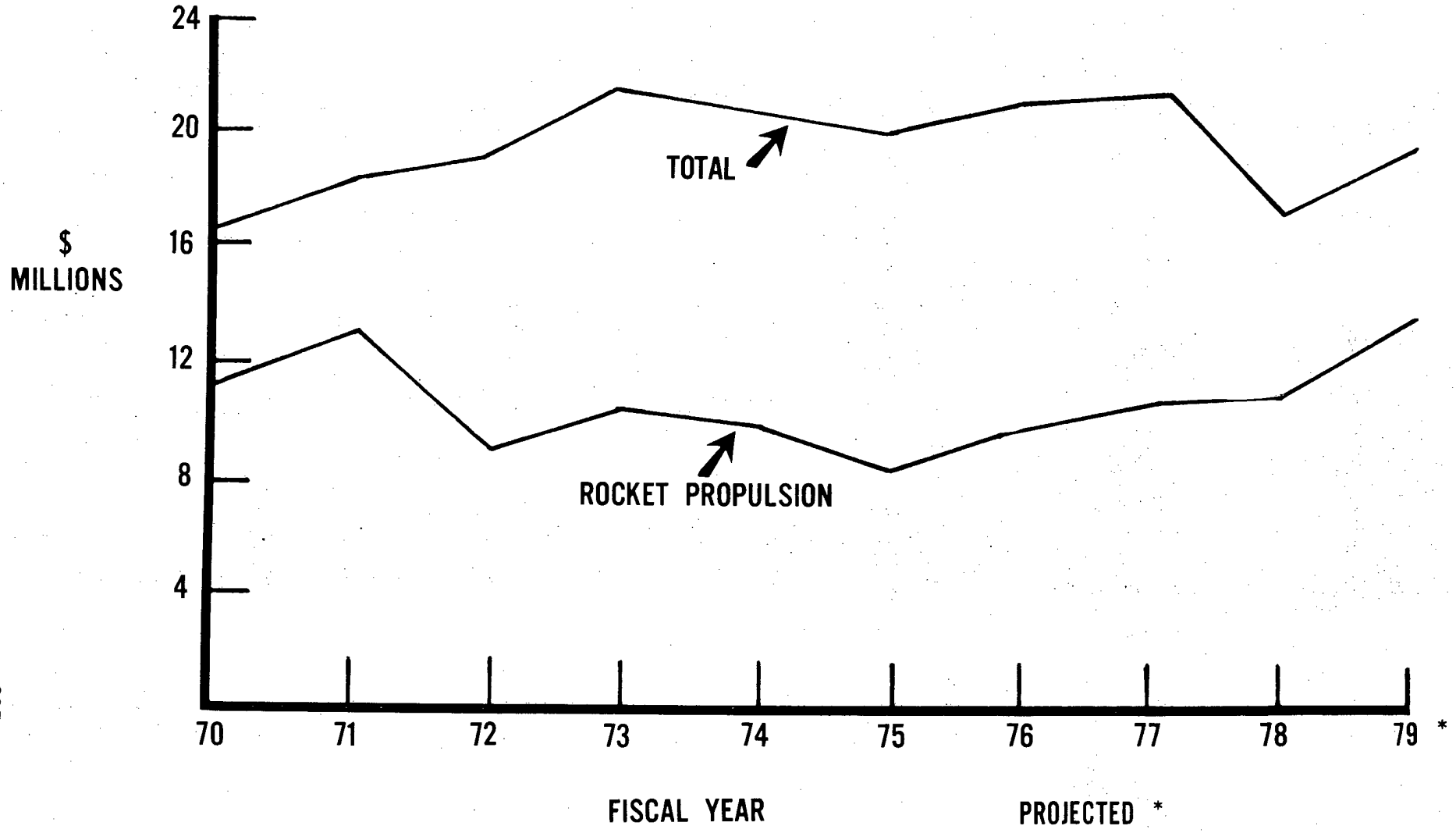

FIGURE 6

AIR FORCE

AIR LAUNCHED MISSILE PROPULSION

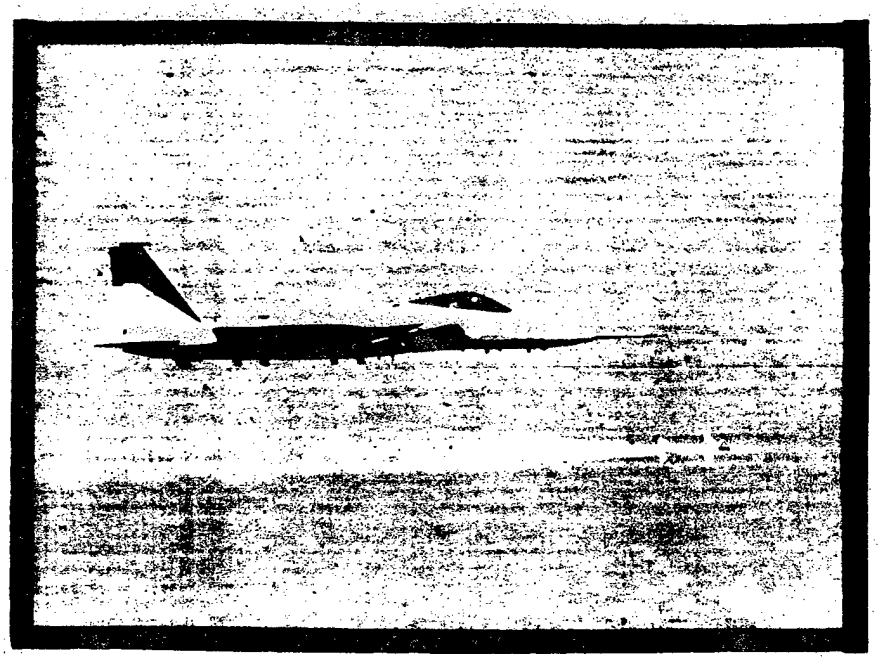

DEVELOPMENT:

- SIDEWINDER, AIM 9L
- SRAM
- ADV. MEDIUM RANGE AIR-AIR MISSILE (6.3)
- LIGHTWEIGHT MISSILE MOTOR (6.3)
- LOW COST MISSILE MOTOR (6.3)

TECHNOLOGY:

- SIGNATURE
  - –MINIMUM SMOKE PROPELLANTS
  - –UV/IR
- PERFORMANCE
  - –RADIAL PULSE MOTORS
  - –HIGH DENSITY-IMPULSE PROPELLANT
  - –HIGH PERFORMANCE MOTOR DEMOS
- LOW COST
  - –MOTOR DEMOS
  - –NOZZLELESS MOTORS
- INTEGRAL ROCKET RAMJETS
  - –BOOSTER MOTORS
- DUCTED ROCKET PROPELLANTS

FIGURE 7

NAVY ROCKET PROPULSION

DEVELOPMENT:

- TRIDENT
  - –CROSS-LINKED DOUBLE BASE PROPELLANT
  - –ORGANIC FIBER CASES/PG NOZZLE INSERTS
  - –ALTERNATE PROPELLANT PROGRAM/HAZARDS
- HARM
  - –REDUCED SMOKE HTPB PROPELLANT
- INTEGRAL ROCKET-RAMJET BOOSTERS
  - –HARPOON
  - –TOMAHAWK
  - –STAND-OFF TACTICAL MISSILE

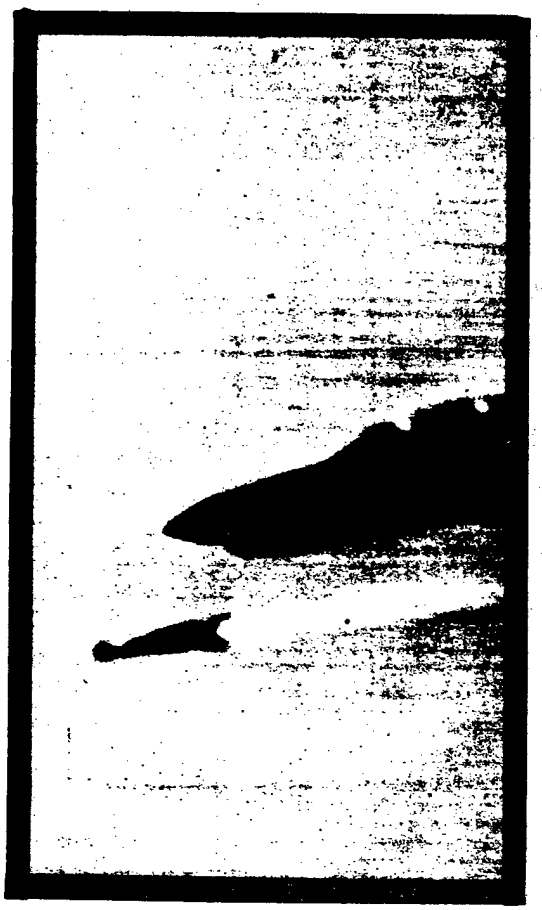

TECHNOLOGY

- –HIGH PERFORMANCE IRR BOOSTER MOTOR DESIGN
- –HIGH IMPULSE PROPELLANT EVALUATION
- –DUAL CHAMBER BOOST SUSTAIN MOTOR DESIGN
- –LOW COST TVC/ AERODYNAMIC CONTROL SYSTEM
- –AIR LAUNCHED MOTOR HAZARD EVALUATION
- –MINIMUM SMOKE PROPELLANTS/COMBUSTION INSTABILITY
- –LOW SIGNASTURE PULSE MOTOR DEMO
- –LIFE CYCLE COSTING METHODOLOGY (TRI-SERVICE)
- –VERTICAL LAUNCH BOOSTER

FIGURE 8

ARMY ROCKET PROPULSION

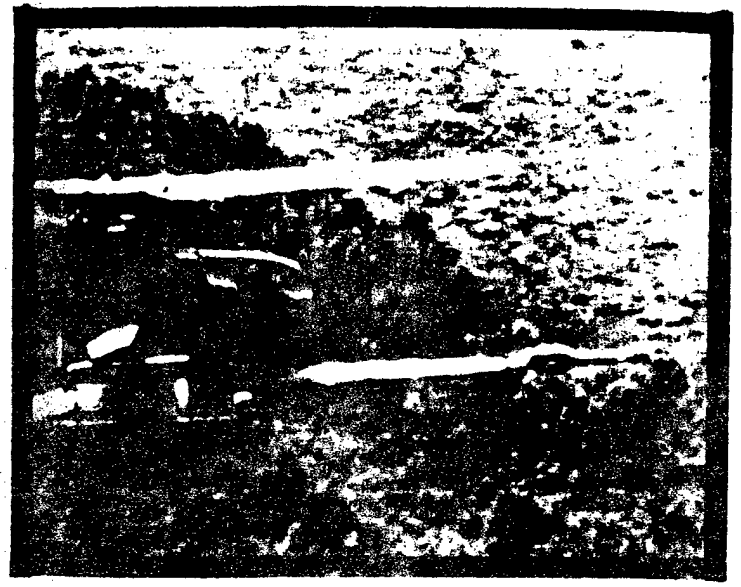

ENGINEERING DEVELOPMENT

- HELLFIRE: – AIR LAUNCHED ANTI-TANK MISSILE

  REDUCED SMOKE (HTPB) PROPELLANT

- CHAPARRAL: – SURFACE LAUNCHED AIR DEFENSE MISSILE

  HIGH ENERGY (XLDB)/MINIMUM SMOKE PROPELLANT

- VIPER: – SHOULDER FIRED ANTI-TANK ROCKET

  HIGH BURN RATE, LOW TEMP SENSITIVE PROPELLANT

ADVANCED DEVELOPMENT

GSRS: – GENERAL SUPPORT ROCKET SYSTEM

- 29-MONTH VALIDATION PROGRAM STARTING IN FY-78

TECHNOLOGY

–CONTINUED WORK ON ABM TECHNOLOGY RELATED TO ULTRA-FAST TERMINAL INTERCEPTOR

–CONTINUED EMPHASIS ON MINIMUM SMOKE PROPELLANTS COMPATIBLE WITH BEAM RIDER MISSILE CONCEPTS

–LOW COST MOTOR TECHNOLOGIES

FIGURE 9

SUMMARY

- ROCKET PROPULSION STATE–OF–HEALTH IS GOOD

- MAJOR DRIVERS ARE:
  - –INCREASED RANGE & MANEUVERABILITY
  - –REDUCED MISSILE SIGNATURE
  - –BALANCED PERFORMANCE & COST

- DOD PROGRAM VERY COMPLIMENTARY

FIGURE 10

COLONEL WILLIAM F. MORRIS

Colonel William F. Morris is the Commander of the Air Force Rocket Propulsion Laboratory (AFRPL), Edwards Air Force Base, California. The Laboratory's primary mission is to provide advanced rocket propulsion technology for future Air Force ballistic missile, air launched missiles and space systems. It also provides rocket propulsion expertise to other organizations, primarily AF System Program Offices for problem solving and effective technology transfer.

Colonel Morris was born in Oneonta, New York on May 11, 1932, grew up in Binghamton, New York and graduated from Central High School there in 1950. He graduated from Purdue University with a Bachelor of Science degree in Air Transportation Corp in May 1954. A distinguished Air Force Reserve Officer Training Corp graduate and Cadet Air Division Commander, he was commissioned in the US Air Force in May 1954, and entered active duty the following month. He holds a second Bachelor of Science degree in Mechanical (Aerospace) Engineering from Oklahoma State University and a Master of Science in Mechanical Engineering from the Jet Propulsion Center at Purdue University.

After attending Supply Officer School at F.E. Warren AFB, Wyoming, Colonel Morris was assigned as supply officer of the 48th Installation Squadron, Chaumont Air Base, France. In November 1957, he became a special agent for the 11th District Air Force Office of Special Investigations, Tinker AFB, Oklahoma. From February 1959 until August 1962 he was commander of Detachment 1107, Air Force Office of Special Investigations at Blytheville AFB, Arkansas.

Colonel Morris attended Oklahoma State University from August 1962 to February 1965. Upon graduation, he was assigned as a rocket propulsion analyst with the Foreign Technology Division, Wright-Patterson AFB, Ohio. He became chief of the Aerospace Technology Division in July 1966 and head of the Propulsion Technology Group in August 1967. He left the Foreign Technology Division for Purdue University in May 1968.

After earning his master's degree, Colonel Morris returned to the Foreign Technology Division at Wright-Patterson AFB, Ohio from January 1970 through June 1976. During this time, he served as a missile analyst and assistant chief of the Advanced Ballistic Systems Branch; chief of the Medium and Intermediate Range Ballistic Missiles Systems Branch; assistant deputy chief of staff for Plans and Programs; chief of Advanced Projects Division; and Assistant Director of Engineering.

Colonel Morris was assigned to the Air Force Rocket Propulsion Laboratory in June 1976 as chief of the Technology Division. He became director of the Test and Support Division of AFRPL in October 1977 and held that post until he assumed his present position on June 20, 1978.

His military decorations and awards include the Legion of Merit and the Air Force Commendation Medal. He wears the Senior Missileman Badge.

The colonel and his wife, the former Thelma L. Arthur of Santa Barbara, California have four children; William and Michael who live in Venice, California, and Jennifer and Tedi who live with their parents at Edwards Air Force Base.

THE ROLE OF TURBINE ENGINE TECHNOLOGY ON LIFE CYCLE COST

BY

Robert F. Panella, USAF

Michael A. Barga, USAF

Richard G. McNally, USAF

Turbine Engine Division

Air Force Aero Propulsion Laboratory
Wright-Patterson AFB, Ohio

The Role of Turbine Engine Technology on Life Cycle Cost

Abstract

The turbine engine is a major contributing subsystem in the life cycle cost (LCC) of an aircraft weapon system. The impact of turbine engine technology on LCC is addressed in this paper. To adequately assess this technology, LCC techniques are being developed which are sensitive to performance, structural design, manufacturing processes, reliability and maintainability. These techniques will then be used to determine the performance/life/cost trade-offs of advanced technology. An overview of current efforts in this area is given.

INTRODUCTION

The overall objectives of our efforts in the area of life cycle cost (LCC) are two: first, to determine the cost impact of our advanced technology, and second, to identify and pursue those technologies which offer the greatest potential in cost reduction. This paper will include a perspective of turbine engine LCC, and then an overview of current efforts on the methodology and application of design-to-life-cycle-cost.

Figure 1 shows the LCC of the top five subsystems of an advanced fighter weapon system. The cost of each subsystem is shown as a percentage of total system production cost and logistics support cost. As can be seen from this figure, the engine subsystem is a major component of weapon system cost.

LIFE CYCLE PHASES

In the development phase, the major cost drivers are hardware and test. A study of previous engine development programs suggests that a relationship exists between these two parameters. Current efforts are being conducted, using these parameters to develop estimating relationships for the development phase.

In the acquisition phase, previous cost estimating efforts for this phase determined that the single most significant parameter in estimating the acquisition (or production) cost of an engine is its thrust. It follows then that the cost per pound of thrust is a relative measure of the acquisition cost of an engine. Figure 2 is a graph of cost per pound of thrust, for engines in the inventory, plotted against their Military Qualification Test (MQT) date. The cost of engines was normalized to constant year dollars and equivalent production rate and production quantity. The slope of the curve shown is a measure of the increase in cost of engines over the last 30 years. This increase is a moderate one.

In estimating the cost impact of advanced technology, it is possible to be too narrow in scope, and therefore the analysis can lead to erroneous conclusions. For example, consider the bore entry design of a turbine disk compared to the more conventional rim entry design. Figure 3 is a cross-section schematic of the rotating assembly of the gas generator. Shown are the compressor assembly (minus blades), shaft, and turbine wheel. The primary difference between the design in the upper half of the schematic, and the design

in the lower half is in the turbine area. The upper half shows bore entry turbine cooling, the lower half shows rim entry turbine cooling. The relative production cost of the two-disk designs is shown in the figure. The relative cost of the bore entry disk is more than two times that of the rim entry disk. However, if the rotor cost is estimated for those parts shown on the figure, the relative cost of the two rotors are approximately equal, as shown on the right of the figure. This is so because the secondary flow system, in the case of the bore entry design, is simpler. It is important that the scope of the analysis be broad enough to identify the impact of the advanced technology.

Let us now consider the operations phase. One of the difficulties in this phase is summarized in a Government Accounting Office (GAO) report, dated Dec 74, which states, "It is almost universally held that the greatest obstacle to preparing reliable life cycle cost estimates is the absence of a data base segregating total ownership cost by weapon." However, we are making gains in this area. Hardware failures in the operational phase are a cost driver. Figure 4 shows the basic causes of engine failure, and the approximate percentage of failures attributed to each cause. Some of the causes are well understood, others are not. A difficulty encountered in understanding failures, is the combination of two or more basic causes contributing to a failure. The mechanism of failure of these combined causes is difficult to analyze, and the failure difficult to predict.

The operational use of the engine is a major factor in determining its operational and support (O&S) cost. Efforts are going on to understand and quantify this usage effect. Figure 5 is a set of graphs comparing the engine related operational characteristics of two airplanes flying formation. As can be seen from the graphs in Figure 5, the power setting, engine speed, and tailpipe temperature for the wingman are considerably different than that of the flight leader, even though both airplanes are flying at the same speed and altitude. The resultant temperatures, pressures, and stresses throughout the engines are quite different, and, hence, the useful life of the engines can be significantly different. Figure 6 is a pictorial summary of major efforts to predict life of engine components. The tasks to be accomplished to make these predictions and validate them, are shown on the figure.

Fuel is becoming a very important factor in the O&S phase. Figure 7 shows the Air Force cost and consumption of fuel for the last five years. The vertical bars represent the amount of fuel used, and the curve represents the cost of fuel, in cents per gallon, over the time period shown. Both cost and availability of fuel will continue to be an important factor.

AIR FORCE/INDUSTRY TURBINE ENGINE LCC MODEL

The key to life cycle cost assessment is a standard, usable methodology. A methodology for use during source selection was developed by the Joint Air Force/Industry Working Group July 1975-April 1976. The methodology defines and organizes all engine chargeable costs. It can discriminate between engine designs and can be tailored to accommodate the amount of detailed information known about the engine at the time of source selection.

The methodology developed by the Joint Air Force/Industry Working Group includes equations, definitions, and ground rules. The engine LCC model has twenty-four detailed equations, see Figure 8. Most of those equations are used in more than one phase of LCC. The X's on Figure 8 denote use of an equation in a particular LCC phase. Twenty-three equations are used to calculate Research Development Test and Evaluation (RDT&E) costs, fourteen equations to calculate acquisition costs, and sixteen equations to calculate O&S costs. Each of the equations has several input terms. Each term was completely defined. Definitions were also provided for all output terms to provide clarity in using the model. General instructions and guidelines for model use are as follows: (1) The model was developed to be used in source selections as opposed to other applications such as implementing warranties. (2) The model's primary value is not for absolute engine LCC, but comparative LCC of alternate engine designs. (3) The model was designed to break down the engine to the part level. However, the capability of going to the part level should be used only as required. (4) Of the twenty-four equations in the engine LCC model, only the appropriate equations for a given application should be used. (5) Costs are shown in fiscal years and will include General and Administrative cost (G&A), but will exclude profit and fee.

A report of this methodology titled, "Turbine Engine Life Cycle Cost Model", dated February 1977, describes the model in detail. Several tasks have been identified for follow-on effort before the methodology could be easily applied in a source selection. These tasks include programming the engine LCC model, and model verification.

REDUCED COST TURBINE ENGINE CONCEPTS PROGRAM

There are major efforts underway to adapt the methodology described in the previous section for life cycle cost analysis during advanced technology programs. In June 1977, the Reduced Cost Turbine Engine Concepts program

was initiated. The objectives of this effort are to: (1) assess reduced cost turbine engine concepts prior to engineering development in terms of their impact on engine RDT&E cost, engine acquisition cost, engine O&S cost, and system LCC; (2) select an engine component concept which offers significant cost reduction based on this assessment; (3) design, fabricate, and test the selected component concept; and (4) reassess the component concept LCC impact based upon the design, fabrication and test results. This effort will demonstrate the use of LCC as a major design parameter.

Reduced Cost Turbine Engine Concepts Approach

The Reduced Cost Turbine Engine Concepts Program will first develop an LCC model based on the Air Force/Industry Turbine Engine LCC model to determine engine RDT&E cost, engine acquisition cost, engine O&S cost and system LCC as a function of turbine engine component design parameters. These component design parameters will include performance, weight, life, maintainability and acquisition cost. The LCC model will then be used to determine the LCC of some advanced technology aircraft system for use as a baseline. Trade studies will then be conducted relative to this baseline. The results of the trade studies will be used to select a component concept for design, fabrication and test. As data is obtained during the design, fabrication, and test phases, the LCC model will be updated and the impact on LCC determined.

Reduced Cost Turbine Engine Concepts LCC Model

The cost elements used in the LCC model to define turbine engine LCC were obtained from the Air Force/Industry Turbine Engine LCC model addressed previously. Not all cost elements given on Figure 8 will be used in the developed model. The equations marked with an "X" on Figure 9 will be used in the appropriate LCC phase. For example, cost element 3 will be used during RDT&E and O&S. Equations were selected for use on the basis of their percent contribution to engine LCC in the most likely case. For example, results to date indicate that Scheduled Maintenance accounts for approximately 35% of engine LCC, Petroleum, Oil, and Lubrication accounts for approximately 28% of engine LCC, and Engine Manufacturing accounts for approximately 23% of engine LCC. The other cost elements given on Figure 8 account for the remaining 14% of engine LCC.

The LCC model to be developed by this effort uses both accounting and parametric cost estimating relationships.

Figure 10 gives examples of parametric cost estimating relationships and accounting cost estimating relationships. A parametric cost estimating relationship is an empirical equation for some element of cost in terms of design parameters. An accounting cost estimating relationship is a summation of labor costs, material costs and overhead costs.

Figure 11 is a simplified schematic of the LCC model to be developed by this program. The model will calculate engine RDT&E cost, engine acquisition cost, engine O&S cost and system LCC as a function of engine component life, weight, performance, maintainability and acquisition cost. Engine RDT&E costs will be calculated using parametric cost estimating relationships. Engine acquisition costs will be calculated using accounting cost estimating relationships. Costs will be accumulated at the component level. Learning curves will be used to account for changes in cost with production quantity. Scaling laws will be provided to account for changes in baseline engine size. Engine O&S costs will be calculated using either a simulation or a discrete model. A complete explanation of a simulation versus a discrete model is beyond the scope of this paper. It will simply be stated that the simulation model provides a more realistic representation of the O&S phase of the engine life cycle. The discrete model has the advantage of using less computer time and storage. Both models account for scheduled maintenance as a function of engine operating hours, flights or periods and employ learning curves for required maintenance actions. Both models account for unscheduled maintenance by employing failure distributions for individual engine components and learning curves for resultant maintenance actions. Fuel is determined as a function of usage and engine fuel flow. All phases of airframe LCC will be determined using parametric cost estimating relationships. These cost estimating relationships will define airframe RDT&E, Acquisition, and O&S costs in terms of engine and airframe interface parameters. These cost estimating relationships will be developed for the baseline aircraft by an airframe subcontractor. In the future, it is planned to use the system life cycle cost model currently being developed by the Air Force Flight Dynamics Laboratory, Figure 12. The developed model will have the capability to account for inflation, discounting or constant year dollars.

Reduced Cost Turbine Engine Concepts Methodology

All LCC trade studies will be conducted relative to the baseline system LCC. During these studies, the following

parameters will be constant: mission, lifetime, fleet buildup and peacetime usage rates. The baseline engine and airframe will be scaled in size to meet fixed mission requirements, and the cost impact then determined. The trade studies will be conducted applying inflation and discounting, and constant year dollars.

Figure 13 shows that a change in baseline engine component performance will require the use of an engine performance model, an aircraft sizing/mission analysis model and the LCC cost model. A change in baseline engine component weight will require a reassessment of baseline engine weight, resizing of the baseline aircraft, and the use of the cost model to determine the cost impact. Changes in baseline engine component life, maintainability, and acquisition cost require only the use of the LCC model.

Reduced Cost Turbine Engine Concepts - Results to Date

To date, several trade studies have been completed during the Reduced Cost Turbine Engine Concepts Program. This section of the report will address some of those trade studies. It should be noted that all trade studies are done relative to a baseline and the baseline varies from contractor to contractor.

Figure 14 is a cross-section of the General Electric (GE) Joint Technology Demonstrator Engine (JTDE). GE is considering the use of powder metal (Rene 95) to manufacture the parts identified on Figure 14 to near-net shape, using the HIP (Hot Isostatic Pressing) processing technique. Figure 15 shows that this process results in decreased forging operations and improved material utilization.

A reduction in engine manufacturing cost is realized as shown in Figure 16. Note that baseline engine performance, weight, reliability, life and maintainability are not affected and no scaling of the baseline engine or aircraft is required to determine the LCC payoff.

Detroit Diesel Allison (DDA) has developed a transpiration cooling material called Lamilloy which is a laminated photoetched, diffusion bonded structure. Triply Lamilloy shown in Figure 17 has three laminates. Cooling air enters and leaves each layer through discrete holes. Because of the alignment of adjacent sheets, the air must travel around the etched pins in each sheet. Lamilloy has a higher heat transfer effectiveness than conventional film cooling and when

compared to other transpiration materials, Lamilloy has improved structural integrity and oxidation resistance, and more tolerance to clogging.

Figure 18 is a cross-section of a Lamilloy DDA Combustor rig. The parts made of Lamilloy are depicted.

DDA is currently considering the use of Lamilloy in the construction of their JTDE combustion liner. Figure 19 shows that Lamilloy will result in a decrease in baseline engine cooling flow, a reduction in baseline engine weight, an increase in baseline engine life and a lower baseline engine manufacturing cost. The LCC problem becomes somewhat more involved than just considering an improved manufacturing process as was the case with the GE powder metal high spool. The reduction in engine cooling flow and weight necessitates engine and system scaling to identify the full LCC payoff of the Lamilloy combustor liner. Figure 19 gives the results once the baseline engine and airframe are scaled.

Teledyne CAE is considering the use of a low aspect ratio fan in their JTDE, see Figure 20. Figure 21 indicates that the low aspect ratio fan will result in an increase in baseline engine performance, an increase in baseline engine weight, an increase in baseline engine meantime between failure (MTBF) and a lower baseline engine manufacturing cost. Note that with the exception of the increase in baseline engine weight, all baseline engine changes should result in a decrease in LCC. Scaling of the engine and airframe is required to determine the LCC impact. Figure 21 gives the LCC impact once the baseline engine is scaled.

AiResearch is considering the use of a low aspect ratio turbine in their advanced technology turbine engine, Figure 22. Figure 23 indicates that the low aspect ratio turbine will result in an increase in baseline engine performance, an increase in baseline engine weight, a decrease in baseline engine reliability, a decrease in baseline engine maintainability and increase in baseline engine cost. Note that all of the baseline engine changes with the exception of Specific Fuel Consumption (SFC) and thrust would result in an increase in baseline engine and aircraft LCC. Scaling of the engine and airframe is required to realize the LCC payoff of the low aspect ratio turbine. Figure 23 gives the results.

CONCLUSIONS

The turbine engine is a major contributor to weapon system LCC. The consideration of this contribution early in the design phase will result in a substantial LCC savings. When determining the LCC impact of an advanced technology engine component, the following should be considered: (1) weapon system LCC, not just engine LCC, (2) engine component interaction, (3) duty cycle, (4) fuel usage, and (5) engine component maintenance and life prediction. The accurate determination of all of these parameters is essential to the prediction of the LCC payoff of advanced technology turbine engine components.

An assessment of the payoff of advanced technology must include the effect of three fundamental characteristics of that technology. These characteristics are performance, structural life, and cost. Figure 24 shows what this assessment process involves when applied to turbine engine technology. As the figure shows the assessment is involved, and the performance, structural life, cost characteristics are very much interactive.

ADV. FIGHTER SUBSYSTEM LCC
(TOP FIVE SUBSYSTEMS)

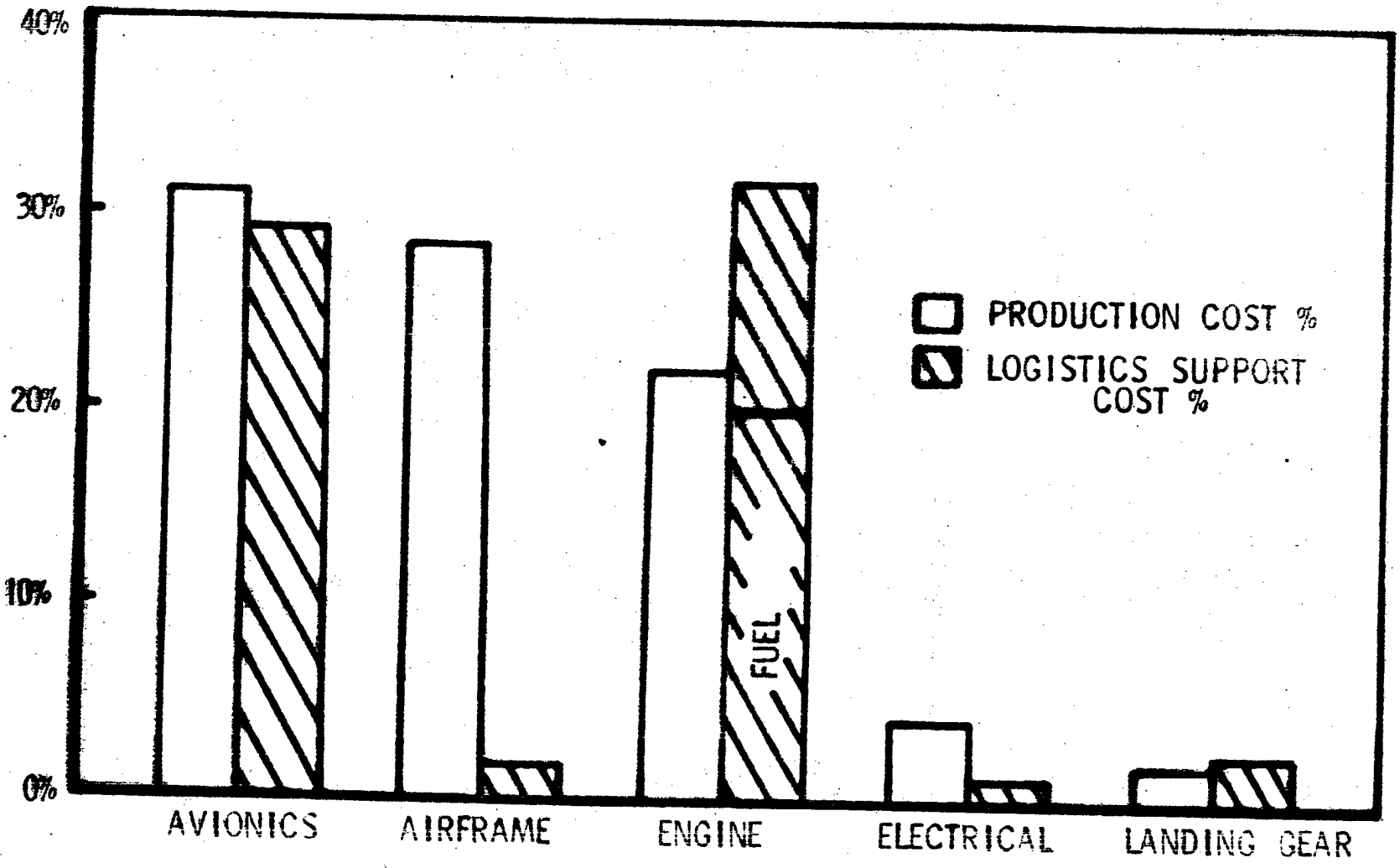

Figure 1

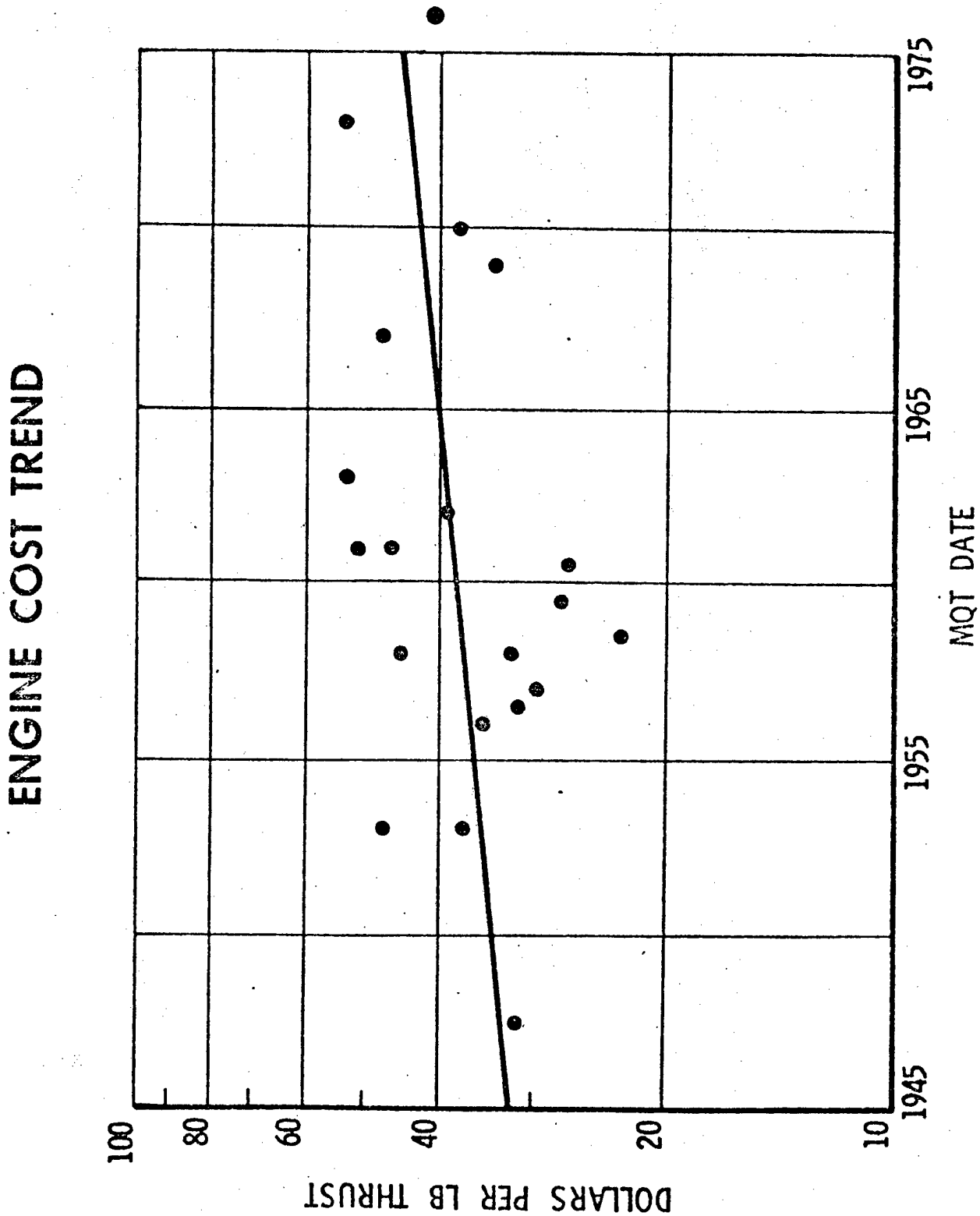
ENGINE COST TREND
DOLLARS PER LB THRUST
100
80
60
40
20
10
1945
1955
1965
1975
MQT DATE

Figure 2

Cost Estimates for Bore Vs. Rim Entry Study Engines

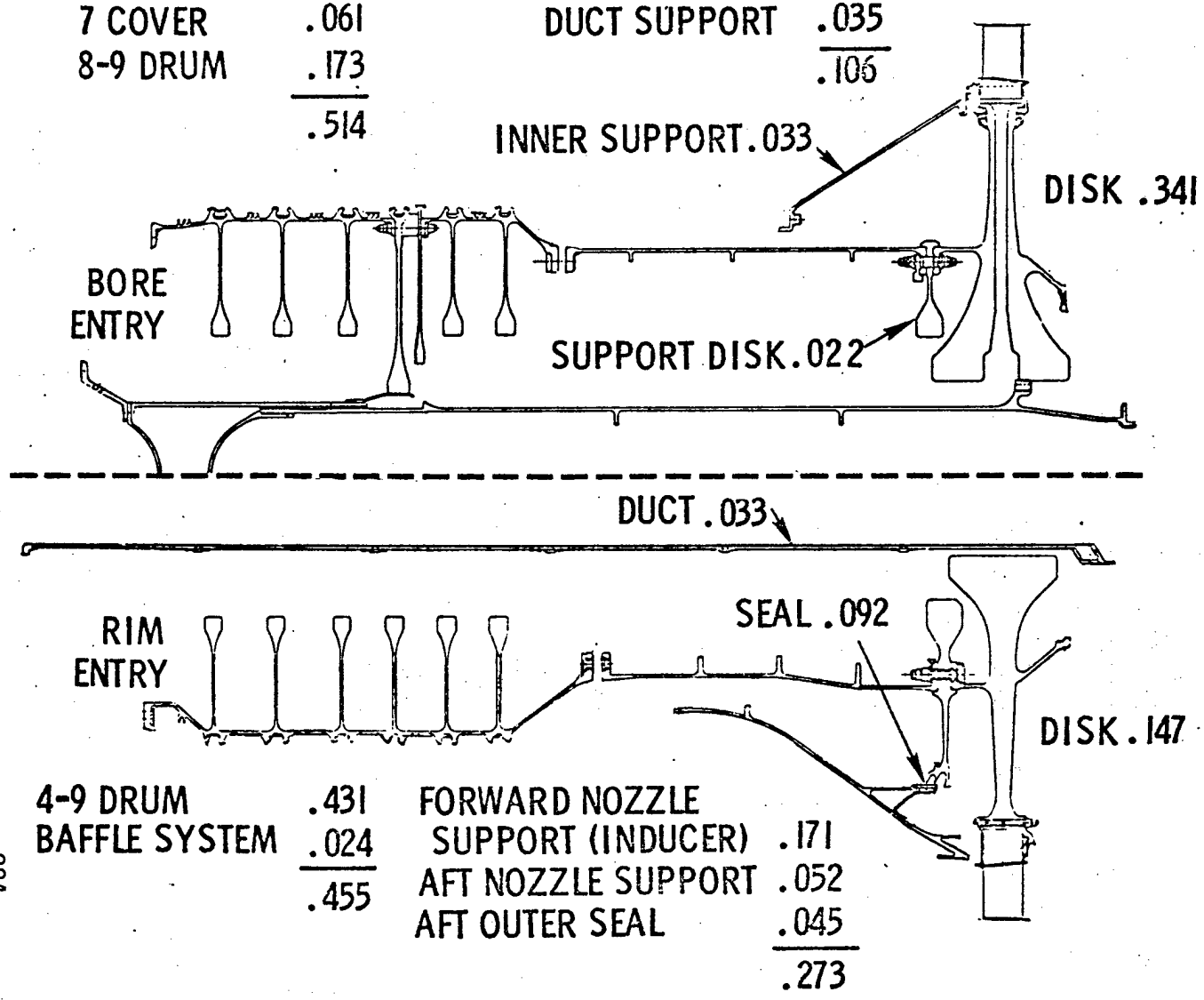

Figure 3

CAUSES OF ENGINE FAILURES

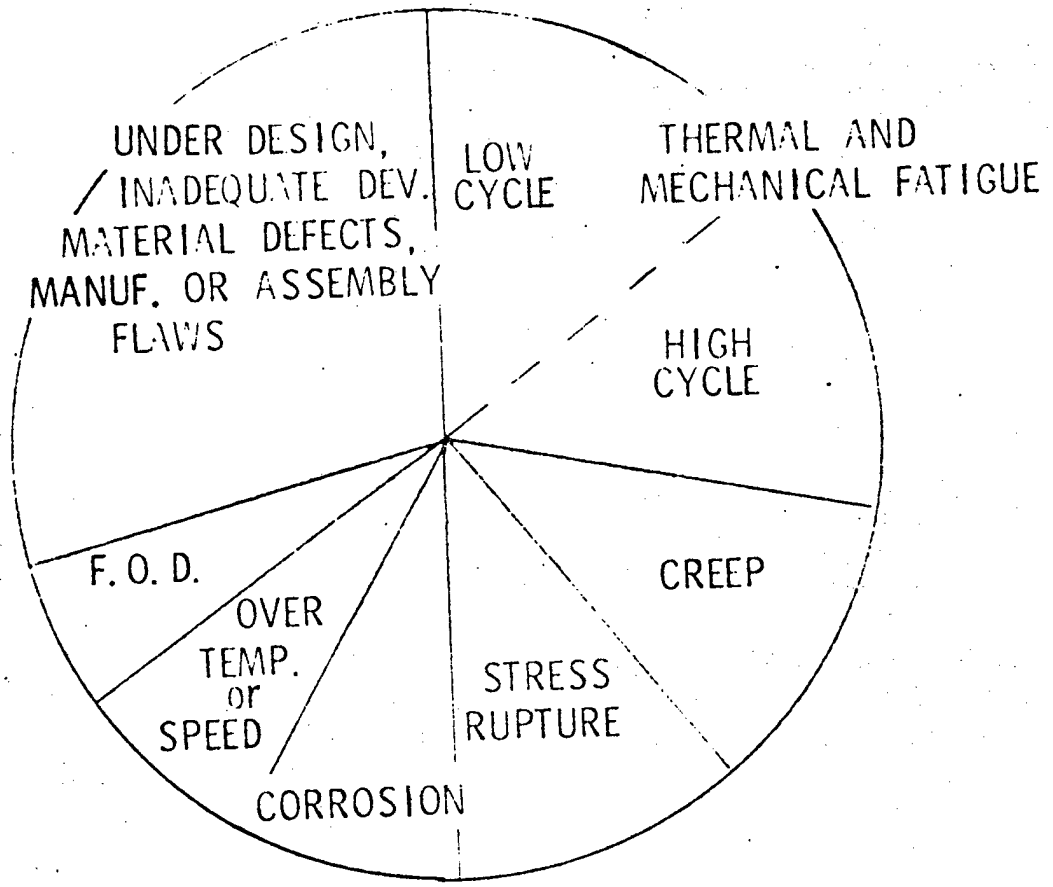

Figure 4

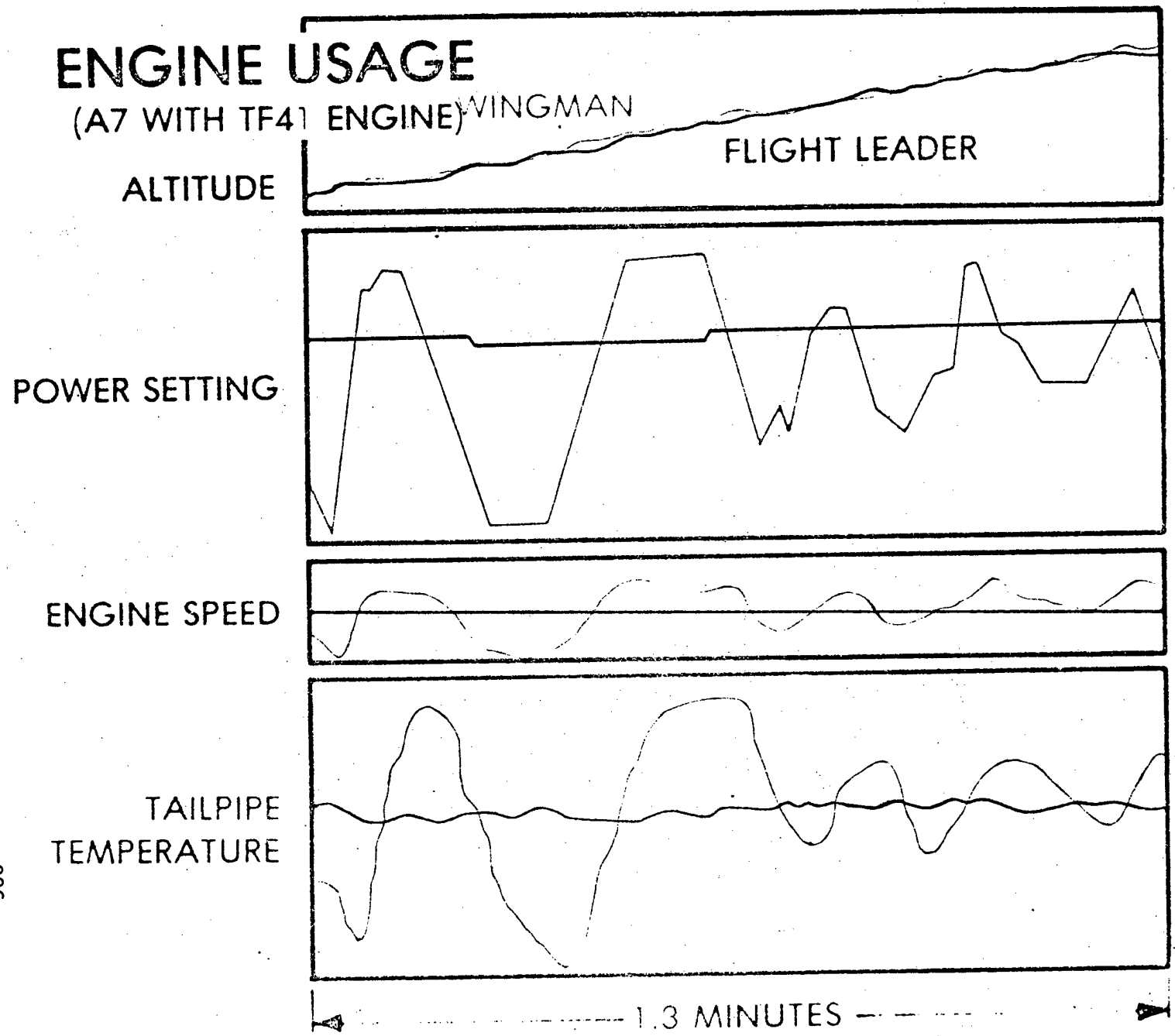
ENGINE USAGE
(A7 WITH TF41 ENGINE)
WINGMAN
FLIGHT LEADER
ALTITUDE
POWER SETTING
ENGINE SPEED
TAILPIPE TEMPERATURE
1.3 MINUTES

Figure 5

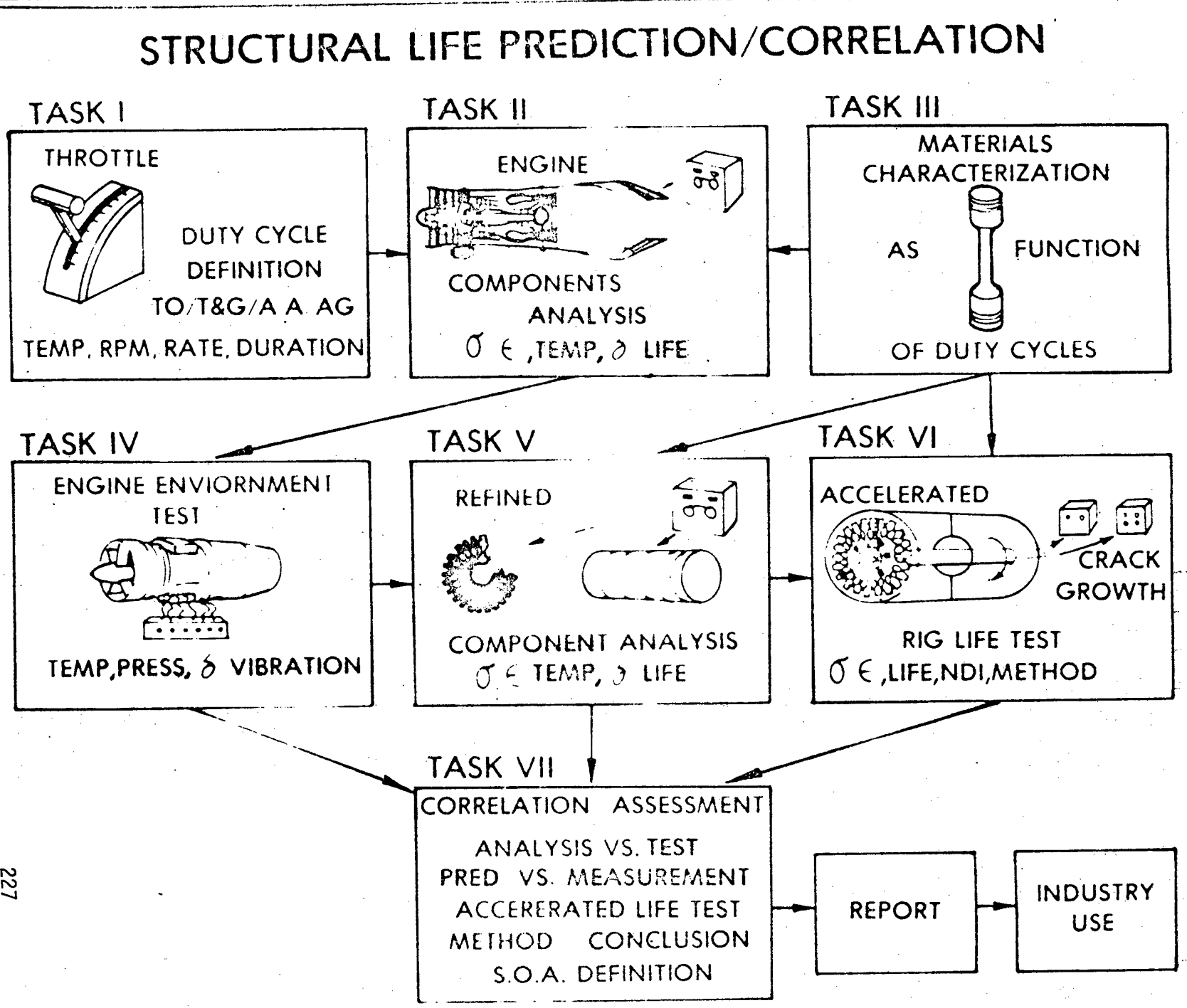
STRUCTURAL LIFE PREDICTION/CORRELATION
TASK I
THROTTLE
DUTY CYCLE DEFINITION
TO/T&G/A A AG
TEMP, RPM, RATE, DURATION
TASK II
ENGINE
COMPONENTS ANALYSIS
σ ε ,TEMP, ∂ LIFE
TASK III
MATERIALS CHARACTERIZATION
AS FUNCTION
OF DUTY CYCLES
TASK IV
ENGINE ENVIORNMENT TEST
TEMP,PRESS, δ VIBRATION
TASK V
REFINED
COMPONENT ANALYSIS
σ ε TEMP, ∂ LIFE
TASK VI
ACCELERATED
CRACK GROWTH
RIG LIFE TEST
σ ε ,LIFE,NDI,METHOD
TASK VII
CORRELATION ASSESSMENT
ANALYSIS VS. TEST
PRED VS. MEASUREMENT
ACCERERATED LIFE TEST
METHOD CONCLUSION
S.O.A. DEFINITION
REPORT
INDUSTRY USE

Figure 6

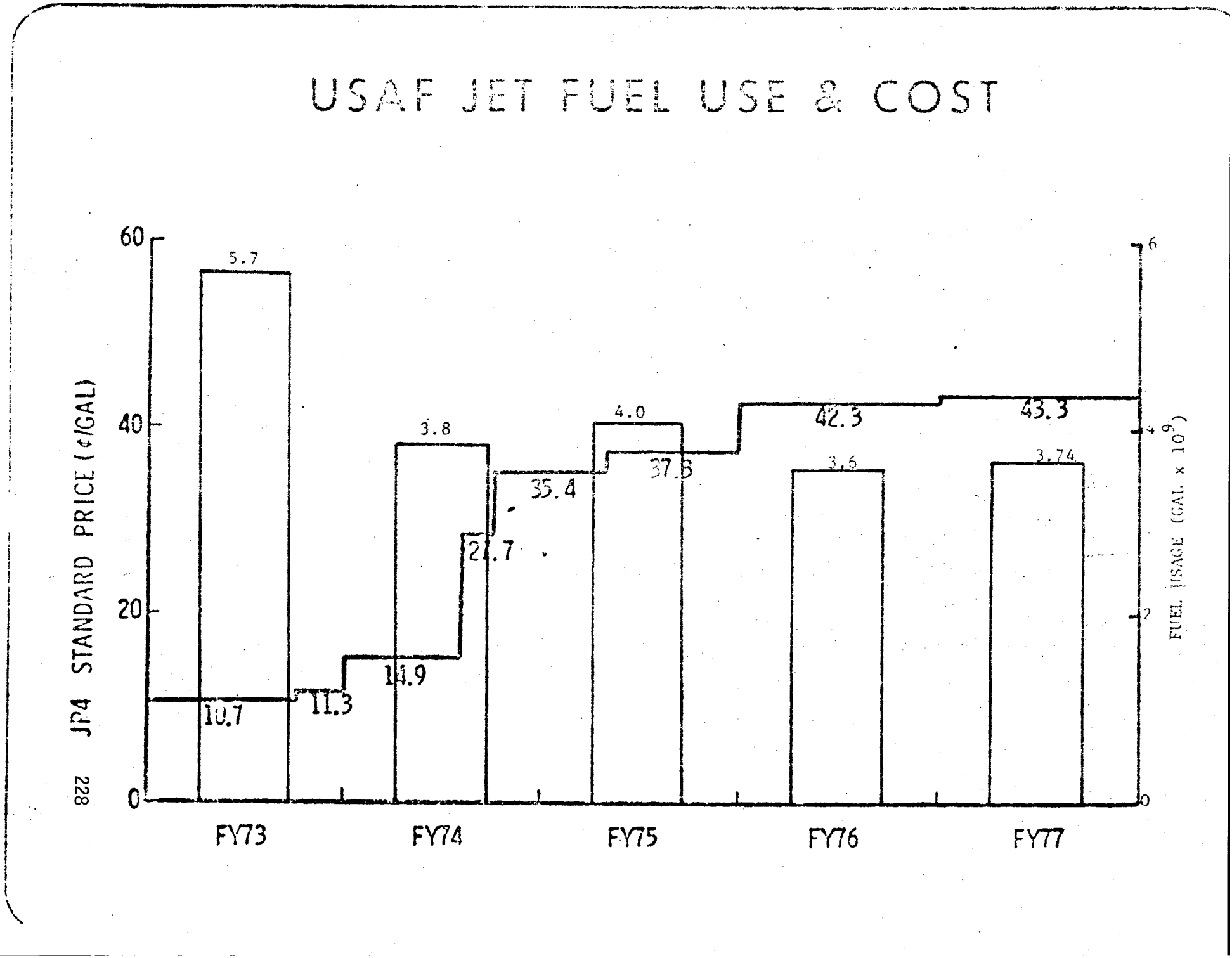
USAF JET FUEL USE & COST
JP4 STANDARD PRICE (¢/GAL)
FUEL USAGE (GAL x 10^9)
60
40
20
0
6
4
2
0
5.7
3.8
4.0
3.6
3.74
10.7
11.3
14.9
21.7
35.4
37.8
42.3
43.3
FY73
FY74
FY75
FY76
FY77

Figure 7

AIR FORCE/INDUSTRY TURBINE ENGINE LCC MODEL

COST ELEMENT	R	A	S	COST ELEMENT	R	A	S
1. Conceptual Study, Cycle and Configuration	X			15. Contractor Field Support	X	X	X
				16. Data	X	X	X
2. Mock-up	X			17. Initial Inventory Management	X	X	
3. Detail Design	X		X				
4. Tooling	X	X		18. Recurring Inventory Management	X		X
5. Engine Manufacturing	X	X	X				
6. Spare Sections Assemblies and Parts	X	X		19. Scheduled Maintenance	X		X
				20. Unscheduled Maintenance	X		X
7. Peculiar Support Equipment	X	X	X	21. Recurring Maintenance Management	X		X
8. Common Support Equipment	X	X					
9. Special Test Equipment	X	X	X	22. System Engineering/ Project Management	X	X	X
10. Packaging and Shipping	X	X	X				
11. Facilities	X	X		23. Petroleum, Oil and Lubrication	X		X
12. Contractor Test	X		X				
13. Government Testing	X		X	24. Production Program Start-up		X	
14. Training	X	X	X				

R - Research Development Test and Evaluation

A - Acquisition

S - Operation and Support

Figure 8

REDUCED COST TURBINE ENGINE CONCEPTS

LIFE CYCLE COST MODEL

COST ELEMENT	R	A	S	COST ELEMENT	R	A	S
1. Conceptual Study, Cycle and Configuration				15. Contractor Field Support			X
				16. Data			
2. Mock-up				17. Initial Inventory Management			
3. Detail Design	X		X				
4. Tooling	X	X		18. Recurring Inventory Management			
5. Engine Manufacturing	X	X	X				
6. Spare Sections Assemblies and Parts	X	X		19. Scheduled Maintenance	X		X
				20. Unscheduled Maintenance			X
7. Peculiar Support Equipment				21. Recurring Maintenance Management			
8. Common Support Equipment							
9. Special Test Equipment	X			22. System Engineering/ Project Management	X		
10. Packaging and Shipping			X				
11. Facilities				23. Petroleum, Oil and Lubrication	X		X
12. Contractor Test	X						
13. Government Testing				24. Production Program Start-up			
14. Training							

R - Research Development Test and Evaluation
A - Acquisition
S - Operation and Support

Figure 9

REDUCED COST TURBINE ENGINE CONCEPTS

LIFE CYCLE COST MODEL

PARAMETRIC (COST ESTIMATING RELATIONSHIPS)

COST = f (THRUST, WEIGHT, ETC.)

ACCOUNTING

$$\text{COST} = \sum_{i=1}^{n} \Big[(\text{LABOR RATE}_i)(\text{MAN-HOURS}_i) + (\text{MATERIAL WEIGHT}_i)(\text{MATERIAL PRICE PER POUND}_i)\Big]$$

n = TOTAL NUMBER OF PARTS

Figure 10

REDUCED COST TURBINE ENGINE CONCEPTS

LIFE CYCLE COST MODEL

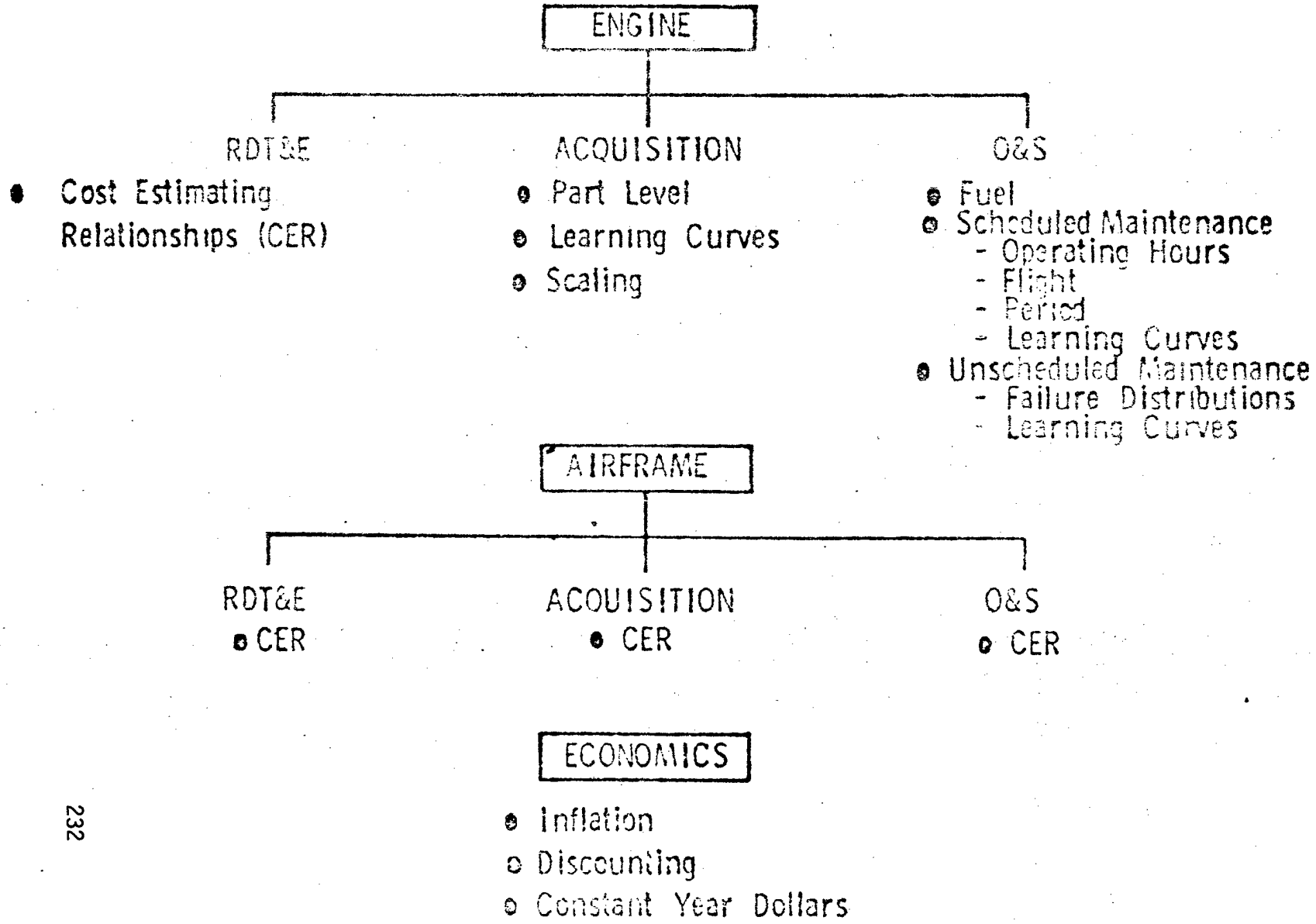

Figure 11

FLIGHT DYNAMICS LABORATORY SYSTEM LIFE CYCLE COST MODEL

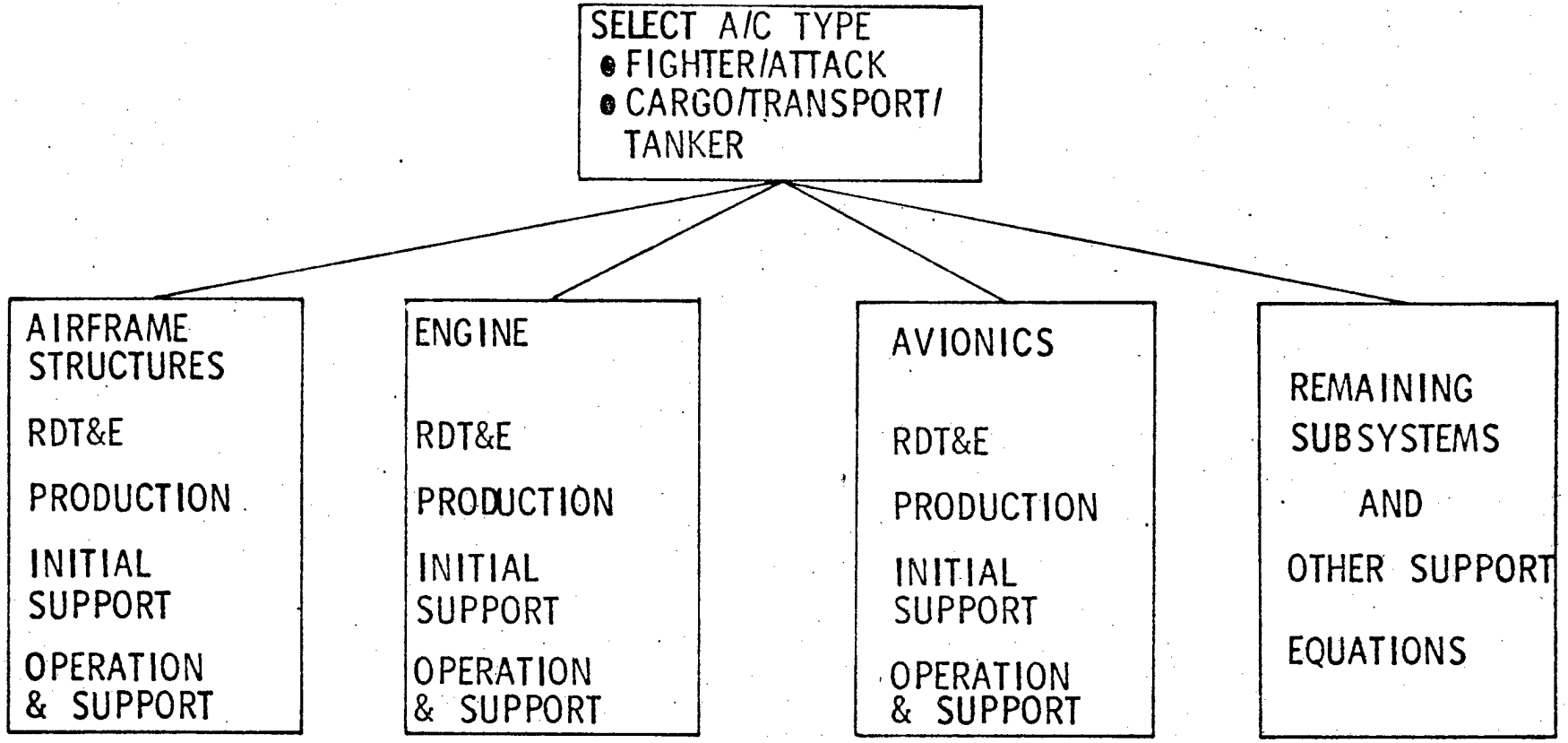

Figure 12

REDUCED COST TURBINE ENGINE CONCEPTS

LIFE CYCLE COST METHODOLOGY

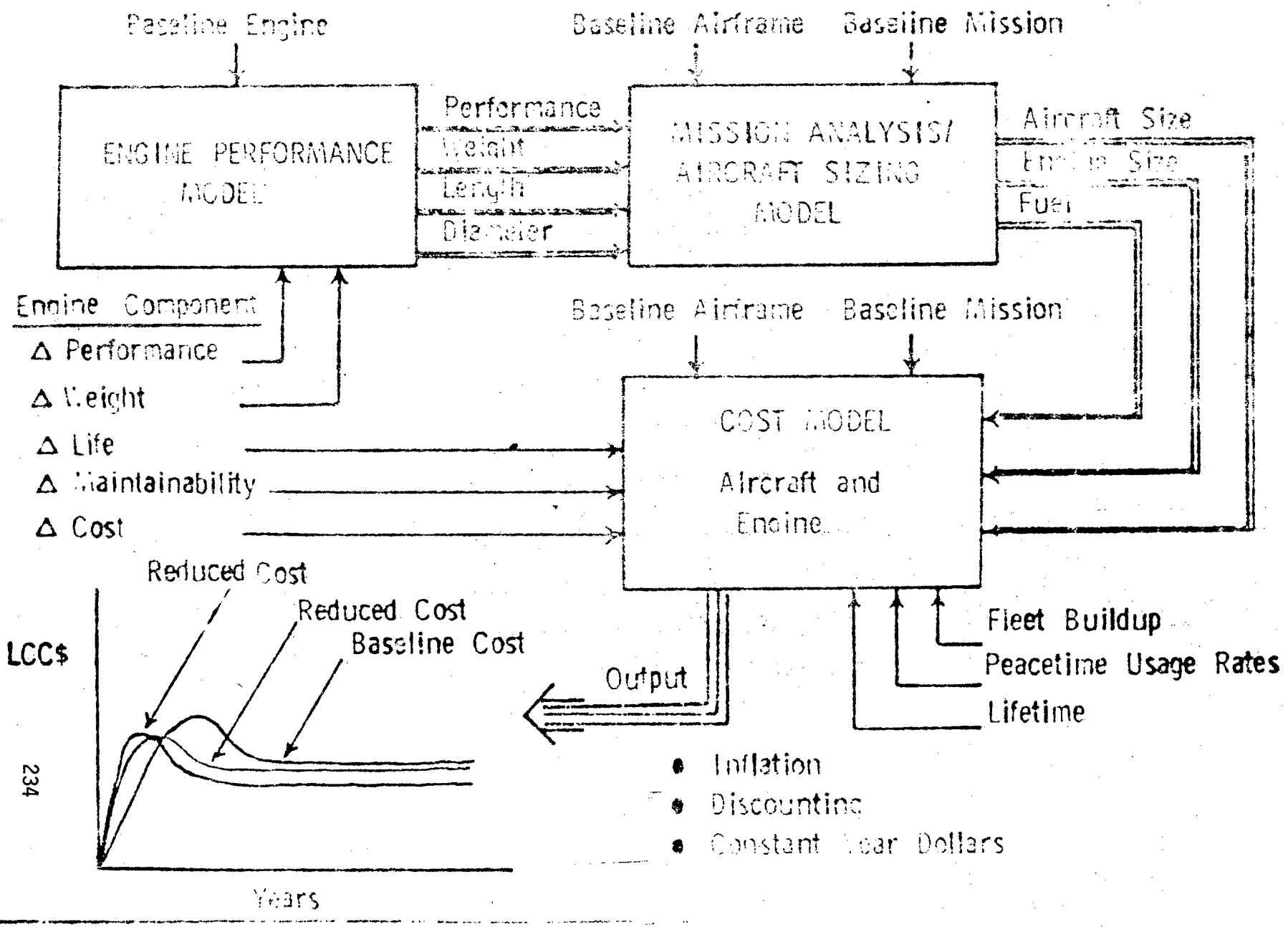

Figure 13

GE23/F1A1 JTDE APPLICATION OF AS-HIP RENE'95 TO HP SPOOL

PART POSITION	PART NAME	PART POSITION	PART NAME	PART POSITION	PART NAME
(A)	BORE VANES	(D)	CDP SEAL	(G)	COMP'R FWD SHAFT
(B)	HPT FWD SHAFT	(E)	STG 6 DISK & COVER	(H)	STGS. 4, 5, 7 & 8 DISKS
(C)	STG 3 DISK	(F)	HPT AFT SHAFT	(I)	HPT FWD FLANGE SUPPORT
				(J)	FORWARD & AFT BLADE RETAINERS

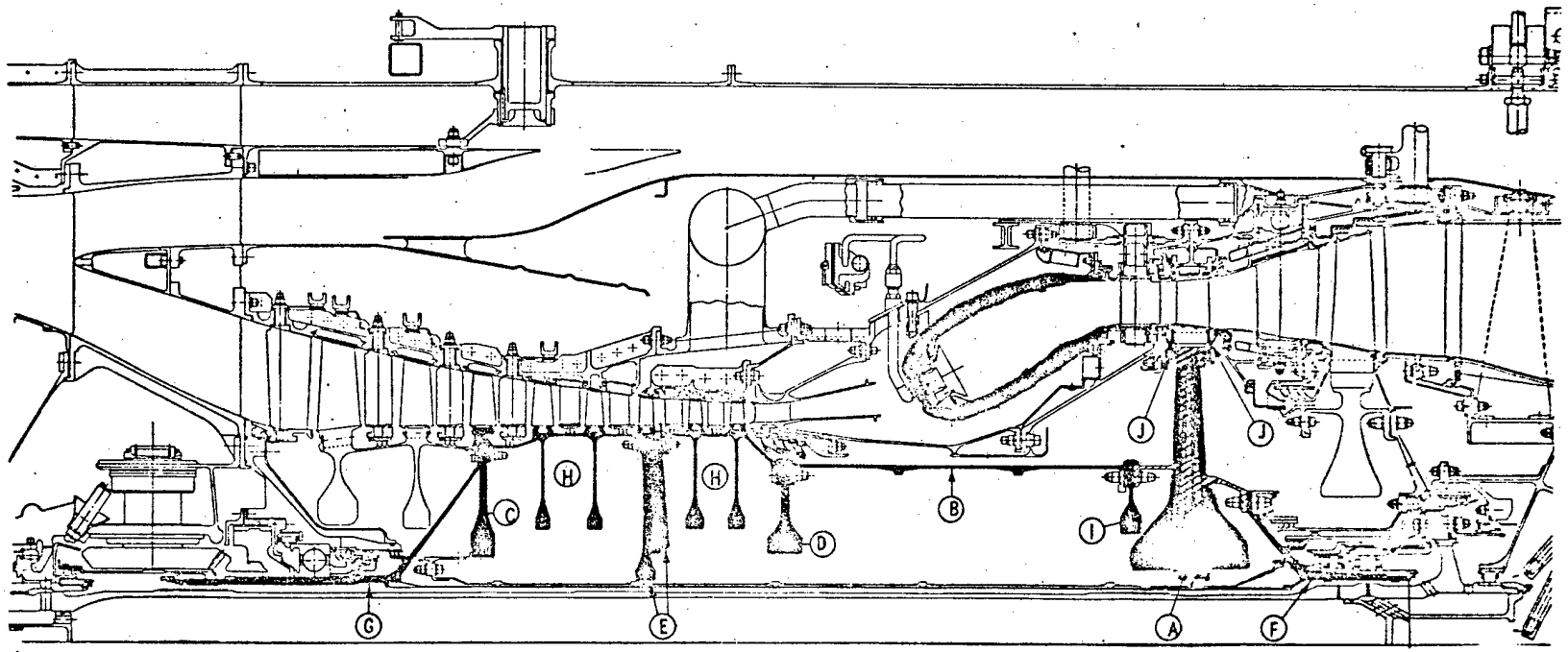

Figure 14

PROCESSING SEQUENCES FOR JTDE COMPRESSOR DISK

HOT ISOSTATIC PRESSING (HIP) RENE'95

(STAGES 7 OR 8)

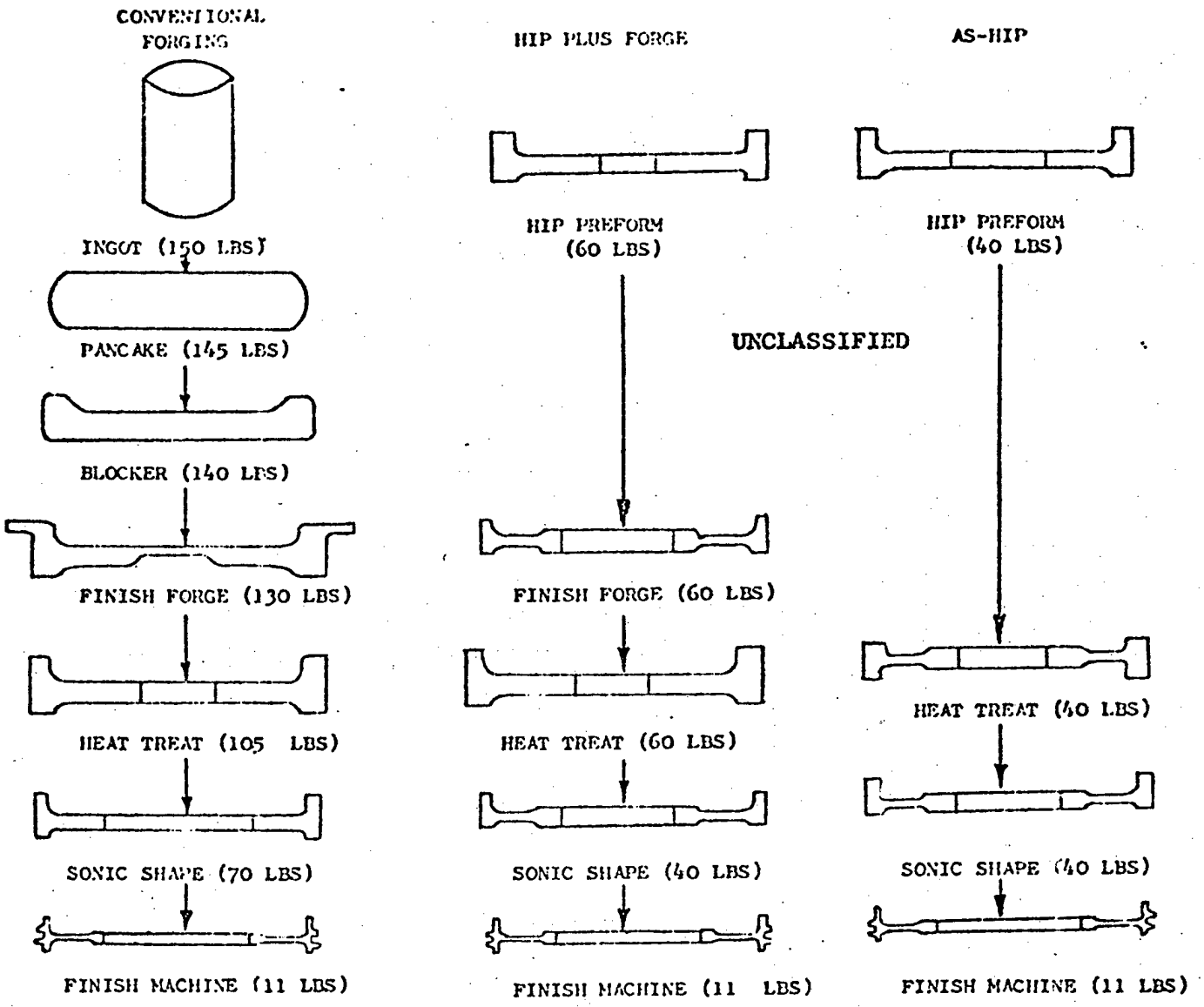

UNCLASSIFIED

Figure 15

AS-HIP RENE 95 HIGH PRESSURE SPOOL LIFE CYCLE COST (LCC) IMPACT IN 1977 DOLLARS

INPUT

OPERATIONAL LIFE = 20 YR
ENGINES/AIRCRAFT = 2

OPERATIONAL AIRCRAFT = 334
UTILIZATION = 300 HRS/YR/AIRCRAFT

	BASELINE SIZE	SCALED SIZE
ENGINE PERFORMANCE	NO IMPACT	NO IMPACT
ENGINE WEIGHT	NO IMPACT	NO IMPACT
ENGINE RELIABILITY/LIFE	NO IMPACT	NO IMPACT
ENGINE MAINTAINABILITY	NO IMPACT	NO IMPACT
ENGINE MANUFACTURING COST	- $ 17,461.00 (250 unit)	- $ 17,461.00 (250 unit)
OUTPUT		
ENGINE RDT&E COST	- $ 1,560,000.00	- $ 1,560,000.00
ENGINE ACQUISITION COST	- $ 33,721,000.00	- $ 33,721,000.00
ENGINE O&S COST	- $ 39,107,000.00	- $ 39,107,000.00
TOTAL WEAPON SYSTEM LCC	- $ 74,388,000.00	- $ 74,388,000.00

Figure 16

TRIPLY LAMILLOY

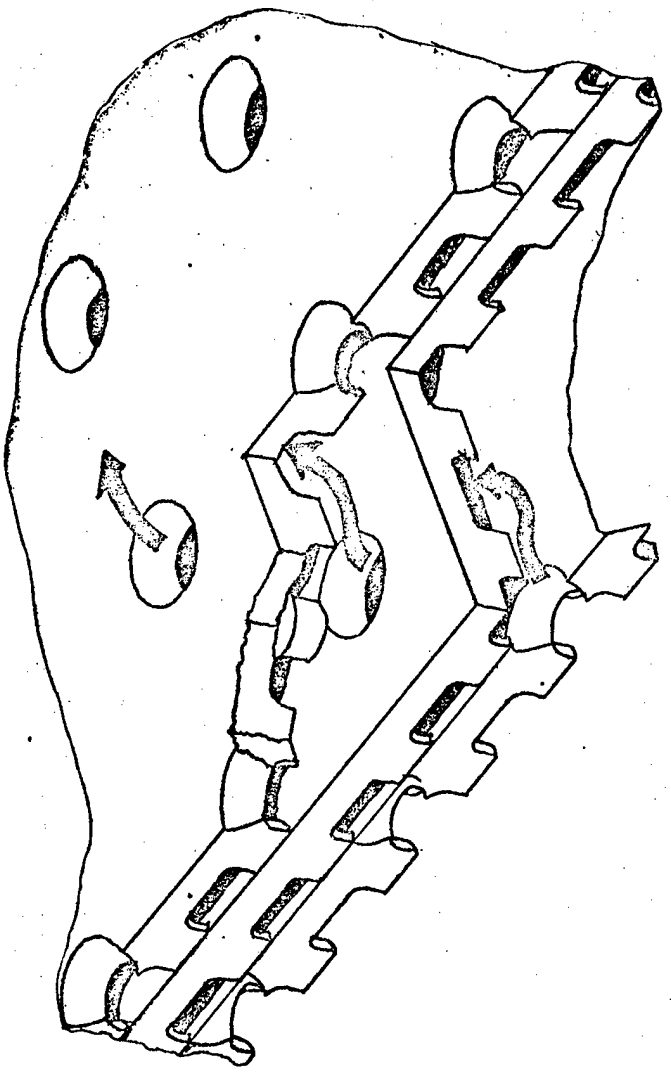

Cooling Air Flow

Figure 17

COMBUSTOR RIG

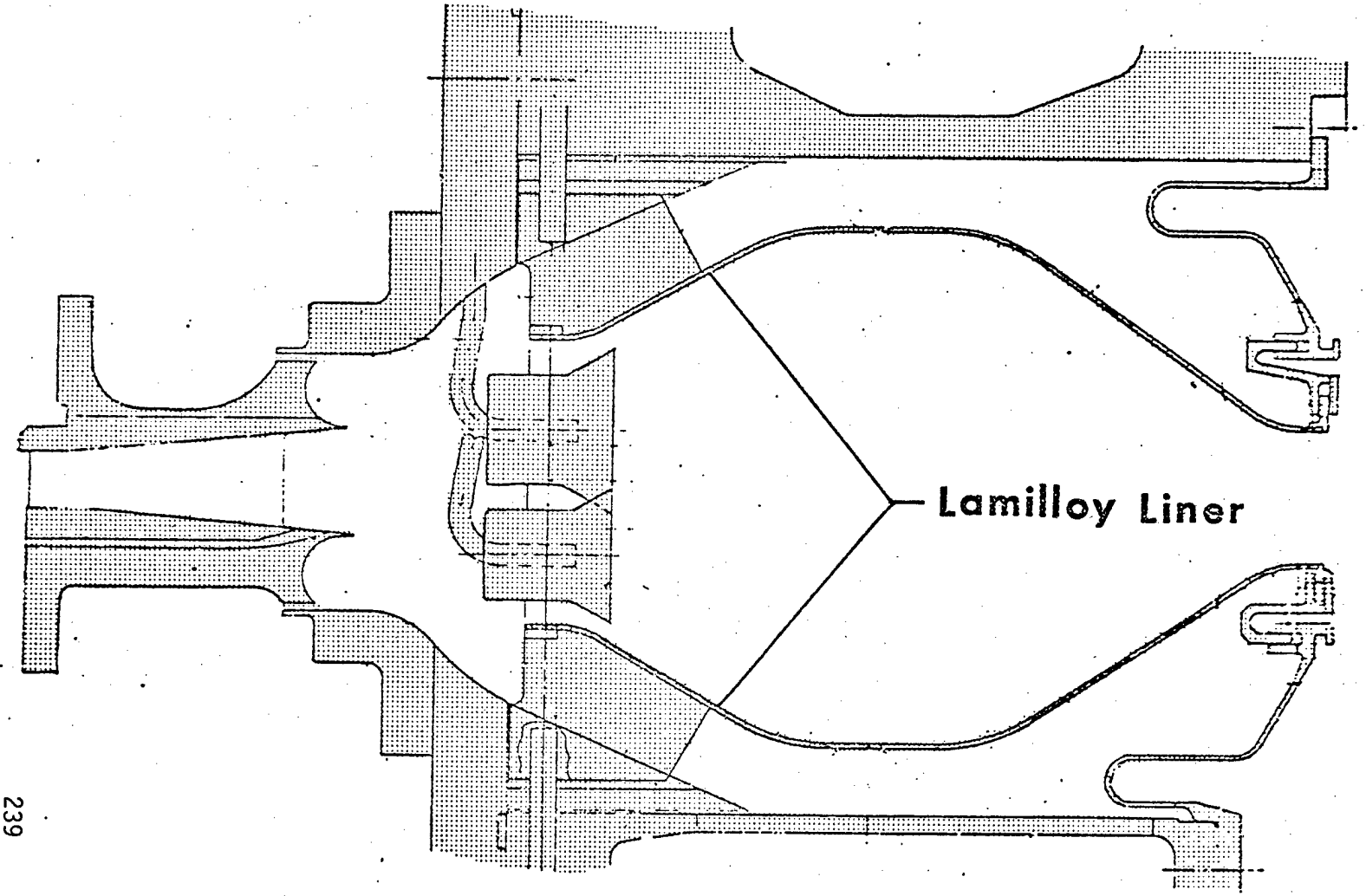

Figure 18

AD6581

Detroit Diesel Allison
Division of General Motors Corporation

LAMILLOY COMBUSTOR LIFE CYCLE COST (LCC) IMPACT IN 1974 DOLLARS

INPUT

OPERATIONAL LIFE = 10 YR
ENGINES/AIRCRAFT = 2

OPERATIONAL AIRCRAFT = 750
UTILIZATION = 300 HRS/YR/AIRCRAFT

	BASELINE SIZE	SCALED SIZE
ENGINE PERFORMANCE	- 27% Cooling Flow	- 3% Airflow
ENGINE WEIGHT	- 17.87 Lb.	- 87.8 Lb.
ENGINE RELIABILITY/LIFE	3x Life	3x Life
ENGINE MAINTAINABILITY	Negligible	Negligible
ENGINE MANUFACTURING COST	- $3,462.00 (Avg. of first 2000 units)	- $ 26,401.00 (Avg. of first 2000 units)

OUTPUT

ENGINE RDT&E COST	- $ 3,300,000.00
ENGINE ACQUISITION COST	- $ 43,000,000.00
ENGINE O&S COST	- $ 24,000,000.00
TOTAL WEAPON SYSTEM LCC	- $251,400,000.00

Figure 19

TELEDYNE CAE

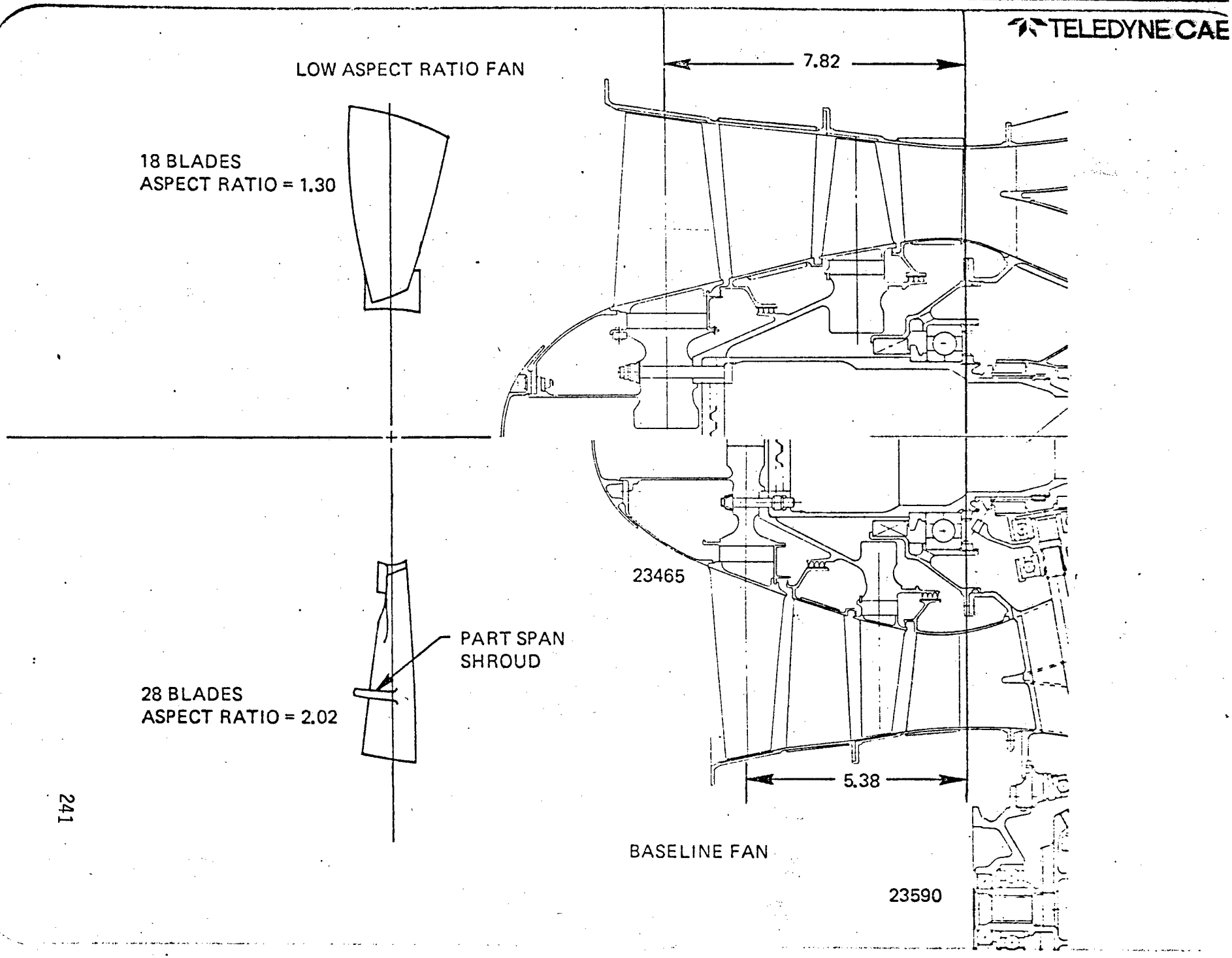

Figure 20

LOW-ASPECT-RATIO FAN LIFE CYCLE COST (LCC) IMPACT IN 1979 DOLLARS

INPUT

OPERATIONAL LIFE = 20 YR
ENGINES/AIRCRAFT = 2

OPERATIONAL AIRCRAFT = 700
UTILIZATION = 1116 HRS/YR/AIRCRAFT

	BASELINE SIZE	SCALED SIZE
ENGINE PERFORMANCE	+4% Thrust -3% SFC	-4% Airflow
ENGINE WEIGHT	+10 Lb.	-14.5 Lb.
ENGINE RELIABILITY/LIFE	+30% MTBF	+30% MTBF
ENGINE MAINTAINABILITY	NO IMPACT	NO IMPACT
ENGINE MANUFACTURING COST	- $ 9,800.00 (Avg. of first 1400 units)	- $ 12,000.00 (Avg. of first 1400 units)

OUTPUT

ENGINE RDT&E COST	NO IMPACT
ENGINE ACQUISITION COST	- $ 18,000,000.00
ENGINE O&S COST	- $ 41,000,000.00
TOTAL WEAPON SYSTEM LCC	- $ 94,000,000.00

Figure 21

GAS GENERATOR CONFIGURATION

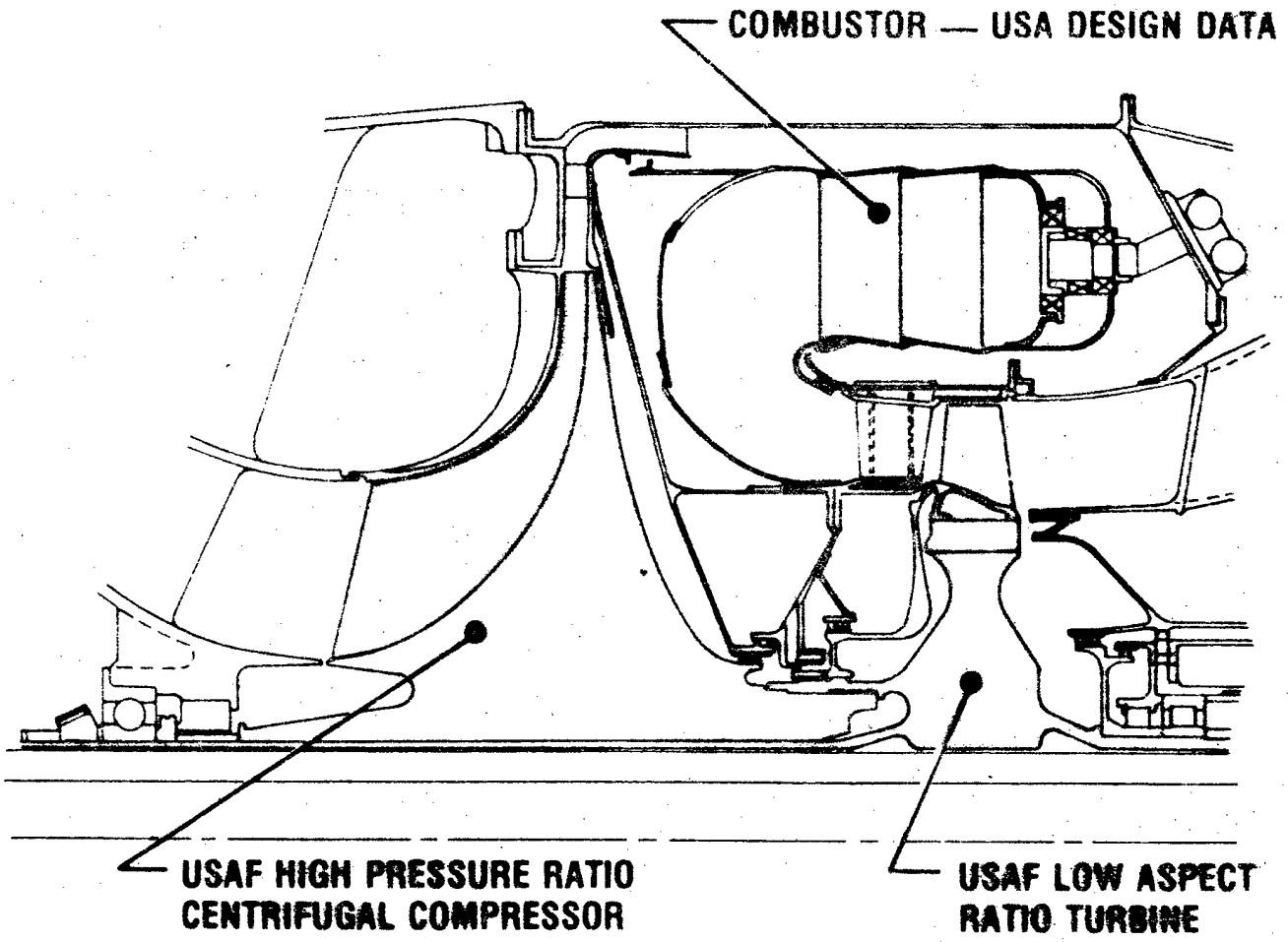

Figure 22

MS 4465-3

LOW-ASPECT-RATIO BLADING FOR HIGH PRESSURE TURBINE LIFE CYCLE COST (LCC) IMPACT IN 1977 DOLLARS

INPUT

OPERATIONAL LIFE = 15 YR
ENGINES/AIRCRAFT = 2

OPERATIONAL AIRCRAFT = 420
UTILIZATION = 300 HRS/YR/AIRCRAFT

	BASELINE SIZE	SCALED SIZE
ENGINE PERFORMANCE	+6.41% Thrust -1.33% SFC	-10.6% Airflow
ENGINE WEIGHT	+7.8 Lb.	-99 Lb.
ENGINE RELIABILITY/LIFE	-10% MTBF	-10% MTBF
ENGINE MAINTAINABILITY	-10% TBO	-10% TBO
ENGINE MANUFACTURING COST	+$2000.00 (Avg. of first 50 units)	-42,000.00 (Avg. of first 50 units)

OUTPUT

ENGINE RDT&E COST	-$ 6,300,000.00
ENGINE ACQUISITION COST	-$34,100,000.00
ENGINE O&S COST	-$ 71,800,000.00
TOTAL WEAPON SYSTEM LCC	-$172,100,000.00

Figure 23

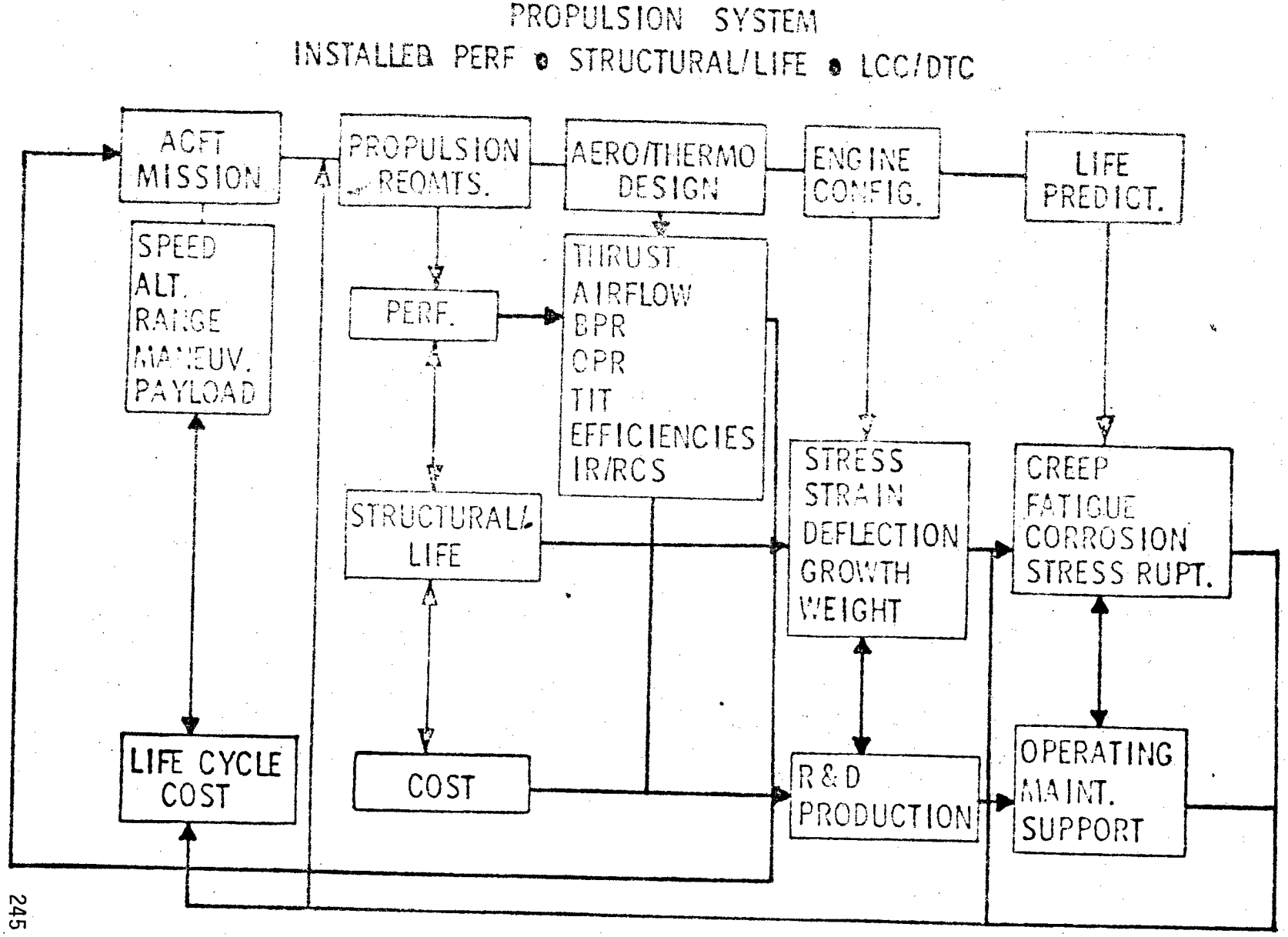
PROPULSION SYSTEM
INSTALLED PERF • STRUCTURAL/LIFE • LCC/DTC
ACFT MISSION
PROPULSION REQMTS.
AERO/THERMO DESIGN
ENGINE CONFIG.
LIFE PREDICT.
SPEED
ALT.
RANGE
MANEUV.
PAYLOAD
PERF.
THRUST
AIRFLOW
BPR
OPR
TIT
EFFICIENCIES
IR/RCS
STRUCTURAL/ LIFE
STRESS
STRAIN
DEFLECTION
GROWTH
WEIGHT
CREEP
FATIGUE
CORROSION
STRESS RUPT.
LIFE CYCLE COST
COST
R&D PRODUCTION
OPERATING
MAINT.
SUPPORT

Figure 24

Biographical Sketch

Robert F. Panella's current position is in the Turbine Engine Division of the Air Force Aero Propulsion Laboratory. He is project manager for the Aircraft Propulsion Subsystem Integration (APSI) Advanced Development program. He is also Laboratory focal point for turbine engine life cycle cost.

Previous assignments in the AF Aero Propulsion Laboratory were staff officer, Plans Office, and project engineer for the Advanced Turbine Engine Gas Generator (ATEGG) program. Other assignments included system program officer, AF Special Project Office, Los Angeles AFS, Calif., and test engineer, AF Rocket Propulsion Laboratory, Edwards AFB, Calif.

Michael A. Barga is in the Turbine Engine Division of the Air Force Aero Propulsion Laboratory. He was on the Acquisition Committee of the Air Force/Industry Working Group. Mr. Barga is currently project engineer on two of the four Aircraft Propulsion Subsystem Integration (APSI), Reduced Cost Turbine Engine Concepts programs. He has worked in the area of turbine engine cost for the previous five years.

Richard G. McNally currently works in the Turbine Engine Division of the Air Force Aero Propulsion Laboratory (AFAPL). He is the project engineer on two of the four Aircraft Propulsion Subsystem Integration (APSI), Reduced Cost Turbine Engine Concepts programs. Mr. McNally started working in the AFAPL in March 1967; since then, he has worked in the following technical areas: airframe inlet integration, mission analysis, ramjet powered missile effectiveness, advanced technology fuels and turbine engine performance simulation. From November 1975 to January 1977, Mr. McNally was collocated in the Productivity, Reliability, Availability, and Maintainability (PRAM) program office, working in the area of turbine engine operation and support cost reduction.

VORBIX AUGMENTATION - AN IMPROVED PERFORMANCE AFTERBURNER FOR TURBOFAN ENGINES

BY

William W. Wagner

Research and Technology Group

Naval Air Propulsion Center
Trenton, New Jersey 08628

Vorbix Augmentation

Abstract

In 1973 the Navy initiated an Exploratory Development program directed at substantially improving the performance and reliability of afterburning turbofan engines. The objective of the program was to investigate the feasibility of a new augmentor which would result in improved system performance and reliability.

Combustion driven instabilities coupled with a characteristic "drop off" in efficiency are inherent limitations in the performance of conventional mixed flow augmentors. The effects are pronounced in the upper left-hand corner of a fighter/interceptor flight envelope where both transient and steady-state operational limits could curtail full use of the aircraft envelope.

The investigation of several innovative designs resulted in a concept identified as the VORBIX (Vortex Burning and Mixing) configuration. A successful rig test program, which included simulated altitude conditions, showed that a VORBIX configuration was intrinsically stable and could result in high, steady (flat) efficiency curves indicative of thrust improvement throughout a typical flight envelope. The program has continued into a full-scale design and evaluation phase with a VORBIX installed on a slave F401 engine. Sea level verification tests have recently been initiated with altitude testing to follow.

The presentation will briefly review the development process to date and include a comprehensive description of the design. The benefits to the Department of Defense (DOD) will be addressed in terms of operational effectiveness, reduced complexity, the potential for reduced length propulsion systems and Survivability/Vulnerability (S/V) improvement.

Introduction

The afterburner was proven in early turbojet engine development as a reliable and systems effective device for thrust augmentation as required to perform advanced portions of the DOD mission. Developmental problems associated with afterburner performance, reliability, and durability were to a large extent satisfactorily resolved through "cut-and-try" fixes. The stiffest challenge, and perhaps the largest effort, was directed at "screech" elimination. Screech, a high frequency acoustical instability which once encountered rapidly leads to catastrophic effects, was and is today resolved by afterburner liner acoustical oscillation damping patterns. Fundamentally, the afterburner attachment to a turbojet engine was a sound concept from a combustion standpoint, since hot vitiated gas and relatively constant inlet conditions are conducive to good fuel vaporization, ignition characteristics, and efficient burning.

With the advent of the mixed-flow augmentor in turbofan engines, development problems increased significantly. There remained the problems common to any afterburner development; i.e., screech elimination, flameholder and liner durability, and the "last component" syndrome; however, in addition, fundamental problems relating to ignition, flame stability and propagation, and combustion efficiency were readily apparent. To initiate the design of a mixed-flow augmentor, heady assumptions must be made as to the probable inlet conditions at an arbitrary mix-and-match plane. Often through engine development, the assumed pressure profile and velocity (for both the core and fan bypass) change significantly leading to poorer efficiency than predicted, unreliable ignition, and combustion driven instability. In essence, the aerothermal design and resultant chemical kinetics reaction is now farther removed from the more common design practice which was established with primary combustors and was extended to early afterburners. Characteristics of the conventional augmentor design and their specific problems will now be addressed followed by a description of the VORBIX design.

Conventional Design

The typical mixed-flow augmentor today is comprised of bluff-body flameholding devices in varying locations downstream of a low pressure turbine and diffusing section.

The flameholders or V-gutters consist of a series of circumferential and radial bluff-body blockages which serve to create low pressure regions relative to adjacent streamlines in which combustion is initiated and stabilized. Additionally, radial V-gutters aid in transverse flame propagation from the core outwards through the fan stream constituent. At various distances upstream of the flameholders, fuel is introduced through a series of circumferential fuel rings or radial fuel spray bars. The fuel distribution is dependent on geometry effects, flameholder location, radial pressure gradients, and combustion stability and efficiency results. Usually the pattern of fuel distribution is continually tailored in an attempt to achieve the overall design goals. The major or fundamental problems associated with the conventional design can include the following:

Fuel Vaporization. Any fuel must be sufficiently vaporized for reliable ignition characteristics and stable and efficient burning. Since spray rings are positioned in a relatively large cross-sectional area with large differences in inlet conditions, multi-phase fuel sources, i.e., combinations of liquid and vapor are generated. Insufficient residence time, adverse pressure and temperature conditions, and unsheared large fuel droplets result in inefficient burning and combustion-driven instabilities due to a non-uniform stoichiometric profile.

Flameholder Geometry. The geometry of the flameholder exerts the greatest influence on flame stability and yet, from a fluid dynamics standpoint, the geometry is optimized for a single-point design. Early turbulence studies resulted in a widely accepted flat plate theory which, simply stated, relates an ideal quench dimension to the minimum distance (flameholder width) which will support steady flame. The optimum width of a V-gutter from a stability standpoint is a strong function of approach pressure (altitude) and therefore, the design is compromised when operated over a wide envelope. In addition to this fundamental concern, inevitably the solidity, width, and positioning of the flameholders are modified/tailored in the final stages of development to optimize the tradeoff in augmentor pressure loss and durability versus "rumble" characteristics.

Development Cost. The time and cost to develop the afterburner has become a major consideration and often a stumbling block to meeting QT development schedule. Engine simulators and full-scale test rigs are utilized

for early augmentor development experience. Yet, often the developed performance and resulting durability predictions are not demonstrated in later engine performance and endurance testing prior to PFRT. Recent DOD engine development experience documents extensive, dedicated altitude test programs in an attempt to improve upper-left hand corner (ULHC) operational capability, eliminate rumble from the air combat maneuver (ACM) area, and establish acceptable steady-state performance and durability.

Engine Stall. The augmentor is a contributing factor in a variety of engine stalls in today's fighter/air superiority aircraft. The two primary categories are transient (light-off) stalls in the ULHC which restrict transient operation to intermediate power levels and fuel scheduling (retard stalls) related to multi-zone fuel introduction.

These problems have been encountered in various degrees in all afterburning tubofan engines; e.g., TF30, F100, F101, F404, and RB-199 engines. I believe that it is a fair assessment that if any one mixed-flow afterburner has performed better or more reliably, or demonstrated expanded operational capability in any of the above systems, it is probably not due to a more sophisticated design practice or better understanding of the physical processes involved.

New Approaches

In 1973, the Navy initiated an Exploratory Development program directed at substantially improving the performance, reliability, and operational effectiveness of turbofan augmentors. Advanced military propulsion systems require reliable and efficient thrust augmentation for acceleration, maneuvering, and supersonic flight. To this end, the controlling parameters which effect rapid, efficient combustion at near-stoichioimetric conditions were evaluated in terms of conventional design improvement and several totally new approaches. Acknowledging that mixed-flow augmentation presented unique problems not experienced in main combustors or turbojet afterburners, NAPC chose a piloted design in an attempt to desensitize the augmentor from the cold, low pressure fan stream. The pilot would perform much the same as the primary zone of a main combustor; i.e., to create a low velocity (sufficient residence) region to ignite and stabilize a combustion reaction. Non-uniform fuel distribution and poor fuel vaporization would be circumvented by injecting all of the fuel flow into the pilot. The incorporation of strong

mixing elements or turbulence generators would control the rate of chemical reaction by means of gaseous diffusion burning. Should rapid mixing and burning take place simultaneously, a secondary benefit would be a significant reduction in the total length required for conventional augmentors. The early experimental work was conducted by PWA under Navy cognizance and resulted in the Vortex Burning and Mixing (VORBIX) concept.

To guide the early efforts, the TF30-P-412 augmentor was chosen as a baseline configuration from which to compare new or modified designs. Improving the performance of the more conventional bluff-body flameholder designs proved futile with marginal performance gains. Other more novel approaches such as burning around a vane, termed the vaned cascade concept, were pursued through experimental evaluations but were eventually discarded as candidates either due to excessively high dry pressure loss levels, poor combustion efficiency, or inherent life limiting concerns. A complete discussion as to the feasibility of the VORBIX and other approaches is contained in Reference 1.

The VORBIX Concept matured through several modifications and resulted in a most promising hardware configuration which will be further developed in an altitude test cell at NAPC during the coming year.

Description of the VORBIX Augmentor

The VORBIX design is a unique approach which has been demonstrated through component rig and engine sea level testing and offers potential to enhance turbofan augmentation operation and performance with good system stability. Figure 1 is a cross-sectional view of a representative VORBIX augmentor installed in a turbofan engine. Excellent ignition and stability characteristics are generated as a result of the pilot burner. The inlet conditions to the pilot are supplied solely by the core discharge gas, as seen in Figure 1. Thus, desensitization from the colder fan bypass stream is accomplished, at least as it effects ignition and combustion stability. The pilot is in fact performing the role of the primary zone in a main burner; i.e., it sees steady, relatively constant inlet conditions throughout the flight envelope and the pilot F/A ratio can be easily modulated to prevent lean blowout at high altitude. The velocity within the pilot is reduced to an acceptable level for residence time as occurs in a main burner. External to the pilot and found in both the core and fan streams are turbulence or vortex generators.

Both swept and delta wings of various wing angles, including compound angles, were evaluated for experimental data. In the case of a wing, vortices are created as the flow separates off the tips of each wing. To control mixing strength both the solidity (wing density) and angle of attack were varied. In addition to the wings, mechanical swirlers (not unlike swirlers in the dome of a main burner) were installed and evaluated. The mixing strength was determined as a function of solidity, swirl vane angle, and exit diffuser area ratio. Fuel is introduced through two zones. The pilot fuel is injected at the inlet of the pilot to establish ignition characteristics and once ignited, to maintain the flame (stability). The remainder of the fuel is also injected into the pilot farther downstream where it is then vaporized prior to mixing with the core and bypass streams.

Fundamentals of the VORBIX Concept

Dr. Richard Reilly best described the physical/chemical process in Reference 2. "Figure 2 shows in schematic form the high-rate mixing and burning mechanisms of VORBIX combustion. The swirling jets enter the main augmentor region and interact with the hot fuel-rich pilot exhaust stream. The characteristic radius of the swirling jets is approximately one-tenth that of the duct radius employed in simple annular duct burning. Since the swirl field strengh is proportional to V_t^2/r the net result is a substantial reduction in local spin levels relative to an annular swirl combustor, with a corresponding reduction in associated pressure losses.

Each of the swirling jets grows in size in the downstream passage. The hot, vaporized fuel-rich pilot discharge reacts with the outer radius of each swirling jet in the classical Rayleigh mode in that a dense fluid medium of high angular momentum is located radially inside a hotter, less dense fluid having little or no angular momentum. Consequently, the hot fuel-rich gases are accelerated toward the center of the swirling jet with a high rate of mixing and burning occurring as the hot gases spiral toward the center of the swirling jets as a result of the buoyancy forces, while agglomerates of the combustion air jets are centrifuged into the surrounding mixture. Experimental evidence indicates that, when properly applied, this centrifugal instability phenomenon can have a profound effect on mixing and combustion processes.

The vortex system is comprised of pairs of swirling jets of equal and opposite rotation. These pairs then intermix in the downstream duct, resulting in no net residual swirl in the discharge nozzle.

Since the combustion process in the augmentor combustion zone is of a spontaneous type, conventional flameholding devices with flow recirculation are not required to maintain combustion. In the absence of these deliberately induced regions of slow recirculation, residence time control must be maintained by selection of appropriate bulk velocities and the axial length of the combustor.

Because of the autoignition, diffusion-flame nature of the combustion process in the augmentor, stable combustion is effected from pilot-alone operation through the complete range of secondary fuel flow. From soft pulse lights of the pilot-alone operation, the thrust is continuously modulated up to the maximum level by progressively increasing the amount of secondary fuel injected into the hot pilot exhaust."

Experimental Evaluation

A full-scale test rig was modified into a 45° sector of the TF30-P-412 augmentor which was to be the datum for all experimental evaluations. Actual -P-412 augmentor inlet conditions were supplied to the test rig to simulate both real engine sea level and altitude operation. Since the VORBIX configuration consists of a series of coupled and counter-rotating vortices without a net residual vorticity and since rumble is characteristically a longitudinal mode of instability, the sector rig was judged acceptable for candidate feasibility studies. The goals of the program were as follows:

- 90% Combustion efficiency
  - a flat efficiency curve throughout the F/A operating range
- 4.0% cold pressure loss
- 50% reduction in length
  - compared to the -P-412 configuration
- Rumble-free operation throughout the operating range

- Uniform exit temperature profile - indicative of I.R. reduction potential

A total of twenty configurations were evaluated, which included swept wing and delta wing vortex generators, mechanical swirlers in both fan and core streams, combinations of wings and mechanical swirlers, fuel flow variations between pilot and secondary, and pilot size (volume) variation. A complete description of the test results are included in Reference 1. To summarize the results of the test rig feasibility evaluations; rumble was not encountered in any of the test configurations, several VORBIX configurations were successfully tested (greater than 90% η_c) at a 60% length reduction, the measured exit temperature profile of each configuration showed improvement over the bill-of-material baseline. Combustion efficiency ranged from 60% to 98% (configuration dependent) and the measured pressure loss ranged from 3.0% to 6.0%. In general, mechanical swirlers presented a higher level of combustion efficiency through better mixing (stronger, more developed vortices) but the cold pressure loss tended to be higher also. Conversely, the swept and delta wing configurations resulted in a lower cold loss and an attendant lower efficiency. Late in the program, the size of the pilot was reduced since it also contributes to the total pressure loss. The primary criterion effecting pilot size is a function of the volume needed to energize (vaporize) the complete range of secondary fuel. The most promising design resulting from the experimental program was a hybrid VORBIX configuration consisting of a pilot sized to accept 6% to 10% of the total airflow, mechanical swirlers to generate mixing in the fan stream and delta wings in the core stream. This hybrid configuration as tested met the performance goals of the program. The configuration as adapted to a F401 turbofan engine is shown in Figure 3.

"Rumble" and its Effects

As mentioned in the Introduction, a type of low frequency instability known as rumble has become a serious problem in mixed-flow afterburners. Rumble is a periodic afterburning combustion-driven instability occurring mainly at high fuel/air (F/A) ratios, combined with flight Mach numbers and altitudes which yield low inlet air temperatures and pressures. Thus, rumble is encountered on the left side of a flight envelope extending to the ULHC. The predominant region for susceptibility is in or very near

to the air combat manuever region of the envelope. Rumble can lead to afterburner stall and blowout and/or fan surge and engine stall. The frequency of oscillation is unpredictable but usually lies between 30 and 100 hz. Its behavior often is not repeatable indicating that a potential chemical combustion problem is reacting with the fan duct airflow dynamics. The VORBIX augmentor, rumble-free to date, utilizes a bulkhead with mechanical swirlers at the interface of the fan duct and afterburner duct and in fact provides an impedance which serves to isolate the fan duct from the augmentor, essentially decoupling the system from the standpoint of a longitudinal pressure wave.

The low fan duct inlet temperatures and pressures associated with the operating regime of mixed-flow augmentor engines produce a F/A mixture that is difficult to burn. For example, at an inlet condition of 200°F and 14.7 psia, the ratio of the mass of fuel vapor to the mass of dry air is below the combustible F/A ratio limit. Thus to burn the mixture, heat must be added to increase the fuel vapor concentration to a volume above the lean limit. This aspect of the problem is eliminated in the VORBIX design with the positioning of the pilot in the core stream. By design, fuel is fully vaporized in the pilot prior to mixing with cold, low pressure fan air.

VORBIX Full-Scale Design and Fabrication

In order to fully evaluate the VORBIX augmentor for performance gains and overall system effectiveness, a contract was awarded to PWA for a flight-type design and fabrication. The VORBIX was sized to be compatible with a F401 turbofan engine for subsequent altitude exploration at NAPC. The critical design points are shown in Figure 4. Sea level static is the aerothermal design point at which the maximum temperature rise across the augmentor occurs. This point sizes the combustion chamber (length and diameter). Sea level, Mn 0.5, was chosen as the structural design point for the prototype augmentor. Sea level, Mn 1.2, is the aerodynamic loading point at which the maximum fuel system flow limit occurs. Altitude stability checkout is shown at 60K feet/Mn 0.8, a point at which the minimum augmentor inlet temperature and pressure is expected as well as the fuel system minimum flow limit. Two cooling design points are shown at 65K feet/Mn 2.4 and 40K feet/Mn 2.4. Both points experience maximum augmentor inlet temperature and pressure with the 65K feet

point experiencing the maximum case temperature and the 40K feet point experiencing the maximum liner temperature.

The F401/VORBIX configuration will be controlled by a breadboard full-authority electronic control system both during a sea level functional checkout and altitude testing at NAPC. The test stand schematic is shown in Figure 5. The electronic control was required to facilitate the test program. It will allow flexibility to program on-line changes to the augmentor fuel flow and nozzle area (A_j) scheduling. Control parameters are transmitted to on-stand automated data recording (ADR) equipment. Additionally, the control offers latitude in the development of transient time capability without necessitating hardware changes. The intermediate-to-maximum transient goals are five seconds at SLS and ten seconds at 50K/0.8 for the prototype augmentor. The altitude exploratory test program will be initiated during FY79. Table I shows a NAPC preliminary test schedule. The test points are sequentially scheduled to facilitate test cell operating conditions. As seen in Table I, two constant Mach number climbs are scheduled to establish steady-state blowout and transient limits in the ULHC. Selecting Mn 0.6 and Mn 0.8 will also permit a thorough evaluation of what is typically a rumble map. Additional steady-state points were incorporated to document thrust augmentation improvement resulting from increased combustion efficiency.

Conclusions

The VORBIX augmentation system is a new and unique concept which could eliminate many of the recognized deficiencies currently found in conventional mixed-flow augmentors while improving operational performance consistent with tomorrow's advanced weapons systems requirements. The VORBIX augmentor has demonstrated rapid and smooth transient operation from pilot ignition through a F/A ratio of 0.05 (close to stoichiometric). Smooth transient operation is a major accomplishment and is rarely found in the early development stage of a new augmentor. Pressure spikes at ignition which can lead to fan surge in conventional designs are kept within allowable limits in the VORBIX design. The continuous introduction of secondary fuel as opposed to discreet zoning permits higher efficiency at partial augmentation and thus an improvement in cruise performance. Stable combustion, as a result of the pilot feature, insures maximum aircraft acceleration

to the upper F/A ratio limit. Some of today's systems utilize controlled fuel flow restrictions in parts of the flight envelope in an attempt to minimize A/B blowout and engine stall - this is not necessary with the VORBIX design.

Complete fuel vaporization in the VORBIX configuration solves two very significant problems found in today's development process. First, the time and cost required to satisfactorily develop the component should be minimized significantly. Stable, efficient combustion is inherent in the design, and as such should preclude extensive cut-and-try development testing. Secondly, pilot fuel vaporization eliminates the problems associated with cold stream ignition and flame propagation.

In addition to the performance and operational improvement already verified with the VORBIX design, other potential system payoffs include reduced acquisition cost and improved life cycle costs, reduced length, improved durability, reduced engine stall associated with augmentor operation, and reduced IR signature.

The major cost savings is anticipated to be in the less complex fuel system. Should a cost reduction be realized in the fuel system, it would then also include a cost savings in the control system. This cost reduction could be significant if based on a hydromechanical control.

A 60% augmentor length reduction has been demonstrated in a sector rig, and if verified in actual engine operation, could prove very beneficial to future military aircraft, particularly V/STOL and other vectored thrust requirements.

Improvements in durability and a reduction in maintenance time is predicted since flameholders and V-gutters are not required in the VORBIX configuration. The number of sprayrings are reduced and the metal temperature of the liner is reduced.

Reliable augmentor lightoff conditions and smoothly modulated fuel introduction will minimize augmentor related engine stalls.

Initial infrared plume measurements show a potential reduction of up to 50% in the total unaugmented plume signature as the result of improved mixing. A complete infrared survey is planned upon completion of the altitude exploration test.

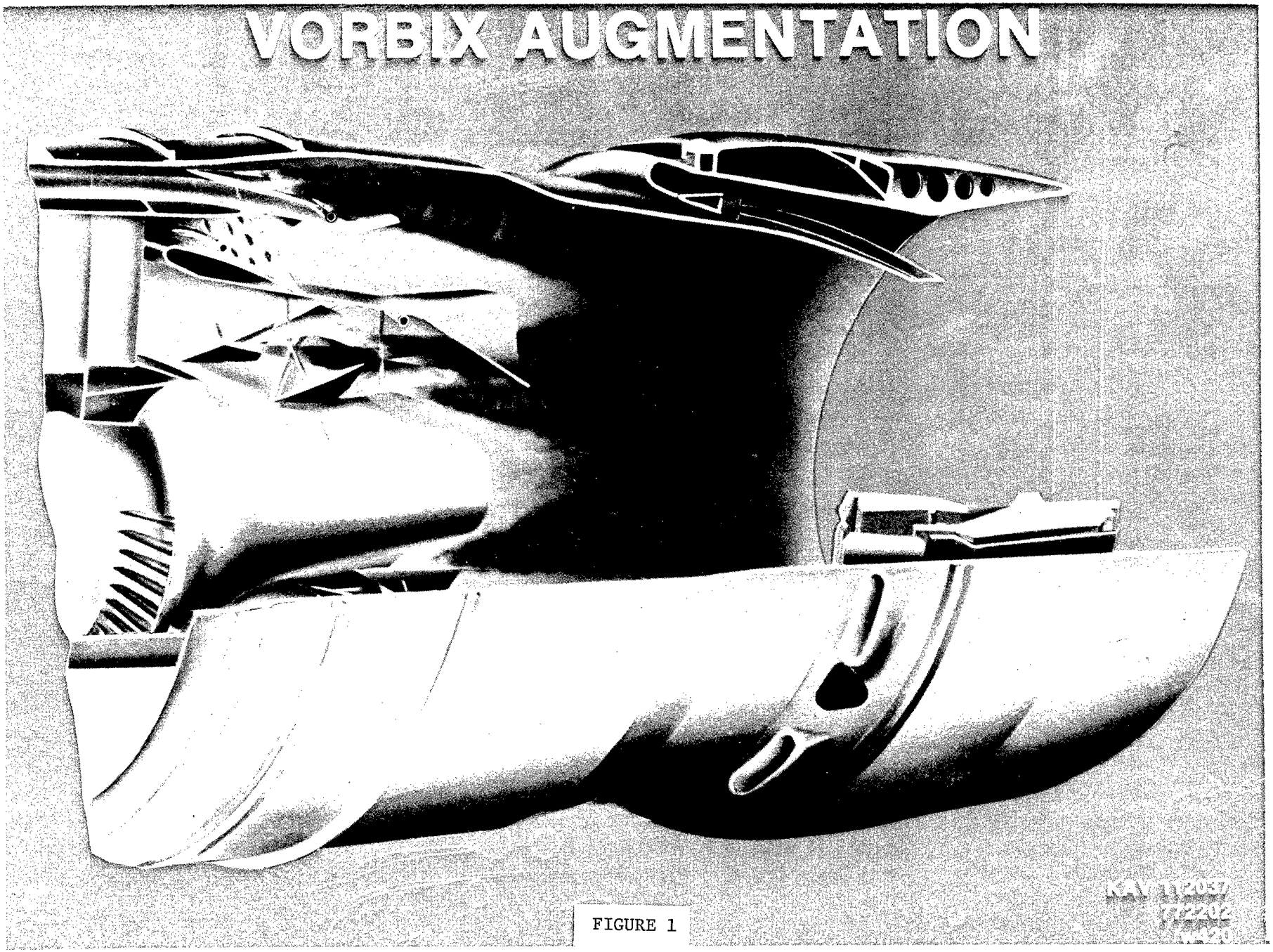

FIGURE 1

Acknowledgment

The author wishes to acknowledge the assistance and helpful suggestions of Dr. R. S. Reilly and Mr. J. P. Rusnak of Pratt and Whitney Aircraft, Government Products Division.

References

1. Reilly, R. S. and Smith, R. D. C., "Advanced Augmentation System," PWA-5261, prepared under Contract No. N0019-72-C-0612, Naval Air Propulsion Center, Trenton, New Jersey, September 1975.

2. Reilly, R. S. and Markowski, S. J., "Vortex Burning and Mixing Augmentation System," AIAA Paper No. 76-678, July 1976.

FUNDAMENTALS OF SWIRL COMBUSTION

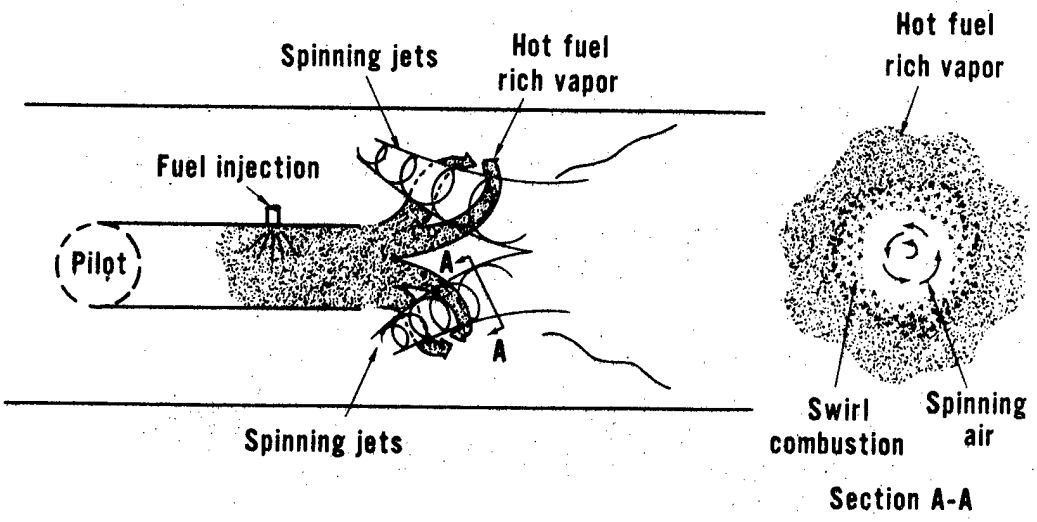

FIGURE 2

J13648-2
760704

YF401-PW-400(II)
VORBIX AUGMENTOR

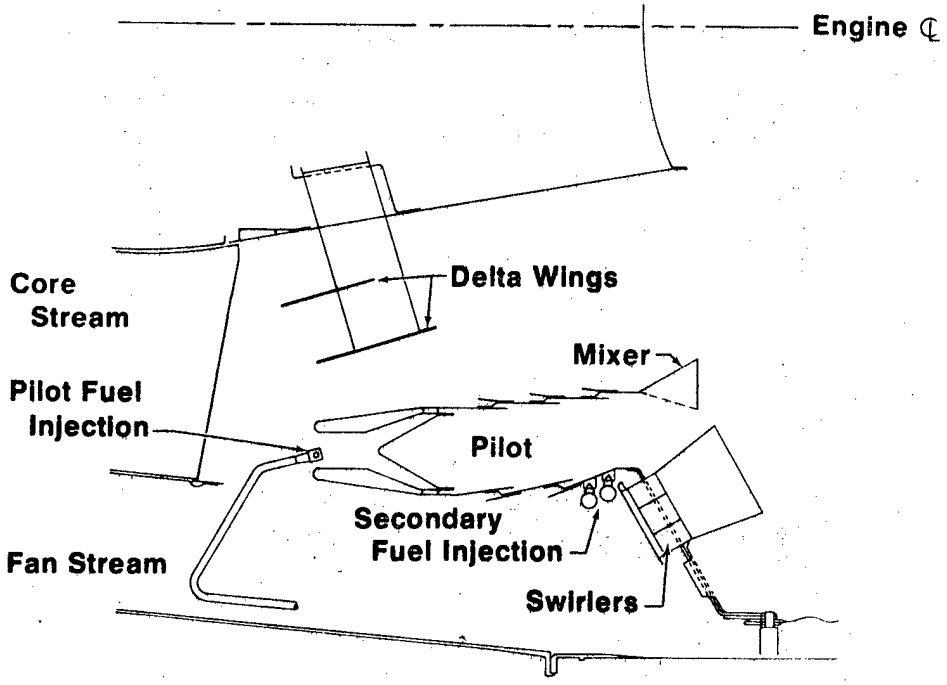

FIGURE 3

AUGMENTOR CRITICAL DESIGN POINTS

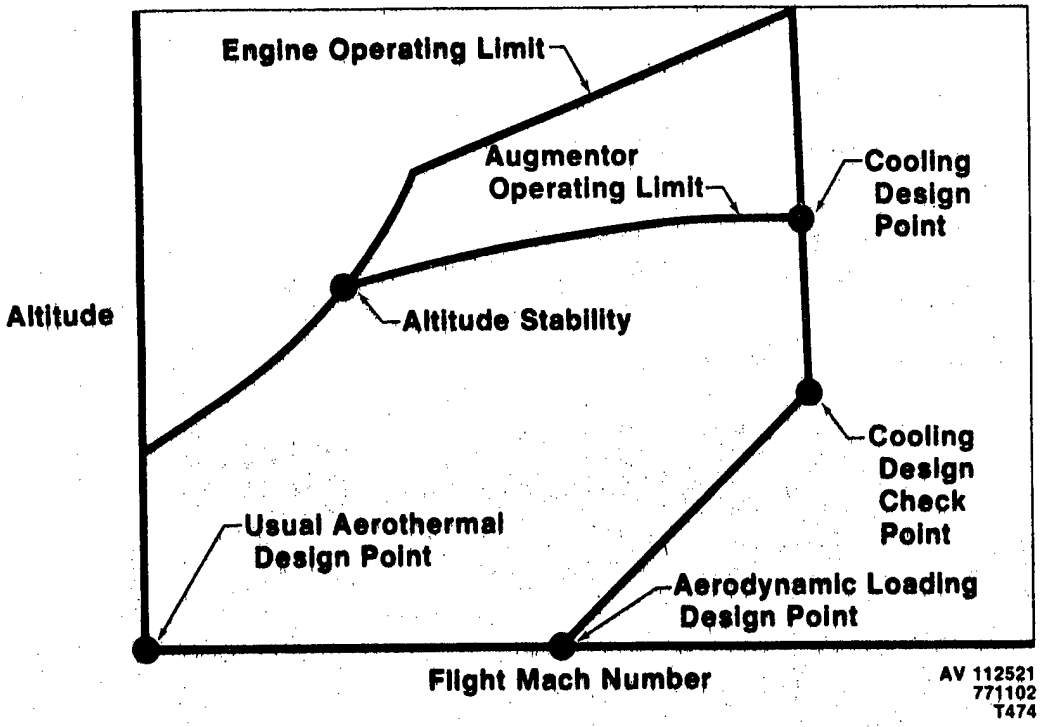

FIGURE 4

TEST STAND SCHEMATIC

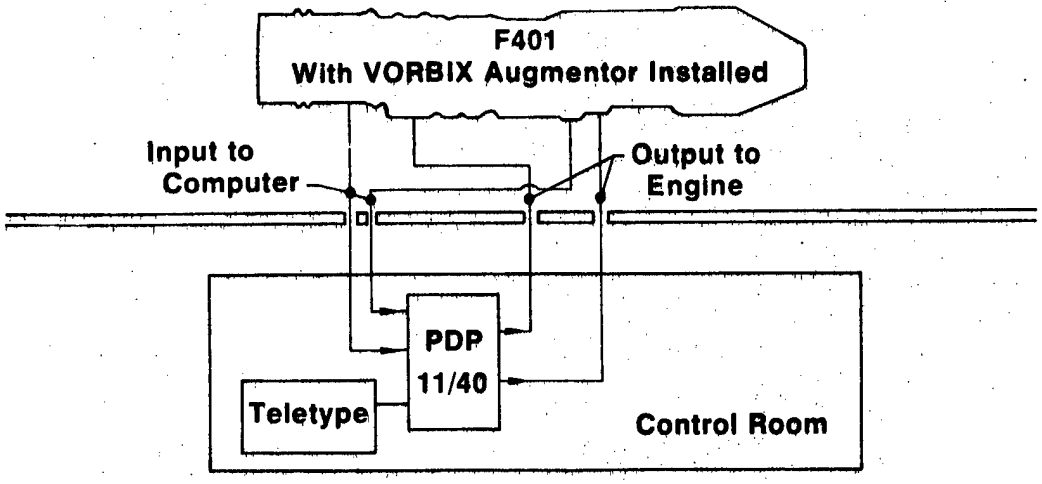

FIGURE 5

TABLE I

VORBIX AUGMENTOR TEST SCHEDULE

POINTS	MN	ALT
1	0	10K
2	0.8	25K
3	0.6	25K
4	0.8	30K
5	0.6	30K
6	0.8	35K
7	0.8	40K
8	0.8	45K
9	0.8	50K
10	0.8	55K
		To Blow Out
11	0.75	40K
12	0.6	35K
13	0.6	40K
14	0.6	45K
15	0.6	50K
		To Blow Out
16	1.2	50K
17	1.2	55K
18	1.2	60K
19	1.2	65K
20	1.2	70K
21	1.3	50K
22	1.3	55K
23	1.3	60K
24	1.3	65K
25	1.3	70K
26	1.2	45K
27	1.2	40K
28	1.2	35K
29	1.3	45K
30	1.3	40K
31	1.3	35K
32	1.0	35K
33	0.6	20K
34	0.6	15K
35	0.8	20K
36	0.8	15K
37	0	0
38	1.0	10K

Biographical Sketch

Mr. William W. Wagner was born in Philadelphia, Pennsylvania on August 21, 1944. He graduated from Drexel University in Philadelphia in 1967, receiving a B.S. degree in Mechanical Engineering. Through a University/ Industry student cooperative program, Mr. Wagner was employed by the South Chester Corporation, plant engineering division during his University enrollment.

In June 1967, he joined the Aeronautical Engine Laboratory of the Naval Air Engineering Center as a project engineer in the Environmental Systems Branch. His responsibilities included experimental evaluation of gas turbine components, including effects from FOD, icing, corrosion, and vibration. He later assumed responsibility for experimental validation of the first salt corrosion specification. In June 1973, he transferred to the Research and Technology Group of the Naval Air Propulsion Center. He is presently Program Manager of the Navy's Combustion Technology programs. Mr. Wagner is an active member in the American Institute of Aeronautics and Astronautics (AIAA).

(U) A RETIREMENT-FOR-CAUSE STUDY OF AN ENGINE TURBINE DISK

BY

Richard J. Hill
Turbine Engine Division/TBP
Air Force Aero Propulsion Laboratory
W-PAFB, Ohio

Walter H. Reimann, Ph.D.
Metals and Ceramics Division/LLN
Air Force Materials Laboratory
W-PAFB, Ohio

Jon S. Ogg
Directorate of Engineering/YZES
Aeronautical Systems Division
W-PAFB, Ohio

A Retirement-for-Cause Study of an Engine Turbine Disk

Abstract

This paper describes a procedure which allows for the retirement of turbine engine disks for actual life exhaustion rather than a statistical minimum limit of a population. The procedure is applied to the third stage turbine disk of the TF33 engine for demonstration purposes. The demonstration included detailed stress and fracture analysis in addition to actual spin pit testing. Limitations of current technologies are discussed which may limit the application of the technique to all advanced engine components; however, the paper shows for most engine components the technologies are sufficiently developed to successfully apply the technique. The effort discussed was a joint program between AFAPL, AFML, and ASD with sponsorship from OCALC. All spin pit testing was done by the Navy at the Naval Air Propulsion Center. The effort was a technical success but could not be implemented for the TF33 engine for logistic reasons.

INTRODUCTION

The design requirements of recent jet engines entering USAF service have emphasized increased performance and higher thrust/weight ratios, which, in turn, result in higher stresses and more severe environments for all components. These high stress levels have resulted in the introduction of a larger number of finite life components. In addition, these same components have rapidly increased in cost due to design complexities and by the use of advanced materials and processing techniques. In order to help minimize Air Force operating costs, it is imperative that ways be sought to optimize the useful service lives of these components.

In this paper, an approach to achieve optimum service life, referred to as Retirement-for-Cause (RFC), is described. It is believed that this approach, which is based upon the use of a fracture mechanics analysis of a component's crack propagation phase for a safety factor, can optimize the service life and thereby minimize maintenance costs.

Using the TF33 third stage turbine disk as the test article, a program is described which details the entire RFC procedure. All aspects of the program from the analytical considerations to the spin pit verification testing considering a low cycle fatigue failure mode are discussed.

RETIREMENT-FOR-CAUSE

Traditionally, component whose dominant failure mode is low cycle fatigue (LCF) have been designed to a "crack initiation" criterion. Under this criterion, all components of a given population are considered to have failed as soon as a crack of some finite size, e.g., .031 inches has statistically formed in the member of the population which has minimum strength properties. No attempt is made to utilize the life associated with the remaining population members which have statistically higher properties and are therefore not cracked.

From a safety standpoint, this approach has been generally very successful since it contains a built-in safety factor by assuming all components to be "minimum". However, for real materials and for real design situations, lifetimes based on time to crack initiation of the minimum member tends to be extremely conservative for a component population. This may be seen by reference to Fig. 1, which illustrates the LCF crack initiation behavior of Inconel 718, a typical nickel-based superalloy, at 1000°F. Because of the statistical nature of engineering materials like Inconel 718, there is significant scatter associated with the number of loading cycles required to initiate a crack at some given stress level for each specimen of material produced. For design purposes, this problem of "material scatter" is usually eliminated by degrading the failure curve to a conservative "design allowable" level where the probability of failure, i.e., crack initiation, becomes very

low. For critical components such as engine disks, this probability is usually set at 0.1%. Fig. 1 shows a design allowable curve established via this philosophy. In service, a component manufactured from this material would be used for the number of load (fatigue) cycles permitted by this design allowable curve and then all such components in the population would be retired. Theoretically, at this cycle count point, only one component in a population of 1000 would have actually initiated a crack and the remaining 999 components would have some undefined useful life to crack initiation remaining. Reference to Fig. 1 shows that in the case illustrated the difference between the number of cycles to reach the "design allowable" curve and the population "average" curve are significantly different and that at the design allowable limit an "average" component would have consumed only 10% or less of its potential useful life to crack initiation. However, under an initiation criterion as in the current Air Force system there is no way to utilize this potential life without accepting a higher probability of failure of the minimum member.

Under the proposed system, this additional useful life can be utilized by adopting a rejection criterion that uses each component in a population until it specifically initiates a crack rather than rejecting the entire population on the behavior of the statistical minimum. The development of fracture mechanics concepts over the last several years has permitted the degree of predictability for crack propagation rates necessary to implement such an approach on a safe basis.

Fig. 2 shows the basic retirement-for-cause concept. For a given component, the number of cycles, N_C, required to propagate a crack from an initial detectable size A_O to critical size A_C can be calculated and verified. An inspection interval is then established at some fraction of N_C designated N_I. The value of N_I is established by considering the non-destructive inspection threshold crack value A_O, cost effective overhaul intervals and degree of conservatism desired. It can be seen that over this interval of time, N_I, no component containing a crack equal to or smaller than A_O could fail catastrophically by reaching A_C.

In using RFC as an operating system, all components would be inspected first at the end of the initial N_I cycles, and only those components containing detectable cracks equal to or greater than A_O would be retired. All others would be returned for additional service. After additional N_I cycles, all components would again be inspected and again all components with cracks larger than A_O rejected and the remainder returned for service. In this way, the crack propagation residual life is continually reset to a safe N_C value. By following this

approach, components are only rejected for cause (cracks) and each component is allowed to operate for its own specific crack initiation life. It should be noted that if a crack is missed at the first inspection interval, another chance exists to find a larger crack, A*, before A_c is achieved.

It is clear that not all fatigue-limited components may be handled in this way, and that each component must be evaluated individually to determine the economic feasibility of RFC. The inspection interval N_I (Fig. 2) must be such that it does not place undue constraints on the operation of the component or that the cost of the necessary "teardown" and inspection does not negate the advantages of the life extension gained. One thousand cycles of crack propagation may represent many years of service for one component and a fraction of a second for another. It seems unlikely that retirement-for-cause can be applied to components limited by high cycle fatigue considerations, but for many high cost components limited by low cycle fatigue, such as engine disks, this approach does appear to offer significant economic advantages.

It is also clear that in applying retirement-for-cause, Nondestructive Evaluation (NDE) becomes a critical factor. The crack length value, A_o, in Fig. 2, determines the residual life of the component and its detection is limited by the resolution and reliability of the inspection system employed. In many cases, the decision as to whether or not retirement-for-cause can be applied to a component will be predicated upon the ability of available NDE approaches to detect a usable A_o with sufficient sensitivity and reliability. However, because the RFC procedure includes an in-depth stress analysis, a component's defect critical locations can be accurately predicted and verified. For this reason, NDE techniques can be selected and refined for a particular area rather than attempting to develop a technique for characterizing the quality of an entire component. This inherently increases the sensitivity of the NDE system to a level where RFC can be utilized.

Preliminary crack growth analyses indicate that the detection and elimination of cracks larger than .030 to .050 inches surface length (A_o) would provide adequate residual life for the safe application of RFC to many older disk designs, and this was the crack size of primary interest in the present study. However, it is also recognized that in some of the more advanced designs, using higher strength, lower toughness material, the acceptable level for A_o must be much smaller for economical use of RFC.

DEMONSTRATION OF THE USE OF RFC ON A TF33 THIRD TURBINE DISK

Engine and Spin Pit Stress Analysis

In order to demonstrate RFC, an entire RFC program was initiated on the TF33 third turbine disk shown in Fig. 3. The TF33 third turbine disk first was analyzed as part of the turbine low rotor system at the mission point of 105 seconds after take-off. This flight point produces the maximum centrifugal and thermal load on the disk. The analysis was done using the "ISOPDQ" family of finite element computer programs (Ref. 1) developed under contract to the Air Force for the purpose of conducting stress analyses of turbine engine components. The analysis considered all blade and attachment bolt loads as well as adjacent hardware interaction.

The result of this analysis is shown as the "engine assembly" curve in Fig. 4. (Only the stresses from the bore up to the bolt hole are shown). The nominal stress at the edge of the bolt hole was calculated to be 84.7 ksi. This value of stress was the value that was used as a goal in creating the spin pit test.

In order to establish the spin pit test conditions, an accurate finite element computer model of the disk was created and analyzed. Both the nominal stress and the actual stress gradients were calculated by using different models. The first model was created from a combination of axisymmetric ring elements and plane stress elements and the second model was created entirely of plane stress elements. The two models were matched through the use of equal bore displacements.

In the first model, shown in Fig. 5, the properties of the plane stress element were utilized by representing the material between the bolt holes by rectangular plane stress elements. The out-of-plane direction was aligned, with the disk tangential direction (θ) and thus the in-plane stress σ_y aligned with the radial direction (R) and the in-plane stress σ_x aligned with the axial direction (Z) of the disk. The thickness of the plane stress elements were set equal to the average thickness of the material between bolt holes. Both the top and bottom of the plane stress elements were constrained to axisymmetric ring elements and thereby the disk bolt circle could support radial and axial loads but would not exhibit tangential stiffness nor transmit tangential load.

The entire model was analyzed at a 6000 RPM, 70°F condition and resulted in an average deflection of .00488 inches

at the bore. (These analysis constraints were chosen to be identical to a spin pit strain survey test which was to be conducted prior to the actual fracture test).

The second model of the bolt hole using only plane stress elements was created as shown in Fig. 6. The deflection value of .00488 inches was used as the required deflection for an equivalent load to produce on the plane stress bolt hole model. The value of the required force was determined by an iterative method to be 1883.2 pounds per nodal point in the radial direction along the top of the model.

The nodal points on each side of the plane stress bolt hole model were free from constraint in the radial direction and constrained to have zero deflection in a direction perpendicular to the radial direction. Constrained in this fashion, the boundaries of the model could only slide on a radial line. The thickness of each element was set equal to the thickness of the disk at the same location with slight adjustments being made for the disk thickness gradient. This model was also analyzed at a 6000 RPM, 70° condition.

In this particular disk, only 10 of the 20 holes are used as "bolt" holes. The remaining 10 holes are "balance weight" holes and are counter sunk .090 inches and are .075 inches less in diameter than the bolt holes. Based upon a tangential plane projection comparison between the bolt holes and counterweight holes, the difference in tangential load transmittal ability is considered insignificant and thus all holes are considered to be identical in the analysis.

The results obtained using this two model procedure on the TF33 engine disk bolt hole geometry are shown in Fig. 7 compared to the experimental strain data. As can be seen, there is very good agreement.

As a result of this good agreement, the two model procedure was expanded to include the actual thermal gradient effect and actual spin pit stress values were calculated for use in the fracture analysis.

Through an iterative method it was calculated that the spin pit test should be run from 0 to 6400 RPM with the thermal gradient that is labeled "Flight Profile" in Fig. 8. However, this desired thermal gradient could not be achieved in the pit and, in fact, the actual test gradient had to be modified three times (shown in Fig. 8 as gradient 1, 2 and 3) to reduce the spin pit cycle time. In addition, the 0

RPM engine shutdown condition could not be achieved in the pit and had to be changed to 500 RPM. All three combined stress (thermal and centrifugal) gradients for the run-up and run-down side of the three pit cycles are shown in Fig. 4 for the nominal stress and in Fig. 9 for the peak stress. The values from these two sets of curves are the values used in the fracture analysis.

Fracture Mechanics Analysis of TF33 Disk

The approach taken in performing the required crack propagation analysis of a low cycle fatigue induced crack in a TF33 disk bolt hole employed the use of the well-known modified Walker equation (Ref. 2). A Bowie correction was also incorporated in the solution procedure to approximate the stress field in the vicinity of the bolt hole crack as it progressed.

As previously mentioned, both an axisymmetric and a plane stress analysis were used to generate the initial conditions for the fracture mechanics analysis considering all three spin pit cycles. Since the axial stress component was found to be small in both analyses relative to the radial and tangential components in the area adjacent to the hole, an assumption of crack growth in a biaxial stress field was considered reasonable. However, before conducting the actual crack growth calculations, an understanding of the material's response was necessary. Since minimal crack growth data was available for the Incoloy 901 material at the temperatures of interest, it became necessary to generate a crack growth curve for the prescribed temperatures anticipated during testing. Fig. 10 portrays the results of this effort.

For the fracture analysis, the modified Walker equation used is equation (1).

$$\frac{da}{dN} = \frac{C(\Delta K)^n}{(1-R)^{(1-M)n}} \qquad (1)$$

where:

$\frac{da}{dN}$ = rate of crack growth per cycle

$C = 1.537 \times 10^{-10}$ } crack growth curve parameters

$n = 2.937$ } crack growth curve parameters

M = .5 empirical weight on mean stress effect

R = minimum to maximum stress ratio

ΔK = change in effective stress intensity

The ΔK expression used to obtain values for equation (1) was equation (2).

$$\Delta K = \Delta\sigma\sqrt{\frac{\pi a}{Q}}\ f\ (a/r) \qquad (2)$$

where: ΔK = change in stress intensity

$\Delta\sigma$ = change in applied stress

a = crack depth

Q = correction factor for geometry and stress distribution in vicinity of crack

f(a/r)= Bowie Correction Factor

Fig. 11 shows the TF33 disk cross-section with the assumed elliptical starting crack superimposed. It should be noted that the Bowie correction factor used in the analysis was for an imbedded crack in a bolt hole exposed to a biaxial stress field. In addition, this expression was modified slightly to account for the fact that the radial component of the biaxial field was lesser in magnitude than the tangential stress. Some conservatism was also applied by assuming that the elliptical crack transitioned to a through-the-thickness crack when the surface length of the crack, 2c, exceeded 75% of the actual disk bolt pad thickness. This assumption appears reasonable considering the geometry of the disk in which the crack front is propagating. The aspect ratio for the crack (crack depth ÷ crack length) was arrived at by breaking open scrap TF33 disks which exhibited cracks in the bolt hole region as shown in Fig. 12. Although the characteristic of the cracks in the bolt holes varied with multiple initiation sites, and appeared to propagate at a changing aspect ratio, a value of .35 was determined to best represent the average aspect ratio and was used in the analysis. Disk failure would occur when the crack depth, a, reached a critical crack

depth value, a_c, which was calculated using the fracture toughness value, K_{IC}, in equation (2). These values are 0.335 inches and 110,000 psi$\sqrt{in.}$, respectively.

It will be shown that this is not truly the case but that residual life still exists once the crack goes beyond 0.335 inches.

Spin Pit Testing

For the spin pit verification, a high time TF33 third stage turbine disk which had been retired from service with an unknown history was used. The particular disk, however, had been cycled beyond the "initiation" point and contained a measured service-induced crack of 0.052 inches surface length. At an aspect ratio of .35, this surface length value calculates to be a crack depth of .0182 inches. This was the starting size used in the fracture mechanics analysis and resulted in a predicted critical crack depth of .335 inches at a propagation cycle count of 15,090 cycles with a growth rate as shown in Fig. 13.

As was discussed, three different thermal gradients were used during the duration of the fracture testing. The amount of testing done under each of the three gradients was as follows: Gradient #1, Cycle 1 to Cycle 597; Gradient #2, Cycle 598 to Cycle 1500; Gradient #3, Cycle 1501 to test completion. These three gradients stress/crack propagation effects were considered in the fracture analysis assuming linear cumulative damage.

The sequence of testing was as follows:

Step 1. Apply temperature gradient.

Step 2. Spin up to 6400 RPM.

Step 3. Spin down to 500 RPM.

Step 4. Flush pit with cooling gas.

Step 5. Repeat Step 1 through 4.

The inspection interval was about every 500 cycles with the following procedure:

Step 1. Clean with solvent (each hole).

Step 2. Obtain trace of eddy current probe reading.

Step 3. Replicate with milar film.

Step 4. Assemble in pit and run next 500 cycles.

Step 5. Repeat Step 1 through 4.

The eddy current inspection consisted of using a Dalton(R) eddy current unit modified with an automatic spiraling mechanism. As the probe transcended the hole, a trace of the signal was recorded. The crack growth was also recorded and measured through standard crack replication methods.

Testing was ended at the 13,860 cycle point after the disk could no longer be spun within acceptable balance limits. Fig. 14 shows the disk after test completion.

The results of the spin pit fracture testing are shown in Fig. 13 compared to the predicted growth. It should be noted that the crack growth in bolt hole #2 (.052-inch starting crack length) showed the same shape and trend as the predicted rate, but it was not the bolt hole that would cause ultimate failure. At approximately the 7500 cycle test point, bolt hole #1 indicated a crack which was also monitored for the duration of the test. Up to about 9000 cycles of testing, this crack in #1 hole grew as expected, but then it "popped" through the thickness and grew at a faster rate to become the dominant crack that ultimately caused the test to be ended. The reason for this change in behavior is not understood at this time. Effort is underway to section this test disk to determine precise aspect ratio of the cracks and to correlate the eddy current traces with the fracture surfaces. A new fracture analysis will be accomplished upon determination of the actual aspect ratio.

Results

It was shown through completion of the spin pit test that over 5-1/2 life times of propagation life exists for this disk as a fracture safety margin. Thus, if RFC was adopted as the replacement philosophy and the inspection interval (N_I) was set equal to one initiation life of 2500 cycles (current throwaway point), there would be five opportunities to find a crack in the disk of increasing surface length from an initial size of .031 inches. Based upon this one disk test data point, RFC would appear safe and practical for this TF33 disk. Fig. 15 shows the potential for cost savings on this disk if RFC was instituted. It was not instituted by the Air Force, however, because there were no third turbine disks of TF33 design to replace the cracked disks that would be found. As a result, the Air Force had

to utilize a JT3D disk in conjunction with a low turbine modification package whenever a TF33 disk needed replacement. Rather than have two different configurations and considering all cost aspects, it was beneficial to the Air Force to replace all TF33 third turbine disks at overhaul, without inspection, with the JT3D modification package. Thus, even though the RFC study was successful, it could not be utilized cost effectively on the TF33 third turbine disk. There are, however, many other LCF limited disk stages in the TF33 engine where RFC could be applied as well as many different engines in the Air Force inventory. Current studies are underway to identify which engine and which stages are the most cost effective RFC candidates.

DISCUSSION

The program described in this paper is one of the first, if not the first, attempt to conduct a full-scale retirement-for-cause validation, and to integrate the various necessary technologies into one program. As such, the results have been very valuable in assessing the state of the technology base and the requirements for implementing a RFC approach.

The primary technology areas required for RFC can be divided as follows: stress analysis, crack growth analysis, non-destructive evaluation and mechanical testing. The following discussion examines each of these areas and attempts to define the work still required for total RFC implementation.

It is obvious that the ability to utilize a RFC philosophy depends first upon the generation of an accurate understanding of the stress field of the component's critical areas(s). It is felt that the current level of stress analysis capability across the turbine engine industry is such that this aspect of the RFC method is not the limiting factor. In fact, there is even significant effort to improve the "standard design" elastic stress analysis capability to include three-dimensional inelastic time independent and dependent effects. Other areas where advances are being achieved include the determination of stress intensity factors for crack tips that are in biaxial and triaxial stress fields.

However, as demonstrated by the success of this project, one does not have to wait upon these newer technologies to come fully of age before implementing an RFC overhaul concept. A rigorous two-dimensional elastic analysis will provide data of sufficient accuracy to adequately implement RFC on many existing and development engine components that do not exhibit gross plastic flow. The components which do, however,

exhibit this non-recoverable deformation will have to wait upon the validation of the newer analysis technologies prior to their inclusion in an RFC philosophy.

It was also demonstrated that an accurate fracture mechanics analysis, along with NDE, are two additionally critical requirements for the successful implementation of an RFC system. The fracture analysis performed in this study was relatively unsophisticated, and under the circumstances, it is remarkable that the correlations observed were so good. However, since 1975 when this analysis was initiated a very significant volume of research has been devoted to high temperature fracture mechanics and the technology appears to be maturing rapidly. For example, the problems of a K-analysis of complex geometries, crack growth in complex stress fields and the transition of part-through to through-cracks appear to be solvable through the use of linear superposition techniques (Refs. 3, 4, 5), as well as recently developed experimental approaches for a K-analysis (Ref. 6). The relationships between crack growth and many of the engine load parameters such as temperature, hold times and stress ratios have also received considerable attention and again promising solutions appear to exist (Ref. 7).

One problem exposed by this study that is currently not receiving much attention is that of multiple crack initiation. Traditionally, fracture mechanics assumes a single "engineering" crack and predicts its growth. Fig. 16 shows a typical bolt hole crack observed by dye penetrant in one of the TF33 third turbine disks. As cycling proceeds, these microcracks grow individually and eventually merge into one dominating macrocrack. Observation of this phase reveals that there is an undefined interaction between the cracks that produces an accelerated growth. Since this microcracking phase persists for a significant portion of the crack growth life, it is clearly imperative that analytical approaches be developed to handle this case.

One major problem inhibiting the immediate reduction to practice of an RFC system for all components is the lack of an acceptable probabilistic prediction method for crack growth. In the present study, no attempt was made to account for materials variability, even though the material, Incoloy 901, is known to show considerable scatter in its crack growth behavior. Based upon minimal crack growth testing, observations reveal that the crack growth tended to be faster than predicted, and while this can be explained in part by the microcracking process described above, it probably also suggests that the crack propagation behavior

of the test disk was faster than the average values used in the analysis.

As stated earlier, NDE is a critical factor in the implementation of an RFC approach. Since with RFC the rejection of a component now becomes based on the presence or absence of a crack, it is essential that the NDE technique employed be capable of finding cracks above some defined threshold (A_O) with a very high degree of reliability. The current Air Force practice of using penetrant inspection techniques almost certainly will not provide the required sensitivity or reliability levels for an RFC system. The development of automated processes using inherently more sensitive techniques (e.g., eddy current) will be required. It would also be highly desirable to develop NDE techniques capable of more quantitative information (e.g., both length and aspect ratio of surface cracks). Finally, it is essential that the statistical aspects of NDE be included in the RFC analysis.

The spit pit verification, while costly and time consuming, is a necessary step in developing the confidence levels necessary to implement the RFC approach. In the present study, considerable effort was devoted to simulating both the mechanical stress and thermal environment of the TF33 engine in order to best verify the analytical predictions. However, provided that the engine environment is well understood so that it can be handled analytically, a simpler isothermal spin pit test may probably be adequate for many disks.

In considering the application of RFC to other engine disks, it is clear that additional complexities may exist which must be considered. In the present case, the engine mission is relatively simple with few load interactions and the critical location is located in an area where fatigue/creep interactions or superimposed vibratory stresses are not likely to have an influence. In other disks both of these factors may have to be considered in the analysis. In addition, the higher design stresses and high strength, lower toughness alloys used in many advanced engines will result in smaller critical crack sizes thus placing even more emphasis on improved NDE techniques. Nevertheless, the significant economic advantages of an RFC approach does appear to provide adequate incentive to continue the development of this approach for optimizing engine component life.

REFERENCES

1. "Turbine Engine Components Stress Simulation Program", AFAPL-TR-77-72, November 1977

2. "Fracture and Control of Fatigue in Structure, Application of Fracture Mechanics", S. T. Rolfe, J. M. Barsom, John Wiley and Sons

3. "Stress Intensity Factors for Some Through-Cracked Fastener Holes", International Journal of Fracture, A. F. Grant, Jr., April 1975

4. "Two-Dimensional Stress Intensity Solution for Radial Cracked Rings", AFML-TR-75-121, A. F. Grant, Jr., October 1975

5. "Stress Intensity Factors for Cracked Holes and Rings Loaded with Polynomial Crack Face Pressure Distributions", International Journal of Fracture, A. F. Grant, Jr., August 1978

6. "Theoretical and Experimental Analysis of Surface Cracks Emanating from Fastener Holes", AFFDL-TR-76-104, February 1977

7. "An Interpolative Model for Elevated Temperature Fatigue Crack Propagation", AFML-TR-76-176, Vol I, II, III, November 1976

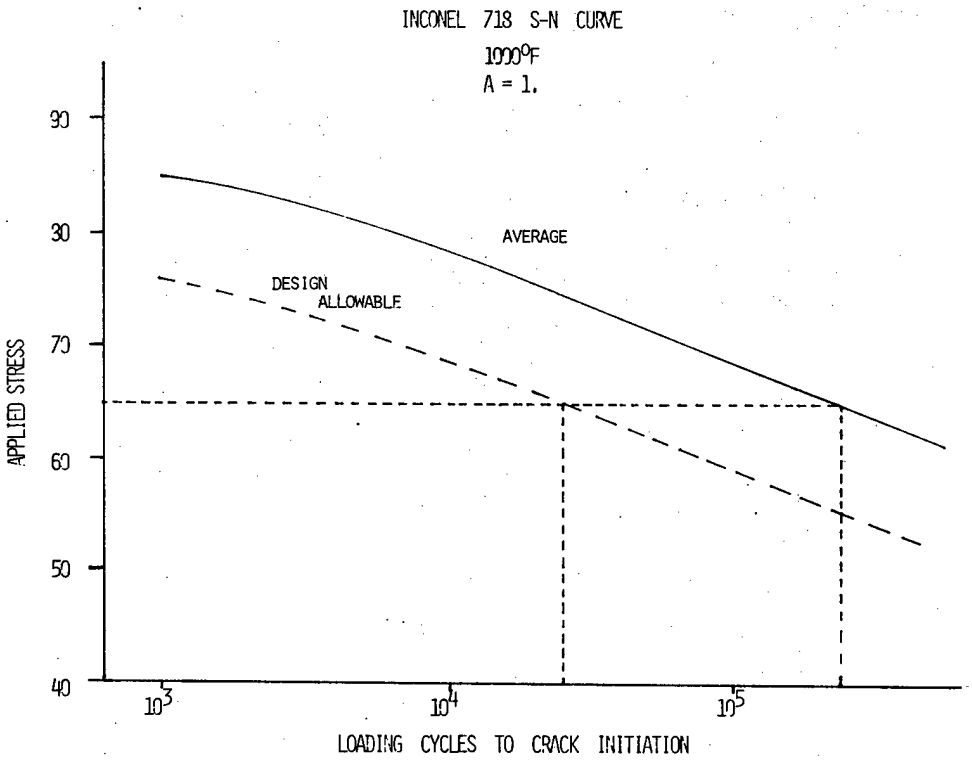
INCONEL 718 S-N CURVE
1000°F
A = 1.
90
80
70
60
50
40
AVERAGE
DESIGN
ALLOWABLE
APPLIED STRESS
10^3
10^4
10^5
LOADING CYCLES TO CRACK INITIATION

Figure 1

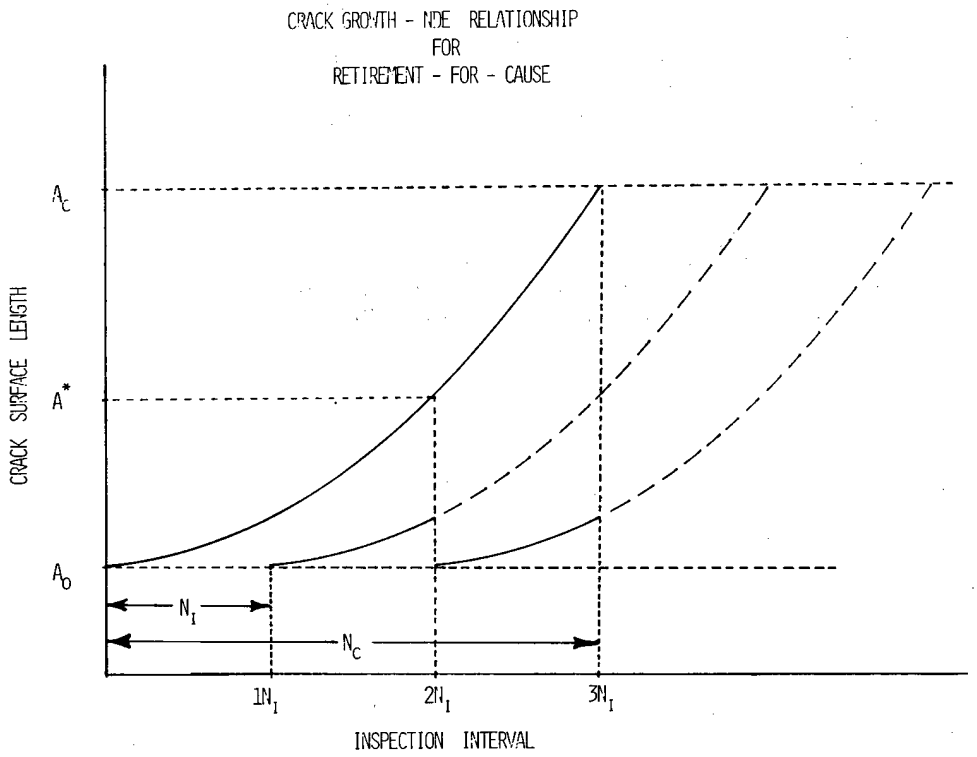
CRACK GROWTH - NDE RELATIONSHIP
FOR
RETIREMENT - FOR - CAUSE
CRACK SURFACE LENGTH
A_c
A^*
A_o
N_I
N_c
$1N_I$
$2N_I$
$3N_I$
INSPECTION INTERVAL

Figure 2

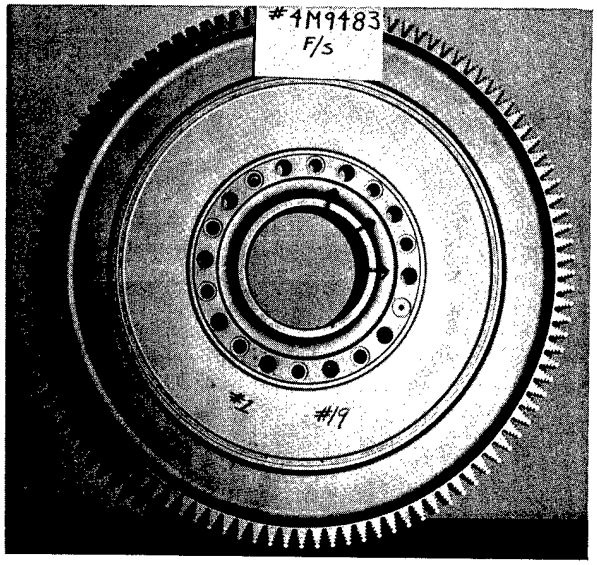

TF33 THIRD TURBINE DISK

Figure 3

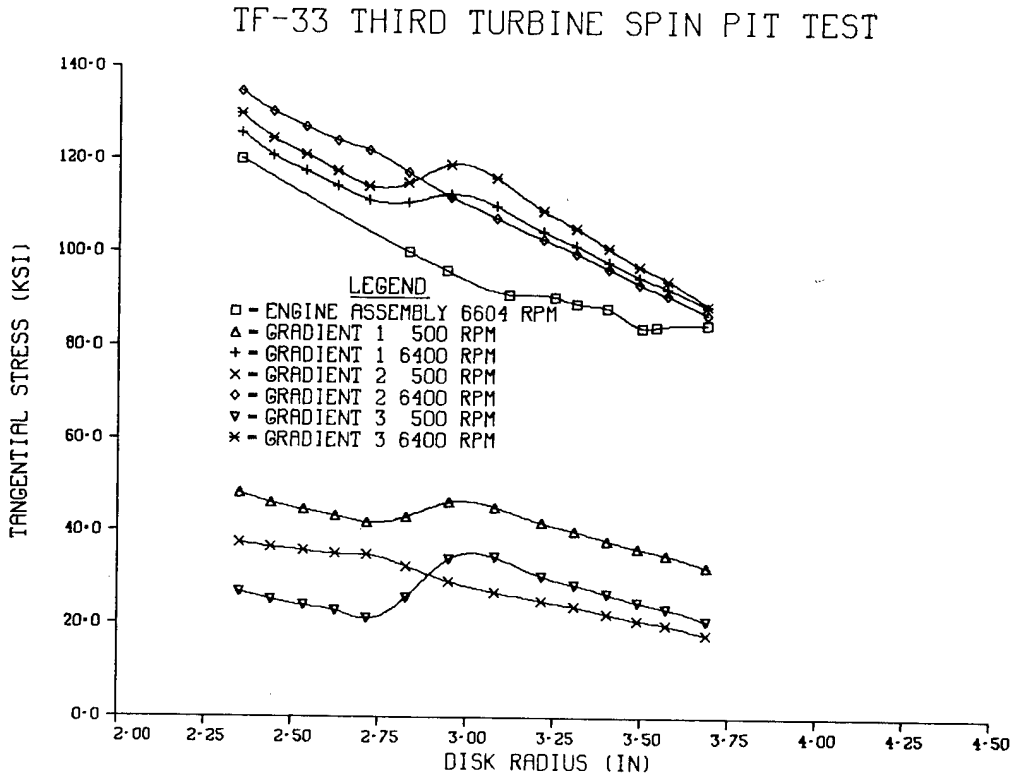

NOMINAL STRESS GRADIENT

Figure 4

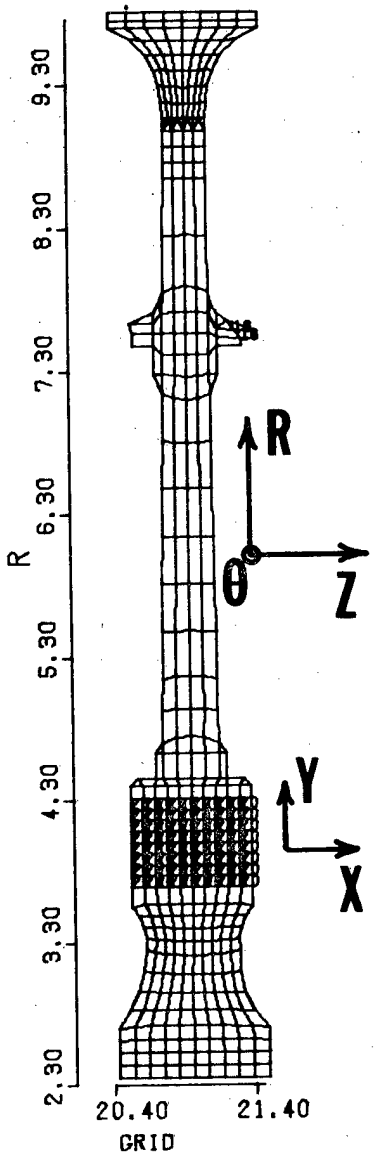

AXISYMMETRIC ELEMENTS

PLANE STRESS ELEMENTS

DISK STIFFNESS MODEL

Figure 5

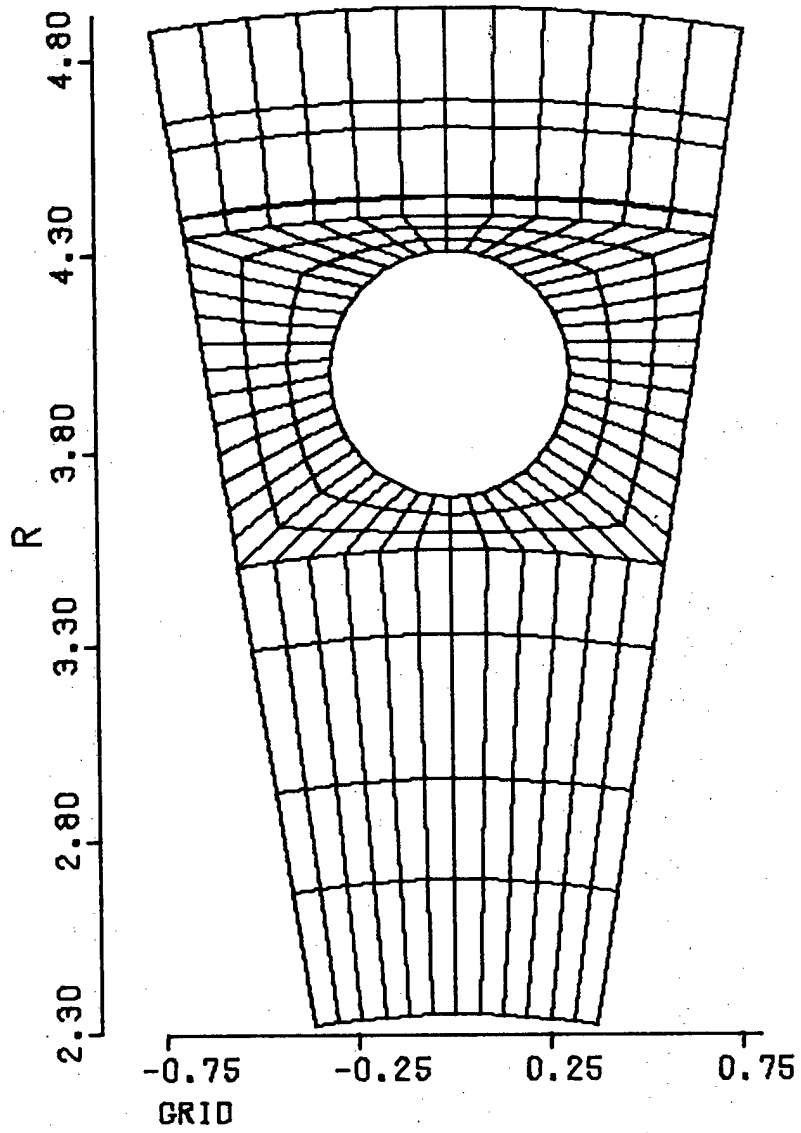

PLANE STRESS BOLT HOLE MODEL

Figure 6

284

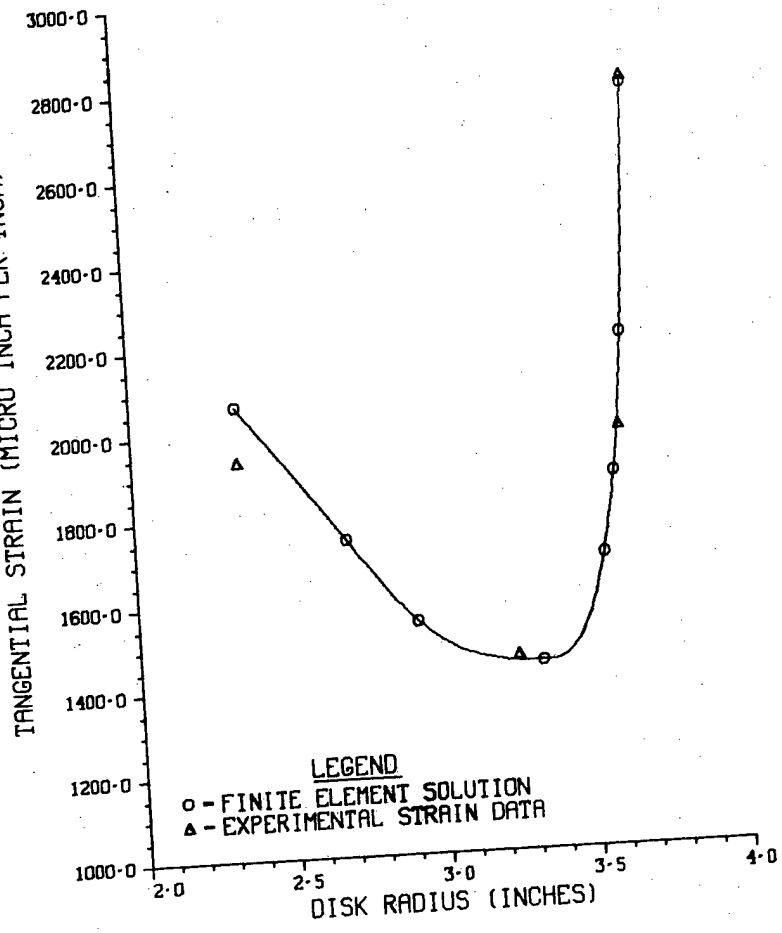

SPIN PIT STRAIN TEST RESULTS

Figure 7

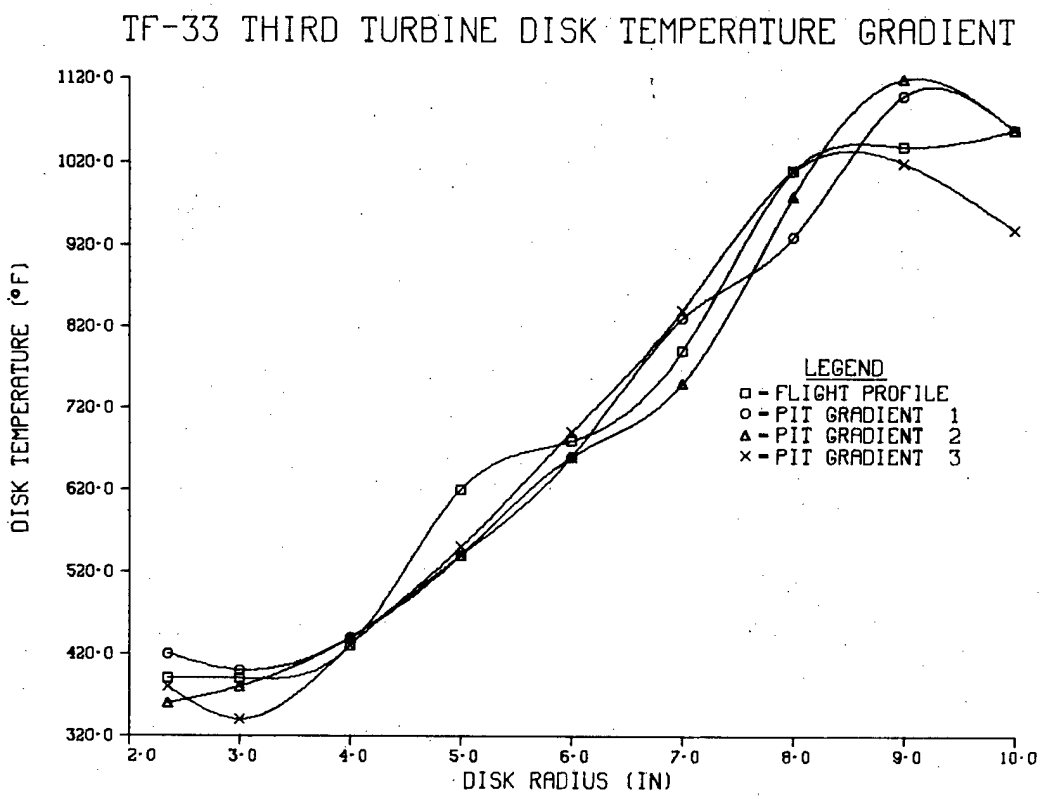
TF-33 THIRD TURBINE DISK TEMPERATURE GRADIENT
DISK TEMPERATURE (°F)
1120·0
1020·0
920·0
820·0
720·0
620·0
520·0
420·0
320·0
2·0
3·0
4·0
5·0
6·0
7·0
8·0
9·0
10·0
DISK RADIUS (IN)
LEGEND
□ - FLIGHT PROFILE
○ - PIT GRADIENT 1
△ - PIT GRADIENT 2
× - PIT GRADIENT 3

Figure 8

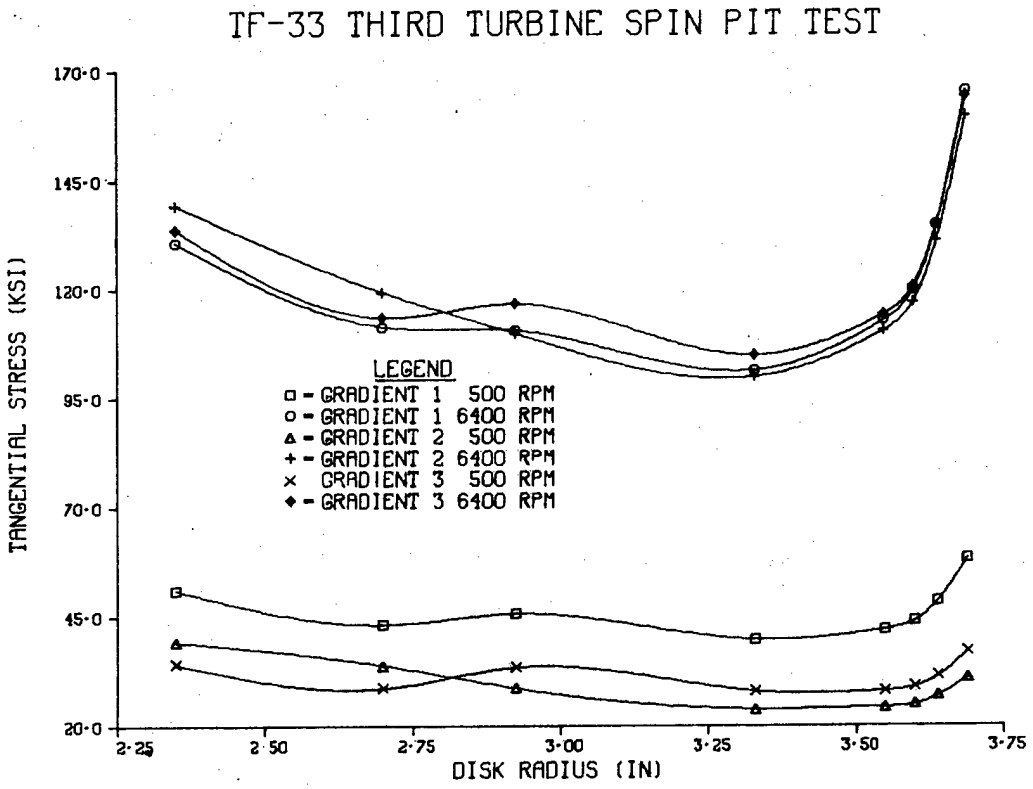

PEAK STRESS GRADIENT

Figure 9

INCOLOY - 901

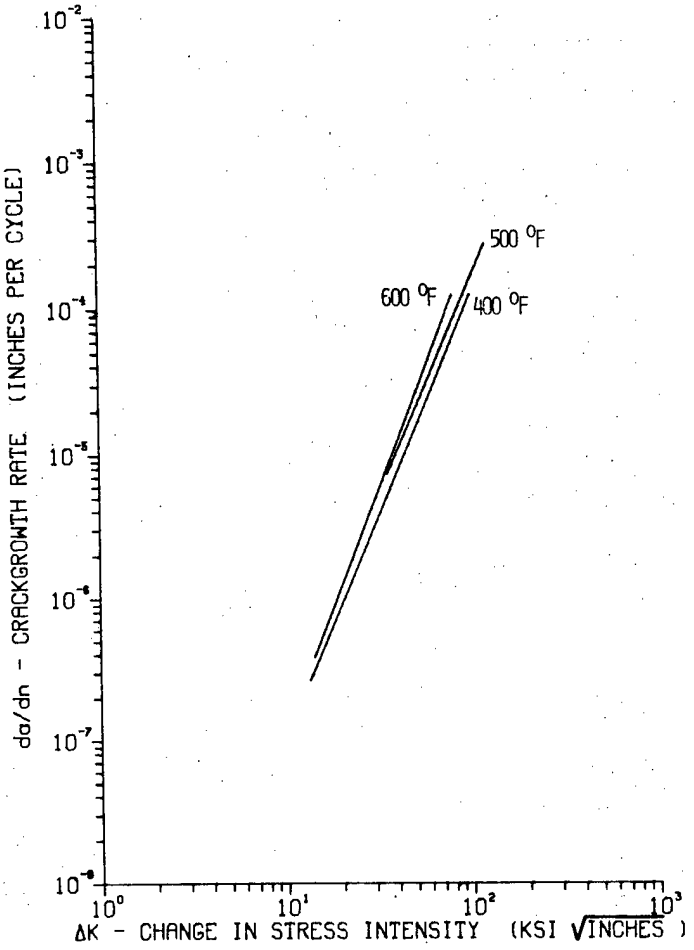

CRACK GROWTH CURVE

Figure 10

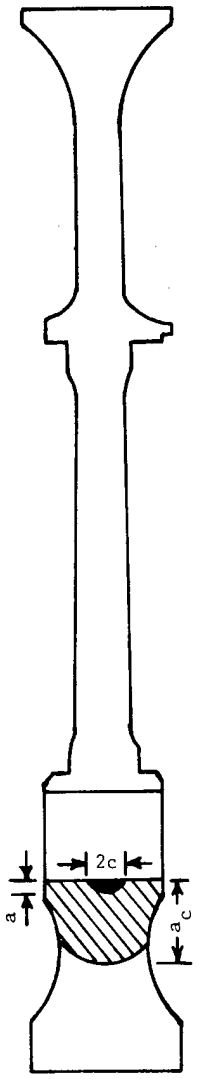

BOLT HOLE CRACK GEOMETRY

Figure 11

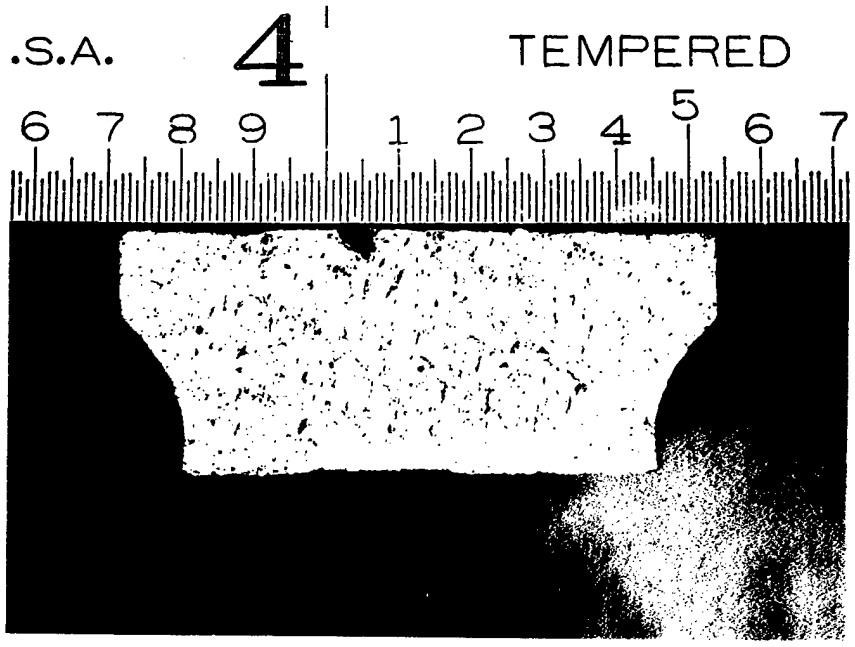

TYPICAL BOLT HOLE STARTING CRACK

Figure 12

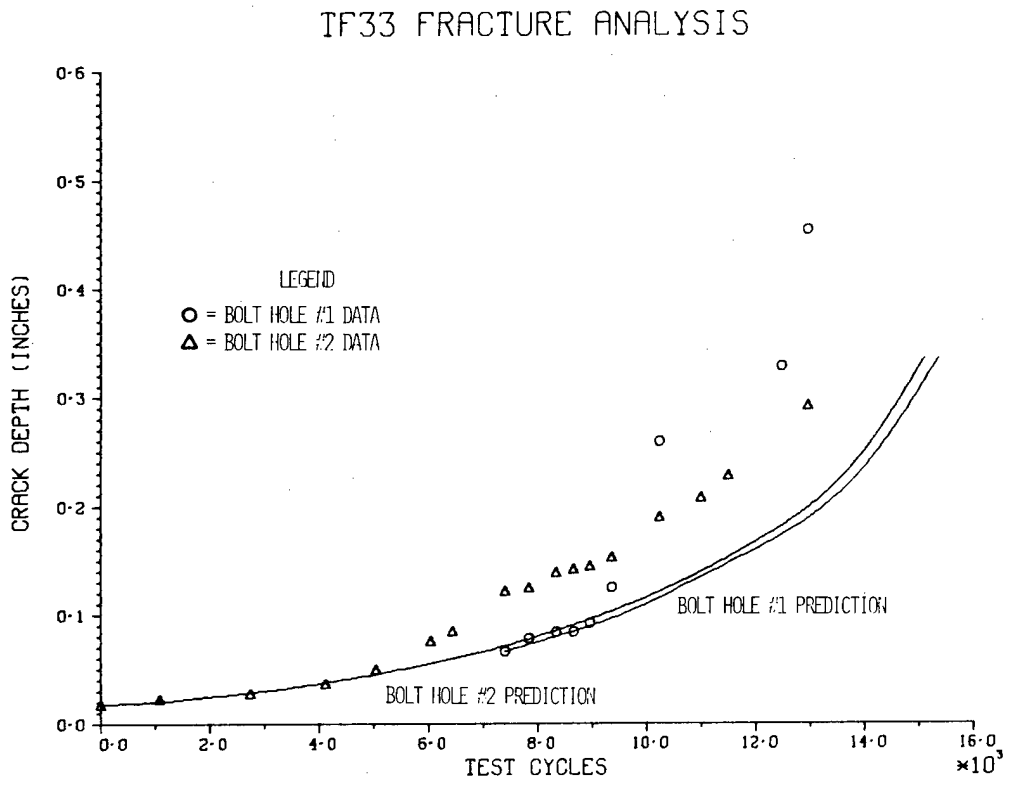

SPIN PIT CRACK GROWTH TEST DATA

Figure 13

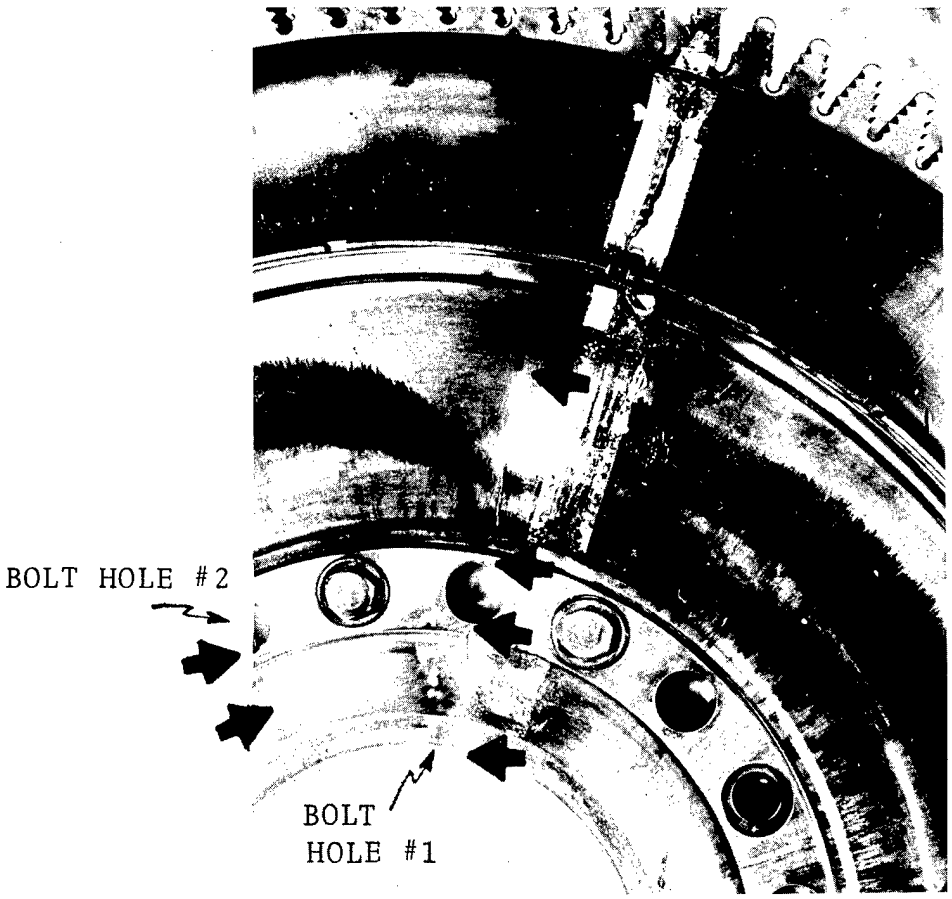

BOLT HOLE CRACKS AT TEST COMPLETION

Figure 14

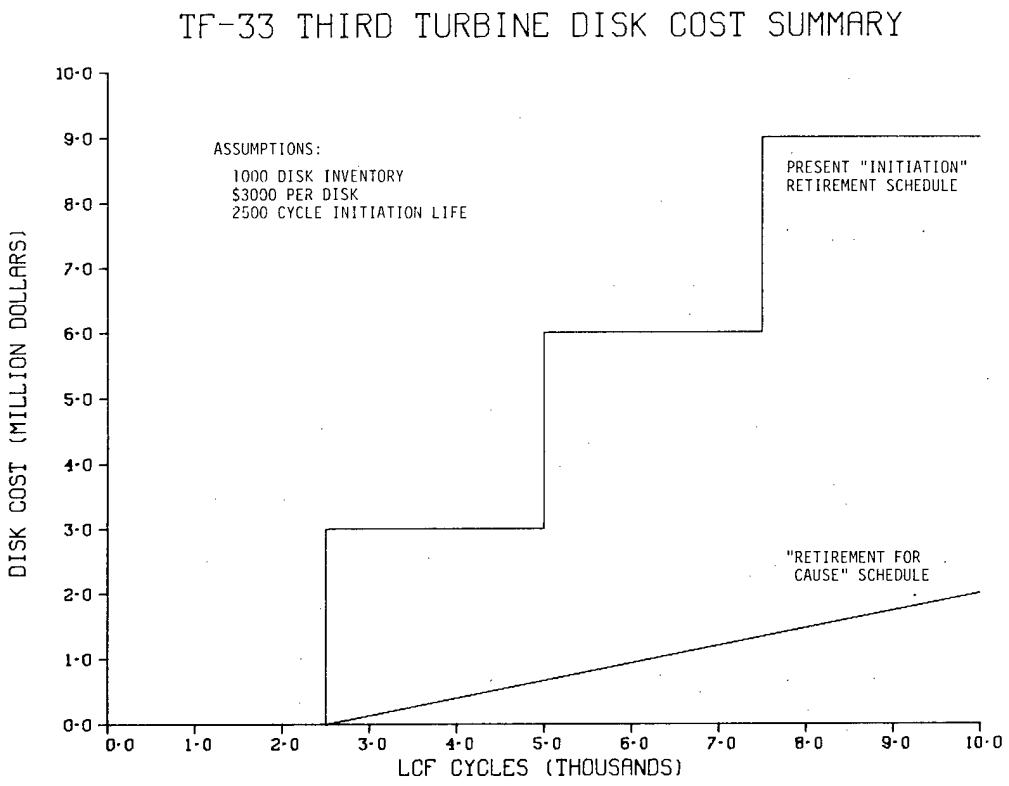

DISK REPLACEMENT COST SCHEDULES

Figure 15

BOLT HOLE SURFACE MICROCRACKS

Figure 16

Biographical Sketch

Mr. Richard J. Hill was born in Pittsburgh, Pennsylvania on October 8, 1945. He graduated from Wichita State University in 1971 with a B.S. degree in Aeronautical Engineering. He received his M.S. degree in Aeronautical Engineering from Ohio State University in 1977. Mr. Hill has been employed by the Air Force Aero Propulsion Laboratory since 1971 and has responsibility for developing and applying technology for turbine engine component structural analysis, life-assessment, and durability advancements.

Dr. Walter H. Reimann was born December 23, 1938 in Maryborough, Australia. He received his B.S. degree in Metallurgy in 1962, his M.S. and Ph.D. in Metallurgy in 1964 and 1967; all from the University of Melbourne. While working on his Ph.D., he attended Columbia University as an exchange research associate. He accepted employment in 1967 with the Metals and Ceramics Division of the Air Force Materials Laboratory conducting research studies in fatigue and fracture, first in airframe materials and then in high temperature engine materials. Since 1972 he has been responsible for the development of advanced life prediction techniques for engine components. He is currently a Research Group Leader in the Metals and Ceramics Division and the AFML Focal Point for Metallic Materials Behavior.

Mr. Jon S. Ogg was born on November 28, 1952 in Columbus, Ohio. He received both a B.S. degree and a M.S. degree from Ohio State University in 1973 and 1977, respectively. He is employed by the Directorate of Engineering of the Aeronautical Systems Division and has responsibility for conducting life assessments and durability improvements for all propulsion systems under ASD sponsorship.

ACKNOWLEDGMENTS

The authors wish to thank their many Air Force colleagues who contributed during the course of this study, and are particularly indebted to Mr. Guy Mangano and his colleagues at the Naval Air Propulsion Center for the very considerable effort they devoted to the development and execution of the spin pit testing.

PAYOFFS OF VARIABLE CYCLE ENGINES FOR SUPERSONIC V/STOL AIRCRAFT

BY

Richard T. Lazarick

Paul F. Piscopo

Research and Technology Group

Naval Air Propulsion Center
Trenton, New Jersey

Payoffs of Variable Cycle Engines for Supersonic V/STOL Aircraft

Abstract

Future airbreathing engines will require lower fuel consumption and greater operational flexibility than obtained with present engines because of low worldwide fuel reserves and the expanded requirements projected for advanced aircraft. Since high bypass ratio engines operate efficiently at subsonic Mach numbers and low bypass ratio engines operate efficiently at supersonic Mach numbers, a fixed cycle engine which is required to operate in both speed regimes is obviously compromised. In addition to diverse flight Mach numbers, V/STOL aircraft require a large variation in thrust levels. At takeoff and landing, the engine must produce a very high level of thrust and thus, is oversized for many of the forward flight conditions. Variable cycle engines (VCE) offer a potential approach to the solution of these problems.

The Naval Air Propulsion Center (NAPC) sponsored a VCE evaluation using advanced V/STOL fighter designs. A systematic engine/airframe evaluation procedure was developed and used to assess advanced engine concepts for lift plus lift/cruise (L+L/C) aircraft designs.

In order to determine the impact of VCEs, a baseline aircraft utilizing fixed cycle turbofan engines was designed. Variable geometry turbofan and variable geometry turbojet-powered aircraft of the same technology level were then designed and compared to the baseline in terms of aircraft takeoff gross weight (TOGW), performance, life cycle cost and operational flexibility. This paper covers the efforts under this program as well as NAPC's follow-on efforts.

Introduction

The inherent operational flexibility of variable cycle engines (VCEs) may provide significant benefits in supersonic Vertical/Short Takeoff and Landing (V/STOL) fighters. The combination of powered lift and forward flight performance requirements of supersonic V/STOL fighters necessitates extensive compromises in the design and scheduling of fixed cycle engines. These compromises have resulted in high aircraft takeoff gross weight (TOGW) and relatively poor payload and range performance in many designs when compared to conventional supersonic fighters. VCEs can potentially reduce the compromises necessitated by fixed cycle engines with attendant improvements in weight and performance.

In 1975 the Navy began a thirty month, three-phase VCE Selection Program to evaluate V/STOL VCE concepts which were defined under Navy contract by Detroit Diesel Allison (DDA) and General Electric (GE). These concepts were postulated to meet the needs of supersonic V/STOL propulsion systems. Both axisymmetric and 2-D V/STOL nozzle concepts were included in the evaluation. In Phase I, preliminary screening was conducted to estimate the potential impact of each VCE on V/STOL fighter TOGW and to select the most promising concept for more detailed evaluations. As a result of this preliminary screening, the Naval Air Propulsion Center (NAPC) selected a GE designed modulating bypass turbofan concept for detailed evaluation in Phases II and III. This concept provides the versatility to be used in either lift plus lift/cruise (L + L/C) or lift/cruise (L/C) V/STOL fighters. In addition, the GE 2-D Augmented Deflector Exhaust Nozzle (ADEN) was selected by NAPC for the Phase II and III evaluations. Since this nozzle provides the capability to augment in the vectored thrust operating mode, single spool variable area turbine turbojets with augmentation were reconsidered in Phases II and III.

In order to assess the payoffs of the VCEs, a baseline L + L/C aircraft powered by fixed cycle turbofans and direct lift engines (DLE) was parametrically optimized. The variable geometry turbine turbojet (VGT-TJ) and VCE-turbofan (VCE-TF) powered L + L/C aircraft were then compared to the baseline system in terms of TOGW, performance, fuel usage, life cycle cost (LCC), and operational flexibility. Another concept developed and evaluated utilized the VCE-TF to provide fan air to a remote augmentor lift system (RALS). The RALS concept eliminates the need for a DLE as the forward thrust vector and results in a L/C aircraft configuration.

At the conclusion of the three-phase VCE Selection Program, additional programs were developed to further evaluate the feasibility and value of the RALS/VCE concept for supersonic V/STOL fighter applications. The Navy also commenced a concurrent in-house study effort to evaluate various propulsion concepts and develop aircraft TOGW sensitivities to various engine design parameters. This paper summarizes the activities under the VCE Selection Program and describes the follow-on programs which are currently being conducted.

VCE Selection Program Description

In order to assess the potential of VCEs for supersonic V/STOL application, NAPC sponsored a three phase airframe/propulsion study. Phase I was a concept screening effort where a variety of engine configurations were evaluated using a simplified analysis procedure. The most promising concepts were selected for more detailed analysis in Phases II and III. Phase II consisted of the development of an automated V/STOL aircraft sizing and performance computer program, definition of a baseline fixed cycle engine (FCE) powered lift plus lift cruise aircraft, and definition of the VCE performance characteristics. In Phase III, aircraft utilizing the VCEs were designed and the VCE payoffs assessed. GE and DDA (Phase I only) performed the propulsion effort while McDonnell Aircraft Company (MCAIR) performed the airframe effort.

A. Phase I

In the Phase I screening activity, a wide variety of engine concepts were developed and evaluated as shown in Figure 1. The figure of merit used in this screening phase was TOGW reduction for a VCE powered aircraft as compared to a fixed cycle turbofan engine (FCE-TF) powered baseline aircraft. All aircraft were required to perform the two diverse design missions illustrated in Figure 2. The Deck Launched Interceptor (DLI) mission emphasized high power performance for vertical takeoff (VTO), maximum power climb, supersonic dash, and supersonic combat. The Subsonic Surface Surveillance (SSS) mission emphasized efficient low power fuel utilization in the long range subsonic cruise mission legs and long loiter on station. Since the DLI design mission was used to define aircraft internal fuel volume, the SSS mission was accomplished by adding external fuel and performing a short takeoff (STO) instead of a VTO. In both cases, aircraft performance requirements such as acceleration time, maneuverability, specific excess power, and combat ceiling were quite

demanding. Superimposing the performance, VTOL and STOL requirements produced aircraft with high thrust to weight (T/W) ratios. Thus, the aircraft required engines with high thrust capability for performance, good high power fuel consumption characteristics for supersonic cruise and combat, and good low power fuel consumption and aircraft installation characteristics for subsonic cruise and loiter conditions.

The principal result of the Phase I effort was the identification of the GE modulating bypass (double bypass) turbofan engine as the strongest candidate VCE for a multi-mission supersonic V/STOL application. This VCE-TF, Figure 3, is a dual rotor, mixed-flow engine incorporating a three-stage fan, a variable stator compressor, a high temperature rise combustor, a high work high pressure turbine, and a variable area low pressure turbine. In addition, the first two stages of the fan are driven by the low pressure turbine rotor, the third stage is driven by the high pressure turbine rotor, and the engine employs two bypass airflow ducts. The bypass ducts incorporate two variable area bypass injectors (VABIs); one to provide for mixing of the inner and outer bypass flows in the fan section and the other for mixing the bypass flow with the core flow in the rear section. The mixed engine exhaust flow then exits through a single ADEN. During transonic and supersonic flight conditions, the outer bypass duct is closed and the VCE-TF operates as a conventional mixed flow turbofan. At part power subsonic cruise and loiter flight conditions, the bypass flow is modulated by a combination of third stage fan stator angle closure and opening of the outer bypass duct, thus increasing the engine bypass ratio. Also included in the Phase I effort was a comparison of axisymmetric versus two-dimensional (2-D) nozzles for VTO thrust vectoring. Since the ADEN, which allows full augmentation in the VTO mode, appeared to have a payoff, it was chosen for continued use in Phases II and III.

Another result of the Phase I effort was the identification of a RALS concept which provides all of the VTO thrust required without the use of a DLE. This concept, also shown in Figure 3, utilizes a double bypass VCE with an oversized front block fan, and ducts fan airflow forward to a remote augmentor which provides the forward thrust vector. In addition to indicating the potential for reduced TOGW, this concept eliminates the need for DLE development and acquisition, and their associated costs.

Another important finding in Phase I was that, for a

DLI mission alone, a non-afterburning variable geometry turbine turbojet (DRY VGT-TJ) powered aircraft was very competitive with the other VCEs. However, for the SSS mission, the engine was significantly oversized for forward flight. This was due primarily to the non-afterburning restriction for VTO which became the engine sizing point. Because of the oversizing, the DRY VGT-TJ did not meet the SSS range requirements for this study. (Note that if the SSS range requirements were reduced, this engine would be a candidate). An afterburning variable geometry turbine turbojet (VGT-TJ) engine concept was included in the Phase II and III effort.

B. Phases II and III

The second and third phases of the VCE selection program performed the detailed airframe/engine integration and design effort and identified the VCE payoffs. The DLI mission was used as the primary mission for these phases. The aircraft were also evaluated on four other missions, illustrated in Figure 4, to assess operational flexibility in terms of mission range or loiter time. The baseline for all comparisons was a FCE-TF powered L + L/C aircraft. An 18:1 installed thrust-to-weight ratio DLE was used in all the L + L/C aircraft. The engine data for the FCE-TF was provided by a GE-developed parametric cycle deck. In addition to the FCE-TF, parametric analysis of a VGT-TJ concept was accomplished utilizing a GE-developed afterburning single spool turbojet parametric cycle deck. Data from the families of engines generated were then input into an automated V/STOL fighter design evaluation procedure along with the mission requirements.

Parametric matrices of aircraft designs were defined by systemically varying engine and airframe design parameters and aircraft thrust and fuel sizing variables. The size, performance, and cost of each aircraft in the matrix were calculated using the MCAIR-developed Computer Aided Design Evaluation (CADE) program. Correlation equations were then generated which describe the relationships between each aircraft size, performance, and cost parameter computed by CADE and the design and sizing variables. Using these relationships, weapons system requirements can be specified in terms of mission radii, maneuverability, load factor, acceleration time, etc. An optimization procedure, the SEARCH program, was used to determine the combination of the design and sizing variables which produced the minimum TOGW aircraft satisfying those requirements. An example of the usefulness

of these correlation equations is shown in Figure 5 for the FCE-TF powered L + L/C system. This figure permits the user to assess the sensitivity of minimum aircraft TOGW to changing the dash Mach number and/or DLI mission radius. Correlation equations were also developed for the SEARCH program which provided visibility into engine/airframe interactions, engine operating characteristics in steady-state mission segments, and engine thrust sizing flight conditions.

Because the double bypass VCE concept is relatively new, a parametric cycle deck was not available for the type of analysis and optimization just described. However, a number of VCE-TF point designs were submitted by GE for both L + L/C and RALS aircraft designs. Engine cycle parameters for these engines are shown in Figure 6.

C. Results and Payoffs

The aircraft design evaluation and optimization procedure described earlier resulted in three optimized L + L/C aircraft designs and one RALS aircraft design. All aircraft were designed to the DLI mission with Mach 2 capability, and all aircraft and engine technologies represent 1985 - 1990 Initial Operational Capability (IOC). Figure 7 summarizes the engine and aircraft design variables for the selected designs. The aircraft weights and performance characteristics for these designs are shown in Figure 8.

1. Takeoff Gross Weight

Relative to the baseline FCE-TF system, the TOGWs ranged from a decrease of 10% for the VGT-TJ to an increase of 4% for the RALS/VCE.

a. VGT-TJ - The reduction in TOGW was 3500 pounds, of which 1500 pounds was due to the reduction in required fuel for the DLI mission. At the dash conditions, the Specific Fuel Consumption (SFC) is 13% better than the FCE-TF while the variable geometry turbine feature keeps the subsonic SFC approximately equal to the FCE-TF.

b. VCE-TF - Of the 3050 pound reduction in TOGW, 1640 pounds was due to the reduction in fuel required. This is due to better SFC at both the dash and subsonic cruise operating conditions.

c. RALS/VCE - The RALS/VCE increase in TOGW of 1250 pounds was due to increased propulsion system and

airframe weight. The RALS/VCE engine reduced SFC at dash, combat and cruise (500 pounds less fuel) and reduced propulsion system drag. However, this was offset by the increase in engine and airframe weight resulting from RALS/VCE being sized by the VTO requirement.

2. Operational Flexibility

The operational flexibility achieved through the use of variable cycle engine features was assessed using the fuel required to achieve the tactical strike mission two-hour loiter time as a figure-of-merit. Fuel savings of 5% and 14%, relative to the FCE-TF, were obtained with the VGT-TJ and VCE-TF engines, respectively. Less than a 1% fuel savings was obtained with the RALS/VCE aircraft design.

As shown in Figure 8, the alternate mission radius and loiter capabilities for all the VCE systems exceeded or were roughly equal to the FCE-TF system. Note that the VCE-TF improves all alternate mission capabilities by approximately 8%.

3. Combat Performance

Assessments of the combat performance capability of the several aircraft designs were made to determine VCE impact. Each V/STOL fighter achieved at least the required levels of combat performance. Since the RALS/VCE engines were sized by VTO requirements, the required combat performance levels were exceeded as indicated in Figure 8. Although the RALS/VCE was 4% heavier than the reference aircraft, this aircraft had 40-50% more combat P_s and acceleration capability than the FCE-TF. If higher combat performance levels than those used in this study are required, the RALS/VCE aircraft will become even more competitive.

4. Life Cycle Cost

The variable cycle engines which have been evaluated resulted in aircraft TOGW reductions and one concept, RALS/VCE, eliminated the requirement for separate lift engines. The attendant impact on aircraft life cycle cost has been estimated for a fleet of 900 aircraft, with the results shown in Figure 9. The lowest aircraft LCC were obtained for the L + L/C aircraft powered by the single-spool VGT-TJ engine. The LCC for the aircraft powered by the more complex VCE-TF and RALS/VCE engines were competitive with the FCE-TF aircraft.

The airframe and engine cost for the three L + L/C aircraft and the RALS/VCE aircraft are compared in Figure 9. The cost payoffs achieved with the VGT-TJ engine reflect lower TOGW and, therefore, lower airframe cost and lower engine production cost resulting from the reduced engine size. The lower TOGW, and therefore, lower airframe cost of the VCE-TF aircraft, offset increased engine development cost and resulted in production cost competitive with the FCE-TF. Elimination of the cost of developing and producing separate lift engines (1.67 billion dollars) made the RALS/VCE cost competitive with the FCE-TF aircraft.

Follow-On Programs

At the conclusion of the GE and MCAIR programs, two areas of activity were identified as logical extensions to the VCE Selection Program and essential to evaluating the potential of the RALS/VCE concept. The first activity was a study effort to identify the sensitivity of aircraft TOGW to turbine rotor inlet temperature (TRIT) and RALS/VCE system design complexity. The second activity was a hardware development effort to design, fabricate and test a RALS burner capable of performing over the range of operational pressures, temperatures, flows, and duct Mach numbers visualized for a supersonic V/STOL fighter aircraft. Both of these activities are being addressed under the Navy's Exploratory Development Program. The hardware development activity is a GE-contracted effort which began in FY 1978 and is called the Remote Burner Development Program. The study activity is a planned FY 1979 contractual effort, also with GE, and is called the RALS/VCE Trade Study. A third related effort being conducted concurrently by the Navy is an in-house Naval Air Development Center (NADC)/NAPC supersonic V/STOL fighter study. Detailed discussions of each of these three programs are provided below.

A. RALS/VCE Trade Study

The VCE Selection Program concluded with the results that a viable supersonic V/STOL fighter candidate airplane could be designed which met or exceeded all of the performance requirements using a RALS/VCE propulsion system configuration. The two characteristics of the "D" series RALS/VCEs shown in Figure 6 which enhanced their feasibility as candidate systems are (1) the 3200°F TRIT used in the VCE Selection Program resulted in an engine with a sufficiently attractive propulsion thrust-to-weight ratio (6 - 6.5), and (2) the double bypass VCE features made it attractive from an alternate mission performance standpoint. Since

both of these features translate into increased propulsion system development risk. The RALS/VCE Trade Study Program was formulated to quantify the effect of TRIT and design complexity on the thrust-to-weight, performance, and life cycle cost of a RALS/VCE system. The engine matrix to be studied is shown in Figure 10. The baseline 3200°F double bypass "D" series RALS/VCE is engine A of the matrix. Engines of constant mechanical design complexity and decreasing rotor inlet temperature can be compared by selecting one of the matrix rows while engines of constant temperature and reducing mechanical design complexity can be compared by selecting one of the matrix columns.

Engine cycle data and mechanical configuration drawings will be generated for engines B through I in the matrix. In developing the engines for a given matrix row, changes in TRIT will require rebalancing of the engine's thermodynamic cycle. The net result of rebalancing the cycle at a lower TRIT is a reduction in fan pressure ratio and an increase in HPC pressure ratio. These changes in cycle characteristics caused by holding the overall cycle pressure ratio constant and lowering TRIT manifest themselves as changes in the engine's mechanical design. However, the mechanical design changes required to generate a matrix row will be limited to those required to rebalance the engine cycle and will not result in changes in the RALS/VCE features shown in the first column of Figure 10.

In developing the engines for a given column, the double bypass RALS/VCE-TF represents the highest system complexity. A single bypass RALS/VCE-TF will be developed by removing the forward VABI and mixer features, adjusting the fan and turbine aeromechanical design, and rebalancing the engine cycle. This system represents an intermediate level of system complexity. A single bypass RALS/FCE-TF will be developed by removing the variable area LPT from the single bypass RALS/VCE-TF and creating a fixed cycle turbofan with a rear VABI to provide modulated air control for the RALS. Again, adjustments will be made to the fan and LPT aeromechanical design and the engine cycle will be rebalanced.

After all eight additional engines have been developed, life cycle costs will be generated to identify LCC changes as a function of temperature and technology. These numbers will be compared with those shown in Figure 9. The total RALS/VCE Trade Study Program is a sixteen month effort planned to be started early in FY79.

B. Remote Burner Development Program

In order for the RALS concept to be integrated into a supersonic V/STOL fighter, it is necessary to turn the fan airflow 180°, duct it through the airframe to a position behind the cockpit, turn the flow approximately 30°, burn it to temperatures up to 3200°F, turn it approximately 60°, and then exhaust it through a gimballed nozzle (see Figure 4). Minimizing aircraft fuselage thickness and the resultant supersonic wave drag requires that the RALS ducting and burner arrangement have a small cross-sectional area. Since RALS airflow (thrust) requirements for aircraft balance are relatively high (on the order of 35-45% of the total propulsion system thrust for the MCAIR aircraft design), the duct Mach number must also be high for the RALS burner duct so as to minimize cross-sectional area. Since the burner must have low pressure losses, acceptable efficiency, excellent light-off and stability characteristics, smooth and rapid modulation, and satisfactory structural integrity, the flow must be slowed substantially by the time it reaches the burner. It was concluded that a duct Mach number on the order of 0.3 is a satisfactory compromise considering cross-sectional area constraints and pressure loss for the transfer duct. Also a flow speed reduction of approximately 50% is required to accomplish efficient and stable burning. With the volume, flow velocity, stability, and structural integrity requirements of the burner all being critical to the operation of the RALS concept, the burner was selected as the key RALS component for development. This effort is funded under the Remote Burner Development Program.

The purpose of this three-phase, twenty-five month program is to design, fabricate, and test a remote burner system. The burner will be tested over a range of inlet temperatures from 300° to 500°F, inlet pressures from 40 to 50 psia, and altitudes from sea level to 10,000 feet. These pressure, temperature, and altitude conditions roughly approximate the limits envisioned for a RALS/VCE V/STOL fighter application. The burner is also required to operate smoothly over the steady-state temperature range from 150°F over the inlet air entry temperature to 2800°F. Since aircraft pitch control is obtained by modulating the thrust of the RALS, transient temperature excursion as high as 3200°F are permitted.

The Remote Burner Development Program schedule is shown in Figure 11. In the nine-month Phase I effort the burner was designed to meet all of the performance require-

ments and a preliminary test plan was formulated defining instrumentation requirements and the method of test. In addition the fuel system, cooling system, and the associated mechanical hardware were also designed. The nine-month Phase II effort, which is about to begin, includes the manufacturing and assembly of all the necessary hardware to perform the rig test. The nine-month Phase III effort is the test and evaluation phase in which the remote burner combustion system operation and performance characteristics will be demonstrated. The performance parameters of interest include dry losses of the burner, light-off temperature rise, modulation characteristics, and combustor efficiency. The program is scheduled to be completed in February 1980.

C. Navy In-House Supersonic V/STOL Fighter Study

In order to come up with an independent Navy assessment of aircraft TOGW, system design, and performance, the Navy embarked on an in-house design study of supersonic V/STOL fighter aircraft in the fall of 1977. In this study NAPC provided engine cycle definition, performance, and engine weight and size data to NADC for installation into an NADC-designed airframe. NAPC developed three double bypass RALS/VCE systems and five VGT-TJs for the study. The purpose of the study was to assess the impact of TRIT and engine cycle on aircraft design parameters. The engine cycle characteristics of the eight engines provided for the study are summarized below:

1. RALS/VCE Temperature Study

The RALS/VCE Temperature Study was similar to the effort being conducted under the RALS/VCE Trade Study with the exceptions that (1) the temperature study developed the engines only in the first row of the Figure 10 matrix, (2) the engines were approximations of a double bypass VCE, and (3) the temperature range studied was not as wide as that of the trade study. A summary of the impact of temperature on engine design point cycle parameters is shown in Table I below. For this study, the bypass ratio (BPR = 1.0), overall pressure ratio (OPR = 24.3), thrust (FN = 27100), and thrust split (35/65) were held constant, and TRIT, fan pressure ratio (FPR), core pressure ratio (CPR), and inlet corrected airflow (WA2C) were variable.

TRIT	FPR	CPR	WA2C	T/W
3200	3.60	6.75	277	6.1
3000	3.42	7.11	285	5.8
2800	3.25	7.48	300	5.5

TABLE I

The impact of TRIT on engine T/W is shown in the last column of Table I above. These results are currently being evaluated to determine their effect on aircraft design performance.

2. VGT-TJ Temperature and Bleed Flow Study

If the double bypass VCEs represent the most complex propulsion systems for a V/STOL fighter, then the VGT-TJs represent the other side of the coin. The VGT-TJs were one-spool single stage turbine systems. Two families of engines were provided: (1) TRITs of 3000°, 2600° and 2200°F, and (2) reaction control bleed levels of 0, 7½ and 15% at 2600° TRIT.

The VGT-TJs were substantially shorter engines than RALS/VCEs and had higher T/W at lower TRITs A summary of the VGT-TJs is shown in Table II below:

TABLE II

TRIT	BLEED %	OPR	FN	WA2C	T/W
2600	0	13.36	20000	183	6.8
2600	7½	11.62	20000	209	5.9
2600	15	9.98	20000	242	4.6
3000	0	12.79	20000	176	6.9
2200	0	13.63	20000	196	6.4

Although the VGT-TJ cycle provides its maximum benefit at a slightly higher OPR, the engines in this study are constrained by the turbine work limitation and resulted in slightly lower compressor pressure ratios. These results, like those of the RALS/VCE, are being evaluated to determine their effect on aircraft design and mission performance.

Conclusions

The VCE Selection Program identified and evaluated a number of concepts which appear to have a potential payoff when utilized in a supersonic V/STOL fighter application, including the double bypass turbofan VCE, the RALS, and the ADEN. The double bypass VCE benefits are derived from the engine's ability to perform efficiently at both supersonic and subsonic operating conditions. The RALS concept allows for a L/C aircraft configuration, thereby eliminating the cost and development risk of a high performance DLE. The ADEN concept permits augmentation during VTO, which allows the engine to be sized by the other mission requirements.

The payoff of the VCE features do not show up so strongly in TOGW, but rather in fuel utilization and alternate mission performance. Since the future of aircraft fuel price and availability is unclear, this may be an even more significant payoff than now realized. Also the utilization of Naval aircraft in the fleet is often quite different than the design missions used in concept formulation. The adaptability of the VCE can significantly enhance the aircraft's ability to perform the modified missions.

Finally, if an increased combat performance requirement is forthcoming for supersonic V/STOL fighters, the RALS/VCE concept can provide that additional performance with the same size/cost class aircraft as is necessary to meet today's combat performance levels.

FIGURE 1.

CANDIDATE VCE CONCEPTS

	AXISYMMETRIC V/STOL NOZZLES						TWO-DIMENSIONAL V/STOL NOZZLES	
	DETROIT DIESEL ALLISON				GENERAL ELECTRIC			
DESIGN CYCLE CHARAC-TERISTICS	VGT TF	VGT DRY TJ	PARALLEL TURBINE TF	REVERSE PITCH VGT TF	MODULATING BYPASS TF		MODULATING BYPASS TF	MODULATING BYPASS TF AND REMOTE LIFT SYSTEM
FPR	2.9	–	2.9	FWD = 1.4 AFT = 2.3	4.0	3.5	4.0	4.0
OPR	21	11	21	HP = 7.25	20	25	20	20
BPR	1.35	–	1.7	0.4 - 4.5	0.5	0.95	0.5	0.5 (0.9 VTO)

GP76-0509-1

FIGURE 2.

DESIGN MISSIONS

DECK LAUNCHED INTERCEPT (DLI)

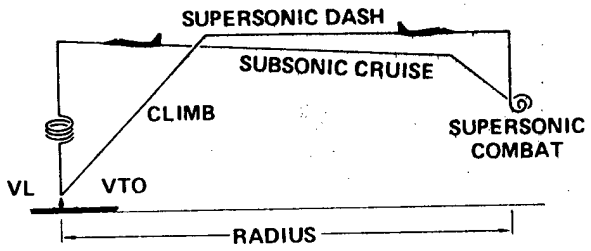

SUBSONIC SURFACE SURVEILLANCE (SSS)
EXTERNAL FUEL (IF REQUIRED)

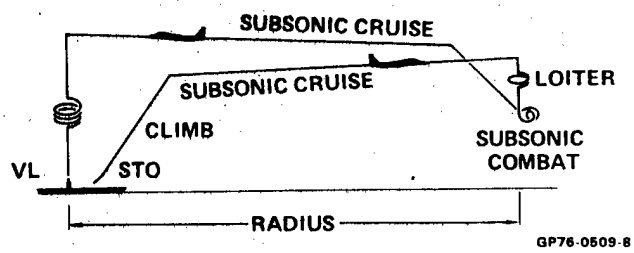

GP76-0509-8

RADIUS 150 NM
DASH MACH NO. 1.6

RADIUS 300 NM
LOITER TIME 2 Hrs.

COMBAT PERFORMANCE

ACCELERATION		
	MACH 0.8 to 1.6 at 35000 FT.	90 Sec.
MANEUVER		
	MACH 0.65 at 10000 FT.	4.75 g
SPECIFIC EXCESS POWER		
	MACH 0.9 at 10000 FT.	750 Ft/Sec

FIGURE 3.

VARIABLE CYCLE ENGINE WITH
REMOTE AUGMENTOR LIFT SYSTEM

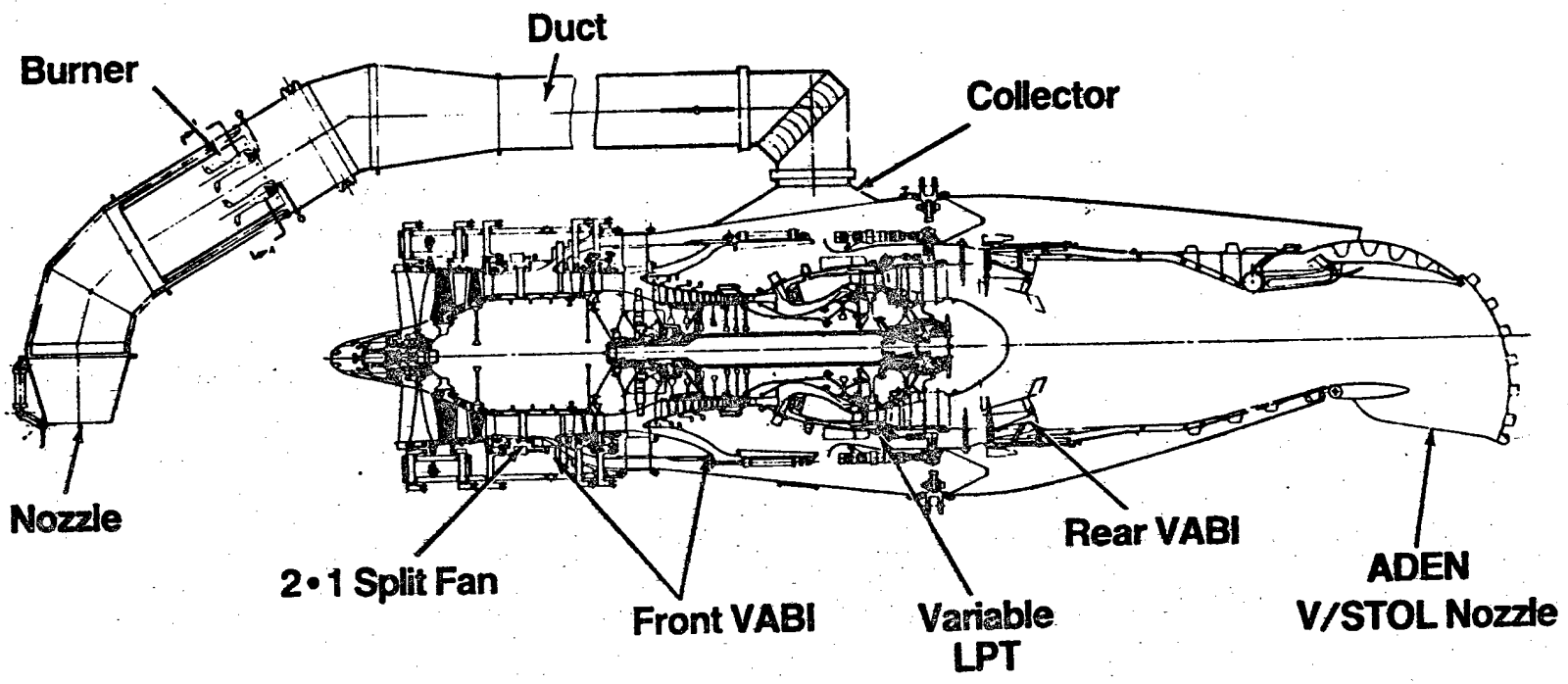

FIGURE 4.

PARAMETRIC ALTERNATE MISSION (STOVL)

- Parametric Escort Mission
  Weapon Load = 2200 lb (Retained)

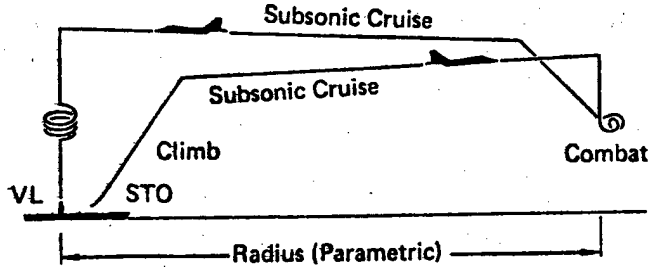

- Parametric Tactical Strike Mission
  Weapon Load = 3400 lb (Retained)

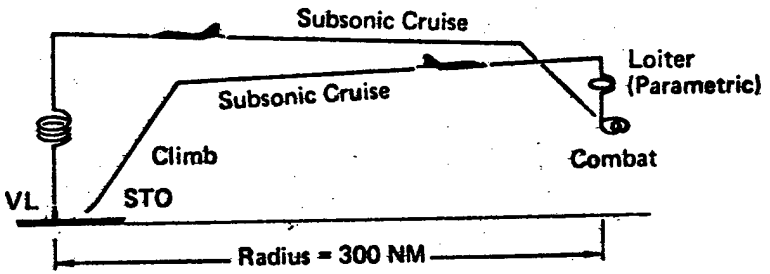

- Parametric Combat Air Patrol Mission
  Weapon Load = 2200 lb (Retained)

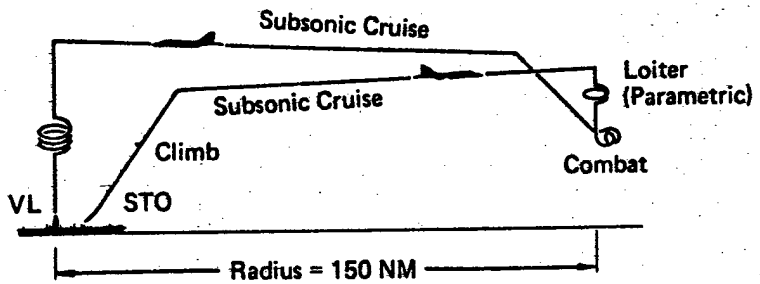

- Parametric Ferry Range Mission
  External Fuel Tanks Retained

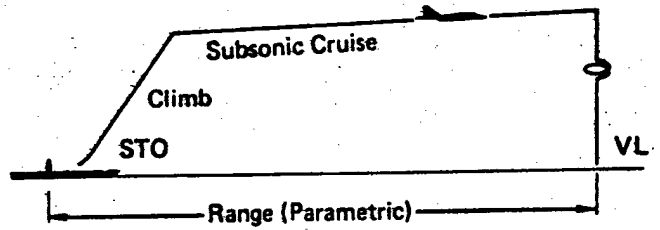

FIGURE 5.

ENGINE/AIRFRAME/REQUIREMENT INTERACTION – DLI MISSION

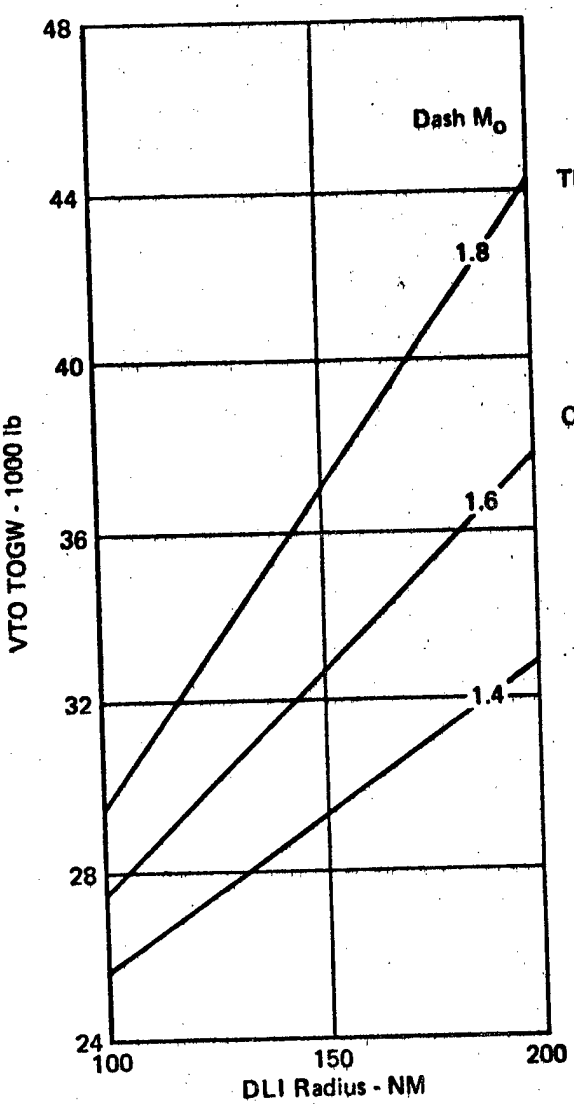

Thrust Sizing

- P_s = 750 fps at M_O = 0.90 and 10,000 ft
- n_z = 4.75 g at M_O = 0.65 and 10,000 ft

Optimized Variables

FPR = 4.0	W/S = 88 lb/ft^2
CPR = 6.6	LAM = 55°
ΔTamb = 50°	AR = 2.5
L/C VTO F_N = 55%-80% Max	

GP77-1058-28

FIGURE 6

VCE CYCLE PARAMETERS

ENGINE	BPR (Nominal)	FAN PR	CORE PR	OVERALL PR	TRIT (°F)		VCE Features
					VTO	Super Cruise	
Single Bypass	.50	4.00	6.0	24.0	2800	3200	Rear VABI, VALPT
Double Bypass	.50	4.00	6.0	24.0	2800	3200	Front & Rear VABI, VALPT
VF19 - A1	.67	4.65	6.0	28.0	3200	3000	Front & Rear VABI, VALPT RALS
- D1	1.00	4.00	7.0	28.0	3200	3000	Front & Rear VABI, VALPT RALS
- C1	1.25	3.35	8.4	28.0	3200	3000	Front & Rear VABI, VALPT RALS
VVCE-5 - D2	.95	4.00	7.0	28.0	3200	2835	Nominal Airflow Schedule
- D3	.95	4.00	7.0	28.0	3200	3000	High Airflow Schedule
- D4	.95	4.00	7.0	28.0	3200	2720	Low Airflow Schedule

FIGURE 7.

ENGINE AND AIRCRAFT DESIGN VARIABLES

	Engine Cycle Characteristics					Aircraft Design Variables		
L/C Engine Designation	FPR	BPR	OPR	Maximum TIT (°F)	VTO(3) Thrust/Weight	W/S (Combat)	Sweep (DEG)	AR
FCE-TF(1)	4.0	0.60	27	3180	6.7	88	55	2.5
VGTTJ(2)	-	0.00	13	2600	6.7	84	55	2.5
VCE-TF	4.0	0.50	24	3200	6.6	88	55	2.5
RALS/VCE	4.0	0.95	28	3200	6.4	88	55	2.5

Notes: (1) Obtained from GE parametric turbofan deck
(2) Obtained from GE parametric turbojet deck
(3) Based on 90°F day and 97% inlet recovery

FIGURE 8.

AIRCRAFT WEIGHT AND PERFORMANCE SUMMARY

			L + L/C Aircraft Designs			RALS/VCE Aircraft
		Requirements	FCE-TF L/C Engine	VGT-TJ L/C Engine	VCE-TF L/C Engines	
• TOGW	(lb)	–	32,650	29,100	29,600	33,900
• Internal Fuel	(lb)	–	10,600	9,100	8,960	10,100
• Mission Performance						
DLI Radius (Int Fuel)	(NM)	150/VTOL	150**	150**	150**	150**
Fighter Escort Radius†	(NM)	400/STOVL	555	580	598	570
Tactical Strike Loiter*	(hr)	2.0/STOVL	2.0	1.95	2.2	2.0
Combat Air Patrol Loiter*	(hr)	2.0/STOVL	2.8	2.75	3.0	2.7
• Combat Performance						
Acceleration						
Mach 0.8 to 1.6 at 35,000 ft	(sec)	90	84	89	78	52
Maneuver						
Mach 0.65 at 10,000 ft	(g)	4.75	4.75**	4.75**	4.75**	4.95
Specific Excess Power						
Mach 0.90 at 10,000 ft	(fps)	750	824	750	832	1,270

GP77-1056-6

†(2) 300 gallon tanks
*(2) 600 gallon tanks
**Sizing constraints

FIGURE 9.

LIFE CYCLE COST COMPARISONS – 900 AIRCRAFT

	L + L/C Aircraft			RALS/VCE Aircraft
	FCE-TF	VGTTJ	VCE-TF	
LCC (1976 Dollars)	19.466×10^9	17.642×10^9	19.077×10^9	18.668×10^9
TOGW (lb)	32,650	29,100	29,600	33,900
$F_{n_{SLS}}$ L/C (lbf)	16,465	13,880	14,783	23,975

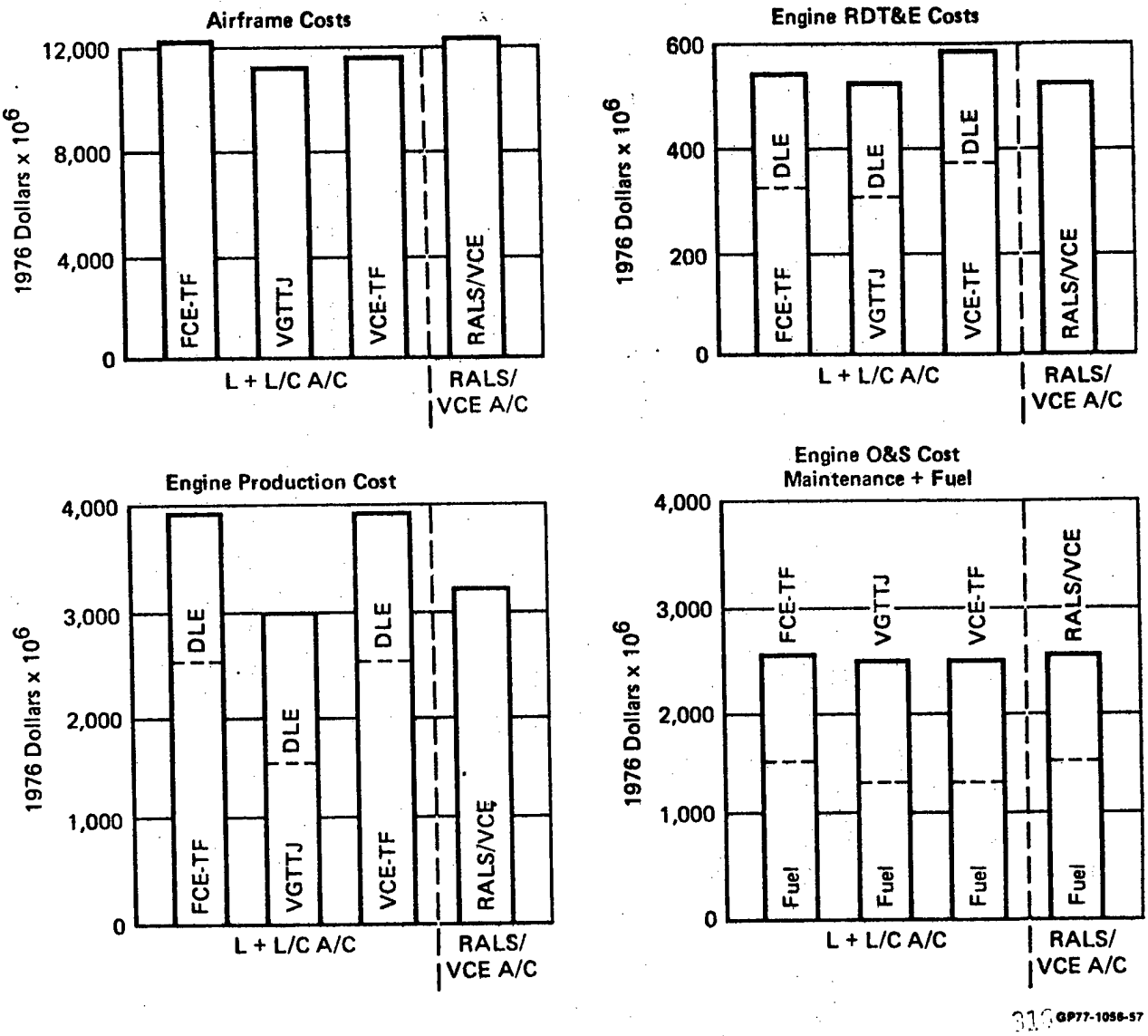

GP77-1056-57

FIGURE 10

RALS/VCE TRADE STUDY ENGINE MATRIX

RALS/VCE FEATURES	TURBINE ROTOR INLET TEMP - °F		
	3200	2900	2600
Double Bypass RALS/VCE-TF 1) Double Bypass & Forward Mixed 2) Variable Area LP Turbine 3) Rear Variable Area Bypass Injector VABI	A	B	C
Single Bypass RALS/VCE-TF 1) Single Bypass 2) Variable Area LP Turbine 3) Rear VABI	D	E	F
Single Bypass RALS/FCE-TF 1) Single Bypass 2) Rear VABI	G	H	I

FIGURE 11.

REMOTE BURNER PROGRAM SCHEDULE

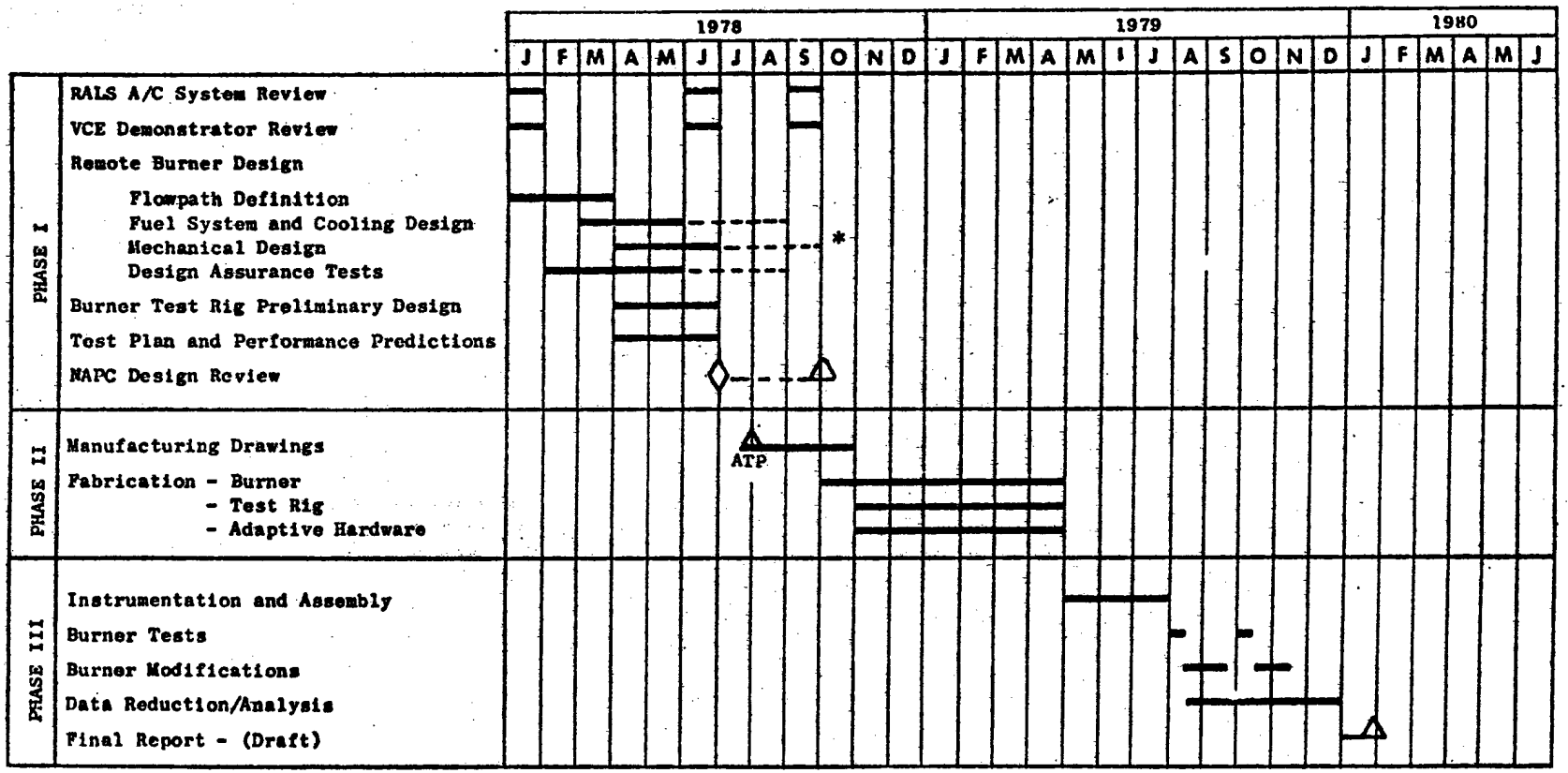

LIST OF SYMBOLS AND ACRONYMS

ADEN	-	Augmented Deflector Exhaust Nozzle
BPR	-	Bypass Ratio
CADE	-	Computer Aided Design Evaluation
CPR	-	Core Pressure Ratio
DDA	-	Detroit Diesel Allison
DLE	-	Direct Lift Engine
DLI	-	Deck Launched Interceptor
FCE-TF	-	Fixed Cycle Engine, Turbofan
FN	-	Net Thrust
FPR	-	Fan Pressure Ratio
FY	-	Fiscal Year
GE-AEG	-	General Electric, Aircraft Engine Group
LCC	-	Life Cycle Cost
L/C	-	Lift/Cruise Aircraft
L+L/C	-	Lift Plus Lift/Cruise Aircraft
NADC	-	Naval Air Development Center
NAPC	-	Naval Air Propulsion Center
OPR	-	Overall Pressure Ratio
Ps	-	Specific Excess Power
RALS	-	Remote Augmentor Lift System
SFC	-	Specific Fuel Consumption
SSS	-	Subsonic Surface Surveillance
STO	-	Short Takeoff
STOL	-	Short Takeoff and Landing
STOVL	-	Short Takeoff Vertical Landing
TOGW	-	Takeoff Gross Weight
TRIT	-	Turbine Rotor Inlet Temperature
T/W	-	Thrust to Weight Ratio
VABI	-	Variable Area Bypass Injector
VCE	-	Variable Cycle Engine
VCE-TF	-	Variable Cycle Engine Turbofan
VGT-TJ	-	Variable Geometry Turbine Turbojet
V/STOL	-	Vertical/Short Takeoff and Landing
VTO	-	Vertical Takeoff
VTOL	-	Vertical Takeoff and Landing
WA2C	-	Inlet Corrected Airflow
2-D	-	Two-dimensional

UNCITED REFERENCES

1. Variable Cycle Engine Evaluations for Supersonic V/STOL Phase II and Phase III Technical Report, McDonnell Aircraft Company, April 1978.

2. Variable Cycle Engine Evaluations for Supersonic V/STOL Fighters, Management Summary Report, McDonnell Aircraft Company, April 1978.

3. Variable Cycle Engine Evaluations for Supersonic V/STOL Fighters, Final Summary Report, General Electric AEG, to be published.

4. Variable Cycle Engine Study, Phase I Final Report, EDR 8695, Detroit Diesel Allison, February 1976 (C).

5. Variable Cycle Engine Program, Phase I, General Electric AEG, May 1976 (C).

6. Variable Cycle Engine Selection Program, Phase I Technical Report, McDonnell Aircraft Company, February 1976 (C).

7. Variable Cycle Engines for V/STOL Fighters, J. R. Facey and F. C. Glaser, AGARD 48th PEP, September 1976.

Biographical Sketch

Richard T. Lazarick was born in Philadelphia, Pennsylvania on May 12, 1949. He graduated from Brown University in 1971, receiving a B.S. degree in aerospace engineering. He is presently enrolled as a graduate student at Trenton State College in a Mathematics and Computer Science program.

In July 1968, he began working at the Naval Air Propulsion Center as a student trainee, beginning full time upon graduation in June 1971. His responsibilities as a project engineer in the large engine test group included engine qualification testing, data analysis and performance verification. He also was responsible for development of an engine health monitoring gas path analysis technique for the TF30 engine. In 1974 he was assigned to the Research and Technology Group where his responsibilities included diagnostic software development, diagnostic and control sensor development, digital electronic control development and computerized engine performance simulations. Mr. Lazarick's current responsibilities include engine performance and weight analysis technique development and monitoring of the propulsion aspects of advanced Navy weapons system studies, including the Maritime Patrol Aircraft.

Paul F. Piscopo was born in Trenton, New Jersey on May 27, 1947. He graduated from the University of Pittsburgh in 1969, where he earned a B.S. degree in aerospace engineering. He is currently attending Trenton State College where he is pursuing a Master's Degree in Mathematics and Computer Science.

In 1969, Mr. Piscopo joined the Naval Air Propulsion Center as a project engineer in the large engine test group. In 1971 he was assigned to the Research and Technology (R&T) Group where he was responsible for managing programs in computerized engine health monitoring and aircraft propulsion system survivability. In this capacity he served as a session Chairman at the 43rd AGARD/NATO PEP Meeting/Diagnostics Symposium, was originator and first Chairman of the Annual Tri-Service Engine Condition Monitoring and Diagnostics Meeting, and was Co-Chairman of the Joint Technical Coordinating Group for Aircraft Survivability Propulsion Committee. He has numerous publications in these fields. In 1976, Mr. Piscopo was assigned responsibility for the development and operation of the R&T Group's thermodynamic and engine mechanical design computer models used in the performance analysis studies of advanced Navy aircraft systems. He served as program manager of the VCE Selection Program Phase III effort and is program manager for the RALS/VCE Trade Study.

THE COANDA/REFRACTION CONCEPT FOR GAS TURBINE ENGINE EXHAUST NOISE SUPPRESSION DURING GROUND TESTING

BY

DOMINIC D. CROCE

PROPULSION DIVISION
GROUND SUPPORT EQUIPMENT DEPARTMENT

NAVAL AIR ENGINEERING CENTER
LAKEHURST, NEW JERSEY

THE COANDA/REFRACTION CONCEPT FOR GAS TURBINE ENGINE EXHAUST NOISE SUPPRESSION DURING GROUND TESTING

ABSTRACT

A new concept in ground run-up test exhaust noise suppression for aircraft turbojet/fan propulsion gas turbines has been developed by the Navy. The so-called COANDA/REFRACTION concept is based upon the Coanda Effect, an aerodynamic phenomenon which deflects the exhaust stream without mechanical devices, and the acoustic refraction characteristic of jet engine exhaust, by which noise refracts from the deflected stream into absorptive elements not in the exhaust flow.

Noise suppressors based upon this concept have been developed for ground run-up tests of out-of-airframe engines in test cells and in-airframe installed engines in complete aircraft acoustical enclosures (hush-houses).

These air-cooled suppressors represent a significant improvement in state-of-the-art equipment. Life-cycle costs are comparatively low for three reasons:

1. The initial cost is low because there are no requirements for supporting water injection equipment, piping and pumps.

2. Maintenance costs are diminished because the simplified design precludes the usual direct impingement of the engine exhaust on suppressor components.

3. Life cycle costs are minimized due to the elimination of requirements for cooling water and electrical power. This feature enhances energy conservation, as well as environmental pollution abatement aspects of the noise suppressor.

Results of the overall program of exploratory and advanced development phases include:

1. A "universal" configuration for demountable type test cell exhaust systems.

2. A "universal" configuration for retrofit of concrete, standard Class "C" test cells.

3. A working technology for designing a specific noise suppressor for any engine in any type test cell enclosure.

INTRODUCTION

One of the most important problems in ground testing of jet aircraft engines is the extremely high noise level energy radiated from the test location to endanger operating personnel hearing and disturb nearby communities. The intense noise levels produced by modern day high-performance jet aircraft is creating hazards, both physiological and psychological, unprecedented in the history of aircraft. To resolve the military aspect of this crucial, nationwide problem, the Navy has initiated a comprehensive developmental program to attenuate noise radiated by Navy/Marine Corps aircraft during ground run-up tests, preflight trim checks and pre-/post-maintenance out-of-aircraft engine testing.

Past equipment procurements and design studies have been limited to state-of-the-art hardware and technology, which have not yet been developed for prolonged durability against the adverse effects of engine exhaust; viz. high impact forces, excessive temperatures and entrained contaminants. These past Navy procurements of noise suppression equipment or test cell acoustic baffles have been diverse in origin and objectives, so that the existing fleet acoustic support gear is not interchangeable; it is specifically designed for only one engine, while the need exists for multi-engine usage; and it lacks commonality to permit a practical, efficient logistics plan for fleet support and replacement of deteriorating parts. Therefore, there are built-in replacement requirements of acoustic absorptive elements and disadvantages in state-of-the-art equipment which necessitate a substantial improvement in noise reduction technology.

Current ground run-up noise suppressors utilize in-stream turning vanes and perforated colanders to direct the horizontal, high temperature jet exhaust upward. This equipment requires heavy structures to withstand the jet exhaust forces. Most internal components (including acoustic absorptive baffles) are subject to deterioration and frequent maintenance.

Another necessary function of the ground run-up suppressor is to reduce the hot exhaust gas velocity to the extent that the noise created by the flow exiting from the suppressor is below the design criteria. In state-of-the-art equipment, the necessary energy transfer is accomplished by the use of perforated colanders to break up the flow and mix it with cooler induced air, or by injecting large volumes of water into the exhaust plume. Both of these methods are

poor for use with afterburning engines, because the flow damages suppressor components and because excessively large amounts of water are required to reduce the exhaust temperature to acceptable levels.

The proposed noise equipment suppression will incorporate design features to enhance transportability/interchangeability, durability, and complete frequency spectrum noise attenuation characteristics. The impact of such equipment on engine test facility design and logistics support planning is as follows:

1. reduction of structural requirements and expenses

2. no cooling water requirements at test sites

3. no need to support test facility with base water supply, especially at air stations in dry locations where water is a critical commodity.

4. a dry system will eliminate the visible plume and harmful fallout of "soggy soot" from proposed test cell exhaust stacks - this problem is prevalent in the vicinity of test facilities, where there are numerous complaints of damage to housing, ground support equipment and automobiles.

5. this feature is favorable for current, related efforts in test cell exhaust emissions pollution control programs.

The general features of the proposed systems are in advance of state-of-the-art hardware, to assure systems commonality for ease of maintenance, personnel instruction and logistics support.

CONCEPT DEFINITION

The COANDA/REFRACTION concept for jet engine exhaust noise reduction depends, essentially, on a combination of aerodynamic/acoustic phenomena which occur simultaneously downstream from the jet engine exhaust nozzle. The concept combines, for the first attempt in noise reduction applications, an aerodynamics phenomenon - the Coanda Effect - for jet exhaust bending/cooling without excessive structural requirements or turning vanes - and an acoustics principle - noise refraction by temperature/velocity gradients for low-frequency tuned absorption, unattainable with present-day acoustic baffles. The refraction principle occurs naturally in all jet engine exhaust streams, but the refracted noise

patterns are more predictable, for exploitation in noise reduction applications, in conjunction with jet sheet bending of the Coanda effect.

The acoustic energy will now be refracted out of the exhaust flow. Acoustically tuned resonant chambers for absorption of specific frequency bands can be located adjacent to the high energy exhaust flow resulting in a significant increase in operating life and providing a much needed method for attenuating low frequencies, which currently cannot be absorbed using state-of-the-art technology.

An additional feature of the Coanda Effect is that it is a natural fluid amplifier - the curved jet flow has a greater capability than normal jets for educting large volumes of ambient air from the immediate vicinity at the outer boundary of the deflected jet. In relation to jet engine testing this means that natural cooling of the superheated jet exhaust (caused by mixing and enthalpy exchange of educted ambient air with the rectangular jet core) is possible without the need for additional structural requirements of secondary air chambers. More important, it eliminates the need for cooling water and associated pump and piping systems.

The Coanda flow-turning technique makes use of a pressure gradient, due to the proximity of a surface to the jet, to cause the jet to turn. This means that there are no components in the flow to create jet exhaust stagnation temperatures and pressures. The deflection surface may be film-cooled with entrained air from cooling air slots along the surface.

The initial concept of a noise suppressor using the Coanda Effect and noise refraction principle is shown in Figure 1. This configuration consists of an adapter/transition section and a Coanda flow turning section. The adapter/transition section serves as an ejector -- it converts the round primary jet exhaust, mixed with entrained cooling air at the inlet, into a rectangular sheet of hot gases at its exit. The curved deflection surface then turns the rectangular sheet flow upward 90 degrees, while reducing the flow velocity and refracting a large portion of the internally generated noise downward and to the rear where acoustic resonant chambers are located.

A comparison of the proposed concept with state-of-the-art technology is presented in Figure 2. It will be found that, in addition to the improvement in operational characteristics, the relative size and component requirements

of the proposed system are less than presently available equipment.

A technical statement of the Coanda Effect, based upon the original work of Dr. Henri Coanda, a Roumanian aerodynamicist, is presented as follows:

A turbulent jet, exiting from a rectangular nozzle into an ambient fluid, entrains fluid from the ambient field. A surface placed near the exiting jet inhibits entrainment on that side of the jet, causing a low pressure region to exist between the jet and the surface. With a pressure gradient thus imposed across the jet, it deflects toward the surface, thereby decreasing the surface pressure even more, until the jet eventually attaches to the surface. If there is a step-gap between the jet and the deflection surface, a trapped vortex will form between jet and surface. This phenomenon is known as the Coanda Effect.

Coanda-deflected jets entrain greater quantities of secondary-air than undeflected jets. Due to the lower static pressure on the bounded side of the jet, the pressure drop across the nozzle is greater, thereby increasing the jet velocity on that side -- the velocity on the bounded side being equal to that of the undeflected jet. The resultant average velocity in the deflected jet is greater than the undeflected jet, assuming equal nozzle exhaust pressure. Consequently, the deflected jet also possesses greater average momentum and greater eduction pumping efficiency than the free-jet mixing capability. As a side-effect to this greater-mass-airflow-entrainment, Coanda flow enhances jet ejector operation with lower ejector exit temperatures.

PROGRAM OBJECTIVES

Based upon the obvious operational need for improved noise suppression equipment, and based upon the potential threat of reduced air defense capability due to non-availability of environmentally compatible engine test facilities, the Naval Material Command sponsored a multi-year comprehensive program of exploratory (R&D CAT 6.2) and advanced (R&D CAT 6.3) development phases.

Under the technical and administrative direction of Naval Air Systems Command, the Naval Air Engineering Center conducted the overall program. The objectives were:

1. To determine the feasibility and configuration

characteristics for applying the so-called Coanda/Refraction Concept to the attenuation of radiated engine exhaust noise from turbojet/fan engine ground run-up testing. The Concept was originally formulated by technically cognizant personnel from Naval Air Systems Command Headquarters and Naval Air Engineering Center.

2. To develop/define an advanced technology for noise suppression, based upon the Concept, which would be a workable technique for usage in future engine/aircraft test facility design projects.

3. To generate functional configurations for exhaust noise suppression systems, based upon the proven technology, which are compatible with Navy/Marine Corps operational procedures for in-airframe and out-of-airframe engine ground run-up tests.

PROGRAM TECHNICAL APPROACH

As a deflection technique for turbojet engine exhaust (mass airflow = 300 lbs/sec; temperature = 3000^{o}F), the Coanda Effect requires optimum geometric configuration of the transition/ejector section and the deflector surface. The transition/ejector device collects the circular jet flow in the bellmouth inlet and ejects it from a rectangular exhaust nozzle slot at the aft end. This rectangular-shaped jet sheet, configured in the form most conducive to efficient Coanda flow, attaches to a curved surface, or series of successively inclined flat plates, which is just downstream of the exhaust nozzle but separated from the nozzle slot by step-gap spacing at the lip of the nozzle slot. This turns the flow into an eddy, or vortex, which generates a low-pressure zone, causing the stream from the slot to bend and thus follow the contour of the deflection surface.

Thus the need is eliminated for massive structural frames to withstand jet impact forces and support turning vanes. Film cooling of the deflection surface by educted ambient air eliminates requirement for water spray rings and associated piping, since the hot exhaust jet does not touch the surface. The mixing of large quantities of ambient air with the original jet greatly dissipates the total energy in the flow, and allows for light-weight acoustical panels for reduction of the characteristic noise spectrum to satisfactory levels.

Research investigations were directed toward refining

this flow phenomenon into a configuration to meet the extreme mass airflow and temperature requirements of jet engine exhausts. A stable Coanda flow effect depends on the appropriate adjustment of many factors, including the texture of the deflecting surface. The primary factor is the maintenance of the balance between the centrifugal force and the suction force as the stream flows from the afterbody of the nozzle around the shoulder. Particularly crucial for this balance is the slot aspect ratio of nozzle exhaust jet sheet width to thickness. It is this ratio which establishes the rectangular dimensions of the nozzle slot, which makes possible the attachment of the jet sheet to the deflector surface.

The initial phase of the overall program technical approach was an exploratory development effort to determine feasibility of the concept application to noise reduction and to conduct initial configuration sizing studies. This work consisted of analytic studies/calculations and breadboard hardware experiments. The theory equations, scientific assumptions and Navy noise suppression requirements were considered in the analytic studies to define feasibility and to determine possible limitations in future designs or operating characteristics. Results and conclusions from these analyses were integrated with an experimental sequence utilizing breadboard, parametric, one-sixth scale models to verify initial calculations and to experimentally demonstrate the feasibility of adapting the two scientific principles to resolve the military problem of engine ground run-up noise reduction. The model test plan consisted of using simulated engine air flows and real temperatures in conjunction with scaled, parametric configurations of Coanda adapters and Coanda curved deflection surfaces to determine the optimum set of adapter/deflector most conducive for jet bending and noise reduction. Dimensions for these parametric models were derived during the initial configuration sizing studies.

The first four model tests were to establish the feasibility of using the Coanda flow turning and resulting noise refraction principles in a jet deflector/noise suppressor and to improve the system cooling and flow attachment. The first model test configuration is shown on Figure 3. The first model test was a parametric test with model variations such as transition ejector area ratio, exit aspect ratio, Coanda surface radius, and cooling slot size. The analytical study output was used to determine the ranges for these parameters to assure a span that encompassed the optimum value for each parameter. The results of this test were used to size following models.

The second, third, fourth and fifth series of tests were conducted on the experimental configurations shown in Figures 4 and 5. It can be seen that an iteration in design improvement takes place between successive models in an attempt to streamline the internal model surfaces and eliminate "square" corners were gas flow stagnation zones may develop.

The second scale model incorporated staged ejectors as a means of improving Coanda surface temperatures. The effect of Coanda surface sidewall configuration was also studied.

The third model test configuration reduced the staged inlet ejectors from three to two while returning to a transition of the flow within the ejectors from round to rectangular at the Coanda entrance. The ejector area ratios were also reduced from that of the previous test. An enclosure with inlet panels was provided to determine the effect on flow attachment and system cooling. The enclosure and inlets were not acoustically treated.

The fourth model test configuration incorporated what was learned from the results of the previous tests relative to flow transitioning, system cooling, and flow attachment.

The fifth model test objective was to isolate and measure the individual system noise sources to determine the necessary acoustic treatment configuration. Four possible noise sources were studies:

1. Noise transmitted through the walls

2. Noise emitting from the secondary air inlets

3. Noise refracting out the exhaust opening from inside the enclosure

4. The residual noise generated beyond the exit by the exit flow.

Based upon the results of all previous tests, the final model tests were conducted on a design which represented a progression of flow streamlining attempts relative to ejector and deflector geometry. The curved surface was a byarithmic spiral radius of curvature instead of a continuous radius. This final model design, shown in Figure 6, represented the acceptable geometry, which would be developed as the full-scale experimental model, and which had been successively "formed" to accommodate the J52, J57 A/B, J79 A/B, TF30,

TF30 A/B and TF41 engines. All these engines exhaust parameters were simulated during each series of model tests to assure all engine compatibility.

The model configuration shown in Figure 7 is the experimental set-up for the aircraft run-up enclosure (Hush-House) series of tests. In order to allow for the physical properties of single, as well as dual, engine aircraft, this flat-plate type ejector system was developed as another advanced technology feature to assure that the Coanda/Refraction concept was adaptable to the complex geometrical requirements of a "universal" exhaust system for a multi-aircraft Hush-House.

The full-scale Coanda/Refraction exhaust noise suppressor system resulting from all the previously discussed analytic and experimental studies was approximately 49 feet long, 23 feet wide, and 40 feet high to the top of the exhaust stack. A further reduced size design, which is recommended for deployment as a standard "universal" suppressor system (for the range of engines previously denoted), is 46 feet long, 15 feet wide, 14 feet high with an exhaust stack height of 40 feet.

Principal components of the suppressor system are the jet deflector system and the acoustical enclosure building.

Within the basic building, the jet deflector system consists of the three-stage ejector, Coanda surface, and support structure. This assembly is shown on Figure 8. All components were fabricated from A36 mild steel. The forward end of the Coanda surface is supported on the ejector stand. The Coanda surface and ejectors contain provisions for thermal growth. The Coanda surface is segmented in three sections for handling ease and supported by a tripod assembly.

The Coanda exhaust system full-scale test setup is shown on Figure 9. The configuration consists of the Coanda exhaust suppressor and J57-P-21 afterburning turbojet test engine.

The final assembly is shown in Figure 10. Since the forward protion of a test cell would normally have the engine enclosed and suppressed, an 18-foot acoustically treated barrier was erected to block engine case and inlet noise radiated into the far field.

Air inlets are required to provide cooling air to the ejectors and Coanda surface to maintain temperatures below 1000°F.

The design of the enclosure walls, to prevent acoustic transmission at low frequency, was one of the more important technical challenges of the program. Using strictly mass to prevent low frequency acoustic transmission would make the modular construction required of a demountable unit somewhat untenable. One might use less mass, but line the interior of the enclosure with sound absorber to lower the interior acoustic levels, but this would be very costly. The scale model results indicated interior lining was not required to meet far field noise goals if the acoustic energy transmission through the structure could be eliminated. The enclosure walls and ceiling design consist of a double-walled steel panel system weighing 20 pounds per square foot. The outer wall is constructed from one-quarter inch steel flat panels attached to 8-inch deep channel frames. The inner wall is constructed from one-quarter inch steel panels, vibration isolated from the channel frames with neoprene isolators. Inner and outer panel sizes were chosen such that their resonant frequencies are less than 30 Hz. This ensures that the panel will be in the mass low frequency range at the lowest frequency of interest (63 Hz octave band). The 10-inch air gap is sealed. The combined double-wall structure with confined air gap exhibits transmission loss characteristics superior to an equivalent 20 lb/ft^2 single-wall structure.

At the time of preparation of this paper, the final series of tests on the Hush-House exhaust system are being initiated. Based upon the success of the initial series, it is expected that a "universal" configuration and an aircraft system design configuration handbook will be developed satisfactorily.

APPLICATIONS

As a result of the final analytic design studies, functional noise suppression systems configurations have been identified for usage in ground run-up test facilities for Navy/Marine Corps turbojet/fan engines and certain fighter/attack aircraft. These systems are also applicable in the present design form to Air Force engines and aircraft which are the same types but which differ only in model number from their counterparts in the Navy inventory.

The standard "universal" exhaust system for prefabricated demountable type test cell is shown in Figure 11. This configuration is specifically designed to accommodate the exhaust airflow, temperature and pressure ratio parameters of the J52, J57 A/B, J79 A/B, TF30, TF30 A/B and TF41 engines. It is noted that the rear wall of the test cell engine enclosure

is the forward wall and ejector inlet plane of the exhaust system.

Figure 12 shows the standard "universal" configuration which has been developed specially as a retrofit for replacement of deteriorated water-injection-type exhaust systems for the Navy standard concrete class "C" test cell.

In addition to these design configurations, a working technology has been formulated and presented in a Design Configuration Handbook. This technology is adequate for designing a specific "tailor-made" noise suppressor for any engine, or closely-related group of engines, in any type of ground run-up test cell enclosure, including Navy/Air Force test cells, Naval Air Rework Facility test cells (which have a variety of non-standard, unique configurations), commercial airlines engine test cells and engine manufacturers test cells. This is considered essential for design studies leading to a configuration for larger, high by-pass ratio turbofan engines, as well as the "Pegasus" or F-402-401 engine for the Harrier aircraft.

For complete aircraft ground run-up tests (in-airframe installed engines), a standard design configuration has been developed as a result of analytic studies, scale model tests and design studies. This exhaust system for aircraft run-up enclosures (Hush-Houses) is shown in Figure 13. Here again, the exhaust system attaches to the rear wall of the standard aircraft acoustical enclosure. The range of Navy/Marine Corps single and dual engine aircraft for which this exhaust system configuration has been developed includes A-4, A-6, A-7, F-4, and F-14. Exhaust systems for other Navy, Marine Corps and Air Force aircraft types can be readily designed by using the technology from the Design Configuration Handbook.

The hush-house exhaust system differs from the test cell exhaust system with respect to the basic transition/ejector configuration. Instead of the round-to-rectangular ejector geometry of the test cell system, the hush-house system incorporates an advanced technology flat-plate type ejector configuration. This approach was originally tested on the scale-model experimental set-up shown in Figure 7. The advantages are that the flat-plate ejectors are less sensitive to aircraft tailpipe movement during power-change surges of ground run-up tests, and dual-engine, as well as single-engine, aircraft can be accomoodated on the same exhaust system without unnecessarily stringent and painstaking aircraft alignment/positioning. The flat-plate

system also assures that the mixed flow from two distinct exhaust nozzles of twin-engine aircraft (e.g. one engine at idle power and one engine at afterburner) will attach to the curved surface and deflect upward.

Hush-house exhaust noise suppressor systems for use during ground run-up tests or in-airframe installed engine pre-flight trim checks for commercial airlines and aircraft manufacturers can also be readily designed by using the technology from the Design Configuration Handbook.

OTHER PROPULSION APPLICATIONS

The Coanda Effect is an aerodynamic phenomenon of jet sheet bending which occurs when proper exhaust nozzle geometry and deflection surface orientation are favorable relative to exhaust flow parameters. In addition to the fluid amplification benefits, propulsive and dispersive resultant forces are induced upon the ambient atmosphere by Coanda-flow deflected jets.

Propulsive Wing - a current aircraft being developed by the Boeing Company for the U. S. Air Force features a Coanda-type wing/engine arrangement for additional thrust in short landing situations. This is similar to the Navy propulsive wing developmental studies program. A reconfigured jet exhaust nozzle is oriented over the wing which has a large curved-effect flap. The resultant thrust force is directed upward. This is exactly opposite to the noise suppressor system where there is a force directed downward along the specially located deflection surface support sheet.

Aircraft/Missile Exhaust Dispersion - a Coanda-type exhaust nozzle has potential for cooling and dispersing the hot exhaust flow from aircraft and missiles, thereby reducing the threat from enemy heat-seeking missiles. An exhaust configuration is feasible, which would cool the exhaust immediately downstream of the propulsion system and deflect the remaining heated gas away from the aircraft.

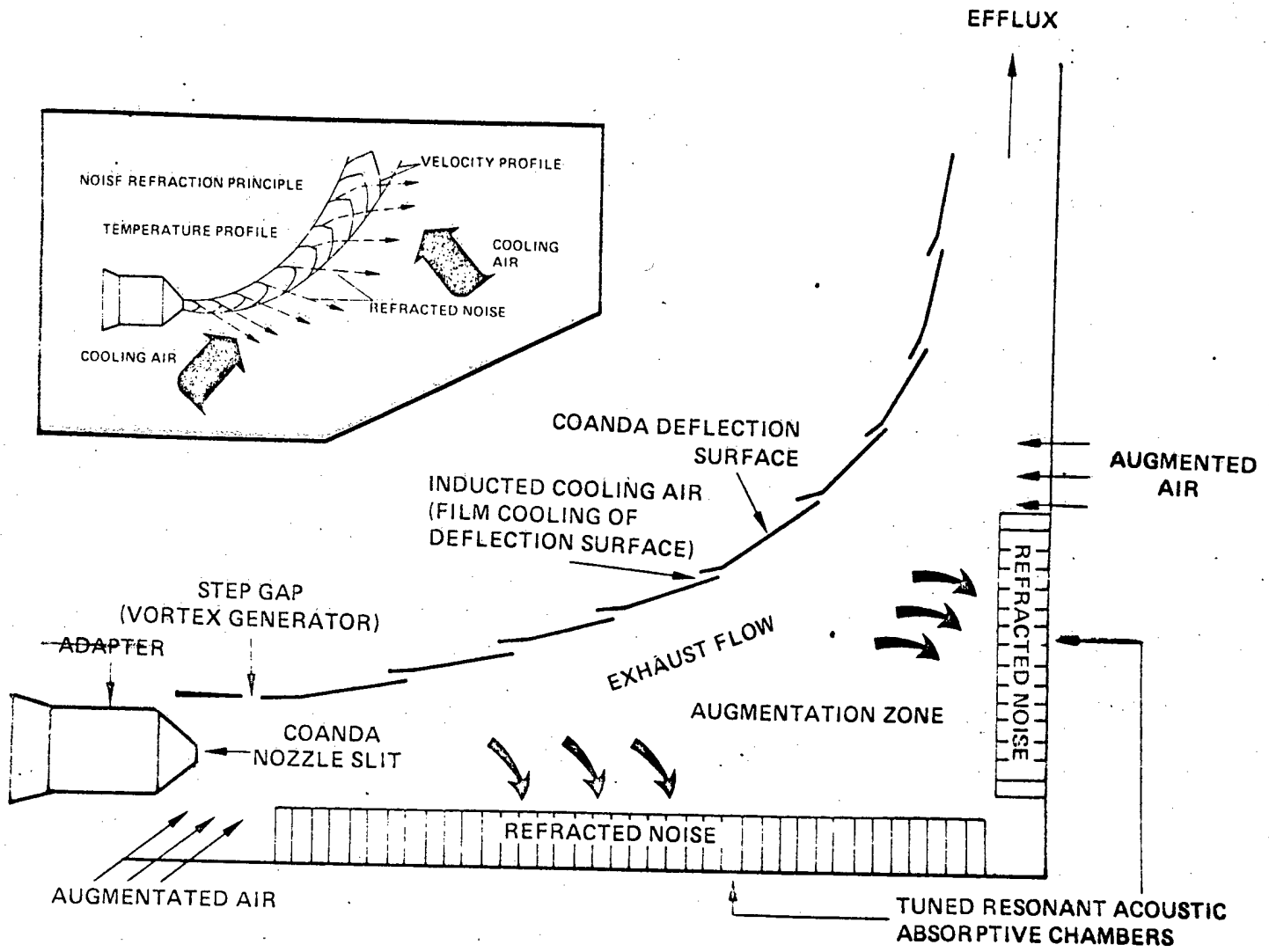

FIGURE 1. THE COANDA/REFRACTION NOISE SUPPRESSION CONCEPT

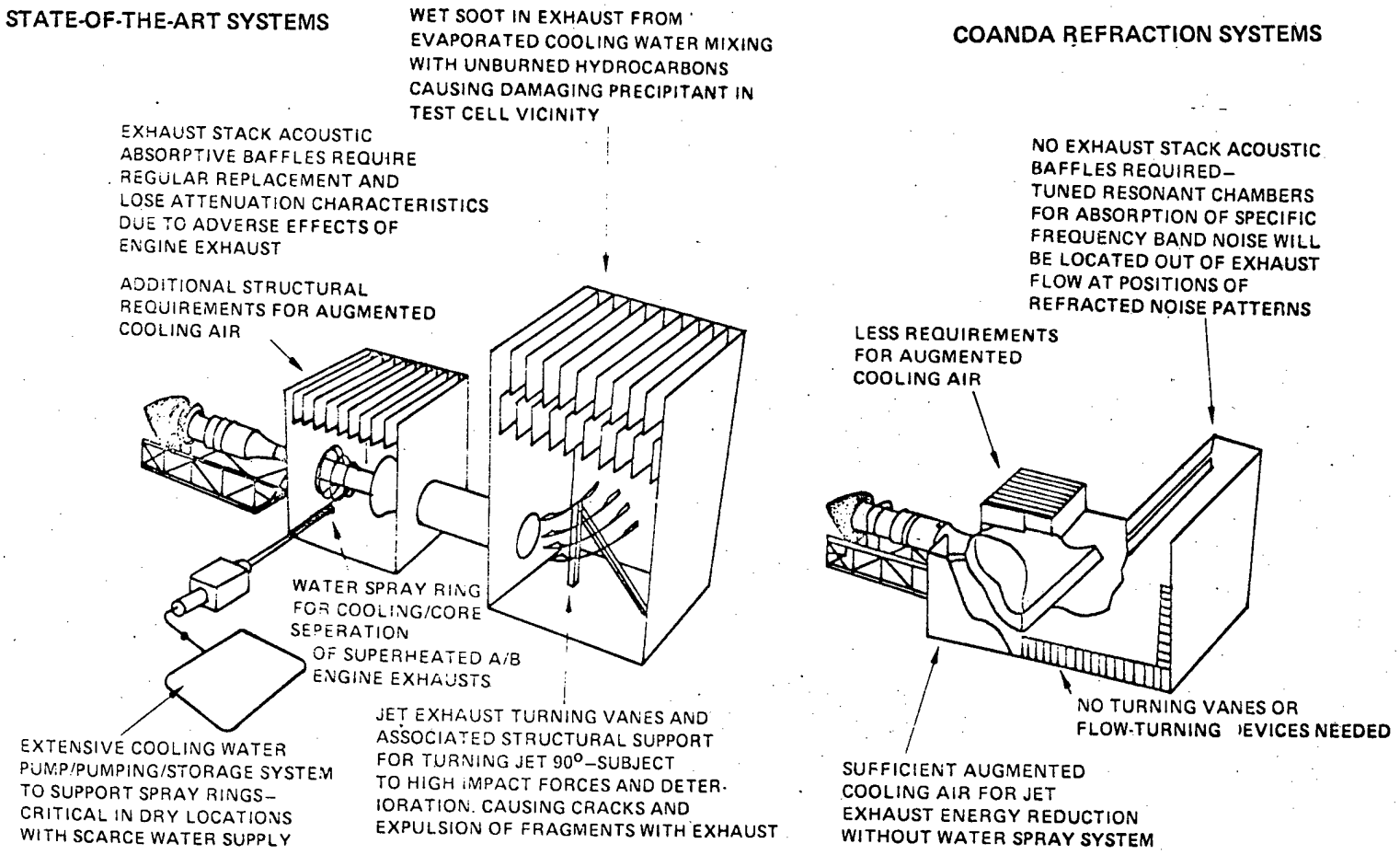

FIGURE 2. Comparison of State-of-the-Art and Coanda/Refraction Noise-Suppression Systems

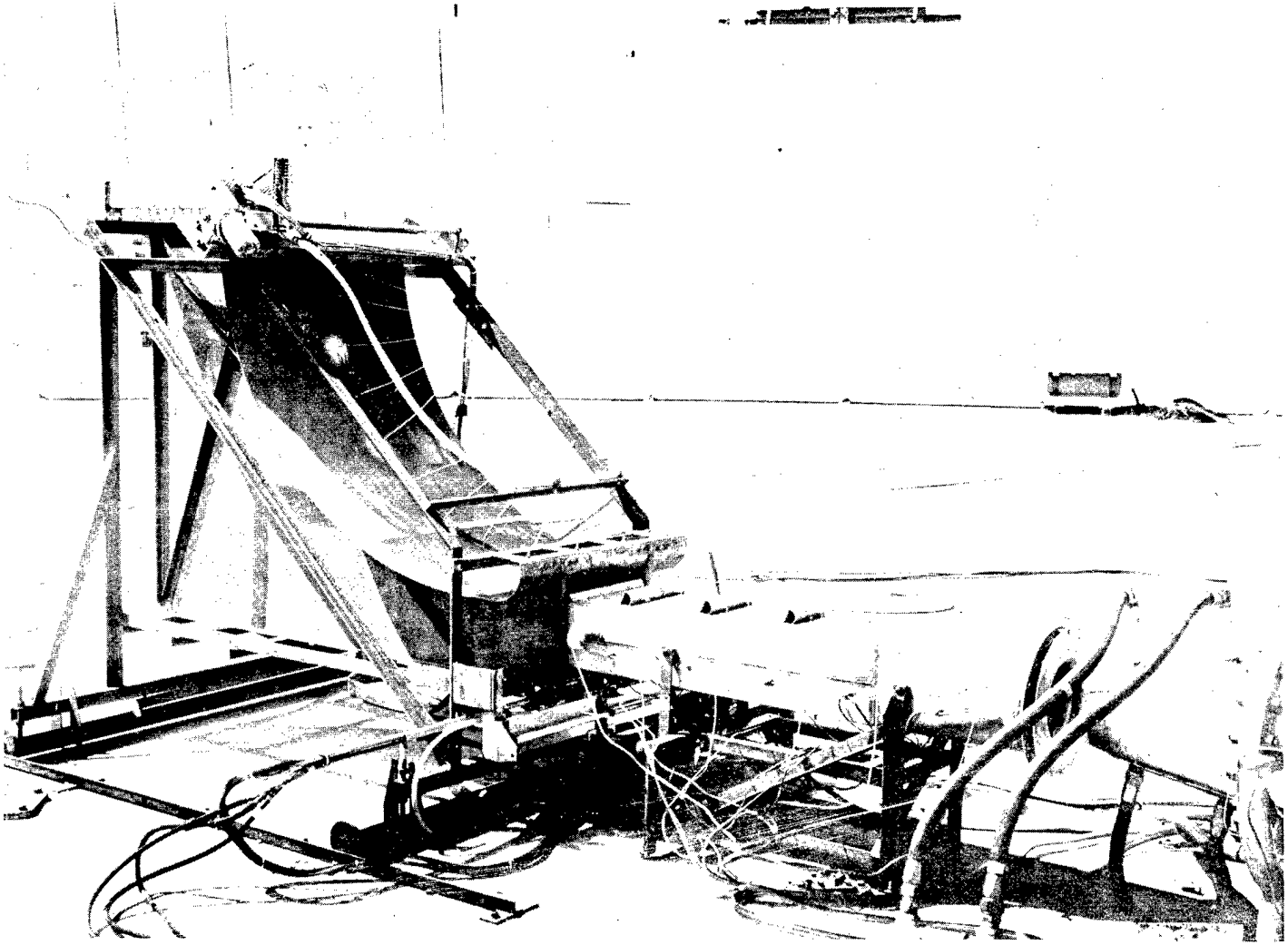

FIGURE 3. INITIAL STUDIES "SQUARE-EDGE" PARAMETRIC MODEL

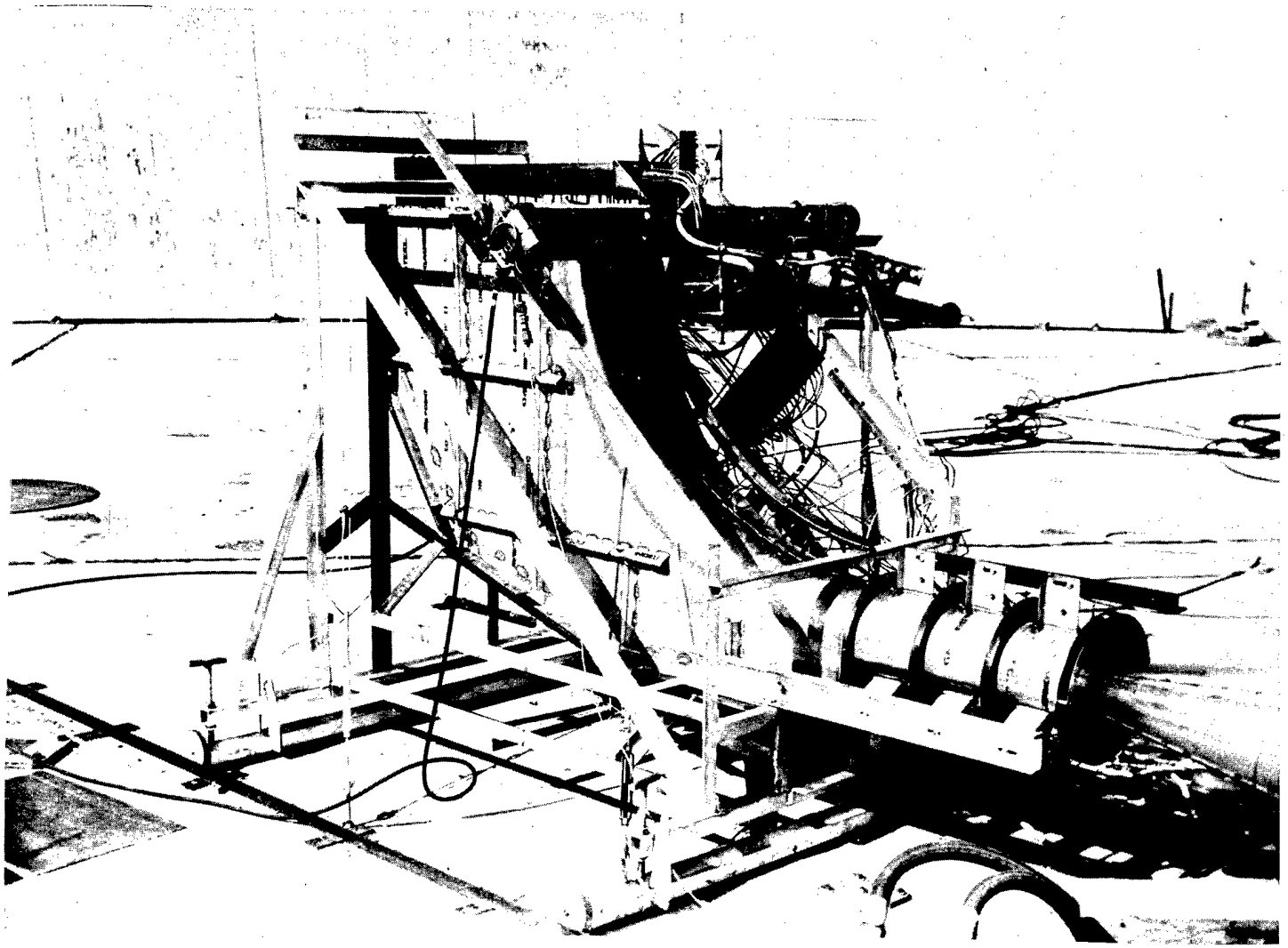

FIGURE 4. STREAMLINED MODEL EJECTORS AND DEFLECTOR

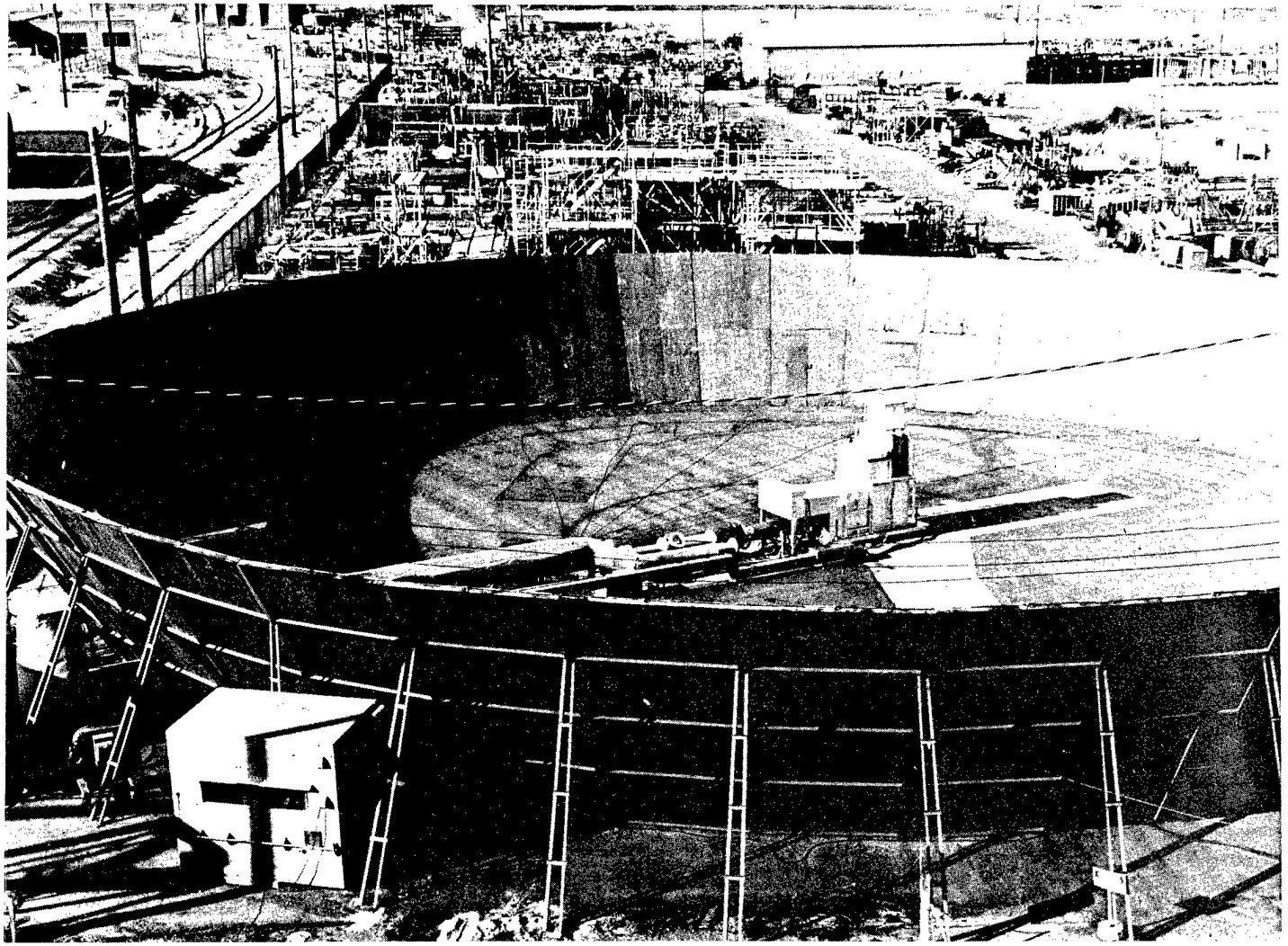

FIGURE 5. MODEL TEST ARENA SHOWING TEST CELL MODEL

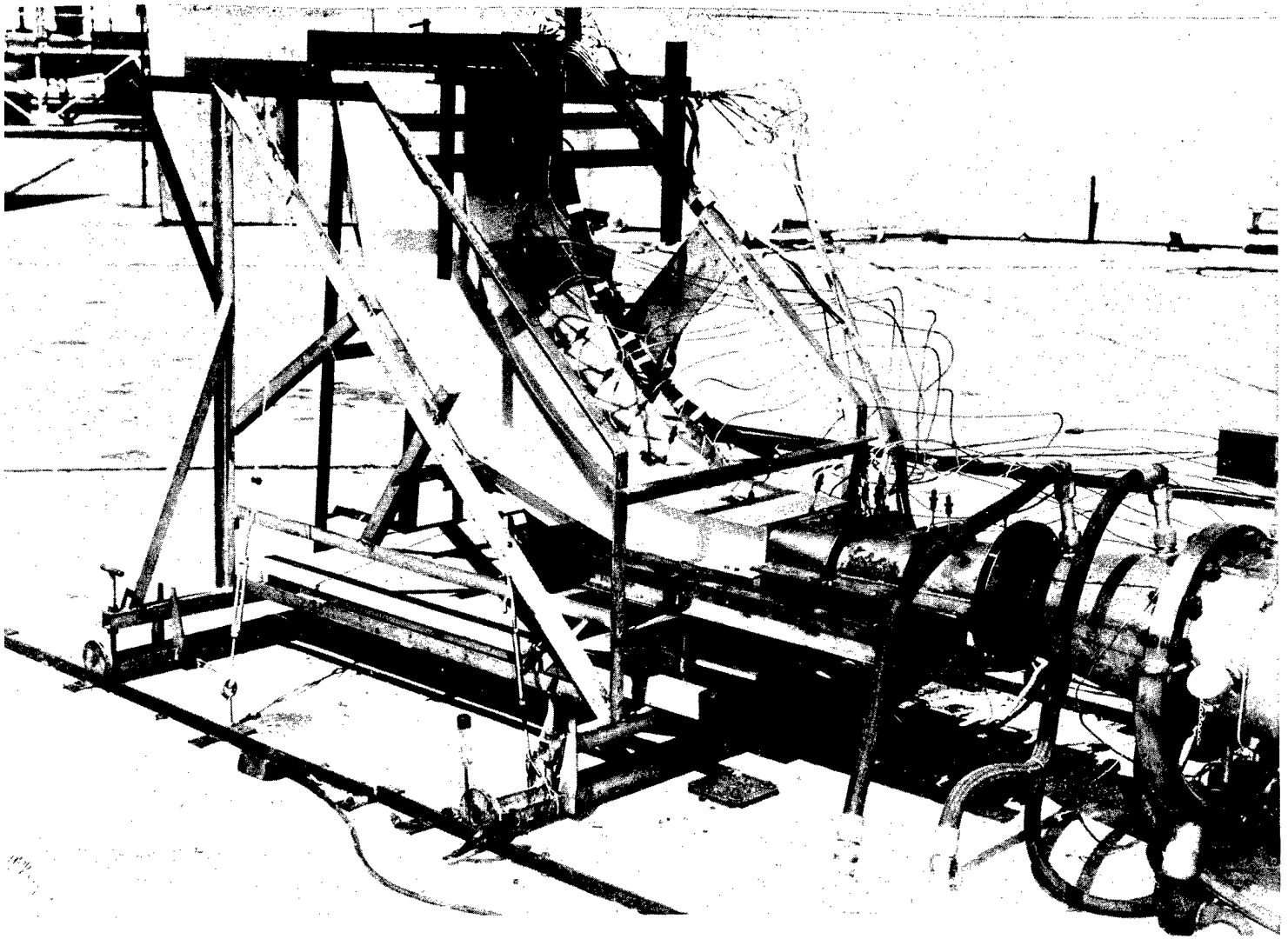

FIGURE 6. FINAL SCALE-MODEL CONFIGURATION - LOG SPIRAL RADIUS

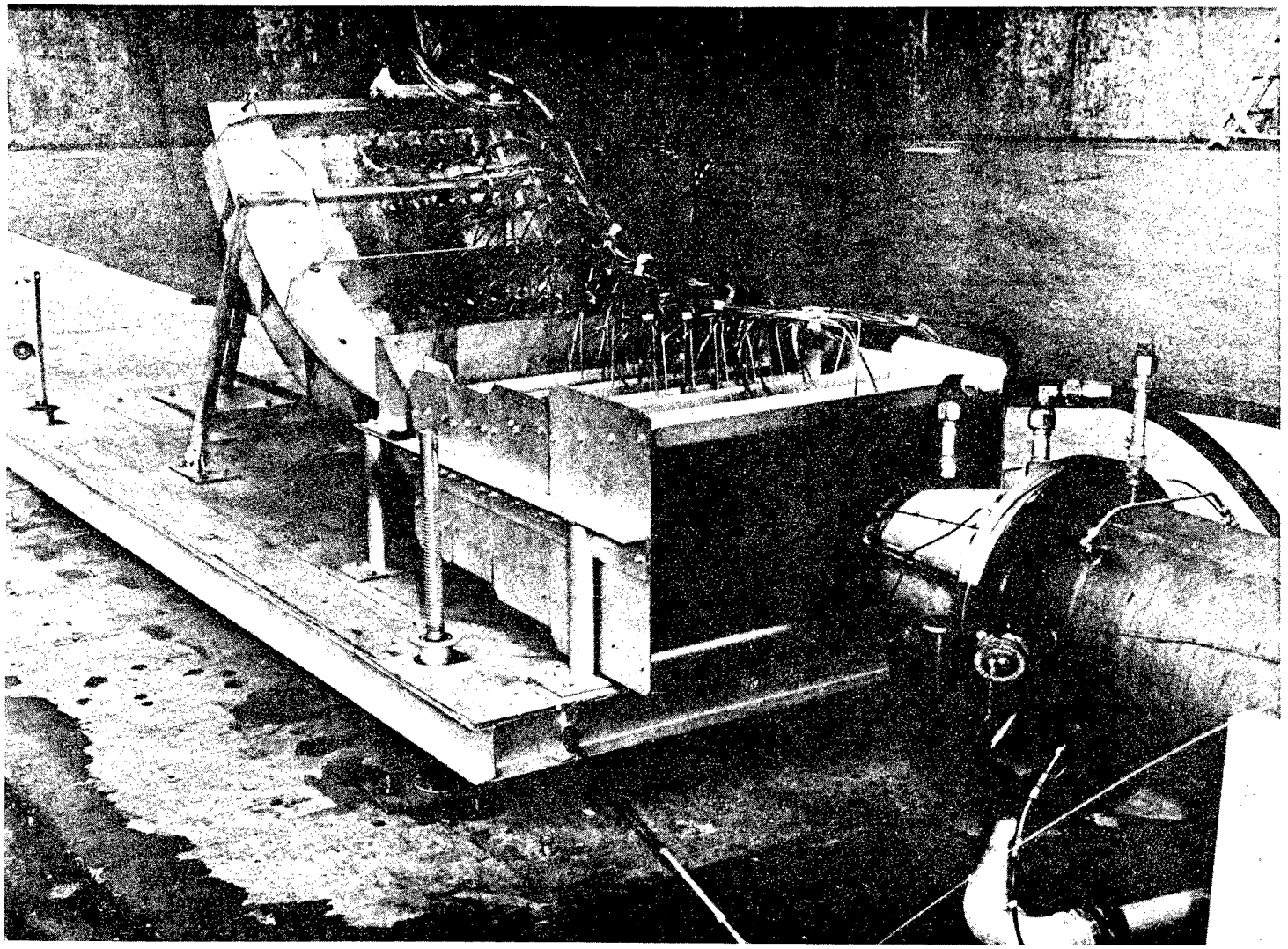

FIGURE 7. AIRCRAFT SYSTEM FLAT-PLATE EJECTOR MODEL

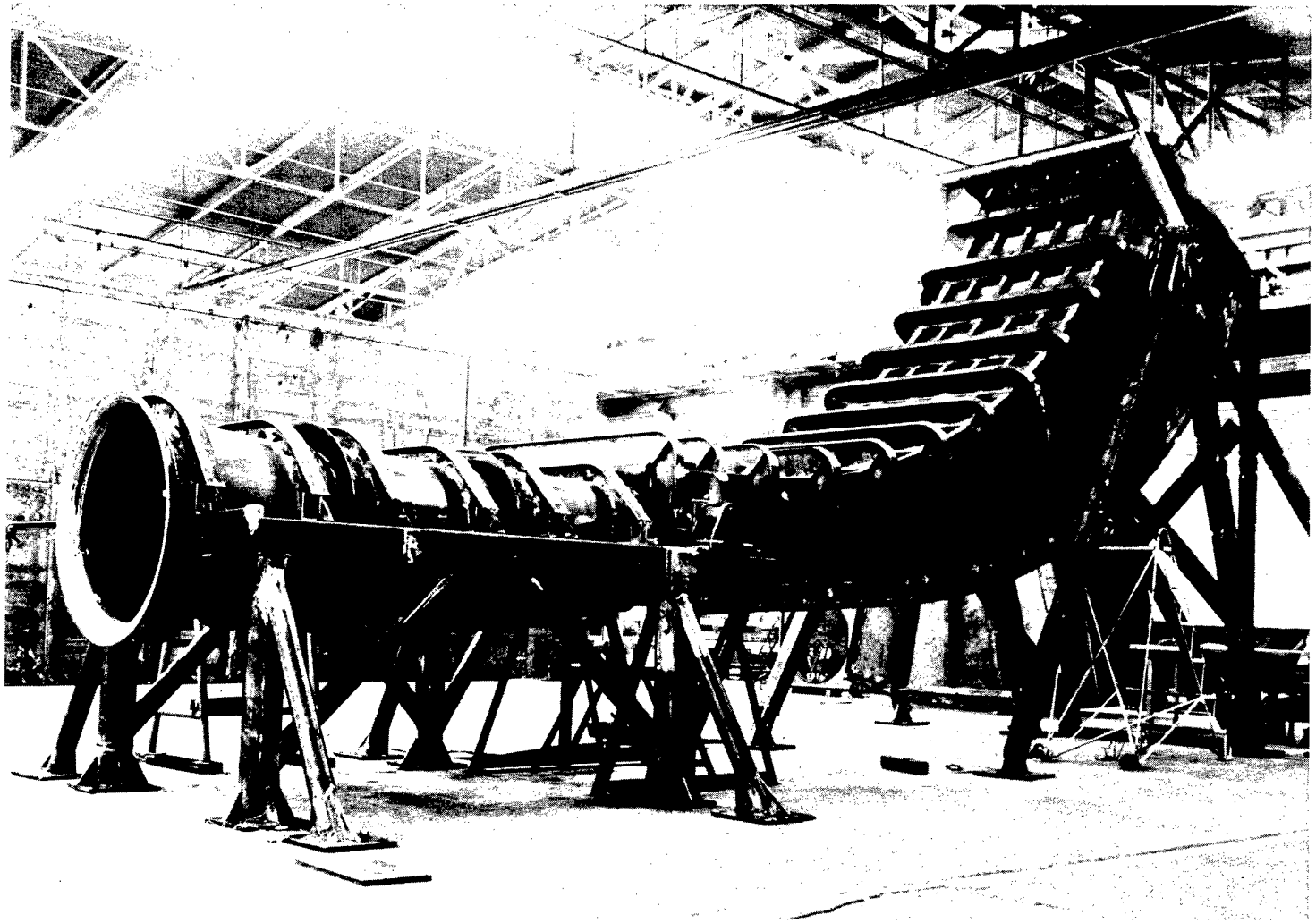

FIGURE 8. EJECTORS AND COANDA DEFLECTION SURFACE.

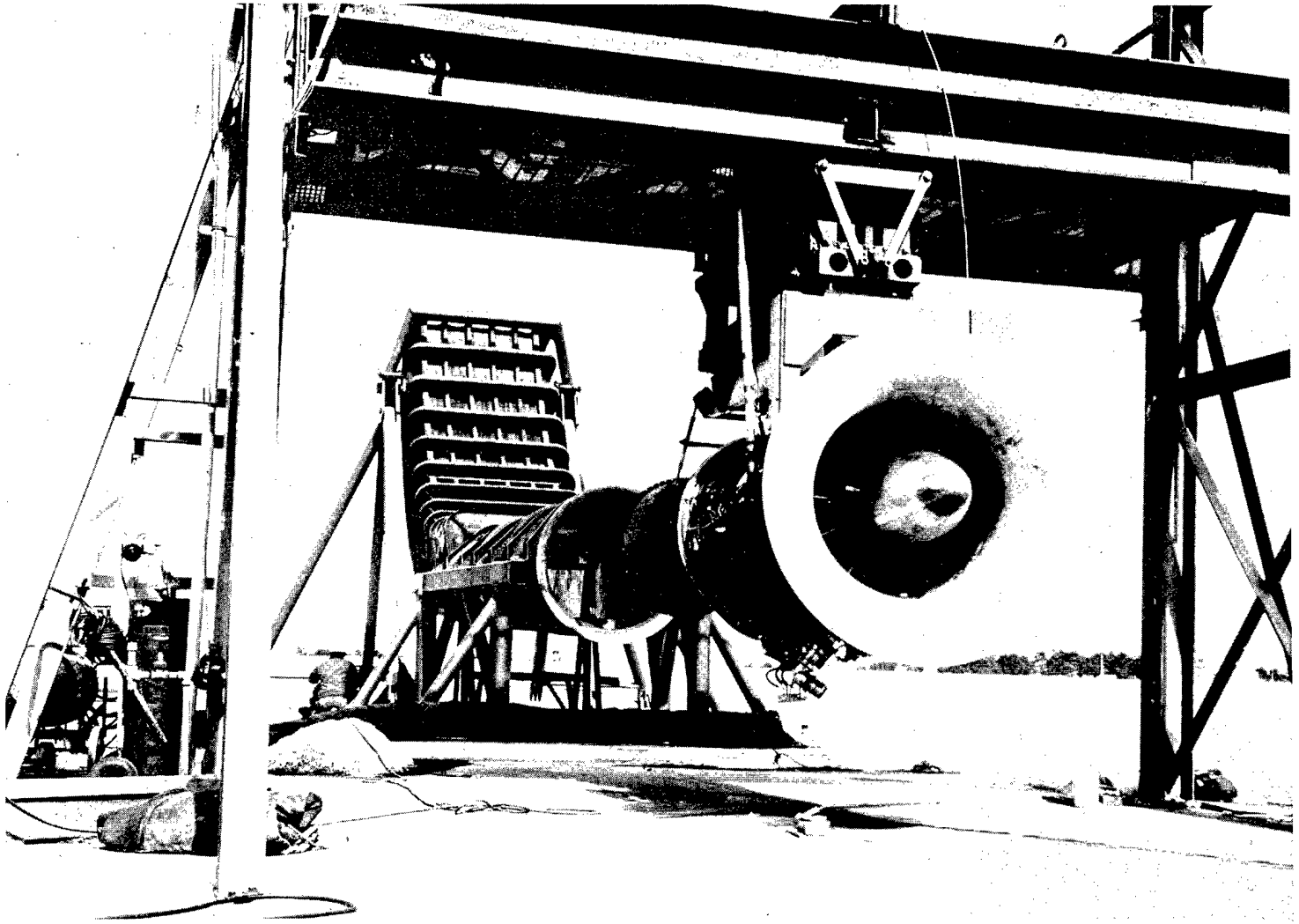

FIGURE 9. J57 A/B ENGINE ALIGNED WITH EJECTORS/DEFLECTOR

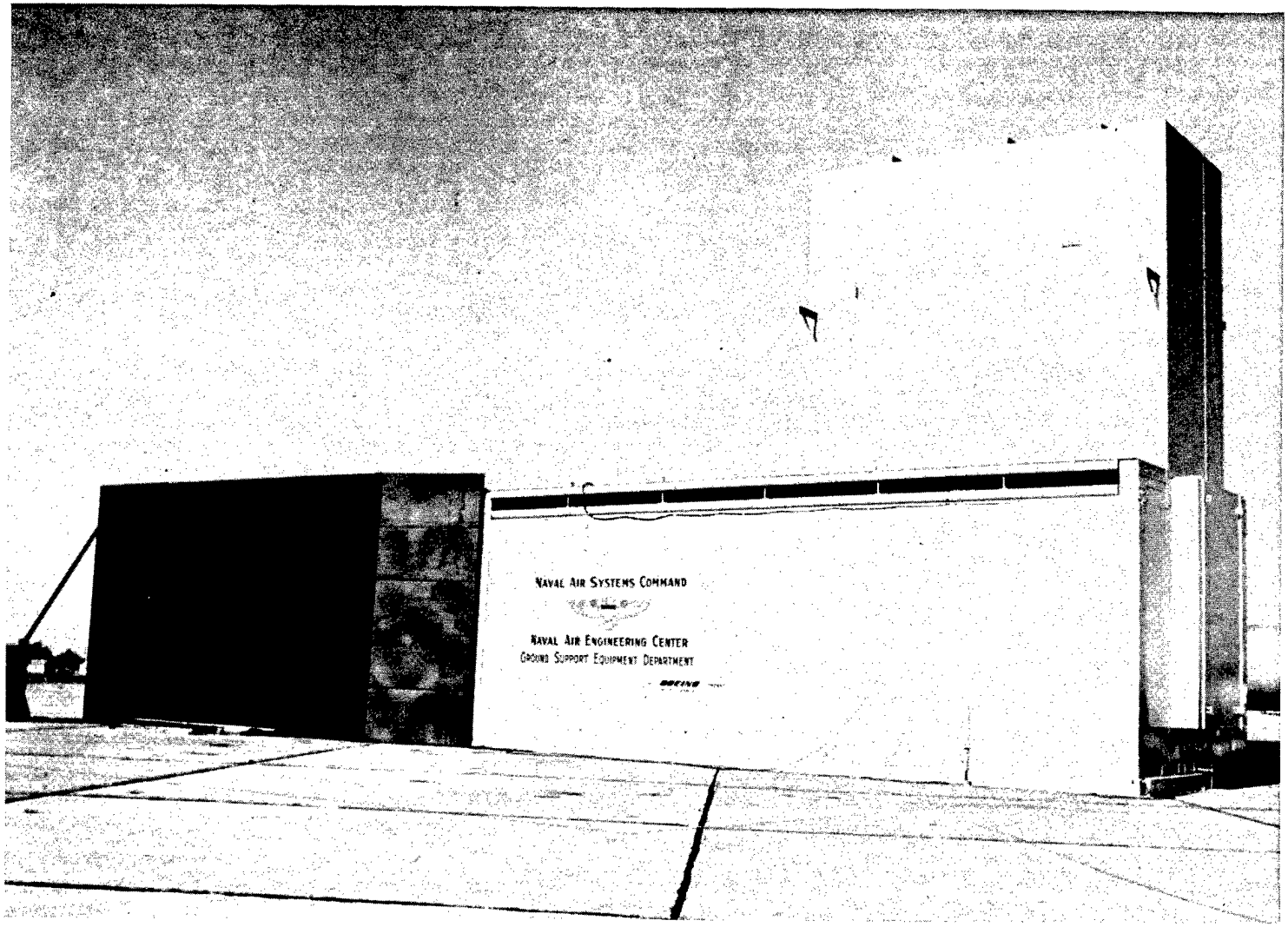

FIGURE 10. FULL-SCALE EXPERIMENTAL MODEL ASSEMBLY

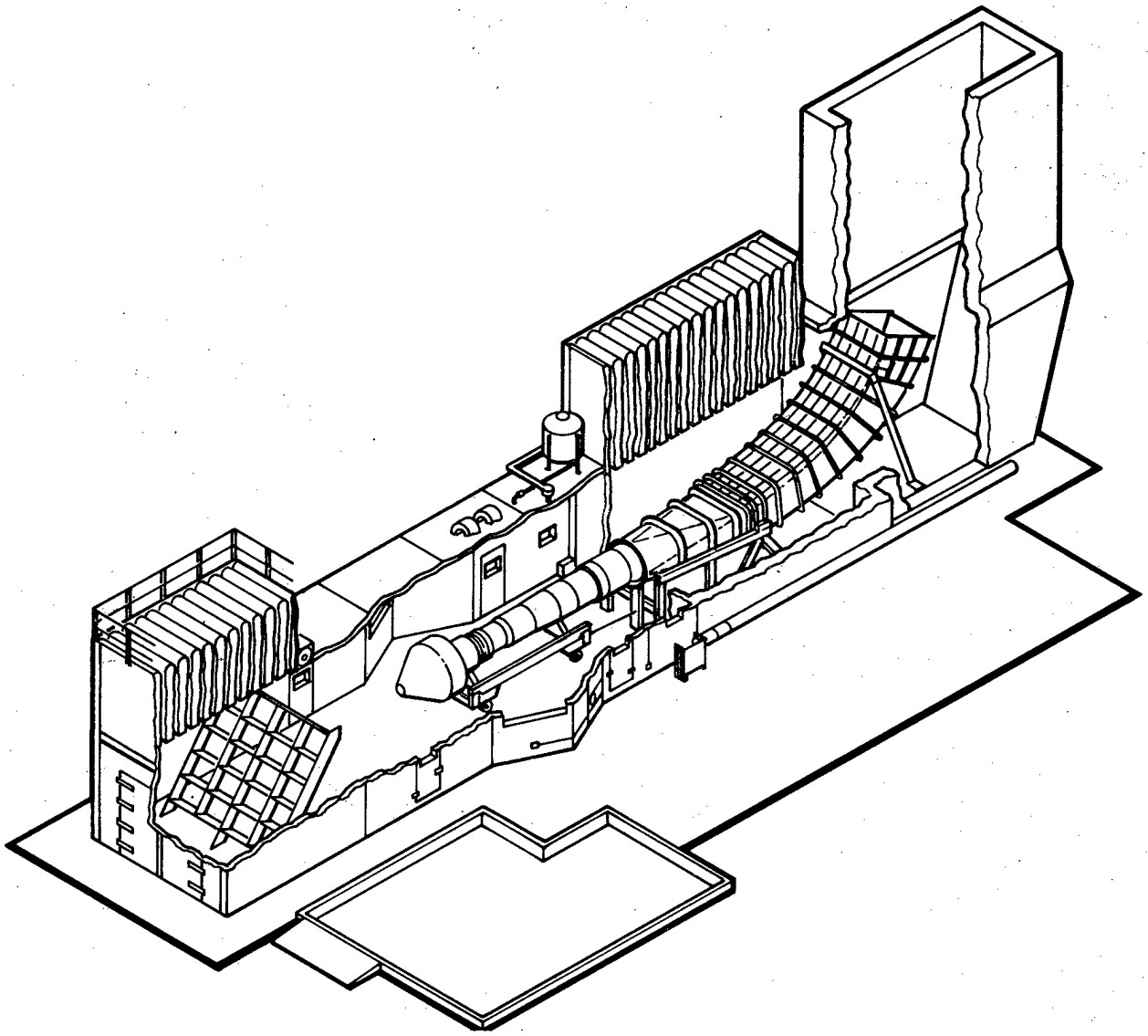

FIGURE 11. TEST CELL "UNIVERSAL" EXHAUST SYSTEM

"C" CELL INSTALLATION
NOISE SUPPRESSOR SYSTEM
COANDA/REFRACTION

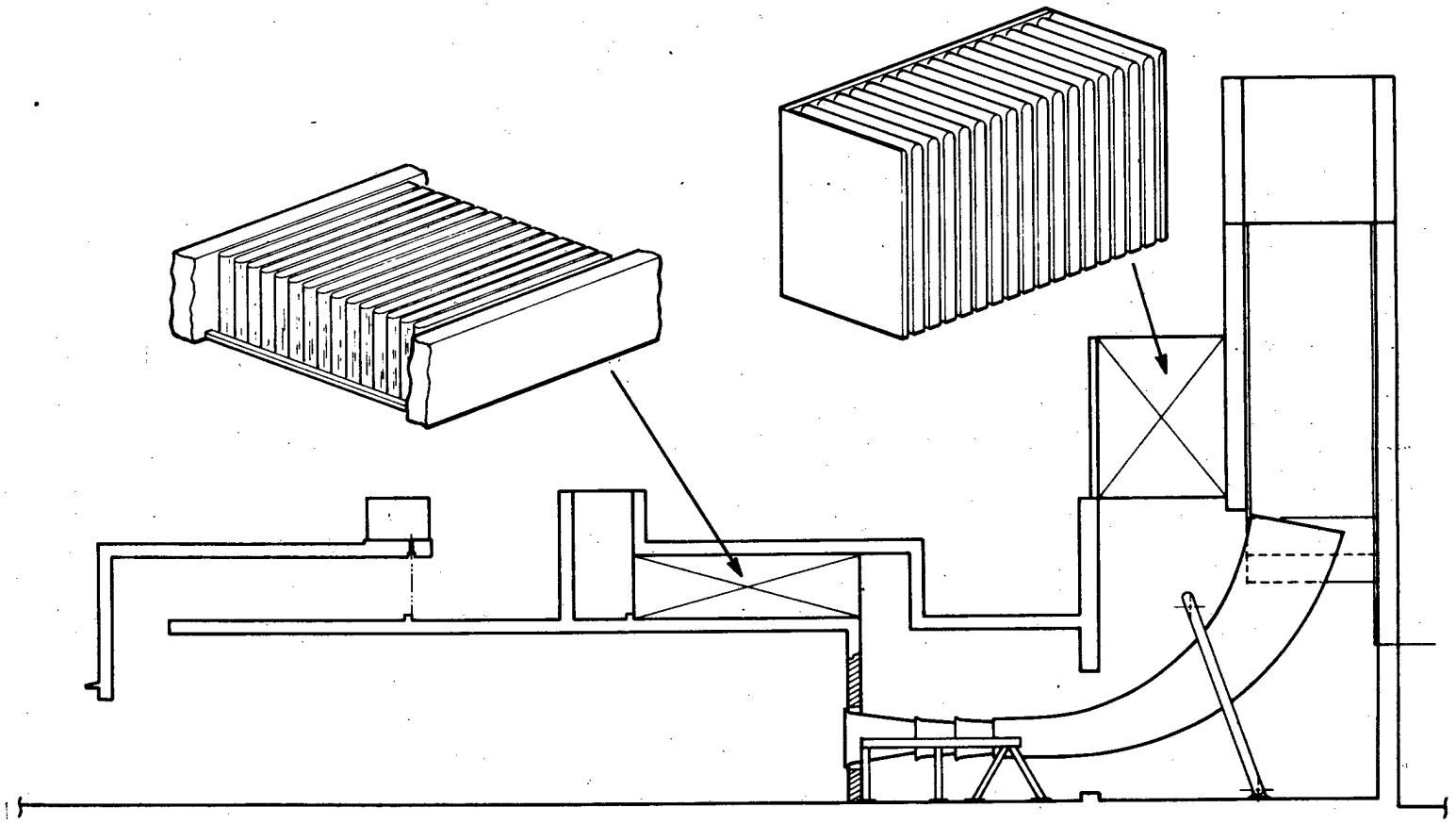

FIGURE 12.

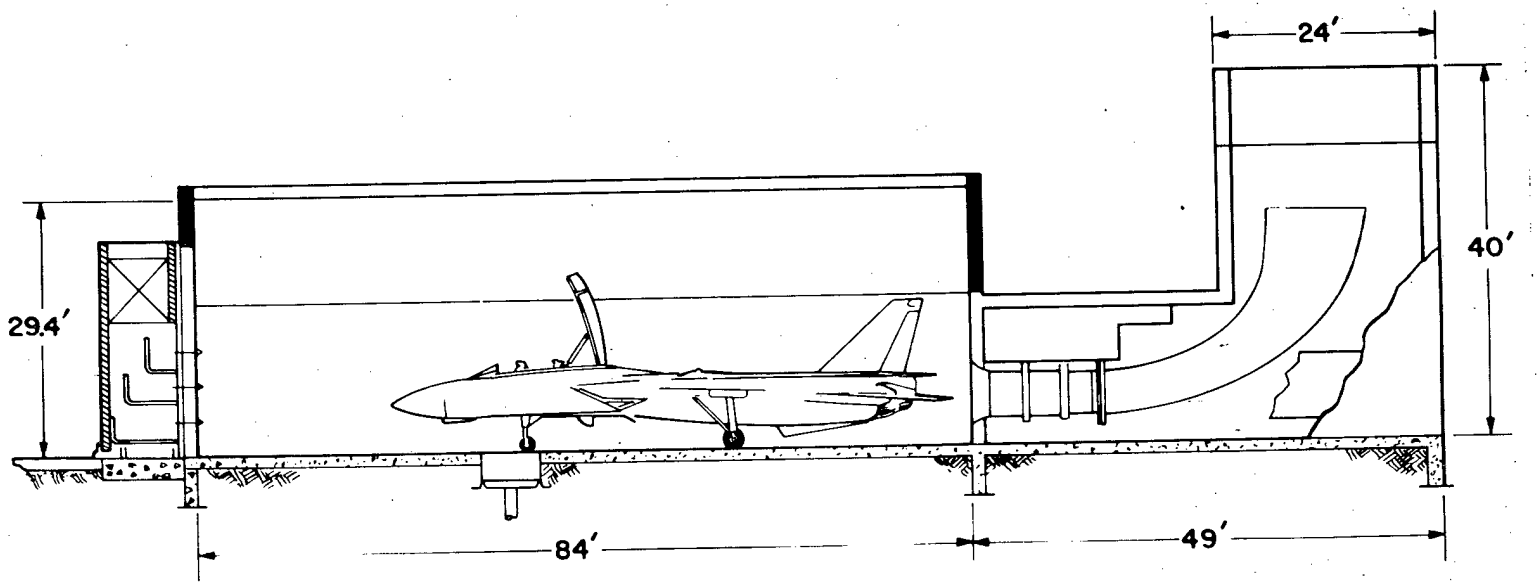

FIGURE 13. AIRCRAFT HUSH-HOUSE EXHAUST SYSTEM

BIOGRAPHICAL SKETCH

Dominic Daniel Croce was born in Philadelphia, Pennsylvania on October 15, 1938. He graduated from Saint Joseph's College of Philadelphia in 1964, receiving a B. S. degree in Physics. He conducted graduate studies at the Pennsylvania State University earning a Master's degree in Engineering Science in 1973.

Upon graduation from Saint Joseph's College, he worked at the Philadelphia Naval Shipyard, Design Division, Noise and Vibration Analysis Section. The work included shipboard test and analysis of airborne noise, submarine underwater noise, hull vibration and machinery vibration. He transferred to the Naval Air Engineering Center, Ground Support Equipment Department, Propulsion Division in 1969, where he has been involved with aircraft run-up noise suppression and environment pollution abatement.

EXPENDABLE DESIGN CONCEPT

Lt. D. C. Hall
Air Force Aero-Propulsion Laboratory, WPAFB, Ohio
and
H. F. Due, Jr.
Teledyne CAE, Toledo, Ohio

Abstract

There are many design concepts available to the aerospace equipment designer. The one most used has been the maximum performance, reusable (or overhaulable) concept. Under this concept, aerospace equipment is designed to maximum performance at the least weight/size and to have the ability to be overhauled and reused after failure. As equipment has become more complex, however, this design concept has led to rapidly increasing costs, without equal increases in performance. This fact requires that different design concepts be explored and adopted. One concept that offers many advantages is the Expendable Design concept.

The expendable design concept has as its basic premise that equipment should be designed to last for a specified period, and after its useful life is expended (or failure), be discarded rather than overhauled and reused. In many cases, this design concept offers much lower life cycle costs for equipment with little or no compromise in performance.

As an example of this design concept, the Air Force Aero Propulsion Laboratory, Aerospace Power Division, has an on-going program to demonstrate a gasifier (gas generator) for use as the core of a jet fuel starter. It was designed to the expendable concept and is expected to meet or exceed the performance of existing engines in its power class at one-half to one-fourth of their life cycle cost.

Introduction

Throughout the development of most aerospace equipment, the emphasis has been on achieving the maximum performance in the smallest and lightest package. This design concept has produced equipment, most notably gas turbine engines. With both remarkable performance and cost. Until recently, this approach was justified in that the level of performance growth roughly equaled the level of cost growth. Today, however, the cost growth can be large for only a very small (or no) performance growth. This fact, coupled with a shrinking budget, now requires the use of a different type of design approach, one that can minimize cost while increasing performance, in other words, an approach to design equipment that will provide necessary performance at the minimum cost.

There are many different ways to design minimum cost equipment, but one of the most promising is the Expendable Design concept. Using this concept, equipment will be designed to operate for a specific lifetime and then discarded at the end of that lifetime rather than overhauled and reused. This paper briefly discusses some of the major life cycle cost factors and the impact proper application of the Expendable Design concept could have on them.

349

Expendable Design Concept

The concept of designing aerospace equipment to be discarded rather than overhauled at the end of its useful life can be used to significantly reduce the costs of many of the factors making up total equipment life cycle cost.

The factors most affected are the following:

a) Acquisition
b) Maintenance
c) Overhaul

The ways they are affected are outlined in the following paragraphs.

The acquisition cost of equipment is reduced due to two factors; 1) the inherently simpler design of expendable compared to overhaulable equipment, and 2) the reduced amount of personnel/paperwork required to transfer the expendable unit into operational status. The inherently simpler design comes about by eliminating the requirements for precision threaded fittings and multiple pilot diameters ability to use simple cast hot and/or cold end components and attach components permanently by techniques like welding rather than disassembly. The reduced amount of personnel/paperwork results from restricting the number of individual components necessary to track.

The maintenance and operational cost of equipment is reduced in three ways. First, much less field level maintenance would be required for each expendable unit since the only requirement is to remove and replace total units. This eliminates subunit repair and replacement. Due to the total unit concept, only one part needs to be shipped/handled, stored and accounted for. This can drastically reduce the amount of shipping/handling from depot to field level and, concurrently, the required personnel and paperwork.

The overhaul cost, which currently averages about 50% of equipment life cycle cost, is virtually eliminated.

Example of Expendable Design Concept

An example of applying the expendable design concept is presently being explored in the on-going AFAPL Expendable Gasifier (EG) program.

The objective of the EG program is to demonstrate a low cost, expendable gasifier for use as the core of an aircraft Jet Fuel Starter (Figure 1). The main emphasis of the program is low cost at a preselected performance level. The low cost is accomplished through the use of many innovative design techniques, however, the entire process is based on the expendable design concept (Table #1) (Figure 2).

Table I - E.G. Design Features

1. Radial pin joint construction
2. Die cast aluminum housings
3. Maximum use of cast components
4. Minimum number of components
5. Low speed rotor design
6. Simple, reverse flow annular combustor with integral fuel manifold

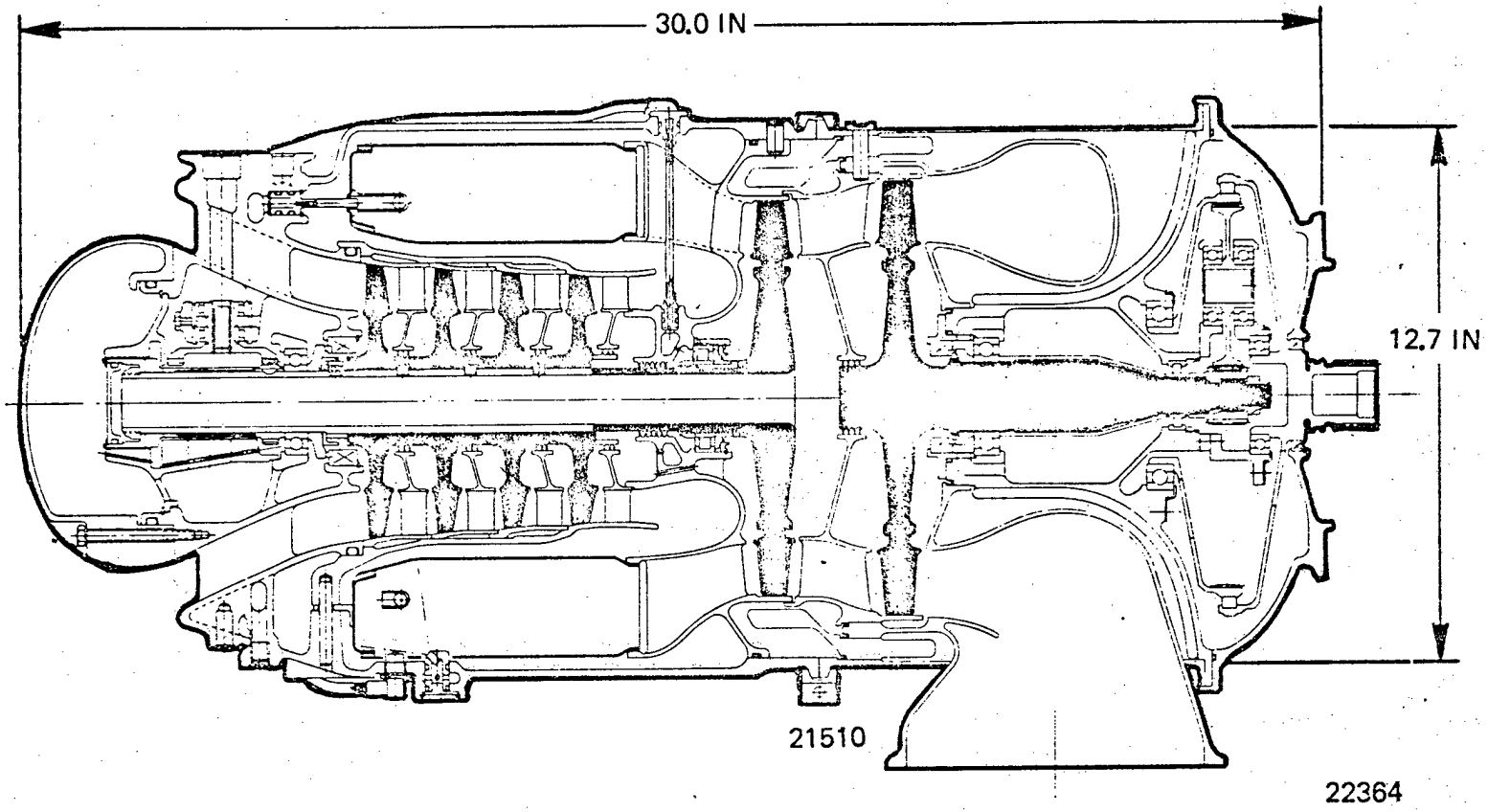

PERFORMANCE (SLS, 59F)			
HORSEPOWER	230	CPR	2.86
SFC	1.43 LB/HR/HP	WEIGHT	150 LBS
AIRFLOW	3.86 LB/SEC	POWER/WEIGHT	1.53 LB/HP
TIT	1800°F	N_{PTO}	3600 RPM

Figure 1. Model JFS 206 Jet Fuel Starter

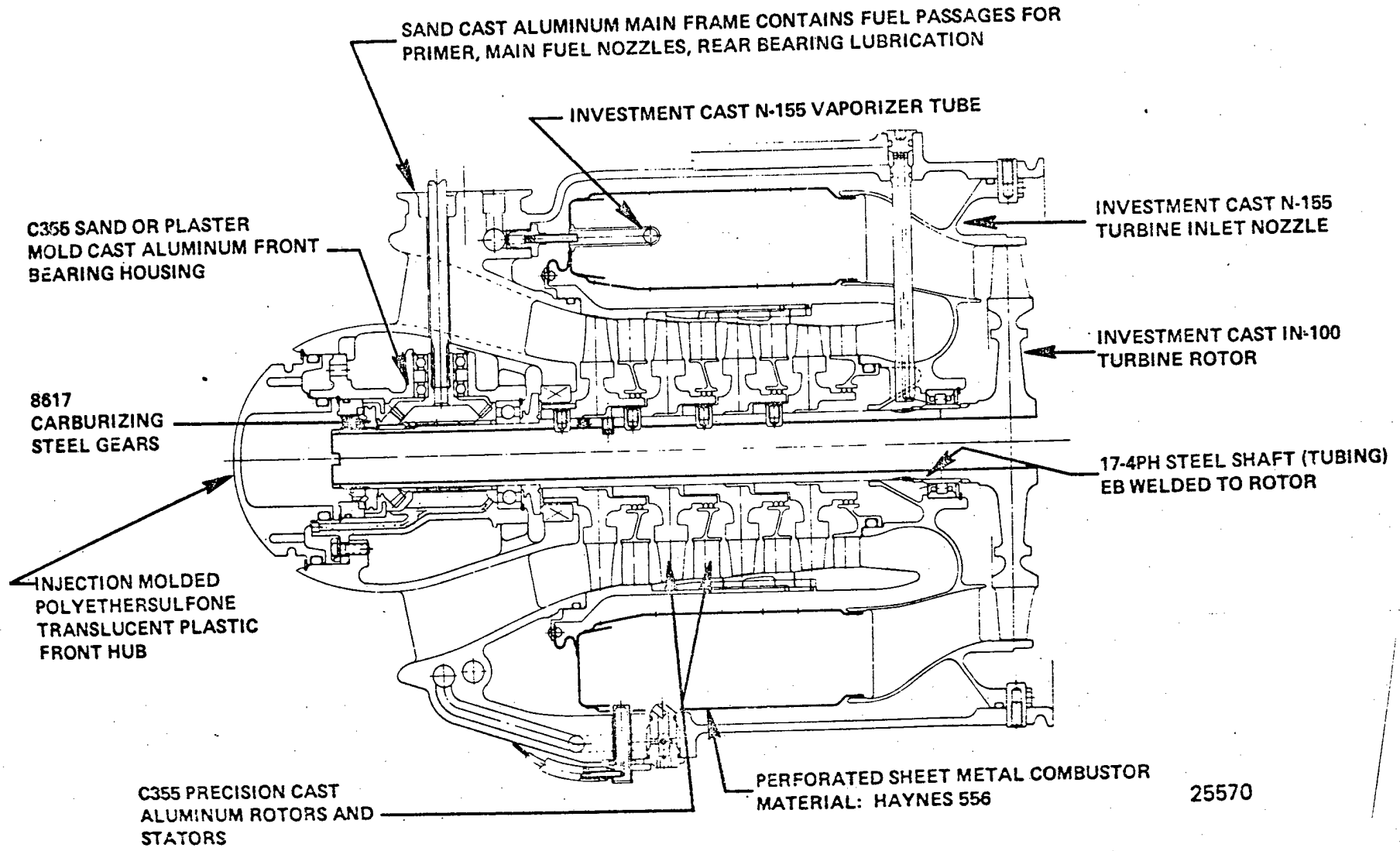

Figure 2. E. G. Material Summary

The program is now in the component testing phase and many of the design features have been demonstrated. The complete gasifier unit is planned for demonstration in early 1979 in the turbojet configuration.

The following are comparisons of existing Jet Fuel Starter technology (ET) now in use in the Aerospace industry and the E.G. technology as applied to a Jet Fuel Starter.

Table II - Comparisons

Parameter	E.G.	E.T.
Acquisition cost	$18,000	$40,000
Lifetime	2000 starts 5 years	1200 starts 2-1/2 years
O&M costs	$5,000/yr	$5,000/yr
Total direct personal required	5	15
Overhaul costs	$500	$15,000
Cost per start	$6.00	$50.00
Performance -	115 HP/FT^3	85 HP/FT^3
	2.3 HP/LB_m	2.0 HP/LB_m

Potentials

Future aerospace equipment must be designed to two usually uncompatible points, maximum performance in the least weight/size package, and minimum life cycle cost. The Expendable Design Concept enables designers to achieve maximum performance at the minimum possible life cycle cost. Almost all types of aerospace equipment can take advantage of the design concept and minimize their life cycle cost. It has not yet been determined where the breakeven point is between the overhaulable and expendable concepts. (Figure 3).

Data is presently being generated to produce the trend curves shown in Figure 3. It has been assumed at this time that the life cycle cost of the system will increase with increasing complexity or application of more advanced technology (i.e., higher pressure ratio cycles). If the expendable design concept is employed to satisfy the requirements of the advanced system, the life cycle cost of the system is expected to be reduced. The difference in cost between overhaul and expendable designs would presumably be greater as the system complexity increases (full up APU's). Likewise, for less complex systems (constant

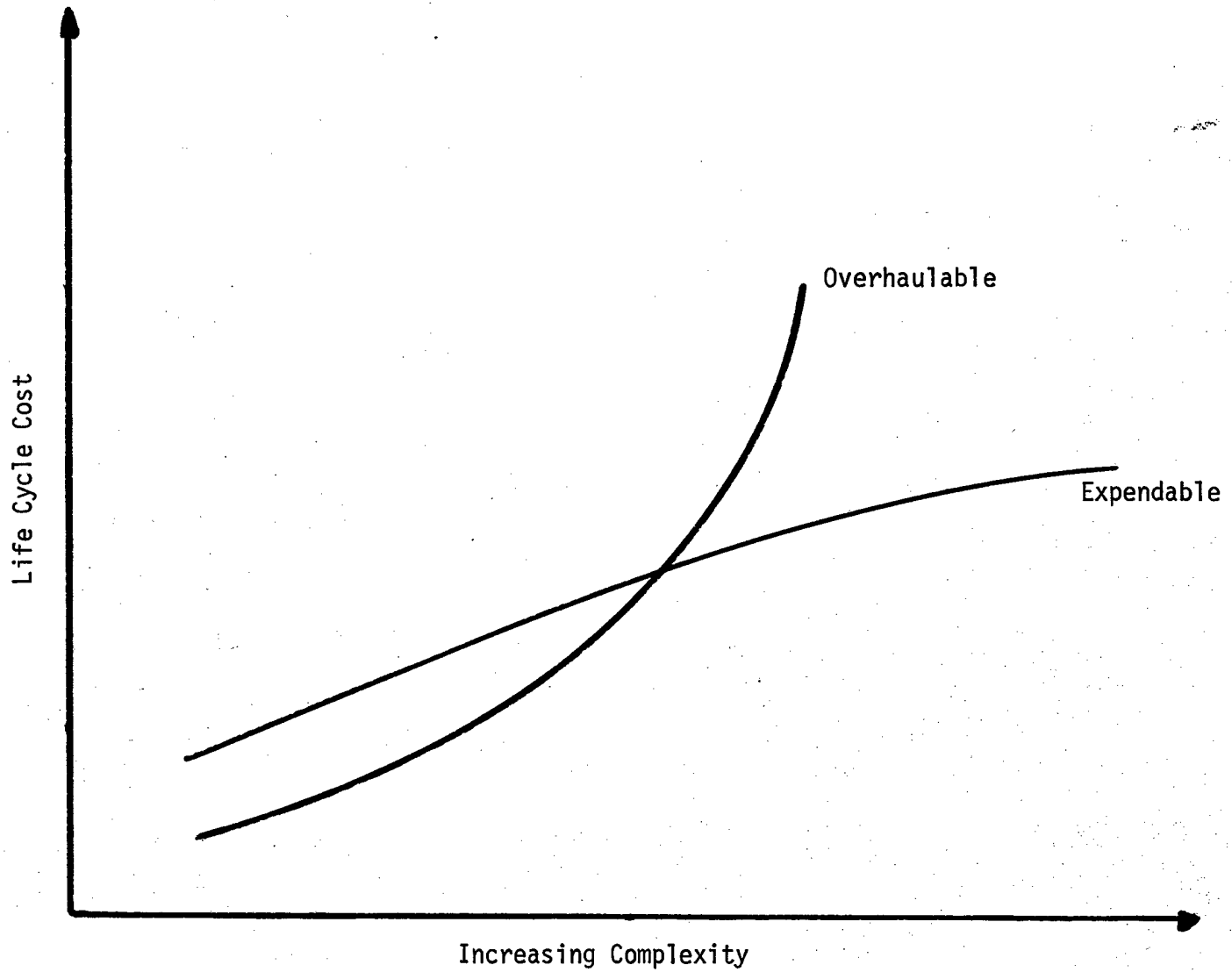

Figure 3. Life Cycle Cost Comparisons

speed drives), the difference in cost is expected to be lower. A breakeven point may exist depending on the relative design complexity of the simpler systems and the ratio cost elements in relation to total costs.

Another approach adopted in the expendable design concept to reduce acquisition cost is to achieve high production rates by multiple uses of the core engine. The expendable gasifier has been designed as a "common core" adaptable to a small turbojet and turbofan as well as a jet fuel starter. Photos of a mock-up of the modules which comprise the various applications are shown in Figure 4. The assembled mock-ups are shown in Figure 5.

Expendable Gasifier Program Status

The expendable gasifier program is presently about seventy percent completed and many of the low cost features of the unit have been demonstrated in the combustor development task which was completed in October 1977. The combustor rig included the main frame aluminum casting, cast turbine inlet nozzle and perforated sheet combustor (Figure 6). The combustor rig was operated for over 50 hours at gas temperatures exceeding 1800°F. The design goal temperature profiles were achieved at design point temperature rise and the simple perforated sheet liner cooling was shown to provide adequate cooling.

Presently the remainder of the EG hardware is being fabricated using the processes selected to achieve the lowest production cost. In 1978, the compressor will be tested as a component followed by the gasifier unit tested in the turbojet configuration in 1979.

References

1. Hall, D. and Due, H.F. "The Expendable Gasifier Program," 1976 JANNAF Conference, Chemical Propulsion Institute, Publication Number 280, Volume 1, Page 369, November 1976.

2. Smith, R., "Low Cost Jet Fuel Starter," SAE Paper 75117, November 1975.

3. Hall, D. and Due, H.F., "The Expendable Gasifier - A Cost Effective Approach to Turbine Power," AIAA Paper No. 77-497, March 1977.

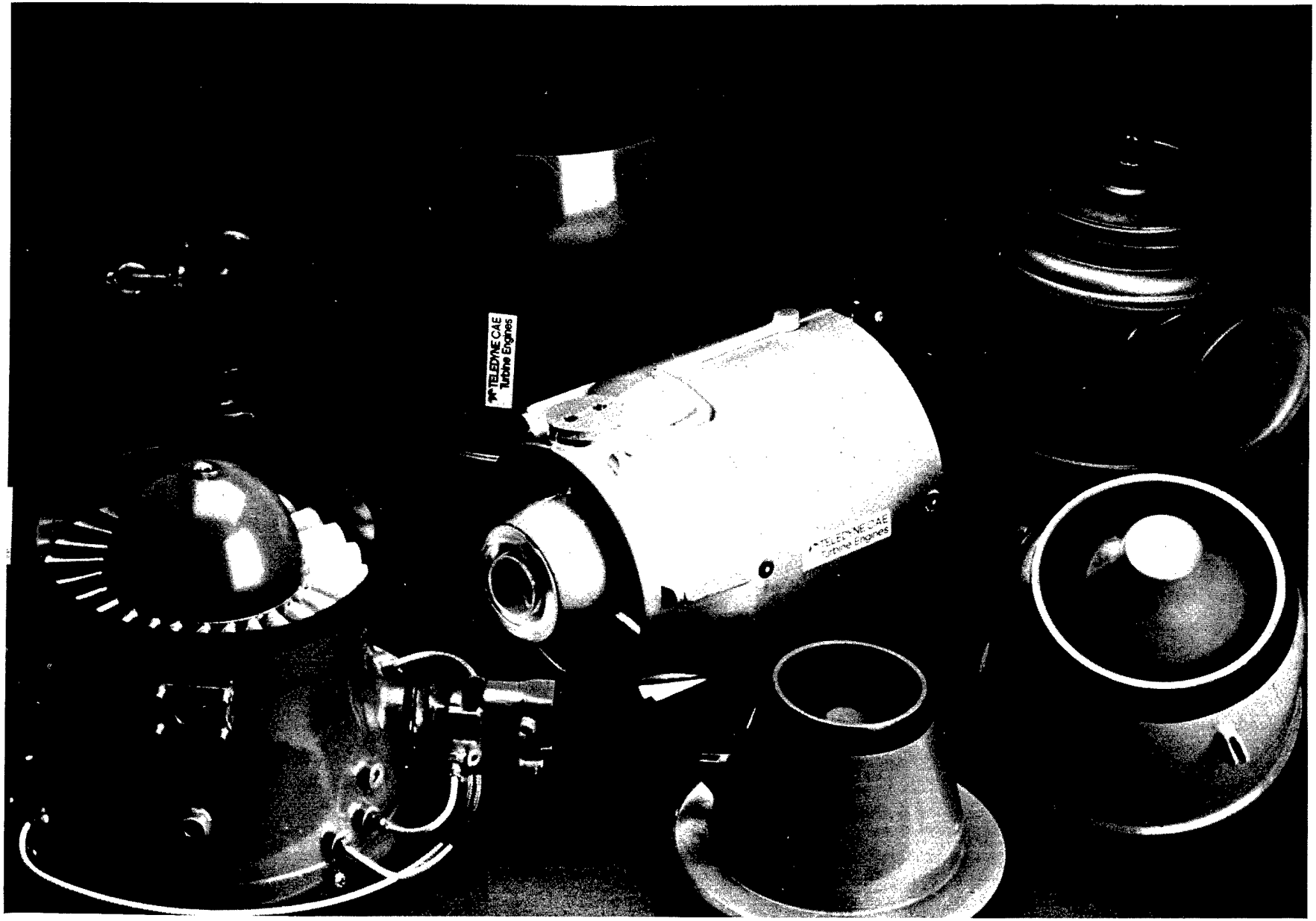

Figure 4. Mockup of E. G. Modules and Components

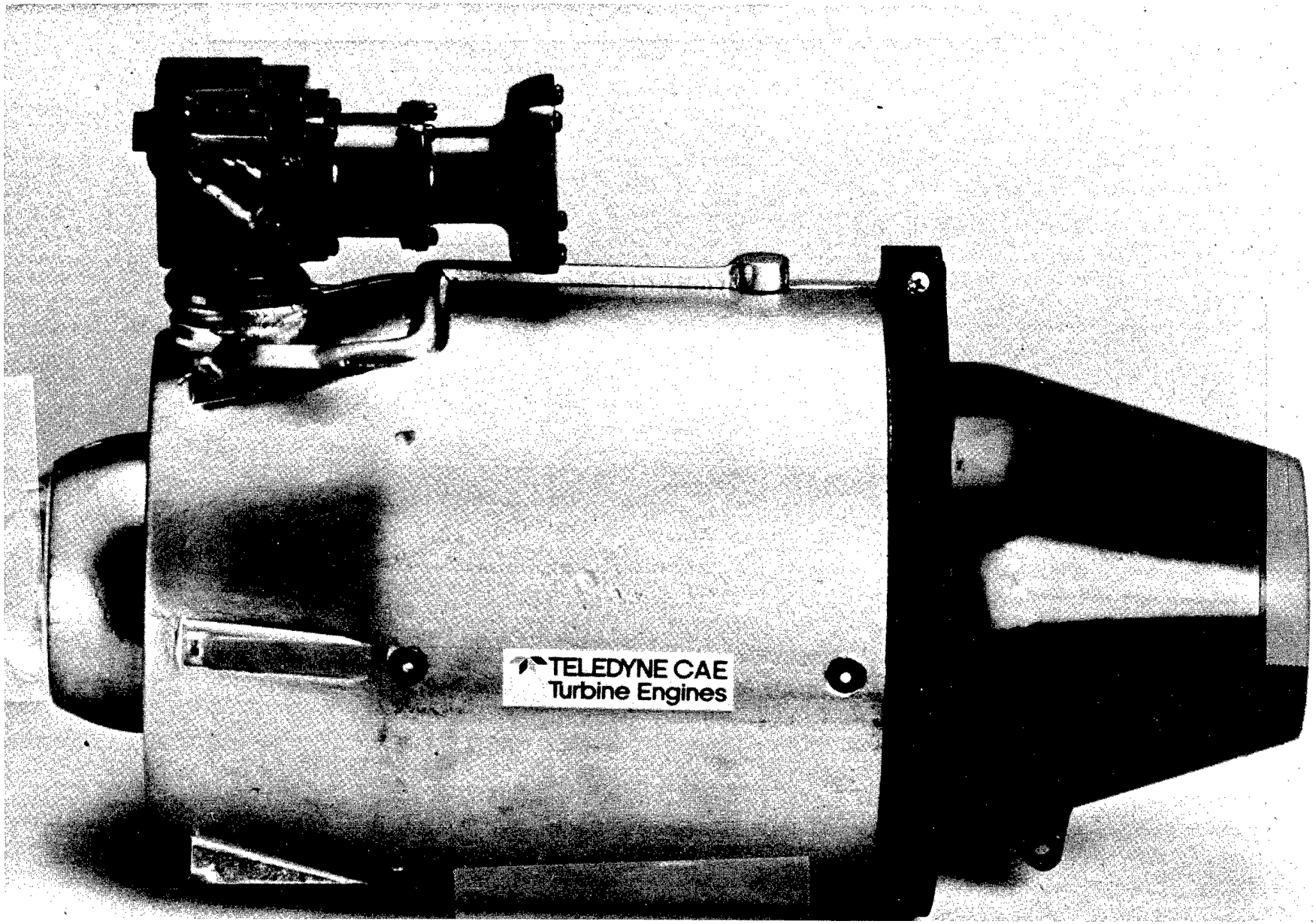

Figure 5a. Turbojet-230 lb S.L.S. Thrust

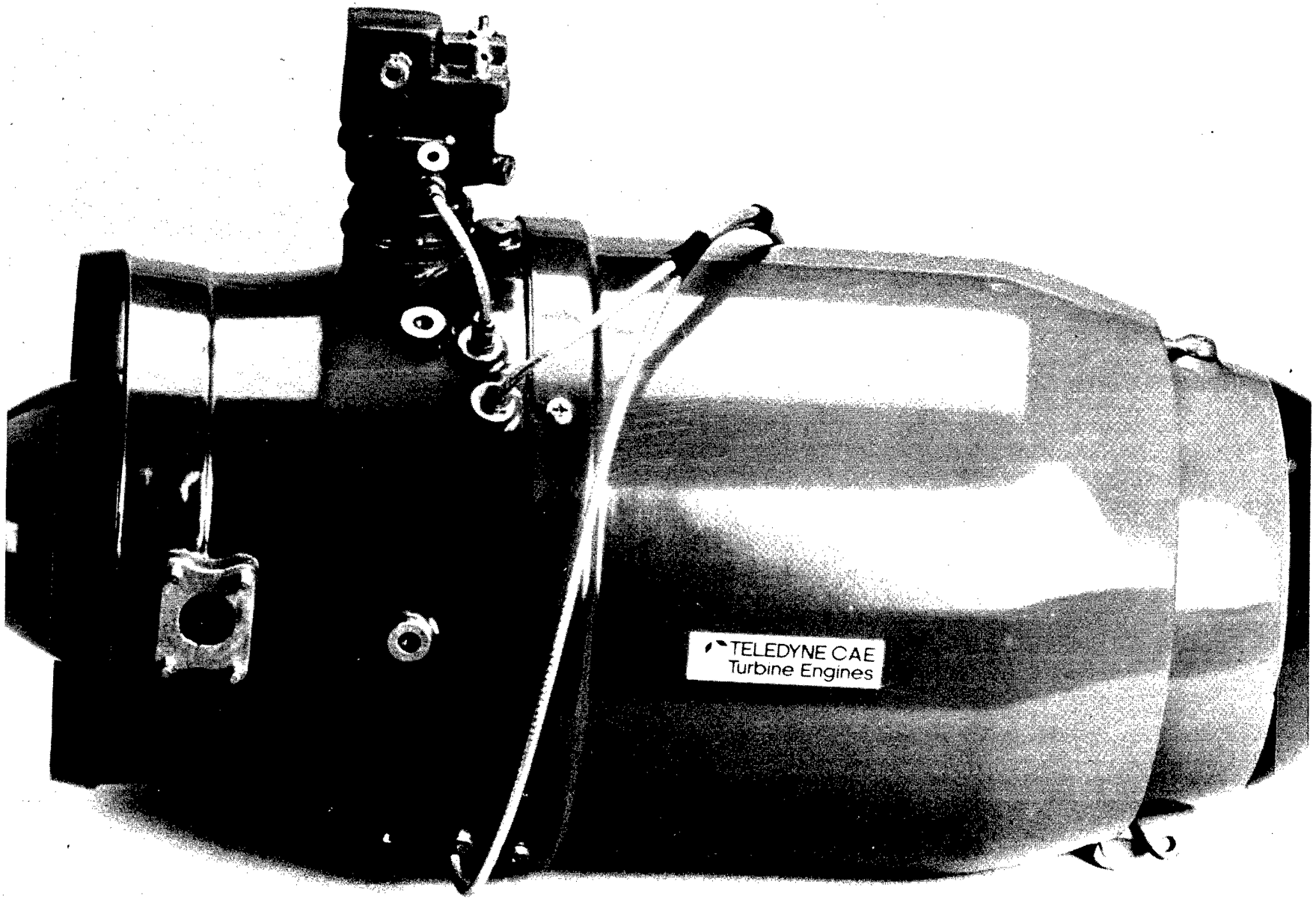

Figure 5b. Turbofan - 500 lb S.L.S. Thrust

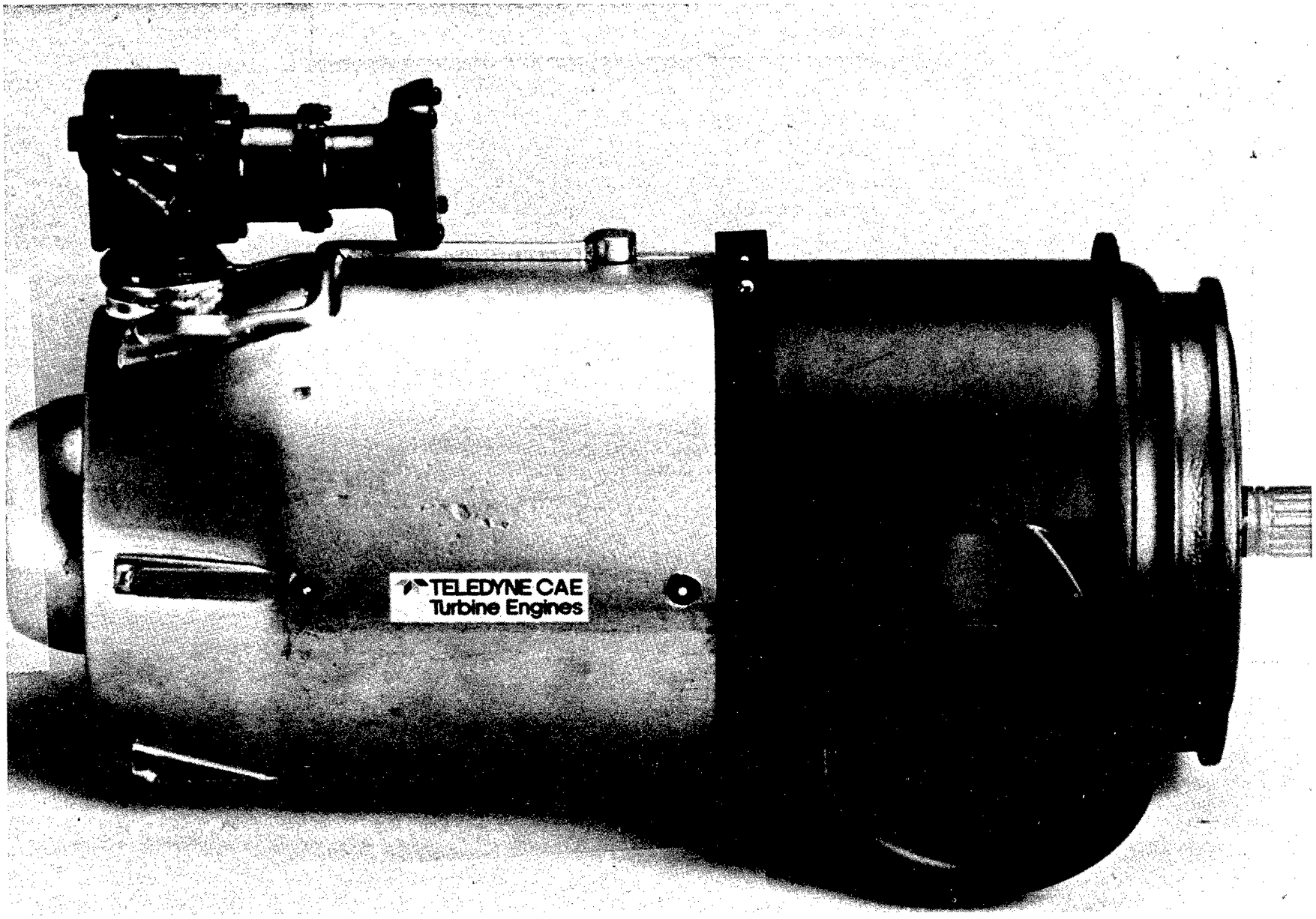

Figure 5c. Test Fuel Starter-230 hp S.L. Std Day

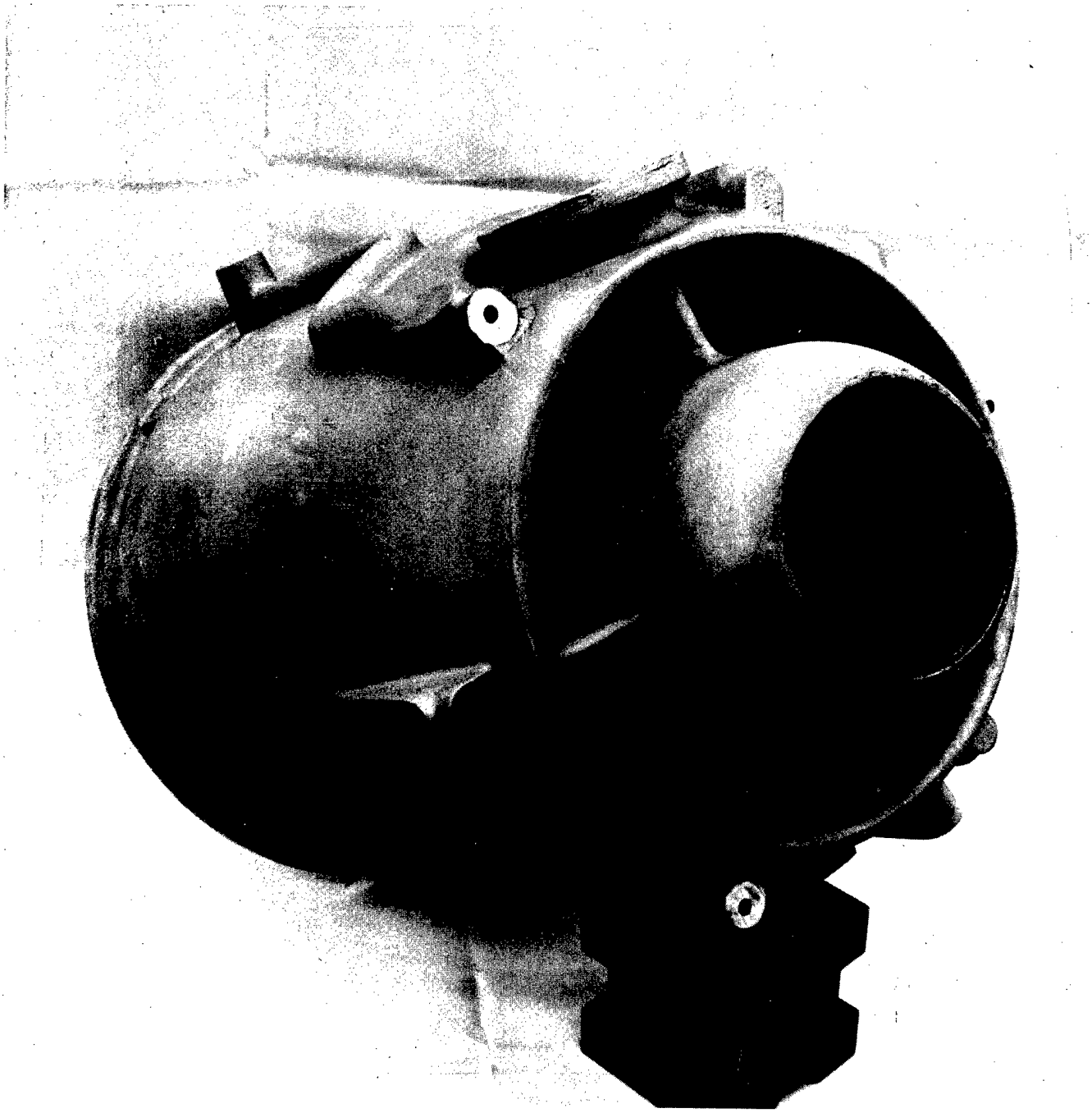

Figure 6a. Main Frame Casting

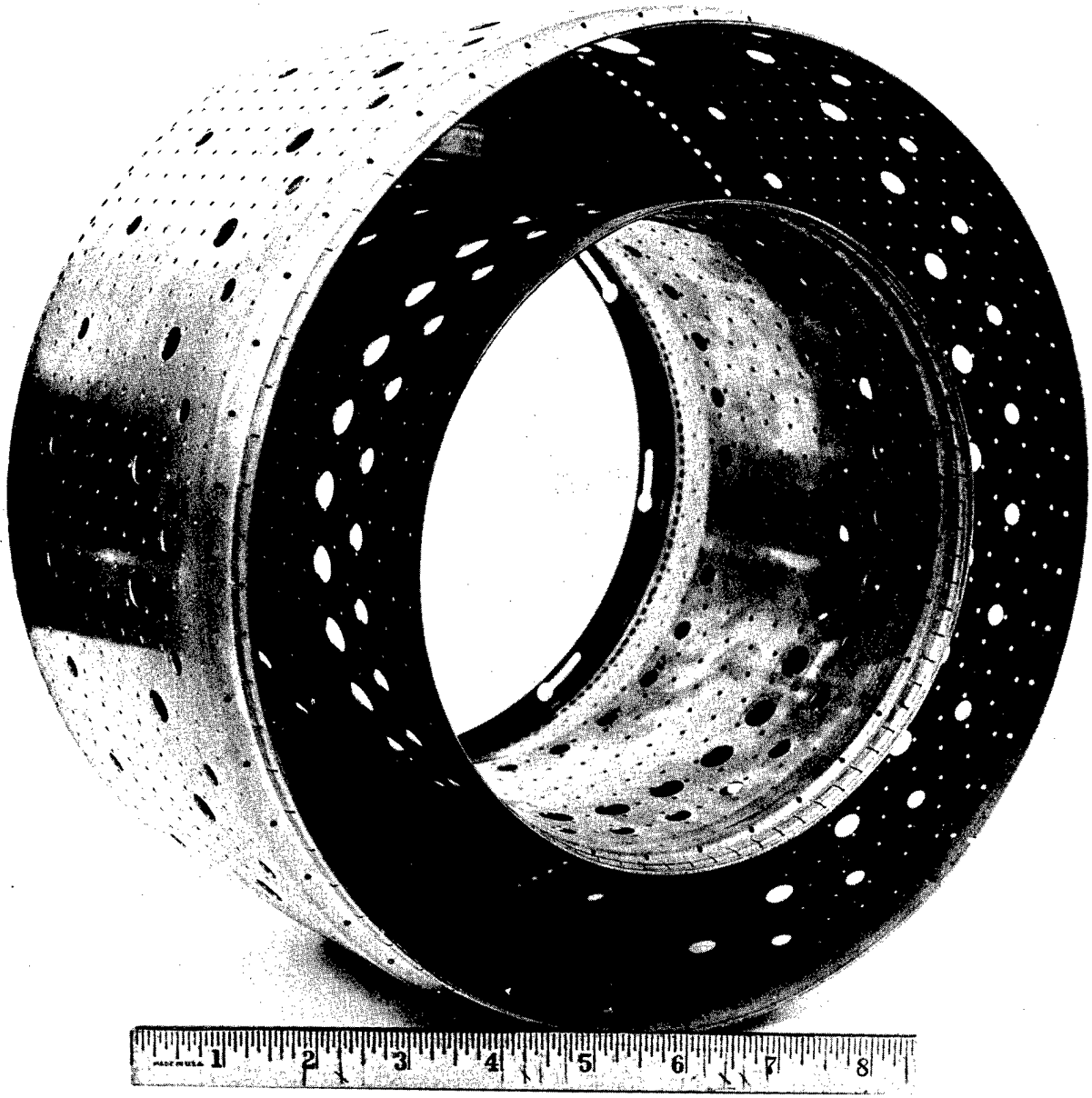

Figure 6b. Combustor Assembly

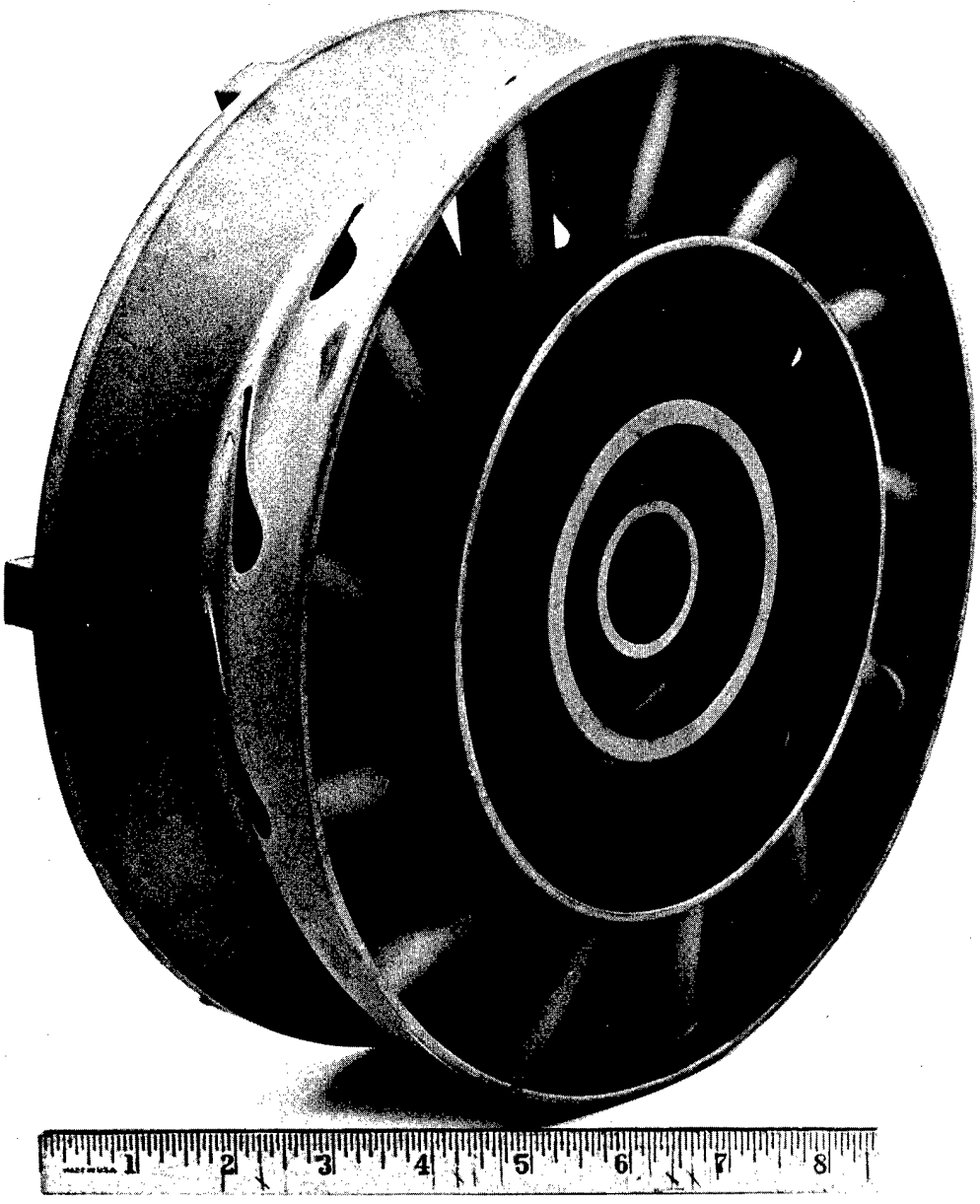

Figure 6c. Turbine Inlet Nozzle Casting

THE SUPERSONIC EXPENDABLE TURBINE

ENGINE DEVELOPMENT PROGRAM

BY

Theodore E. Elsasser

LaFayette College	BSME
Pennsylvania State University	Master Engineering
Naval Postgraduate School	M. S. Management

Research and Technology Group

Naval Air Propulsion Center
Trenton, New Jersey 08628

THE SUPERSONIC EXPENDABLE TURBINE ENGINE DEVELOPMENT PROGRAM

ABSTRACT

The Naval Air Systems Command has been sponsoring the technology for low cost turbojets for supersonic missile applications since 1971. Curtiss-Wright Corporation currently is working under contract N000140-76-C-0499 to develop a gas generator to demonstrate the basic performance and viability of an engine design incorporating low cost design and manufacturing features. The results of the total Supersonic Expendable Turbine Engine exploratory development program to date have shown that advancements in design and fabrication technology make it possible to achieve, at a reasonable cost, the combined capability of range, payload and speed through turbine powered stand off tactical missiles.

This paper reviews the technologies which have been developed under this program, summarizes the results of the gas generator demonstration contract and outlines future plans.

Introduction

The genesis of being able to develop an affordable gas turbine power plant for relatively long-range high-speed stand off missiles is almost a decade old. This general class of missile needs an efficient and powerful propulsion system for long-range and adequate payload, supersonic capability for survivability, and low cost for affordability. Obviously, since the missile will be used but once, the production cost of all components and sub-assemblies must be as low as practical.

Turbojet engines offer a number of desirable features for this type of weapon system: they are efficient, reliable and versatile. Unfortunately, they also tend to be rather expensive for one-time usage.

To address this problem the Navy has been sponsoring the development of technology necessary to reduce the cost of acquisition of turbojet engines for missile applications since 1971. This effort is being conducted under the Supersonic Expendable Turbine Engine (SETE) program. The primary object of the program is to develop and demonstrate low cost design, fabrication and assembly concepts in an engine representative of a propulsion system suitable for a supersonic stand-off missile. Secondary objectives of the program are to develop a technology base for low cost turbomachinery throughout the industry and to foster technology transfer between nonman-rated and man-rated design concepts.

Design Requirements

Although no specific weapon system having a requirement for a SETE is being developed at this time, program planners have endeavored to select engine design goals that would be generally applicable to a number of mission scenarios. The physical size, performance requirements and operating envelopes were established in this manner.

Some general design requirements are listed in Tables 1 and 2 and the operating and starting envelopes are shown in Figure 1.

Table 1 SETE Design Requirements

Size	
Length	44 in
Diameter	14 in
Weight	250 lb
Life	
Operating time	15 min at max thrust 60 min at reduced thrust
Cycles	1 start and operation
Shelf	5 years
Maintenance	None
Starting Time	10 sec
Reliability	98-99%

Table 2 -Sea Level Performance Ratings

Rating	Mach Number	Net Thrust,lb	Duration, min
Maximum	1.5	2300	15
Maximum	0.9	1600	30
Intermediate	1.5	1800	20
Intermediate	0.9	600	60

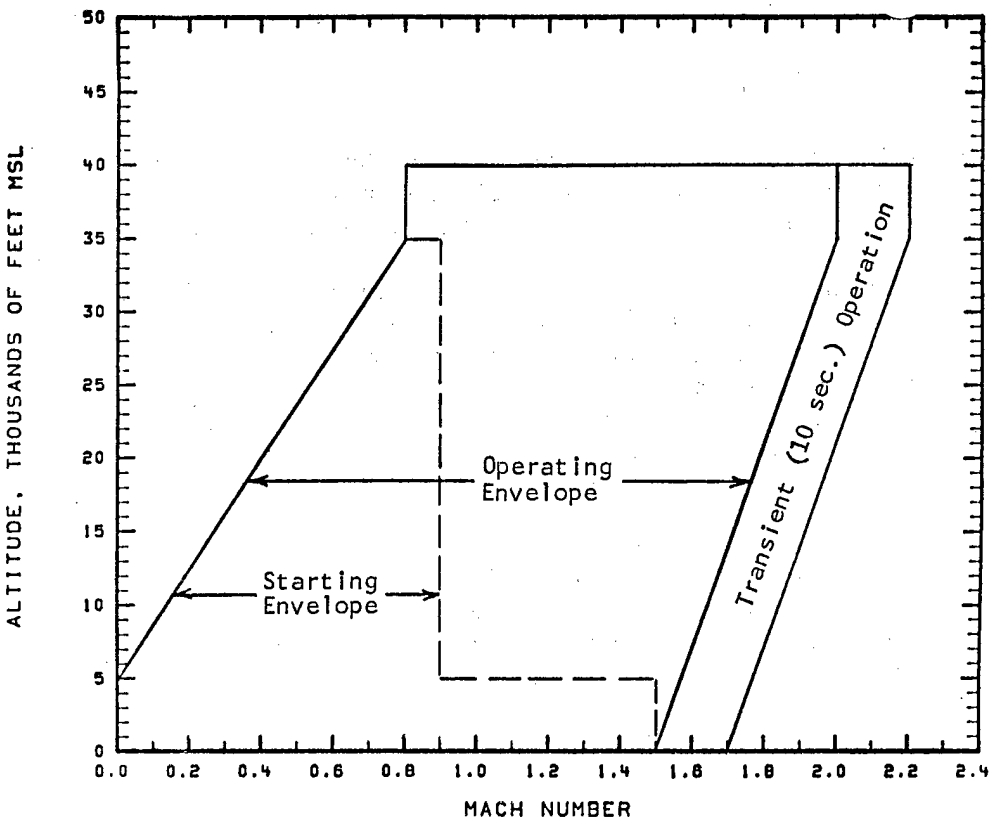

FIGURE 1 - SETE Starting and Operating Envelope

As opposed to performance and size, the concept of low cost is a tough nut to crack. It is perhaps best to discuss low-cost in relative terms. Turbomachinery with high rotatitive speeds and precision airfoil shapes historically has been expensive. Their excellent specific performance, high reliability and long life have nevertheless made gas turbine engines cost effective. The question to program managers of missile weapon systems is: "Can turbojets still be cost effective in expendable, or one-shot, applications?" The basic hypothesis of the SETE program is that by trading off long life and high performance in favor of lower cost, engine designers can reduce the cost of a turbojet engine for nonman-rated applications to affordable levels.

Also unlike performance and size, there are a number of external factors which can influence production costs significantly. Frequently, these variables can not be controlled or anticipated. Examples of these factors are changing production rates or manufacturing overhead rates, the unavailability of critical materials, labor difficulties and, of course, inflation.

Keeping these factors in mind, we feel that a reasonable production cost objective for the SETE program is $20,000 per engine in relatively large (1000/yr) production quantities. Some estimates have been generated

which indicate production costs significantly below this level while other estimation analyses, developed independently, indicate higher costs. Many of the differences lie in the assumptions used.

There is another aspect of cost which needs to be mentioned. What is really desired is low life cycle costs. Obviously, in an expendable type engine, operation and support costs are small and may be neglected. (An exception to this assumption would arise if engine shelf life objectives can not be met with a particular design; in that case the cost of inspection and refurbishment would have to be taken into account.) The remaining elements in most life cycle cost models are development and production costs. Production cost which typically gets most of the attention, has already been discussed. However, development costs also are important and must be minimized to produce an overall affordable engine. It should be quite obvious from the discussion of the program phases which follow, that the SETE program planners and contractors alike have paid particular attention to development costs in negotiating the scopes of work for each phase.

Exploratory Development Program

The Naval Air Systems Command has been sponsoring the SETE program under Category 6.2 Exploratory Development funds since 1971. This effort consists of Phases I through III as shown in Figure 2. The 6.2 program started with design studies in 1971 and will culminate in a gas-generator demonstration at the end of this calendar year. The final report for this phase will be published in March 1979 marking graduation from Exploratory Development and commencement into Advanced Development.

Figure 2 shows the approximate timing of each phase, the contractor involved and the value of award. The final reports from each contract were published with unrestricted distribution. Each succeeding phase was reopened to accept proposals from all qualified companies. In this manner the technology developed under the SETE program had maximum chance for transfer and utilization in other programs, including man-rated development efforts. In exchange, a healthy competition throughout the industry has been maintained for the SETE program and the Navy has been able to draw on the benefits of technology developed under other programs.

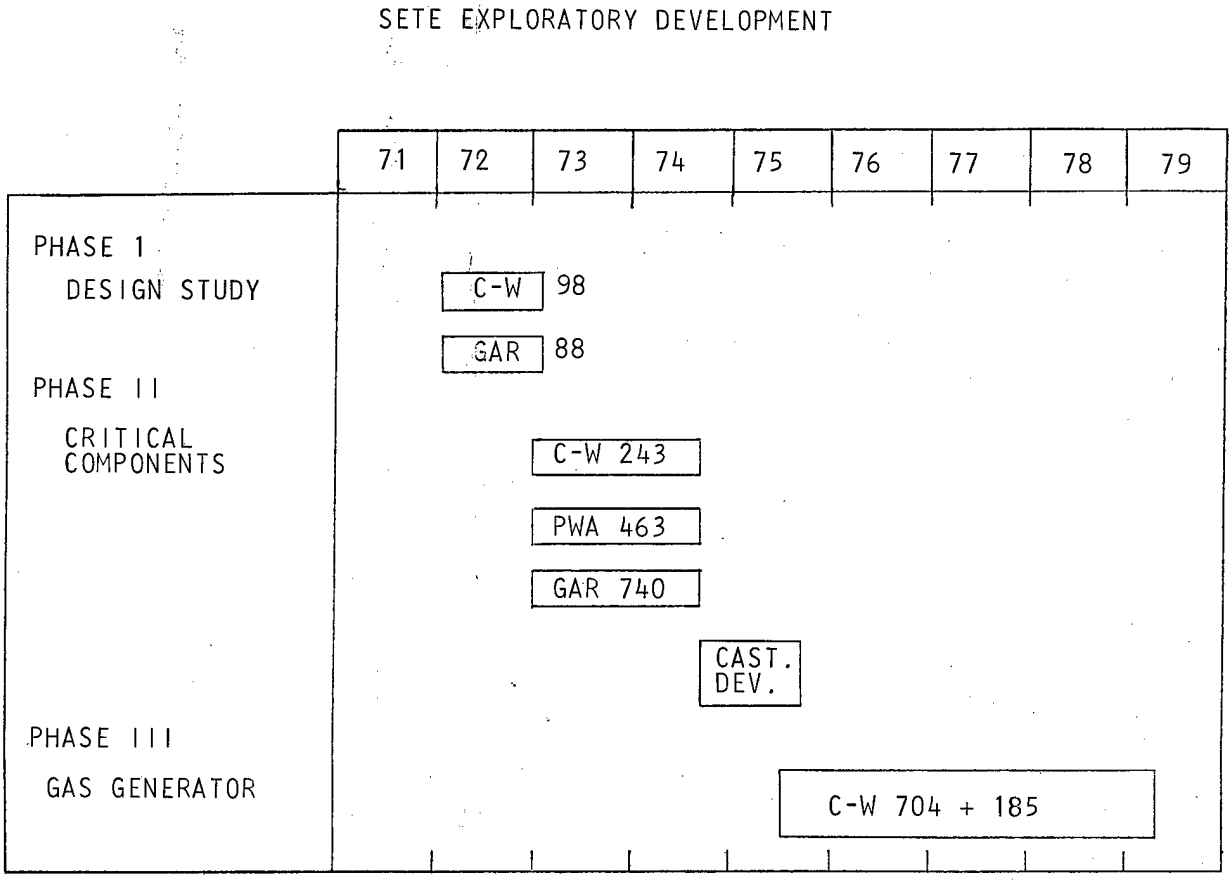

FIGURE 2

FIGURE 2 - SETE EXPLORATORY DEVELOPMENT PROGRAM

PHASE I - Phase I was a design study conducted by Curtiss-Wright and AiResearch. The objective was to prepare a preliminary engine design based on lowest possible production cost, but would meet the basic design goals. The results of this effort indicated that for such an engine designed from its inception for low cost, it would be feasible to manufacture the engine at a unit cost of approximately $10,000 (based on 1971 dollars).

PHASE II - With the favorable results of the design study, the critical technologies for low-cost designs were identified and plans were made to embark on a hardware program. In Phase II, three companies were awarded contracts to perform detailed design of their most critical components, fabricate the component and conduct rig tests. The objective of this phase was to verify the performance of these components without having to commit to an engine program.

The three companies awarded contracts for this phase and their respective designated critical components are listed in Table 3.

Table 3 - Critical Component Designation

Curtiss-Wright Corporation	Combustor
AiResearch Mfg. Co.	Turbine, Compressor
Pratt & Whitney Aircraft	Compressor

All three engine designs employed axial flow compressors, annular combustor, single stage turbines, and pyrotechnic ignitor squibs and starter cartridges. A brief description of each contractor's basic engine design and the results of the critical component effort are presented in the following sections. A comparison of the characteristics of the major engine components is listed in Table 4.

Table 4 - Major Component Characteristics

	AiResearch	Curtiss-Wright	Pratt & Whitney
Compressor			
Stages	3	4	5
Pressure ratio	3.5	4.0	5.3
Airflow, lb/s	17.3	19.8	24.7
Efficiency,%	82	85	80
Combustor			
Pattern factor	0.30	0.19	0.35
Efficiency,%	98	99	98
Turbine			
Inlet temperature,°F	2200	1900	1900
Cooled	Yes	No	No
Efficiency,%	86	88	86

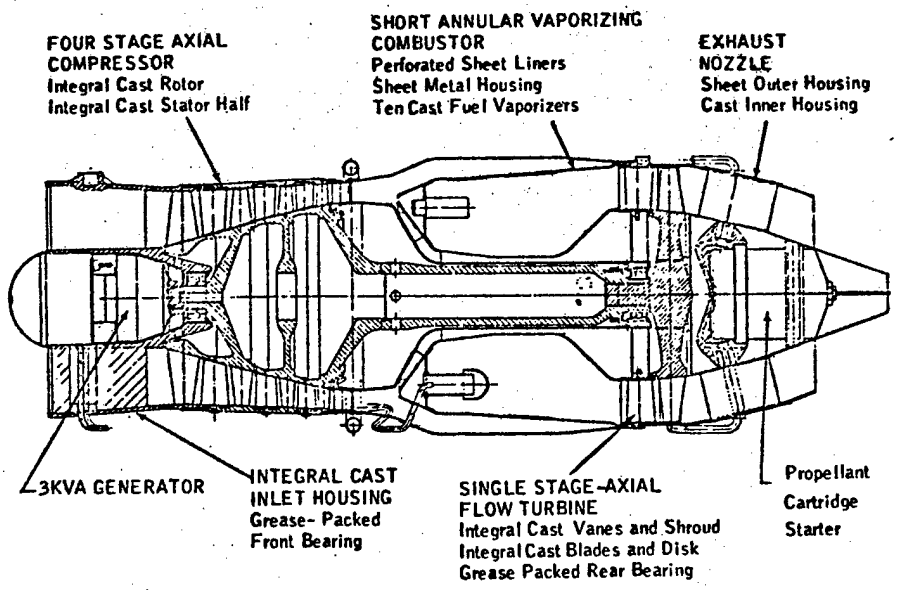

FIGURE 3 - Curtiss-Wright WEJ20 SETE

Curtiss-Wright - The Curtiss-Wright model WEJ20 engine, shown in Figure 3, has a four-stage compressor with an overall pressure ratio of 4.0 and an airflow of 19.8 lb/s. Each stage is integrally cast from 17-4 PH stainless steel and electron beam welded. The stator section is cast in two halves. The only machining is a tipping operation on the blades and vanes. There are no circumferential bolt flanges. Adiabatic efficiency is 85%.

The single-stage uncooled turbine has an integrally cast IN100 rotor. The stator section is a one-piece integral WI-52 casting.

The combustor is a full annular welded composite structure with a sheet metal housing and perforated metal liners. There are ten 1/4 in. diameter fuel metering tubes which discharge the fuel into cast Hastalloy X Mushroom vaporizor tubes. All joints are sealed with "Locitite" sealer to eliminate more common, but costlier, joining techniques. Ignition is accomplished by two pyrotechnic flares.

The engine has a thrust ball bearing located at the compressor first stage and a cylindrical roller bearing located at the turbine. Both bearings will be packed with krytox 280AC fluorinated grease.

The electric generator is illustrative of low cost design techniques in what are usually considered to be minor components. The generator rotor is screwed onto the front of the compressor shaft and is directly driven at engine speed. It has no bearings, splines, or brushes. The generator also serves as a retaining nut for the main engine bearing.

The exhaust nozzle, an extended plug fixed-area design, houses the starter cartridge. Hot gases from the starter pyrotechnic impinge directly on the engine turbine blades. The electronic fuel control is packaged on the outside of the compressor case, while the 3kV-A generator is housed inside the engine bullet nose.

The combustor was selected as Curtiss-Wright's critical component because it's low pattern factor was felt to be essential to satisfactory engine operation and turbine life. A schematic of the combustor is shown in Figure 4.

During the development program, holes in the combustor liners for both primary and secondary airflow zones were modified and relocated as needed to produce the desired temperature profiles. There was only one hot spot in the circumferential profile which would affect stator life. Fortunately, this spot occurred in a region of low stress. The radial pattern affecting the turbine rotor was actually better than anticipated. Accordingly, the results of the critical combustor program were considered satisfactory.

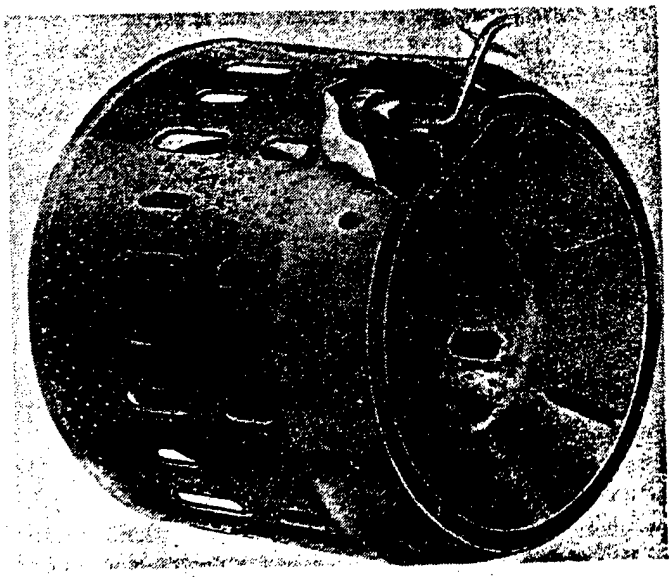

FIGURE 4 - Curtiss-Wright Combustor

AiResearch Mfg. Co. The AiResearch ETJ1000 design, shown in Figure 5, has a three-stage compressor with low aspect ratio blades, a pressure ratio of 3.5 and an airflow of 17.3 lbs/sec. The compressor rotor blades are integrally cast out of 17-4 PH steel as are the stator vanes and casing. The compressor rotor is pressed onto the turbine shaft and retained by a nut.

The combustor is an annular straight-through-flow design which is essentially a scaled-up version of their Harpoon combustor. The fuel injection system is a vaporizing system with 10 air swirlers and 10 J-tube fuel injectors. The air swirlers could be integrally cast with the combustor dome. The combustor was designed to yield a 0.3 temperature pattern factor.

The single-stage turbine has an integrally cast, cooled rotor and cast, cooled vanes. IN100 is used for the rotor while the vanes will be made from GMR-235. Five percent cooling air will be split with 3% going through the stator vanes and 2% to the rotor.

The engine is supported by two preloaded ball bearings. This arrangement will help to prevent brinelling due to static vibratory forces and will also eliminate skidding. The bearings are lubricated from a fiberglass wick system.

The starter system consists of an electrically ignited pyrotechnic cartridge, a small turbine, and a reduction gear. The hot gases are directed onto the small turbine which, in turn, drives the engine shaft after a 2.84:1 speed reduction. The separate starter turbine keeps the hot gases out of the engine airstream; the reduction gear gives better speed-torque characteristics. The entire starter assembly is mounted in the engine's tail cone.

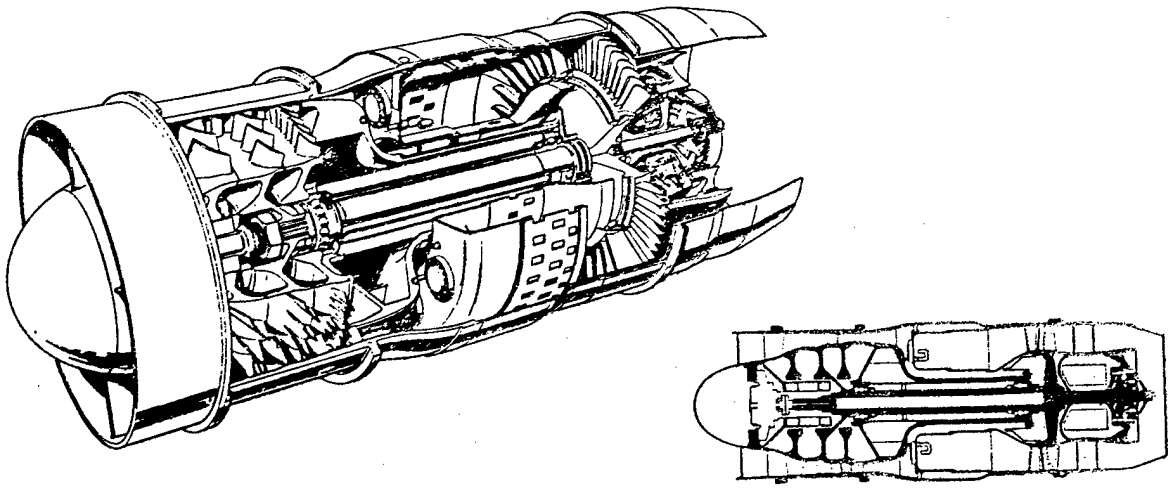

FIGURE 5 - AiResearch ETJ1000 Expendable Turbine Engine

The exhaust nozzle is a recessed plug design made from Hastalloy X. The fuel control is a hydromechanical fuel delivery unit with an electric computer. Electrical power is supplied by a permanent magnet generator (PMG).and a rectifier assembly. The fuel control, PMG, and rectifier assembly will be packaged in the front of the engine.

Both the turbine and compressor of the ETJ1000 design were selected as critical components. The turbine was selected because of the ambitious goal of casting an integral turbine rotor with cooling holes. The compressor was funded primarily because of its potential for high tolerance to inlet pressure distortion.

Some difficulties in obtaining satisfactory turbine rotor castings were encountered. Although this type of difficulty is not unusual in exploratory development programs, it did have the effect of causing a delay in completing the program. An additional casting development was funded as shown in Figure 1. During this effort, casting vendors were successful in developing the process and were able to produce satisfactory turbine rotors. One of these rotors is shown in Figure 6. Unfortunately, there were not sufficient resources remaining in the Phase II budget to fund the turbine performance test program.

In contrast to the turbine program no difficulties were encountered in the compressor program. All objectives were achieved. Efficiency was within 1/2 percentage point of the design goal and the compressor's distortion tolerance also was verified by rig test.

ETJ1000 COOLED TURBINE

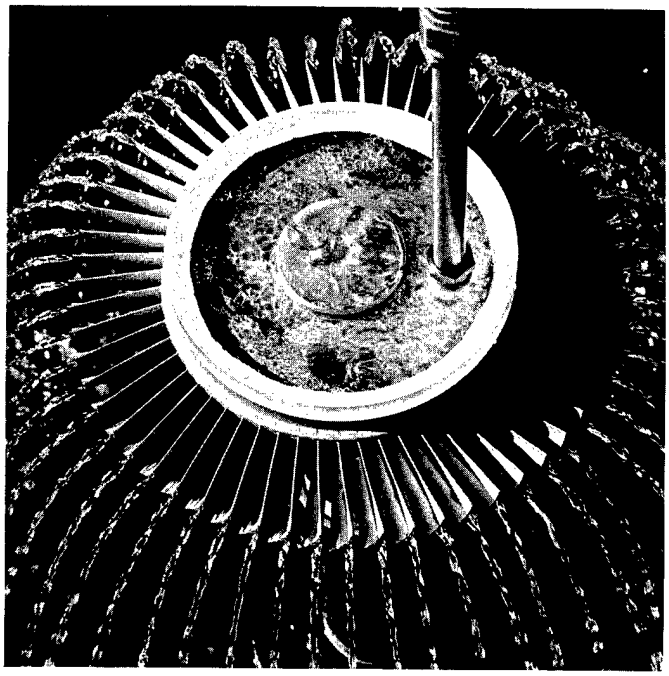

FIGURE 6 - ETJ Cooled Turbine

Pratt & Whitney Aircraft - A schematic of P&WA's model STJ442 engine design is shown in Figure 7. The engine featured a unique approach to compressor design as shown in Figure 8. The compressor consists of 34 bladesticks mounted in a drum rotor with an equal number of broached slots. The circumferential grooves are machined into the drum to allow the chips to escape during the broaching operation. The grooves are located between the rotor blade stages where stresses will be low. Each stick has five blades and is held in place by a U-shaped tab washer and sealed by RTV silicone rubber. The compressor case is a one-piece aluminum casting. The vanes are made from 410 stainless steel airfoil strip stock. The vanes are pierced through the one-piece stator case and then brazed. The result is a five-stage, 24.7 lb/s airflow compressor with a pressure ratio of 5.3:1.

The titanium bladesticks are made by Pratt & Whitney's Gatorizing process. Gatorizing is a hot isothermal forging process which allows fairly complex shapes to be forged in a state of high ductility. After being Gatorized, the bladesticks are ready for assembly as is. No final machining operations are required.

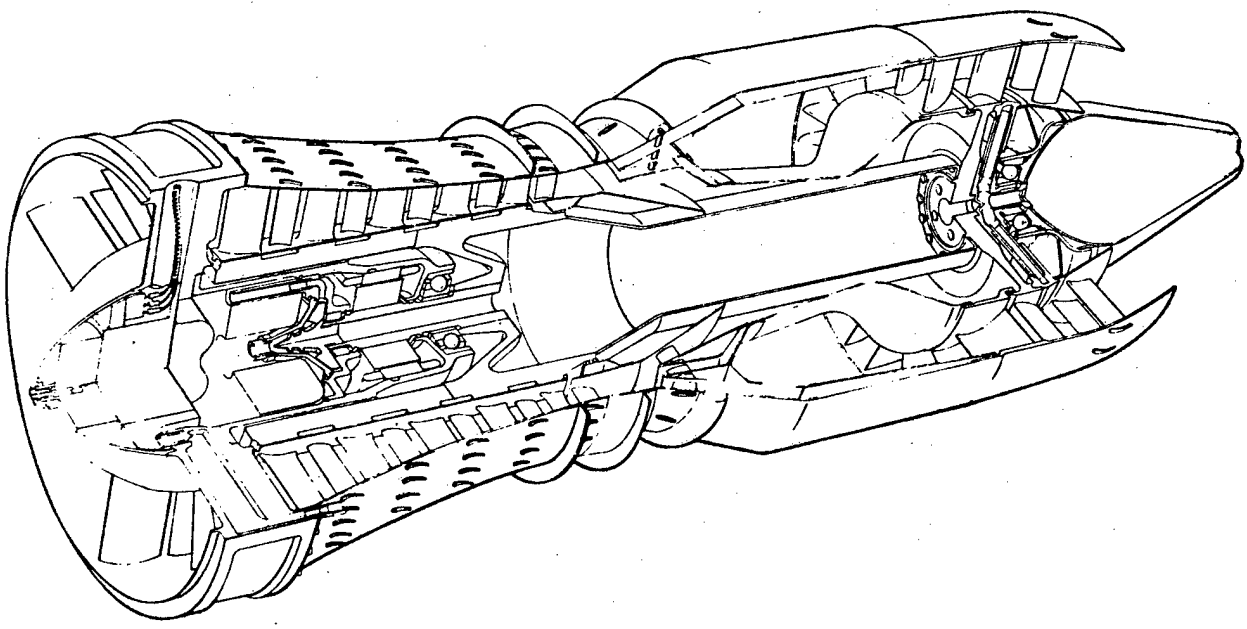

FIGURE 7 - Pratt and Whitney STJ442 Expendable Turbine Engine

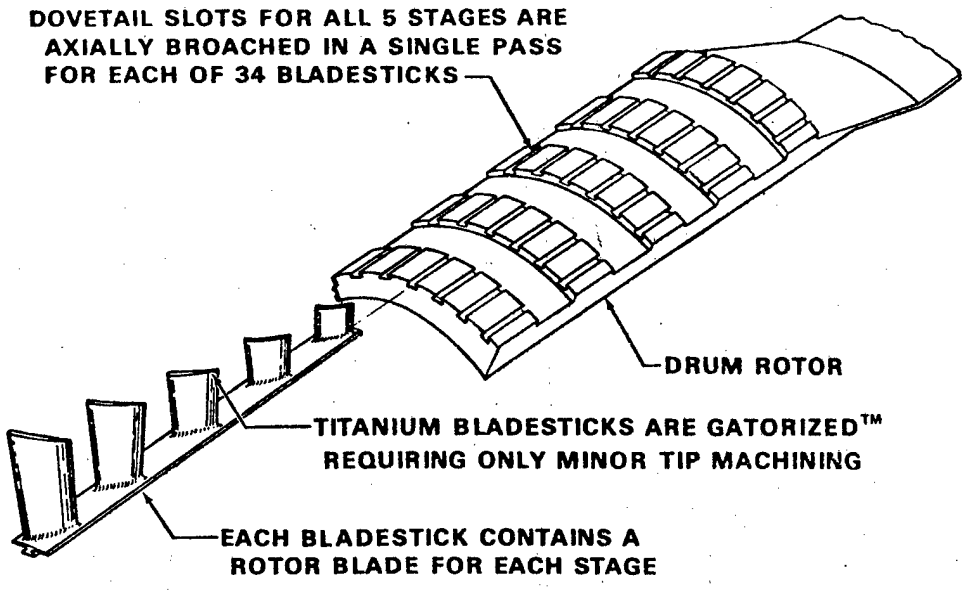

FIGURE 8 - Pratt & Whitney Aircraft Bladestick Compressor

Selection of the compressor as Pratt & Whitney Aircraft's critical component was obvious. While this design potentially offers a low cost manufacturing process for many classes of engines, aerodynamic performance had to be verified along with the capability of fabricating this type of compressor.

As it turned out, the fabrication of the titanium bladesticks proved to be beyond the state of the art of the Gatorizing process at that time. Consequently, the program was terminated after numerous attempts to make the bladesticks were unsuccessful.

PHASE III - Based on satisfactory results of Phase II, a program to continue development of a SETE was warranted. Curtiss-Wright was awarded a contract in September 1975 to complete the development of the remaining major engine components, assemble these components into a gas generator and test the assembly as an engine. The objective of this phase is to demonstrate the basic viability and performance of

the engine design. The gas generator has an identical aerodynamic flow path as a flight worthy engine, but the casings and supporting hardware were modified to facilitate assembly and disassembly of the gas generator, increase operating time capability, and to permit adequate instrumentation for development testing.

A unique aspect of this program is that there was no independent development of the compressor and turbine. The first time these components were operated was as part of the gas generator assembly. This type of approach is necessary to minimize development costs. To put the development cost into perspective one needs only to add the total funding awarded to Curtiss-Wright for all three exploratory development phases. This total effort from design through gas generator test will have been accomplished for approximately $1.23 million.

The results of the initial tests conducted on the gas generator are listed in Table 5. The demonstrated or indicated performance is compared to the engine performance goals. In certain areas, such as compressor efficiency, attaining the engine goals was not anticipated on the first attempt. As it turned out, the compressor efficiency of 82% is considered satisfactory at this stage of development. The thrust levels cited in Table 5, represent the performance level corrected to engine design speed and cycle temperature. The engine times listed at the bottom of the table are the times which were desired to be accumulated during the gas generator program to demonstrate a level of maturity.

Subsequent tests had to be terminated short of attaining 100% rotor speed due to excessive vibration. Extensive analysis of the rotor dynamics revealed that the engine design speed approached the bent shaft critical speed. At this point the most practical solution was concluded to be to modify the rotor system by stiffening the shaft.

Curtiss-Wright is now in the process of making these modifications. Testing is scheduled to resume in November and to be completed by the end of December.

Table 5 - Gas Generator Performance Results

	Engine Goal	Demonstrated
Compressor Efficiency	85%	82%
Turbine Efficiency	88%	88%
SL 1.5 Fn lb	2300	2045
SFC	1.58	1.60
SL .9 Fn lb	1600	1410
SFC	1.42	1.62
SL 1.5 (INTER) Fn lb	1800	1615
SFC	1.59	1.77
MAX Ng RPM	29560	28300
T_2 °F	291	~100
T_4 °F	1900	~1500
Engine Time - Hr	80	11.25
Engine Time @ 95% - Hr	25	1

ADVANCED DEVELOPMENT PROGRAM PLANS

With the gas generator program nearing completion, there is growing confidence that the technology exists within the small engine industry to produce a Supersonic Expendable Turbine Engine. The next logical step is to build and test a number of flight-weight engines and then to demonstrate their capability in a representative flight test.

The purpose of this program, which is Phase IV of the overall SETE development program, is to demonstrate the technology needed for an affordable turbojet powered supersonic stand-off missile.

Procurement activities for the Phase IV program are currently in progress. The anticipated start date is October 1979. A program plan is shown in Figure 9. This schedule is for a five-year program, however, these tasks could be accomplished in less than four years without incurring a significant increase in technical risk. An accelerated program would be conducted at the request of a sponsoring activity to satisfy a specific requirement.

As shown in Figure 9, the Phase IV program has the following major elements:

a. Engine Development - A distinction must be made between this engine configuration and that of a gas generator such as the one developed during the previous phase. The gas generator consisted only of the major engine components and test cell hardware. The engines to be developed in Phase IV are of a flight-weight configuration fabricated essentially as prototype engines. In addition, the minor components, such as the bearings, a fuel control, and an exhaust nozzle will have to be developed.

b. Engine Fabrication - A total of twelve engines will be fabricated for use in the program. Since these engines have been designed for short life, a certain amount of hardware will necessarily be consumed during test and demonstration. Two of the twelve engines will be retained by the engine contractor for development testing. Up to four engines each will be consumed during the Demonstration Flight Rating Tests (DFRT) and Propulsion Test Vehicle (PTV) demonstrations. Two engines will be held in reserve. The engines for the PTV will not be fabricated until after the DFRT has been completed to enable any minor design deficiencies to be corrected for the PTV.

c. Demonstration Flight Rating Tests - A series of tests will be conducted in an altitude engine test cell to ensure satisfactory engine starting capability and operation, and structural integrity before committing any engines to flight tests. These tests will simulate the flight condition which will be encountered during the Propulsion Test Vehicle demonstrations. Any major deficiencies uncovered during

the DFRT will be corrected before embarking on the PTV portion of the program.

d. Propulsion Test Vehicle Design and Fabrication - Three vehicles will be needed for flight tests. The vehicles may be built either under contract or in-house. During the building of the first vehicle, propulsion system integration, including the inlet development, will be conducted. A conceptual schematic of a PTV is shown in Figure 10. The vehicle is considered representative of a stand-off missile. However, there is no intention of developing the PTV into a weapon system, it's sole function being to act as an engine "test cell in the sky".

e. Demonstration Flight Tests - A series of three flight tests are planned, preceded by a captured flight test. During the demonstration program a Navy A-6 or A-7 aircraft will be used to launch the PTV's. The first flight test, a sea-level cruise demonstration, will consist of air launch at Mach 0.6 at 500 feet altitude, acceleration to Mach 1.5 and cruise for six minutes. The second test will be a 20,000 foot altitude demonstration with launch at Mach 0.8, acceleration to Mach 2.0 and cruise for eight minutes. During the third test, a 5-G sinusoidal maneuvering capability will be demonstrated at a sustained speed of Mach 1.5 at 500 feet altitude for a period of one minute.

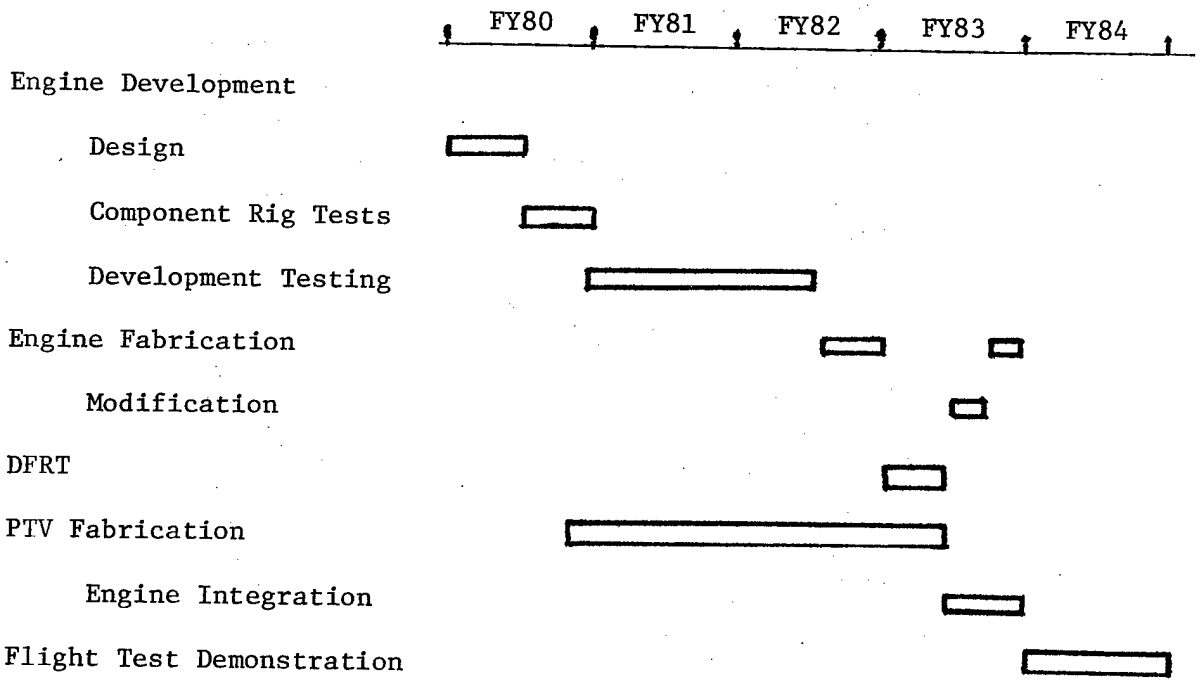

FIGURE 9 - SETE FLIGHT TEST DEMONSTRATION SCHEDULE

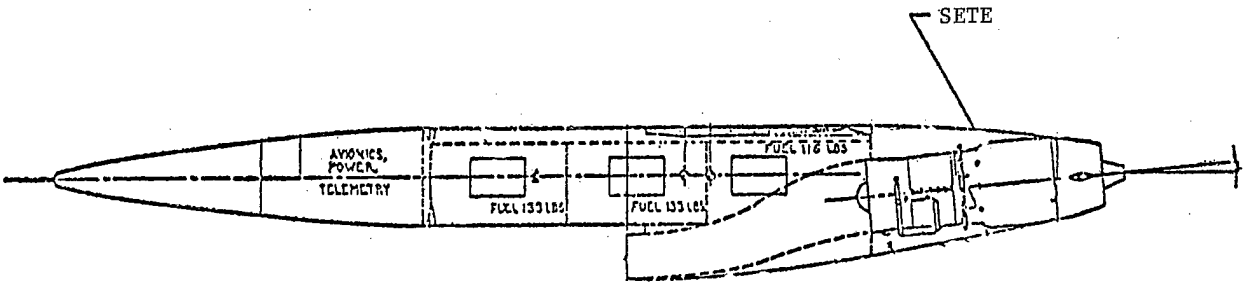

FIGURE 10 - Propulsion Test Vehicle

CONCLUSION

The SETE program has been supported under Exploratory Development to determine the feasibility of developing an affordable turbojet engine to power a supersonic stand-off missile. The technology base to perform this mission has been developed. The next step, which is planned to start early in FY80, is to demonstrate this technology in a series of flight tests. Successful culmination of this program will present a weapons system program manager with a propulsion option filling the void between existing subsonic turbo-powered weapons and high speed, but relatively short range, ram-jet powered systems.

BIOGRAPHICAL SKETCH

Theodore E. Elsasser is the Naval Air Propulsion Center's (NAPC) program manager for small engine technology. As such, he is responsible for formulating program plans to develop the technology base for propulsion systems for missiles, targets, drones, helicopters, trainers and light fighters. Previously, he conducted development test programs on helicopter inlet particle separators and on engine starters and starting systems.

Mr. Elsasser received a Bachelor of Science degree in Mechanical Engineering from Lafayette College and a Master of Engineering from the Pennsylvania State University. In 1975 he was selected for the Naval Executive Management Program and received a Master of Science in Management from the Naval Postgraduate School in 1976.

Mr. Elsasser has numerous publications both in management and technical areas. He is a member of the American Institute of Aeronautics and Astronautics (AIAA) and American Society of Mechanical Engineers (ASME).

A UNIQUE APPROACH FOR REDUCING TWO PHASE FLOW LOSSES IN SOLID ROCKET MOTORS

BY

David C. Ferguson, First Lieutenant, USAF

Robert L. Geisler, Chief, Propellant Development Branch

Solid Rocket Division

Air Force Rocket Propulsion Laboratory
Edwards AFB, California

A Unique Approach For Reducing Two Phase Flow Losses In Solid Rocket Motors

Abstract

The maximum delivered specific impulse (lbs thrust/lbs propellant/sec) in a solid rocket motor is achieved by maximizing the theoretical impulse and then realizing the highest possible efficiency from the motor. The largest degradation of delivered specific impulse, as compared to the theoretical value, is related to the presence of condensed particles in the exhaust, usually metal oxides. The theoretical calculation assumes that these condensed products are in thermal and velocity equilibrium with the flow when, in fact, they rarely are. The theoretical calculation also assumes that any thermodynamically predicted shifts of products from the gas phase to the condensed phase are instantaneous. It also assumes that fusion (conversion from liquid to solid state) occurs when the predicted free stream temperature reaches the condensed substance's melting point. In fact, supercooling, heat transfer delays and crystal nucleation kinetics cause a delay in fusion. The presence of condensed phase also results in particle impingement restrictions on the exit cone half-angle and hence performance loss due to high half-angles.

The general opinion of the propulsion community is that we are presently up against incommutable barriers on all of these parameters. The following discussion addresses conventional wisdom regarding these barriers and one potential solution to transcend them.

The objective of this program is to design and demonstrate a dual chamber rocket motor which will reduce these two phase flow losses in solid rocket motors by effectively reducing the condensed phase particle size. This is accomplished under a four task program: Task I, Design and Analysis; Task II, Propellant Development; Task III, Component Testing; and Task IV, Motor Demonstration Tests.

Introduction (Viewgraph 1)

Metallized solid rocket motors typically experience substantial performance loss due to such parameters as thermal conduction, nozzle erosion, instability, uneven propellant burning, incomplete metal combustion and two-phase flow. Most of these losses can be overcome through propellant tailoring, grain design and hardware construction. The last two parameters, incomplete metal combustion and two-phase flow losses, are the most difficult problems to overcome. It was the purpose of this program to design and demonstrate a dual chamber solid rocket motor to decrease these losses and increase motor performance.

The dual chamber is one possible method of reducing two-phase flow losses, and it should not be assumed that this is the only approach available. Based on hardware availability and simplicity of design, this method was considered to be the most practical approach to demonstrate the principle. The major concern of this program is to create an awareness that two-phase flow losses in metallized solid rocket motors can be significantly reduced for substantial motor performance gains.

Background (Viewgraph 2)

The maximum theoretical specific impulse is most strongly driven by several key thermodynamic features:

$$Isp \propto \sqrt{\frac{Tc}{M}} \qquad \text{and} \quad Isp \propto Pc/Pe$$

where Isp is the propellant specific impulse, Tc is the motor chamber temperature and M is the molecular weight of the exhaust products. Pc/Pe is the pressure ratio, or chamber pressure divided by nozzle exit plane pressure of the motor. In real motors, another important consideration is the nozzle effective half-angle. This is the angle between the flow centerline and the diverging nozzle exit-cone wall of a conical exit cone which gives the same divergence losses as a real conical or contoured nozzle.

The largest single loss of delivered Isp, as compared to the theoretical value, in metallized propellants is caused by the velocity lag of the oxide particles relative to that of the gas flow. In the case of an aluminized propellant, Isp losses of from 2 to 5% of the theoretical value are predicted for very large (60" throat) to very small (1" throat) motors,

respectively. This loss arises from the coarse fraction of the oxide (15-30% by weight of the oxide > 20 micron) failing to accelerate to the gas velocity in the region between the entrance section of the nozzle and the throat. The balance between the aerodynamic shear forces and surface tension forces acting on these particles in this accelerating region result in a maximum stable droplet size for a particular motor. Small motors produce small droplets (2-3 micron) and large motors produce larger droplets (10-15 micron). If the droplets didn't grow with motor size (due to the longer acceleration times in the longer entrance sections), there would be virtually no velocity lag losses in large motors. This, unfortunately, is not the case.

The resulting oxide droplets also create the need for large exit cone divergence angles at the higher area ratios of interest for space motors and ICBM upper stages. The efficiency is degraded to a value of $\xi = 1/2\ (1 + \cos \alpha)$ where α is the half-angle. Typical low expansion ratio solid rockets used in air-launched or lower stage applications operate at 15° and thereby incur a 1.7% divergence loss. High expansion motors are being designed at 17° to 23° half-angles and incur divergence losses of up to 4%.

It can be seen from the above arguments that the presence of a condensed metal oxide phase in the rocket exhaust results in a 5-10% loss in motor Isp as compared to the theoretical value. The metal, is of course, desirable from a density and performance standpoint, even when these losses occur.

One way to produce small Al_2O_3 particles is to cause the aluminum to be reduced in particle diameter before it is oxidized. (Viewgraph 3). The technique was developed under this program to do this aerodynamically in a dual chamber motor with a fuel rich propellant in the forward chamber and an oxidizer rich aft chamber. The molten aluminum droplets generated in the fuel rich chamber are ejected through a nozzle where they are aerodynamically shattered to submicron particles for rapid oxidization. It is thought that this technique was first investigated by the Russians, who developed fuel rich propellants which would form large (> 1000 μ) Al agglomerates.[1] The only utility we could see in this type of formulation was to provide fuel at low oxide level for combustion in a secondary chamber.

It is from these two ideas, reducing Al_2O_3 particle diameter and shattering large Al agglomerates,[2,3] that we decided a dual chamber motor would be the best method to

demonstrate the possibility of reducing two-phase flow losses. (Viewgraph 4). This was accomplished under a four task program: Task I - Design and Analysis; Task II - Propellant Development; Task III - Component Testing; and Task IV - Motor Demonstration Tests.

Task I - Design and Analysis

The basic design utilized 15 lbm BATES (Ballistic Test Evaluation System) motor hardware. (Viewgraph 5). This had to be modified to incorporate a double length and dual chamber with an intermediate nozzle. This intermediate nozzle design is a normal 45° entrance section, a short throat area for minimal Al metal plating, and no exit cone to provide turbulent flow for maximum mixing. Both chambers are 15 lbm center perforated propellant grains. The pressure in the aft chamber must be less than 55% of the forward chamber pressure to maintain sonic flow and prevent perturbations in the aft chamber for affecting forward chamber combustion. Both nozzles were constructed of HLM-85 graphite with the aft nozzle being a typical convergent-divergent design with a contoured throat. The motors are instrumented with 4 pressure transducers (two on each chamber), dual thrust transducers and 12 thermocouples. Visual analysis includes two high speed 16mm movie cameras, 1 still camera and particle collectors to give an indication of Al_2O_3 particle diameter.

Task II - Propellant Development (Viewgraph 6)

Non-aluminized propellants for the aft chamber were already developed under reduced smoke programs so the primary thrust of this task was formulation of the fuel rich propellant for the forward grain. The requirements were to have an overall propellant composition of 18-22% aluminum so the fuel grain required 36-44% Al. (Viewgraph 7). As seen in the figure, the 18-22% Al regime exhibits severe two-phase flow loss; therefore, it is the best area to improve. This plot was a compilation of several hundred BATES motor test firings and covers a broad spectrum of propellant formulations.[2] Motors A and B are 70 lbm and 15 lbm BATES motors, respectively. The burn rate had to be equal to the oxidizer propellant, only at approximately twice the pressure. A propellant with these characteristics was not difficult to develop, the problems came when this propellant was tested in the motor hardware. The Al expulsion efficiency was miserable with the aluminum literally pouring out of the nozzle. In addition, aluminum plated the throat driving the pressure up to intolerable values. Several nozzle design iterations (discussed in Task III) failed to alleviate the problem, and the only

solution to this problem was a higher burn rate to increase the particle velocity and keep them airborne through the nozzle. With an increased burn rate, the fuel grain configuration had to be converted to an endburner to maintain a burn time equivalent to the oxidizer chamber.

The endburner design required a burn rate of approximately 2 inches/sec which proved difficult to meet with a 40% Al propellant. Further analysis of the Russian literature indicated that a new ingredient was being used.[3] We found that this ingredient was silicone and was in the form of a polymer. (Viewgraph 8). Silicone polymers sublime at propellant combustion temperatures, allowing the fuel and oxidizer to burn freely and exhibit a significantly higher burn rate.

Several silicone polymers were analyzed. The low viscosity encapsulating resins were found to be the best with respect to propellant processing and burn rate increase. (Viewgraph 9). Lines 1 through 3 are HTPB propellants and 4 through 7 are silicone polymers, which exhibit a significantly higher burn rate. These propellants provided the required burn rate and produced aluminum agglomerates in excess of 1000μ. Motor testing, however, indicated the same problems as before: low expulsion efficiency and aluminum plating on the throat. This propellant formulation was adopted by Rocketdyne (now Hercules, Inc.)/McGregor, substituting magnesium for aluminum. The propellant became the baseline for their ducted rocket fuel generator and provided an expulsion efficiency of $>99\%$.

We went back to the hydroxy-terminated polybutadiene (HTPB) polymer using a burn rate catalyst developed by the Redstone Arsenal, Carboranyl Methyl Ethyl Sulfide (CMES), to meet the required burn rate. This produced a burn rate adequate for reaching the overall 22% Al desired, when the forward chamber pressure was increased from 2000 to 3000 psig.

Task III - Component Testing (Viewgraph 10)

The components selected for this program were based primarily on existing hardware. The only major change is the addition of the intermediate nozzle and its retainer. So, testing was geared toward evaluation of this design and how it would hold up under high pressure and aluminum flow.

As stated in Task I, the initial design for the shattering (intermediate) nozzle was a solid, one-piece graphite nozzle. This design exhibited severe Al metal plating, which forced the chamber pressure (Viewgraph 11) up to

388

intolerable values and was very unreproducible. Assuming the propellant provided a low flame temperature, the next material tested was a synthetic slate benchtop material. (Viewgraph 12). This material literally melted during the test. The slate failed because the local Al particle flame temperature was extremely high (6000°F), although the overall flame was relatively cool (~3300°F); in addition, the physical erosion due to particle impingement was also a significant factor.

The third nozzle design incorporated an ablative entrance section (asbestos phenolic) to prevent the Al from adhering to the graphite and pouring down into the throat. (Viewgraph 13). This design worked much better than any of the prior designs, but a new problem was encountered. With little or no Al metal coating and protecting the throat, the graphite now eroded giving a regressive pressure trace, thus varying the overall Al% during the test. This erosion was due, in part, to physical impingement, but the main culprit was a chemical reaction between the graphite and Al metal to form aluminum carbide (Al_4C_3).

At this point, the search changed to finding a material with adequate high temperature properties and inert to reaction with molten aluminum. The first material tested was copper, plasma coated with tungsten, zirconium oxide and titanium. (Viewgraph 14). All three components are commonly used for heat shields and high temperature components of liquid rockets. The copper served as a heat sink to conduct the heat away from the throat surface. When tested, the plasma coatings could not withstand the shear forces and peeled off leaving bare copper which quickly melted.

To give high temperature metals a fair chance, the next step was to test a solid piece, instead of just a thin plasma coat. (Viewgraph 15). The material selected was 90% tantalum/ 10% tungsten (Ta10W). Both metals provide good high temperature properties, but the alloy is more practical due to its resistance to thermal shock, machinability and high strength. After this nozzle melted away, we knew that no practical metal could withstand this environment, so we back to graphite.

The final nozzle design incorporated the ablative entrance section and a pyrolitic graphite throat insert. (Viewgraph 16). We assumed this material would chemically erode to form Al_4C_3, but, much to our surprise, it survived the nominal three second

burn time with an erosion rate of only 3 mils/second. This nozzle was incorporated into the motor configuration with the end burning fuel generator as shown in Viewgraph 17.

Task IV - Motor Demonstration Tests

As stated in Task I - Design and Analysis, the initial design was a dual chamber with two center perforated propellant grains and solid graphite nozzles. This design was tested several times with little success due to the erratic pressure in the fuel chamber (Al plating on throat) and the inability to match burn times which made accurate performance calculations virtually impossible. The end burning fuel generator enabled variation in burn time at constant pressure removing the precise burn rate requirements. In addition, the pyrolitic graphite nozzle provided a relatively neutral pressure trace for even more accurate data analysis.

With all major design problems solved, several tests were conducted to demonstrate improved specific impulse efficiency. (Viewgraph 18). These tests exhibited a 1-2% improvement over the baseline at the 21% Al level. The baseline was a double length motor with two center perforated propellant grains of the same formulation. The 16mm movies show a less luminous, more transparent plume indicating better Al combustion in the dual chamber motor and reduced aluminum oxide particle size. The particle sampler results did not support this finding and showed no discernible difference between the tests. This is due to the inability of present state-of-the-art particle sampling techniques to adequately collect the entire spectrum of particle sizes, to collect enough samples to analyze, and to accurately measure the particles when they are collected. Current particle sizing methods cannot completely deagglomerate Al_2O_3 particles and the optical counting system is limited to particles of 2 micron or larger.

In addition to the dual chamber and baseline demonstration tests, two tests were accomplished to determine if the intermediate nozzle was actually required. These tests were dual length, single chamber motors much like the baseline motor, the only difference being one propellant grain contained 40% Al and the other had none. The first test was conducted with the fuel grain in the head end, the second with it in the aft. Both motors performed poorly with a specific impulse efficiency 8% lower than the baseline test. This provides evidence that the intermediate nozzle is required to shatter the aluminum agglomerate for more efficient combustion.

Finally, two more tests were conducted at a lower aluminum level (12-14%) to determine primarily the exhaust plume visibility and see if efficiency improvements could be made with a longer aluminum particle residence time. The residence time was increased by adding another oxidizer grain to the aft end, providing a triple length, dual chamber configuration. The first test had uneven burnout with the fuel grain burning 0.3 seconds after the oxidizer grains extinguished. This made performance calculations difficult and flooded the particle collector with large oxide particles. The second test could not be accomplished in time for this paper, but the results will be reported at the symposium.

Conclusions (Viewgraph 19)

The objective of this program was to demonstrate the feasibility of increasing metallized rocket motor efficiency via two-phase flow loss reduction and improved aluminum combustion. This objective was achieved with a 1-2% specific impulse efficiency increase demonstrated in a dual chamber solid rocket motor. In addition, the silicone propellant discovered under this program was utilized by Rocketdyne as the baseline propellant for the Ducted Rocket fuel generator.

The payoff of this program is primarily demonstration of the dual chamber concept. The dual chamber, in addition to minimizing two-phase flow loss through reduction of condensed phase particle size, can capitalize on the use of staged combustion to allow the use of high energy materials. Development of fluorine containing fuel rich propellants should decrease the condensed phase particle size to less than one micron and, with the dual chamber, higher energy oxidizers in the aft chamber will combust these particles to fine oxide with little or no reagglomeration.

In addition, high energy fuels such as metal hydrides, can be safely used in the dual chamber motor to increase performance as much as 5%. Previously, hydride propellants were plagued with processing hazards and outgassing of hydrogen which made them virtually useless. To utilize hydrides, the propellant must be dry mixed with a low energy oxidizer (e.g., ammonium nitrate) and pressed in the desired grain configuration. This method decreases hazards and allows hydrogen gas to escape due to the porosity of the propellant. In the dual chamber configuration, high energy oxidizers will be used only in the secondary chamber, thus reducing hazards

and increasing propellant performance.

In conclusion, the dual chamber concept will allow use of high energy ingredients at reduced risk to produce a higher performance solid rocket motor. The long range payoff is increased range/payload in tactical and strategic missiles.

LIST OF REFERENCES

1. Kashporov, L. Ya., Frolov, Yu. V., et al., "Investigation of Agglomeration and Dispersion of the Two-Phase During the Combustion of Model Compositions with the High Content of Powder-like Metals", (FTD-MT/ST 75-1988, preliminary translation, September 1975).

2. Geisler, Robert L., Kinkead, Scott A., Beckman, Charles W., "The Relationship Between Solid Propellant Formulation Variables and Motor Performance", AIAA Paper No. 75-1199, October 1975.

3. Ostretsov, G.A., Frolov, Yu. V., et al., "The Mechanism of Agglomeration During the Combustion of Solid Fuels with High Content of Metallic and Organic Fuels", Ordena Lenina Institut Khimicheskoy Fiziki, Akademiya Nauk SSSR, 1974, pp. 1-9, (English Translation, FTD-MT-24-0967-75, March 1975).

A UNIQUE APPROACH FOR REDUCING TWO-PHASE FLOW LOSSES IN SOLID ROCKET MOTORS

BY DAVID C. FERGUSON, 1LT, USAF

ROBERT L. GEISLER, CHIEF, PROPELLANT DEVELOPMENT BRANCH

SOLID ROCKET DIVISION

AIR FORCE ROCKET PROPULSION LABORATORY

EDWARDS AFB, CALIFORNIA

MOTOR PERFORMANCE LOSSES

$I_{sp} \propto \sqrt{Tc/m}$

$I_{sp} \propto Pc/Pe$

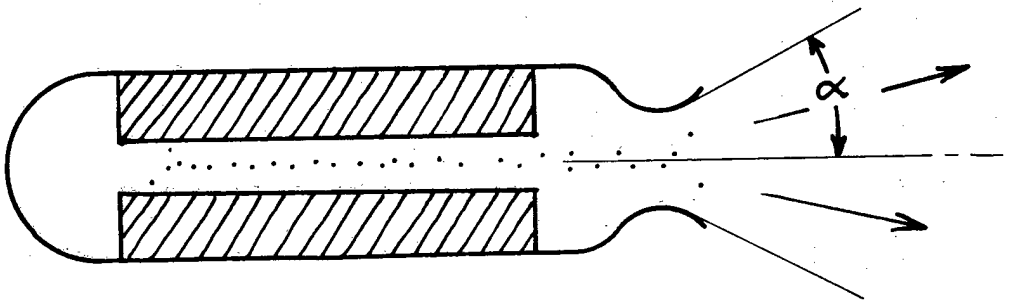

$\varepsilon = \frac{1}{2}(1 + \cos\alpha)$

- HEAT LOSSES
- VELOCITY LAG
- DIVERGENCE

$I_{sp} \propto Wp/Wg,\ Dp$

DUAL CHAMBER CONFIGURATION

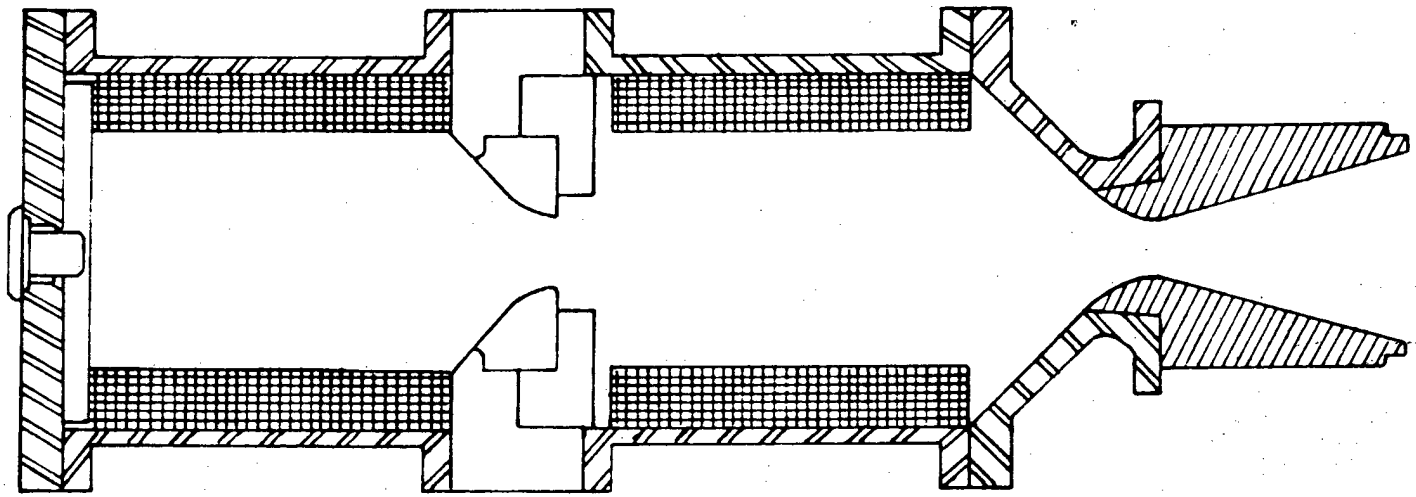

DUAL CHAMBER MOTOR DEVELOPMENT

I - DESIGN AND ANALYSIS

II - PROPELLANT DEVELOPMENT

III - COMPONENT TESTING

IV - MOTOR DEMONSTRATION TESTS

TASK I DESIGN AND ANALYSIS

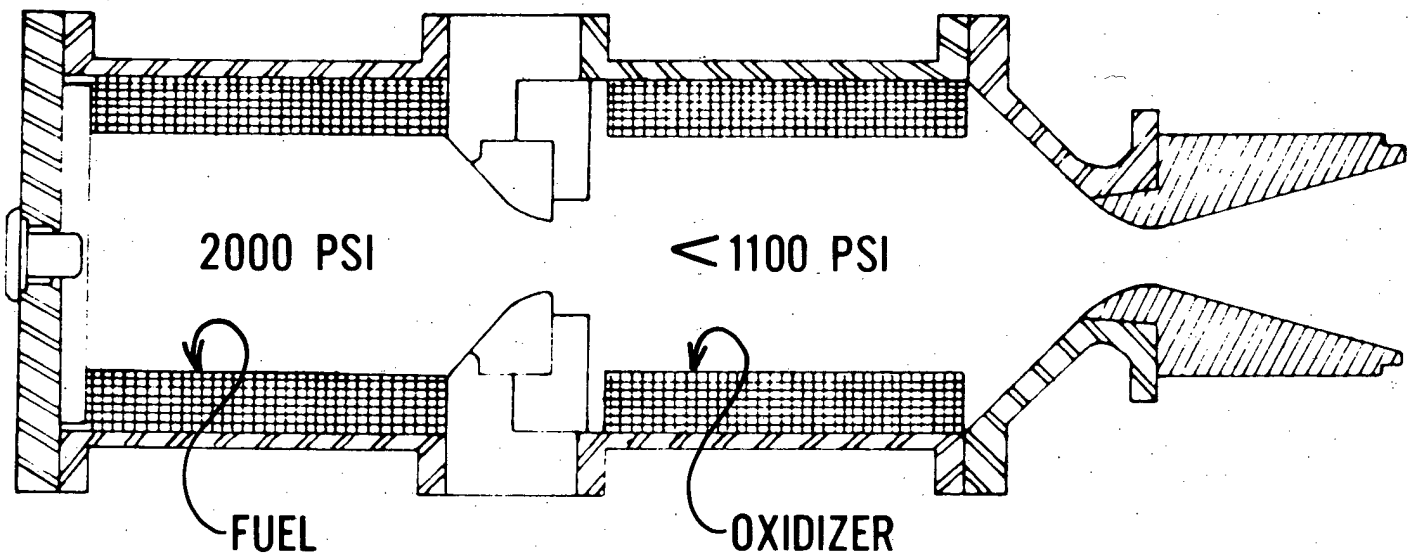

TASK II - PROPELLANT DEVELOPMENT

REQUIREMENTS

- NON-ALUMINIZED PROPELLANT
- FUEL RICH PROPELLANT
- 18 - 22% Al OVERALL
- BURN RATES EQUAL
- HIGH EXPULSION EFFICIENCY

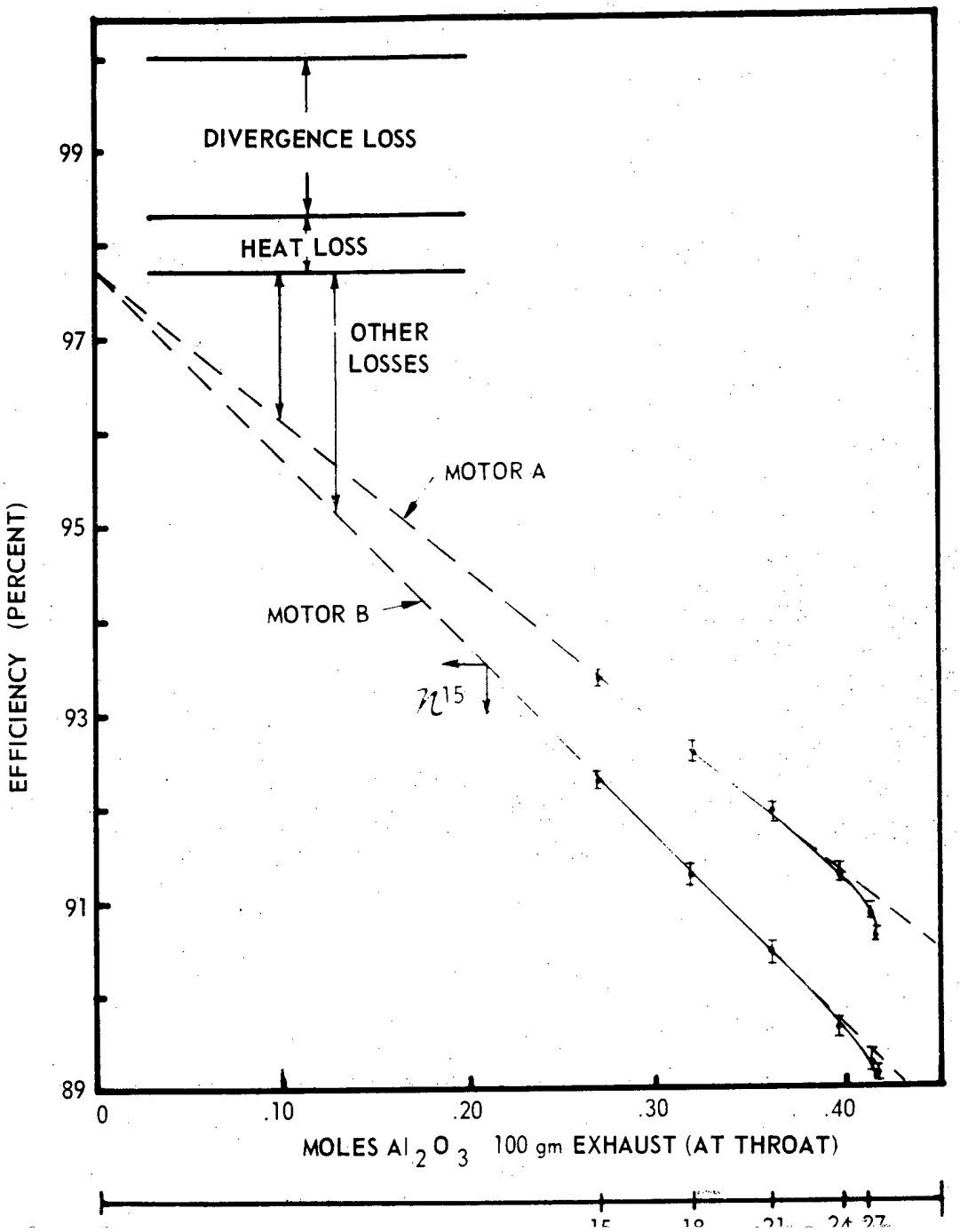
DIVERGENCE LOSS
HEAT LOSS
OTHER LOSSES
MOTOR A
MOTOR B
η_{15}
EFFICIENCY (PERCENT)
99
97
95
93
91
89
0
.10
.20
.30
.40
MOLES Al_2O_3 100 gm EXHAUST (AT THROAT)

SILICONE PROPELLANT FOR HIGH BURN RATE

HTPB PROPELLANT

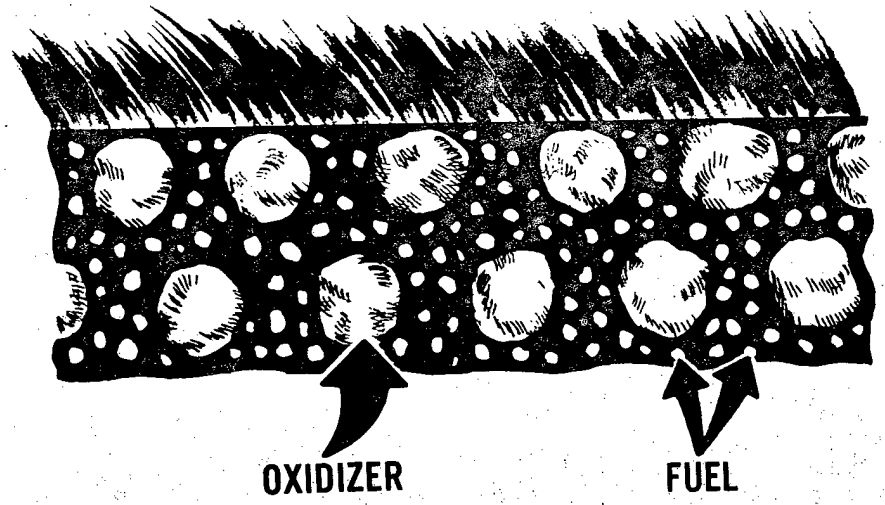

SILICONE PROPELLANT

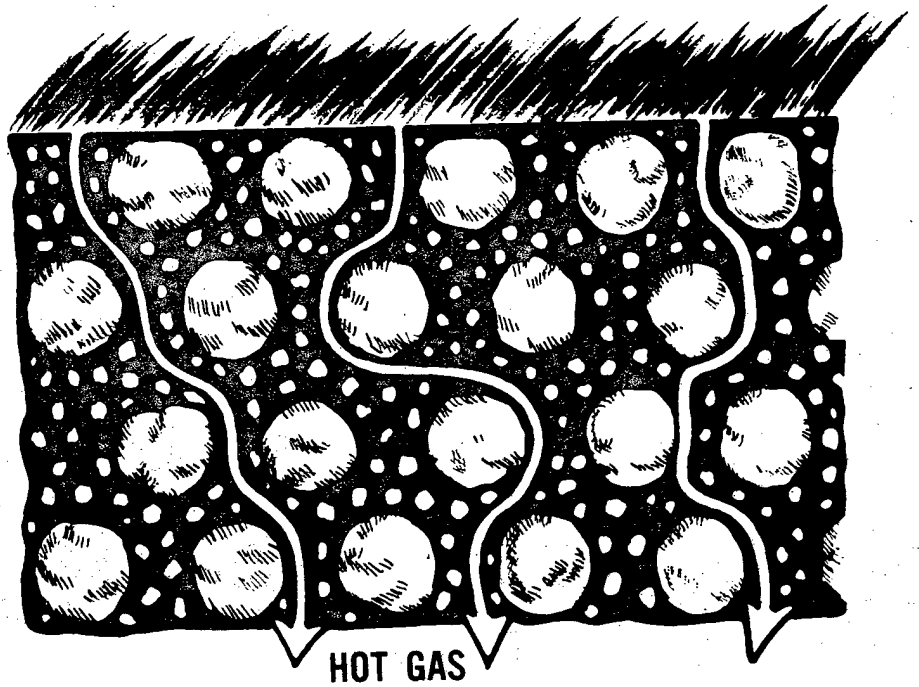

BURN RATE VS PRESSURE FOR SILICONE & HTPB PROPELLANTS

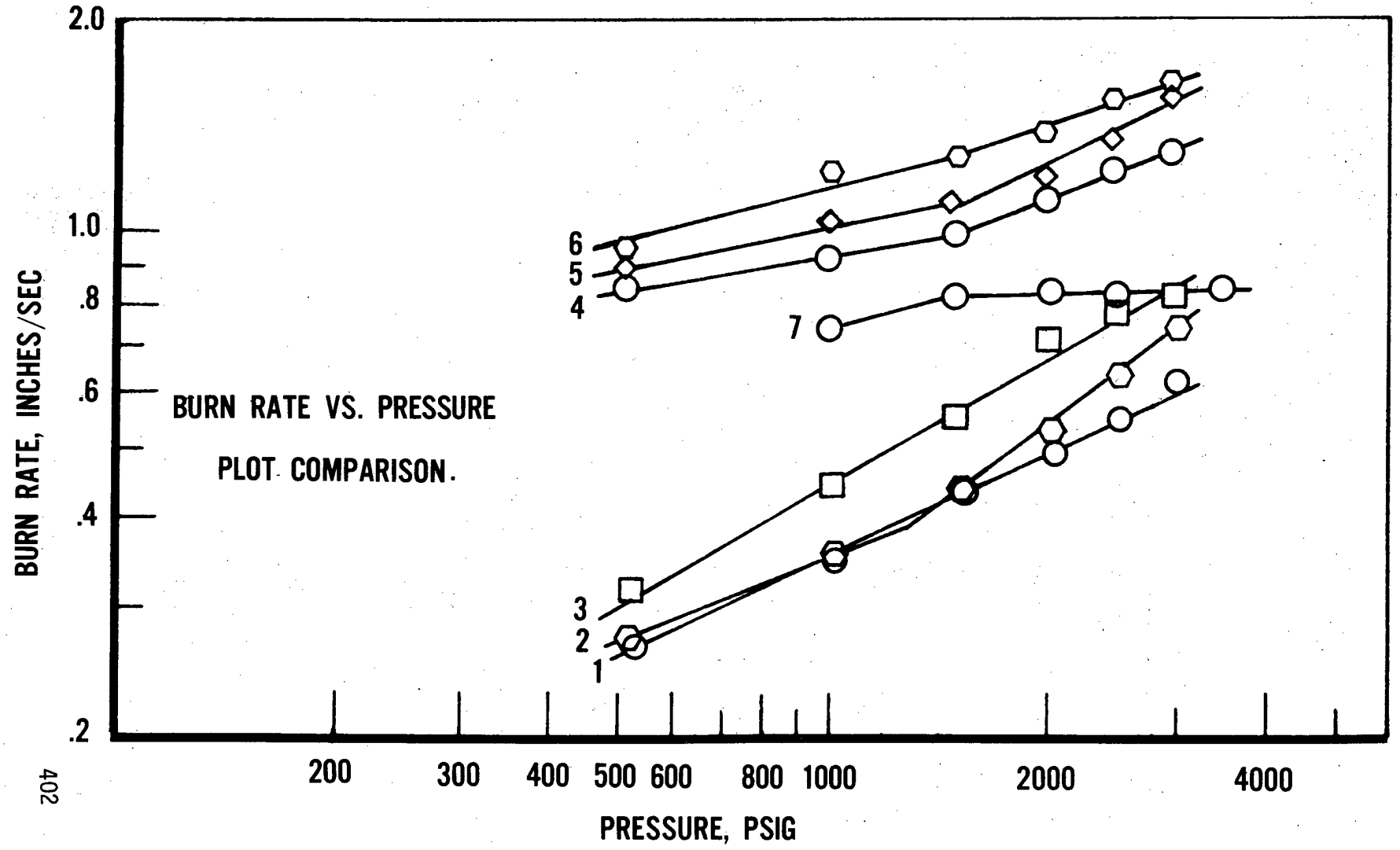

TASK III - COMPONENT TESTING

- EXISTING HARDWARE

- SHATTERING NOZZLE DEVELOPMENT

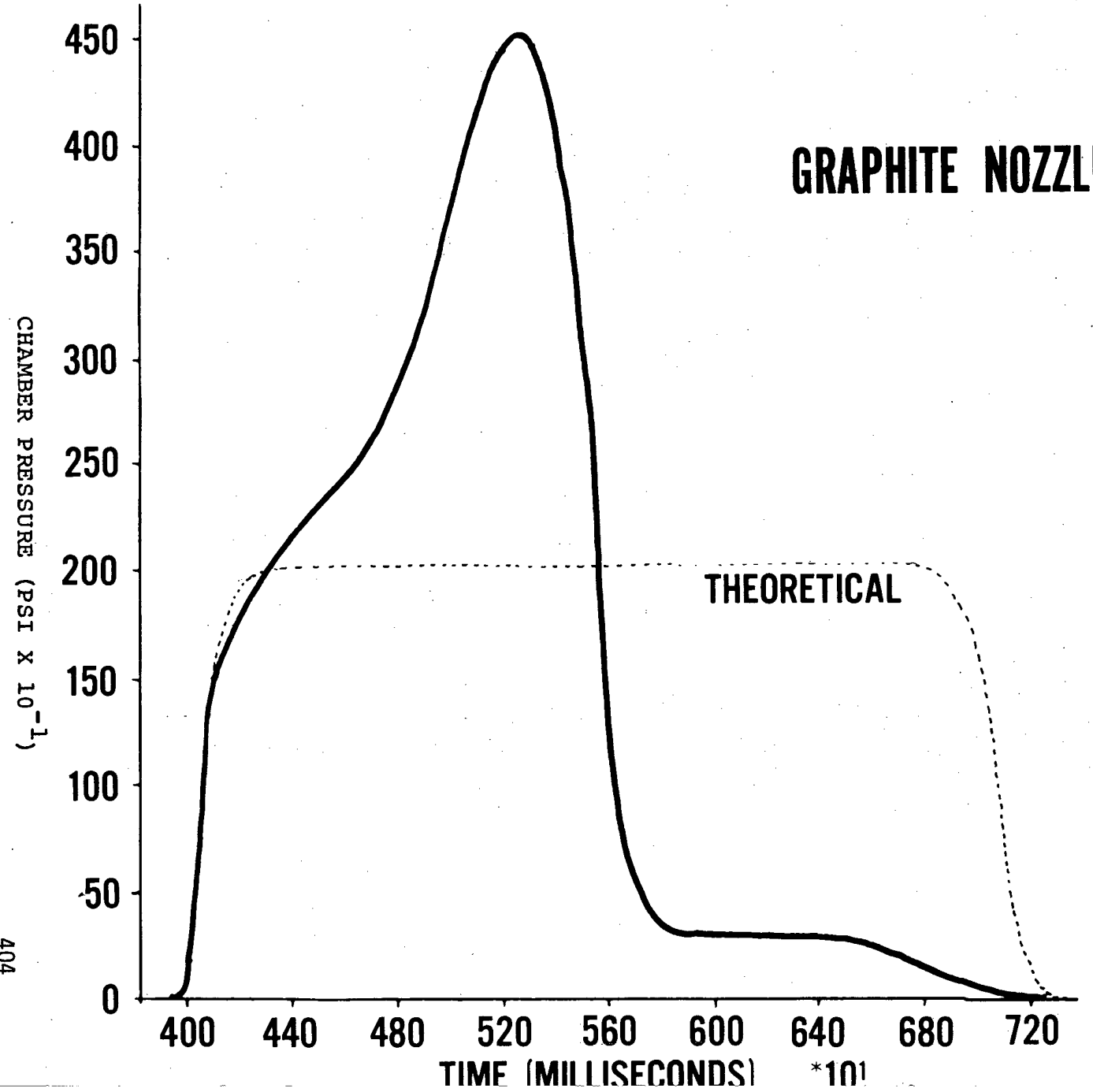
GRAPHITE NOZZLE TEST
THEORETICAL
CHAMBER PRESSURE (PSI X 10⁻¹)
450
400
350
300
250
200
150
100
50
0
400
440
480
520
560
600
640
680
720
TIME (MILLISECONDS) *10¹

SYNTHETIC SLATE NOZZLE

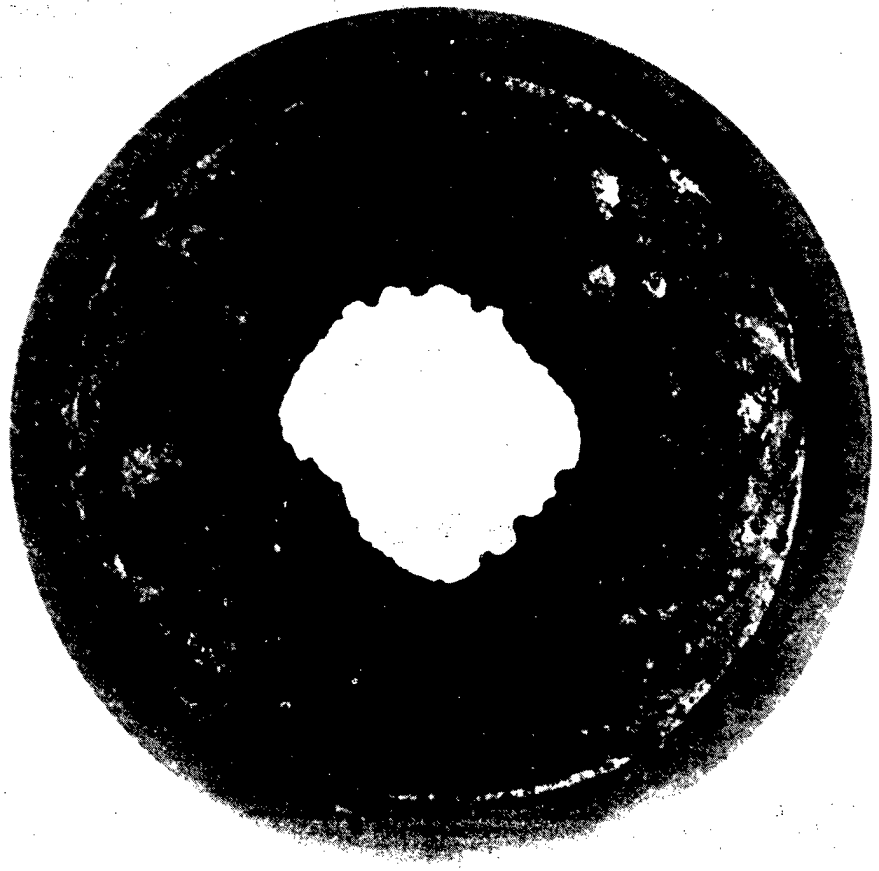

GRAPHITE WITH ABLATIVE ENTRANCE SECTION

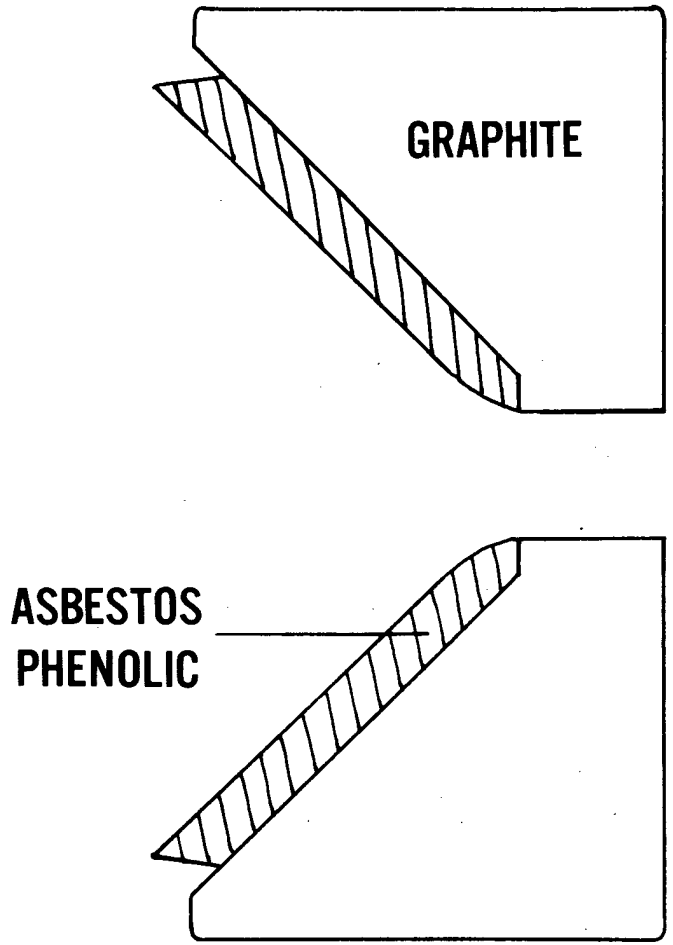

PLASMA COATED COPPER NOZZLE

TA10W NOZZLE

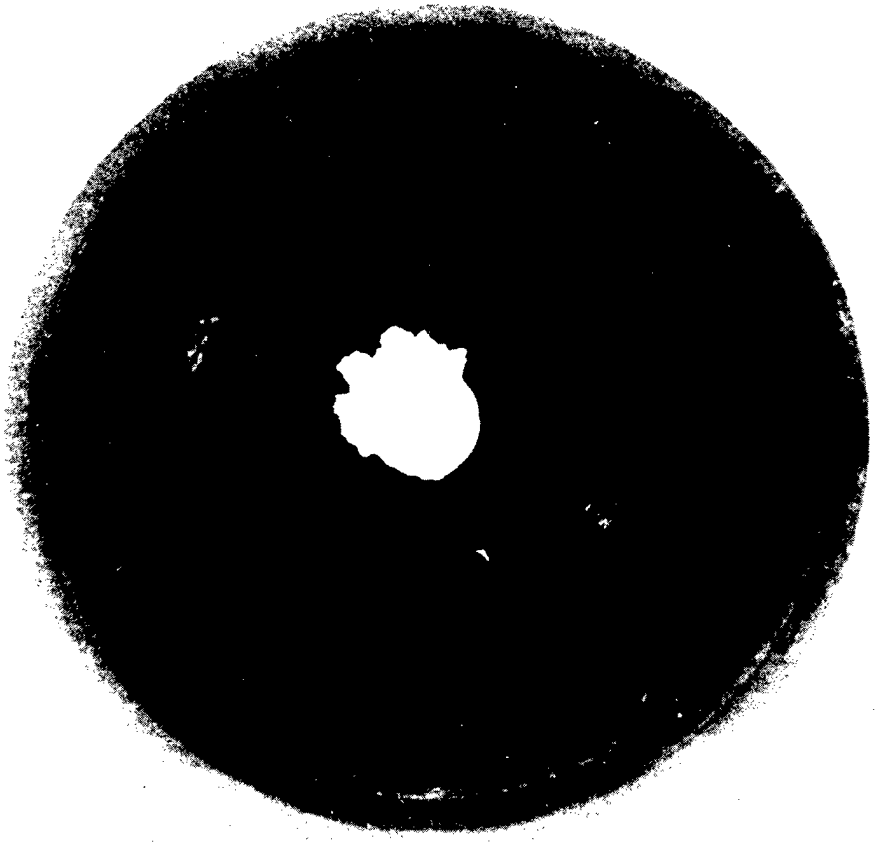

PYROLITIC GRAPHITE NOZZLE

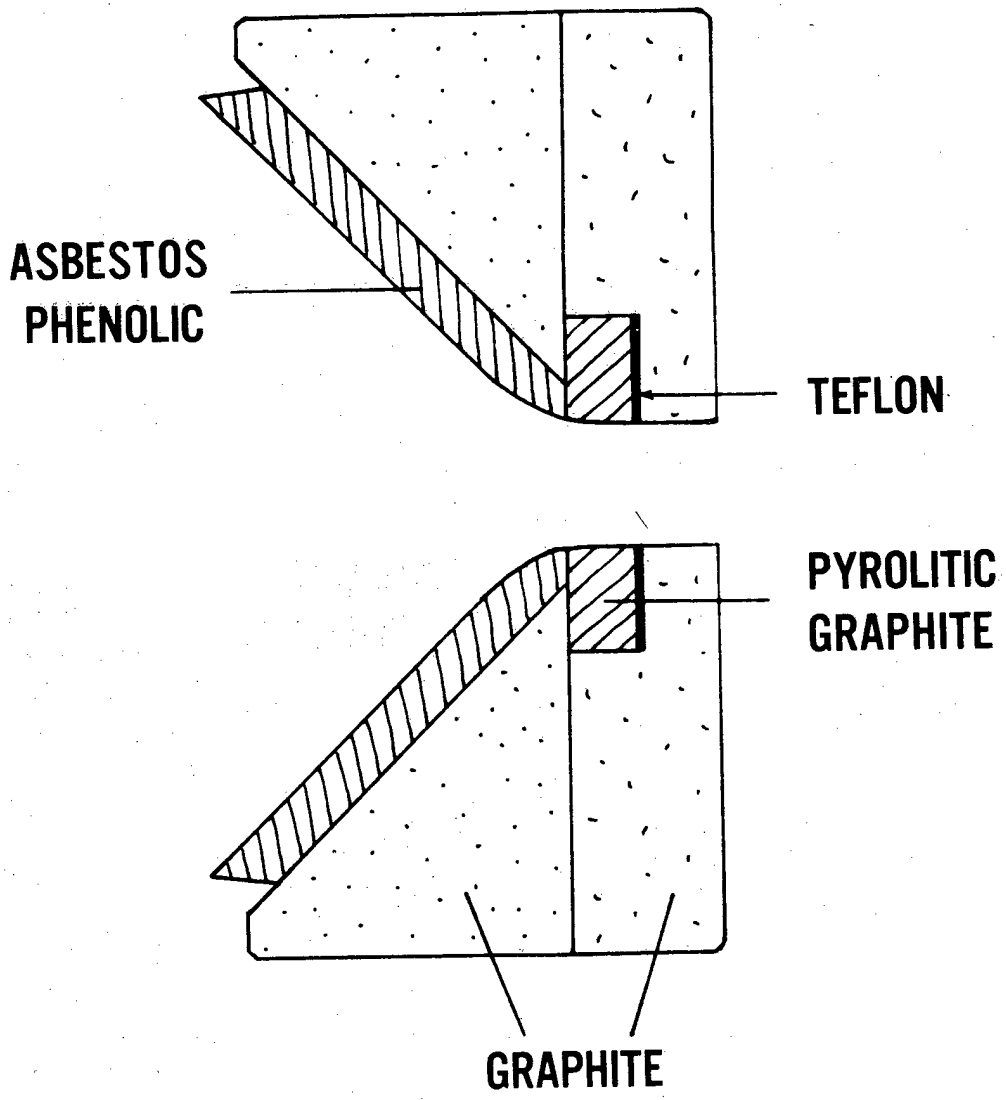

FINAL MOTOR DESIGN

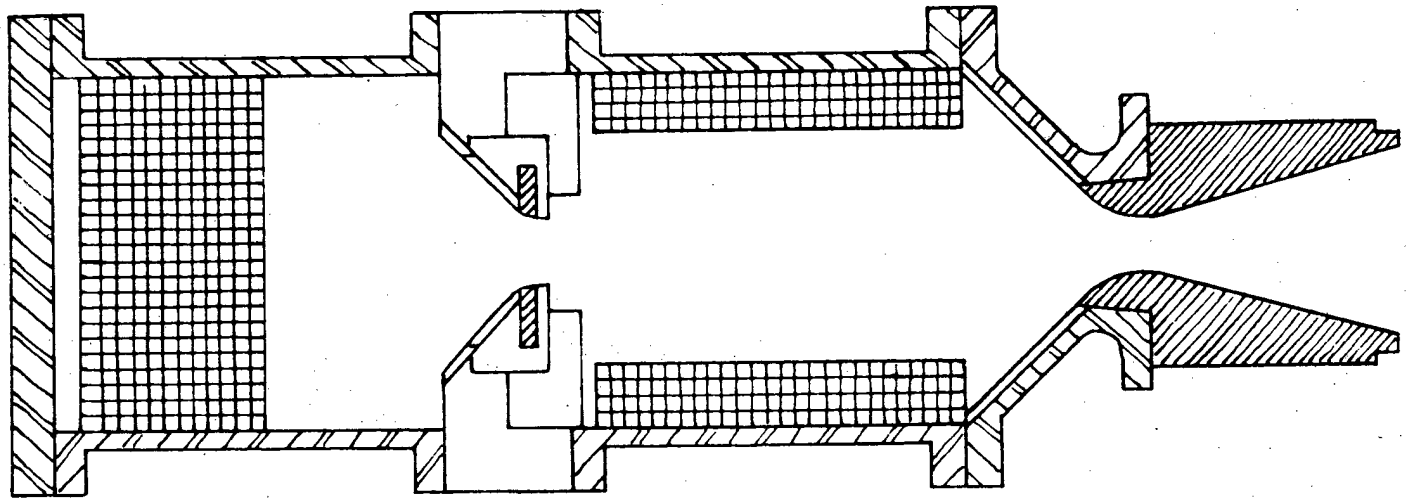

TASK IV - MOTOR DEMONSTRATION TESTS

- DUAL CHAMBER - 1 - 2% ISP EFFICIENCY IMPROVEMENT OVER BASELINE
- OXIDE SAMPLING TECHNIQUES LACKING
- INTERMEDIATE NOZZLE REQUIRED - TWO TESTS WITHOUT
- LOWER LEVEL AL TESTS - NO IMPROVEMENT
- MOVIES

CONCLUSIONS

- DEMONSTRATED DUAL CHAMBER CONCEPT
- DEVELOPED SILICON (RTV) PROPELLANT
- DEMONSTRATED 1 - 2% IMPROVEMENT

FUTURE DEVELOPEMENT

- FLUORINE CONTAINING FUEL RICH PROPELLANTS TO REDUCE OXIDE PARTICLES TO $<$1M
- METAL HYDRIDE FUELS FOR HIGHER PERFORMANCE
- HIGH ENERGY INGREDIENTS

Biographical Sketch

Lt David C. Ferguson graduated from the USAF Academy in 1975 with a B.S. in Chemistry. In August 1975 he arrived at the AFRPL where he began work on an in-house research program investigating the combustion of aluminum in solid rocket propellants. During the past three years, Lt Ferguson has been project manager on three in-house research programs dealing with such problems as zirconium powder sensitivity and burn rate, aluminum combustion efficiency, and reduced hazards/high energy propellants. In addition, he has been project manager on four AFRPL contracts concerned with additives and processing techniques to increase the combustion efficiency and burning rate of solid rocket propellants. Lt Ferguson moved from the Propellant Branch to the Air-Launched Missile Propulsion Branch in October 1977. He is currently the project manager on two Ducted Rocket contracts, an AFAPL Ducted Rocket Support Program and a contract to demonstrate a solid rocket motor for the Wide Area Anti-Armor Munition (WAAM) Minimissile.

Mr. Robert L. Geisler graduated from the University of Cincinnati in 1958 with a Bachelor Degree in Chemical Engineering. He began his career in solid rocketry that year as an Air Force Civilian Project Engineer in the Propulsion Laboratory at Wright-Patterson Air Force Base, Ohio. In 1959 he moved with the functional transfer of the rocket propulsion group to Edwards Air Force Base to form the nucleus of what is now the Air Force Rocket Propulsion Laboratory. He has spent his 20 year career in the Solid Rocket Division of AFRPL, steadily progressing to positions of increasing responsibility to his present position as Chief of the Propellant Development Branch. His Branch is responsible for all USAF exploratory development on advanced solid propellants for Ballistic Missiles, Air-Launched Missiles and Space Propulsion Systems. Mr. Geisler is a highly creative and respected national expert on solid propellants and holds numerous invention disclosures and patents on propellants, combustion and related areas. He is active in the Tri-Service/NASA Propulsion Community and often serves as a consultant on many major weapon systems and projects.

MISSILE SYSTEMS PROPULSION COOK-OFF

BY

Ronald F. Vetter

Propulsion Systems Division

Naval Weapons Center
China Lake, California

MISSILE SYSTEMS PROPULSION COOK-OFF

Abstract

Aircraft carrier ordnance and missiles (both on and off aircraft) are subject to fuel fire at a significant level of occurrence. The hazard level to life and property is high and should be reduced. The testing immediately following the Forrestal incident gave a baseline time to "reaction" of about one minute for rocket motors tested individually with pressure vessel rupture being the typical result. Externally insulated Phoenix did withstand heating for a longer time but was perhaps more violent at reaction. The MK 78 Mod 0 boost-sustain Shrike deflagrated mildly. A large part of our effort has been to elucidate the mechanisms of failure and especially to understand why mild-burning-reaction occurred with one configuration. A "failure map" was deduced. A wide variety of laboratory scale liner/case samples were tested over a flame to observe gross characteristics. Initial attempts with propellant in the "sandwich" showed a great deal of liner and bond failure before the propellant was warmed much. The rather low temperature unbonding and clean release of polyether-based polyurethane liners compared to sticky foaming with most other tactical missile case bonding formulations was postulated to be the cause of mild deflagration observed. Model motors were devised and tested over an array of propane/air burners since visible results were nearly negligible in the JP-5 fuel fires and it was also recognized that the capability of extinguishing the fire at will might provide much more valuable post-test evidence. Development rocket motors have also been tested as well as test motors made expressly for cook-off over JP-5 fuel fires.

The use of external insulation is not recommended for aerodynamics, weight, and cost reasons but primarily is not recommended because it leaves the pressure vessel at near full strength when reaction occurs. The use of normal construction with inclusion of a polyurethane liner and a bladder above this (with special concern that fore and aft sealing of the bladder is accomplished) will often yield mild burning in a cook-off fire. A gassing agent in the case primer may also suffice to provide a gas pocket. Best practice is to include a segment or an entire case wall of plastic bonded filament, tape, or laminate which disintegrates in fire.

(Introduction will be a movie segment of Forrestal fire)

Background. The fast or fuel-fire cook-off environment has been a part of safety testing of aircraft carrier ordnance for many years but the Forrestal and Enterprise catastrophes re-emphasized the importance of minimizing the likelihood of violent pressure vessel rupture, explosion or detonation being initiated by aircraft fuel fire. Much earlier, the carrier USS Franklin on 19 March 1945 lost 724 dead and had 265 wounded with much due to fires from two Japanese 550# bombs (per an April 1969 issue of American Heritage Magazine). NAVAIRSYSCOM has a cook-off improvement plan generated after the Forrestal fire and has imposed the newly generated MIL-STD-1648(AS) on new programs. Retrofit programs on bombs, warheads and rocket pods were priority funded after a baseline test series which tested most of the Naval ordnance used on aircraft carriers.

Some advanced development funding was programmed for concept generation and testing to reduce the hazard level of solid propellant motors in fuel fire (NWC TP 5921 reports the bulk of this effort). Future funding is programmed to continue concept refinement and reduction to acceptable engineering practice; and to attempt preparation of a computer design code to add chemical reactions and structural analysis to the thermal codes now existent.

There is also retrofit and advanced concepts funding supporting work at Pt. Mugu, NWC, NADC and at several contractors. The Safe Transport of Munitions program is also underway and testing has been done related to the railroad car fires where bombs have been involved.

Goals. Imposing MIL-STD-1648(AS) on the propulsion design to make cook-off characteristics as important as motor delivered impulse, environmental suitability, cost and quality goals is one of our prime objectives. Secondly, gaining better understanding of the failure mechanisms and being able to provide valid analysis of design options and recommending proven concepts which provide low hazard reactions in fire are important goals. All of this can save lives and money also.

Status and Results. We have attempted to disseminate what we now know, or believe, to the propulsion community via presentations at meetings and published documents including TP 5921, TM 3299 and TM 3511 from NWC on solid rocket motors. The prime contractors and rocket motor contractors interested in AMRAAM have been supplied with TP 5921 and discussions, opinions, etc.

Some very suitable test results in fuel fires have been obtained. The MK 78 Mod 0 rocket motor has exhibited a mild reaction (see figure 1, photo LHL 179446) in the four tests when it was subjected to fire and has been a "model" or "goal" for this investigator even though the time of reaction was of the order of one minute in enveloping flame, which is typical of all uninsulated rocket motors. The goal of 5 minutes before reaction has been given second place to the goal of not having significant high hazard to the firefighting crew.

Internal insulation may provide both long times to pressure vessel rupture and rupture at low pressure - i.e., "burning" rather than explosion. External insulation has the effect of keeping the pressure vessel at lower temperature which means that the typical steel pressure vessel will rupture at high pressure - above design maximum expected operating pressure (MEOP) - and the gases expansion to atmospheric pressure will carry all the pieces to high velocity causing damage and injury as well as spreading the fire.

Three other designs besides the MK 78 Mod 0 have provided excellent results. Chronologically, these were one of the four Agile cook-off configurations; next, fiber reinforced plastic motor case; and third, the laminated steel strip motor case.

Two of the four Agile motors were judged to have passed MIL-STD-1648(AS) as single samples but one was very mild burning with no noise indication of case rupture and no movement of parts during the test (see figure 2, photo LHL 182922). The first sounds on the video-tape are of propellant burning at low pressure until the inner bore is reached when the added surface area generates some pressure. This motor had a double liner layer with the outer layer containing some calcium formate to produce gas (insulating layer) when high heat was applied. The insulating gas layer is believed to retard heat transfer into the liner and propellant and hold heat in the metal case causing it to soften and thin as it expands due to gas pressure (see figure 3). Several other important factors, as we see it, are the gas-tight fore and aft liner/case seals, the reasonably crush resistant propellant grain configuration, and the low propellant burning rate which does not present as much gas to build high pressures when ignition eventually occurs. It is noted that the MK 78 Mod 0 configuration has a very low burning rate sustainer propellant adjacent to the liner and case wall over the entire length of the rocket motor. Also, its liner is a polyurethane which, when heated by flame, detaches cleanly from the case and forms some gases as well as low viscosity liquid.

The fiberglass/polyester and Kevlar/epoxy novolac cases (one each) constructed and tested have the intrinsic advantages of insulative character and loss of pressure vessel character as they heat up to the temperature where propellant ignition will occur. Also, the gases generated will "percolate" easily through the soft plastic and not deform the propellant grain. Deformation is believed to be a proximate cause of violent pressure buildup and rupture. No significant bore deformation or pressure was detected within the bore of these "motors" during cook-off testing.

The strip laminate construction (of the British Rapier missile) rocket motor was tested on two test items obtained on contract from the Hercules licensee. These were loaded with fresh liner and propellant at NWC, then tested in a propane burner fire facility which allows high speed photography during the test in contrast to the MIL-STD-1648(AS) fuel fire which is an opaque, sooty flame. Both units were nozzleless (12.7 cm dia x 1 meter long cylindrical shape with round bores of 5 cm dia and both ends sealed). The adhesive layers bonding the pressure vessel's three spiral wrapped layers of 0.28 mm thick steel shim give off smoke as the first visible effect of fire. Later, after much smoke at the gap joints, a flame appears and some of the steel strip unwraps (tears, opens up, burns away). This burning and unwrapping increases in area until much of the case is gone and the cylindrical grain outer diameter is visible and burning (we used reduced smoke propellant). Eventually the web burns through, as visible on the film (which will be shown) and corroborated by the bore thermocouples and linear potentiometer. Figure 4 shows the thermocouple measurements from this particular test and figure 5 is a photo of the remains. The second test was identical in result and had only one variation in construction. The end fixture area was more reinforced and insulated to simulate a massive wing holder or other external structure which would reinforce and insulate the tube ends in some missile configurations. Recent British tests of Rapier over small pit fuel fires corroborate the mild failure mode.

These solutions to the problem have other problems. Acceptance of the higher costs, risks, volume and uncertainty of the fiber-reinforced plastic rocket motor may improve as time becomes history. Similar concerns exist for the strip laminate or some such adhesively bonded construction. There is also the unsolved problem of aeroheat capability with production adhesives. The use of fiber reinforced plastic aircraft parts is undoubtedly improving the technology in this area.

Heat activated initiation of exothermic chemicals which softens or cuts the steel case is a scheme (depicted in figure 6) which has not been tried. The heat from this may also ignite the propellant in a small area which may also be desirable. If the burning surface area is small, only a relatively small amount of gas is produced and this will vent easily through a small hole without significantly deforming the grain, nor peeling liner off a large surface area. Then too, the hot gases from the propellant will erode the steel quickly and enlarge the vent hole area. This is excellent for maintaining low pressure burning when the bore surface is eventually ignited.

The anticipated sequence of events in a fire for the adhesive joint concept, figure 7, is that bond strength reduction will occur at an early time. (The adhesive must be a high temperature type to withstand aero-heating.) The adhesive will then decompose and provide a gas exit passage per se plus allow the head and aft sections to separate if enough pressure is generated to part the grain. This latter is not expected early and is not desirable since it would expose a pair of large broken propellant surfaces and the bore to ignition in typical rocket motor configurations.

Conclusions and Recommendations. There are several case constructions which provide mild burning reactions. Insulation extends the time to reaction. However, external insulation keeps the pressure vessel temperature low (thus maintaining high metal strength) and thus may tend to increase the rupture pressure level. Insulation also adds weight, volume, environmental, cost, and aerodynamic drag considerations. Some concepts of clamp and adhesive joints pre-planned as weak sections of the typical steel pressure vessel have not yet been evaluated. Other "active" concepts may be feasible wherein pressure vessel integrity is sufficiently degraded after fire triggers the mechanism. Some too complex - multiple sensors and explosive cutters, etc - concepts of this sort have been considered and rejected with a few or no tests. There may also be merit in a pilot actuated system when he sees fire.

Some other fire environments should also be considered by designers and persons working in the cook-off area. "Slow cook-off" has low pertinence for most modern propellants since the live steam leak or heating equipment malfunction are not likely to provide temperature sufficient for self-heating except for double-base formulations. However, structure or transportation fires do occur. The fire on ship is more serious due to confinement of the personnel, but the wood-fueled fire usually presents a lower flame temperature and has little chance to

soften a steel pressure vessel. The smoldering fire will have a chance to promote self-heating which means most or all of the propellant charge will be at high temperature when reaction occurs. This will be a more violent rupture.

Encouragement and funding of high temperature adhesives for laminate or fiber vessels is needed along with environmental testing of the finished products.

(U) FIGURE 1. Mk 78 Mod O remains after cook–off. (U) (Neg. 179446)

(U) FIGURE 2. Agile variation cook-off test remains. (U) (Neg. LHL 182922)

CROSS SECTION OF CASE AFTER PYROLYSIS GASES HAVE BEEN GENERATED FROM THE CASE PRIMER AND A PART OF THE LINER. NOTE THAT THE PYROLYSIS GASES BUBBLE FORMS ON THE BOTTOM PART OF THE CASE IN A FIRE AND THAT CLEAN SEPARATION IS TYPICAL OF LINER WHICH DOES NOT FORM AN ADHESIVE CHAR. THE HOTTER SURFACE OF THE LINER WILL BE LIQUIDUS (MELTING) AND A BOILING HEAT TRANSFER EXISTS FOR A TIME ON THE INNER WALL OF THE CASE INTO THE BUBBLE.

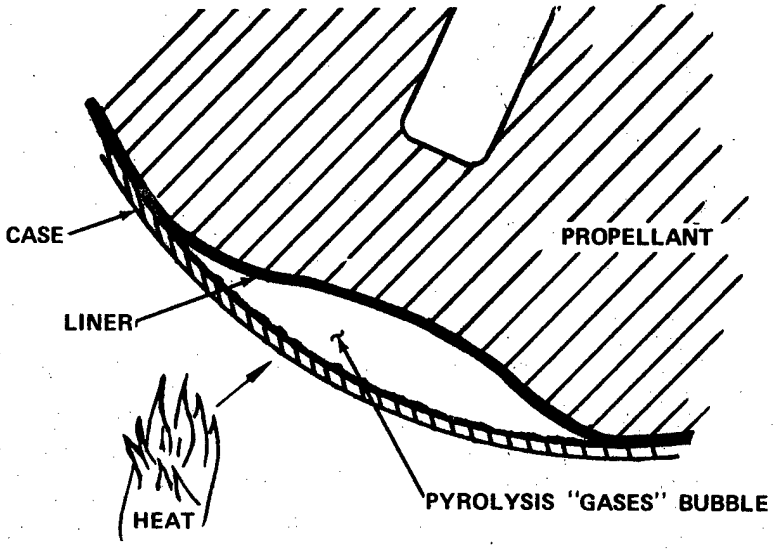

(U) FIGURE 3. Gas Bubble Insulation.

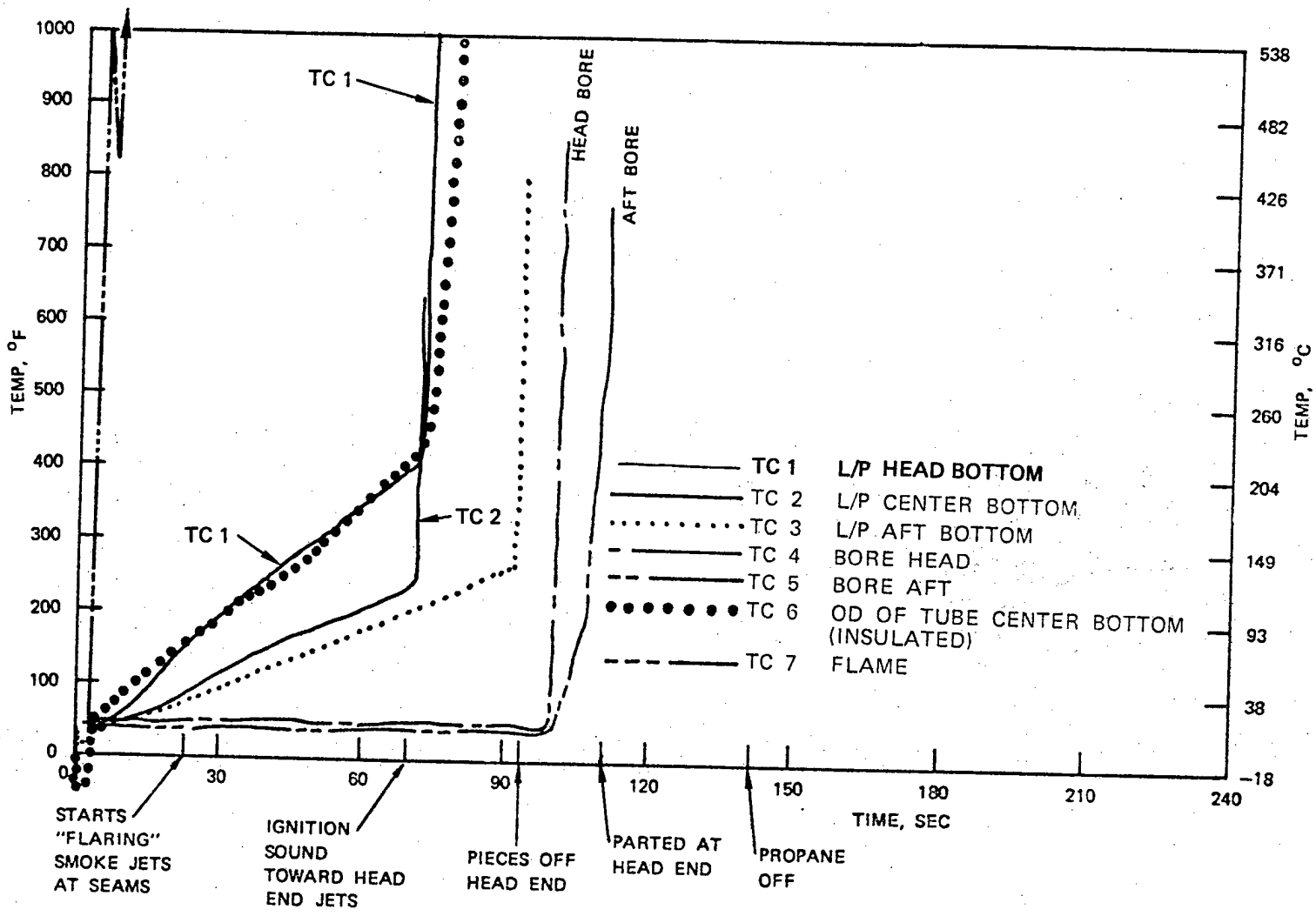

(U) FIGURE 4 Temperatures Recorded During Cook-Off of HTPB Lined Low Smoke Propellant Loaded Steel Shim Spiral Laminated Rocket Motor. (U)

(U) FIGURE 5. Remains of laminated steel spiral wrapped tube cook—off test no. 1.
(U) Neg. LHL 192362)

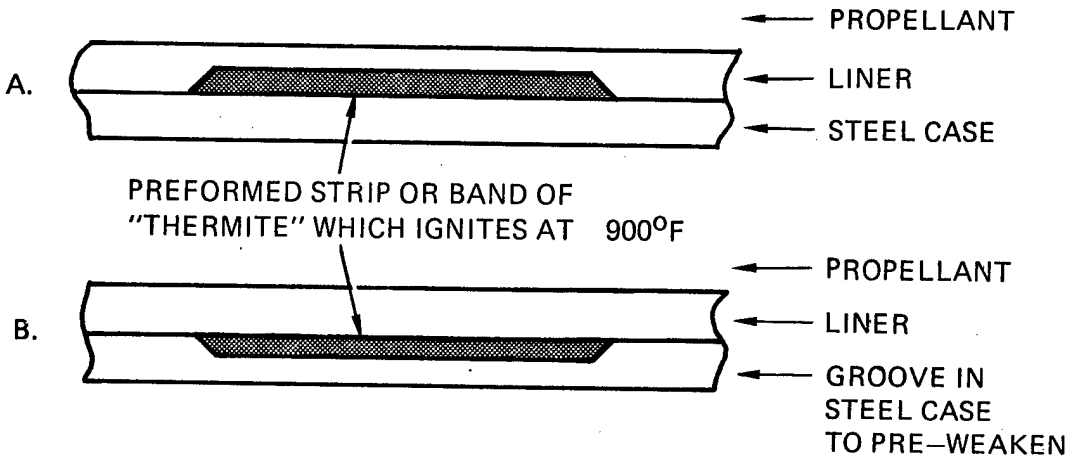

(U) FIGURE 6. Thermite concept.

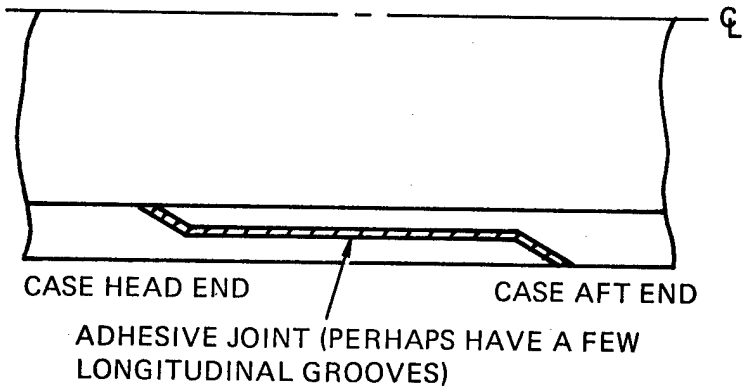

(U) FIGURE 7. Adhesive joint concept.

Biographical Sketch

Ronald F. Vetter was born in Jefferson City, Missouri on 27 August 1936. He graduated from the University of Missouri School of Mines and Metallurgy as a Chemical Engineer.

Ron has twenty years of solid propellants and propulsion experience including pilot plant and projects supervision. He is currently a senior technical project manager and consultant in the Propulsion Systems Division with major efforts in gas generators, mechanical integrity and optimization of solid propellants, plus reduction of hazards of solid propulsion rocket motors in fires.

A POWERFUL NEW TOOL FOR SOLID ROCKET MOTOR DESIGN

BY

Walter S. Woltosz, B.A.E., M.S., M.A.S.

Solid Rocket Division

Air Force Rocket Propulsion Laboratory
Edwards AFB, California

A Powerful New Tool For Solid Rocket Motor Design

Abstract

A new computer tool for automatic, detailed design of a limited family of tactical solid propellant rocket motors is described. This tool, which combines a nonlinear optimization scheme with a sophisticated internal ballistic code, parametric propellant ballistic models, hardware design equations, and motor material cost equations, automatically generates motor designs, including propellant formulation, that meet all performance requirements and design constraints while at the same time minimizing cost or motor weight. This is the first known use of a numerical optimization scheme to drive grain geometry details, propellant formulation, and inert component dimensions in concert to produce a total optimized motor design. The basic optimization problem is described, and a sample detailed motor design is presented to illustrate the power and utility of the approach.

In addition to the rocket motor design problem, the paper presents a call to a new way of doing business. The methods employed here are applicable to a wide variety of systems and can be readily adapted to other design problems.

The author gratefully acknowledges the assistance of Messrs. G. P. Roys and P. R. McFall of Thiokol Corporation/ Huntsville Division for their significant contributions to this joint development effort.

Introduction

The effort described in this paper consists of the development and application of a computer program that automatically designs minimum cost solid propellant rocket motors to meet all performance requirements, design constraints and operating limits. As much as the paper is a description of this achievement, it is also a call to a new way of business in engineering design. This new way of business promises greatly improved performance with existing technologies as well as a more accurate assessment of the potential payoffs of new technologies. Thus, it is seen first as a way to provide more cost effective weapons systems and second as an investment strategy tool for selecting new technology explorations.

The tool or method to be described is automatic computer design. This is not computer aided design, which is currently riding a crest of popularity in many industries. Rather, we speak here of computer generated designs--the computer is given the performance requirements, design constraints, operating limits, and the overall design goal (such as minimum cost, minimum weight, maximum range, etc.) as well as a set of design parameters that can be varied. The computer then finds the optimum values for these parameters which produce the desired result.

In the computer program described herein, the design parameters varied by the computer consisted of dimensions and angles which describe the propellant grain geometry and motor inert components, as well as a series of parameters that describe the formulation of the propellant itself. The capability demonstrated to date is applicable to a class of air-to-ground rockets incorporating reduced smoke composite propellants. This is the first known application of this methodology to drive both motor design and propellant formulation in concert to produce an optimum motor design. The capability provided by this type of tool results in a reduction in manhours of several orders of magnitude to complete designs with as much as 40% greater performance than those generated by previous methods. In fact, design problems that would be impractical to solve at all using conventional methods yield readily to the computer design approach.

Previous applications of similar methods have been demonstrated for trajectory optimization[1], solid rocket motor preliminary design [2,3] (as opposed to the detailed design capability described here), and multistage missile preliminary design[4].

Technical Discussion

In order to illustrate the complexity of the design problem that is handled by this new approach, we will start with a very simple design problem using a manual approach and then add to that starting point step-by-step until we reach the level of the complete problem.

Simple Design Problem

Suppose we wish to design a cylinder that provides a certain required volume, say 200 in^3, with the minimum surface area possible:

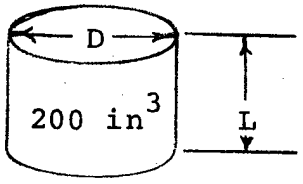

We know that the volume is given by $V = \frac{\pi D^2}{4} L$ and the surface area is $S = 2 \frac{\pi D^2}{4} + \pi DL$. Since the volume is known we can determine

$$L = \frac{800\ in^3}{\pi D^2}$$

Substituting this result in the equation for surface area:

$$S = \frac{\pi D^2}{2} + \frac{800\ in^3}{D}$$

From calculus we know that the minimum surface will occur when

$$\frac{\partial S}{\partial D} = 0,$$

$$\text{and } \frac{\partial S}{\partial D} = 2 \frac{\pi D}{2} - \frac{800\ in^3}{D^2}$$

$$\text{so that } \pi D = \frac{800\ in^3}{D^2}$$

$$D = \sqrt[3]{\frac{800}{\pi}} \text{ in,}$$

which results in $L = \sqrt[3]{\frac{800}{\pi}}$ in also, so that D = h, which is the classical solution to this problem. Thus, we have found the optimum analytically.

Step 2 - Minimum Weight Design

We now take the first problem and add the requirement that the thickness of the material used to make the cylinder must follow the equation

$$T = D/1000 + \frac{L/D}{2000}$$

and we change the design goal from minimum surface area to minimum weight. To provide the required internal volume we must now allow for the thickness of the material. Clearly, weight is minimized when the volume of material is minimized.

The volume of material is

$$V_{mat} = 2\left(\frac{\pi D^2}{4}\right) T + \pi\left(\frac{D^2 - (D-2T)^2}{4}\right)(L-2T).$$

The inside volume is

$$V_{inside} = \frac{\pi(D-2T)^2}{4} (L-2T).$$

In order to solve the problem, we select values for D, iteratively determine the value of L that provides 200 in^3 of internal volume, and calculate the material volume. Our search is in two dimensions, D and L, but one determines the other through the performance requirement of 200 in^3 internal volume. Thus, the search for an optimum can be conducted in one dimension. Having performed the exercise we obtain the following table of values:

D	L	T	V_{inside}	$V_{material}$
5	10.248	0.006025	200.015	1.20413
6	7.118	0.006593	200.002	1.25484
4	16.025	0.006003	200.019	1.35704
5.5	8.470	0.006270	200.020	1.21314
4.9	10.671	0.005989	200.020	1.20734
5.1	9.849	0.006066	199.995	1.20266
5.2	9.475	0.006111	200.019	1.20314
5.15	9.659	0.006088	200.001	1.20267
5.125	9.754	0.006077	200.012	1.20270
5.125	9.753	0.006077	199.992	1.20258

The results of this search are illustrated in Figure 1. Note that the minimum weight solution is neither the minimum surface area solution (L=D) nor the minimum material thickness solution (around D=4.4).

At this point we have seen a single design parameter used to determine an optimum design with a single performance requirement and no design constraints. Our model consists merely of the equations for thickness, internal volume, and material volume. The design goal was minimum weight.

Step 3 - Multiple Considerations

We now consider a problem with multiple design parameters, performance requirements, and design constraints. This problem, which serves to illustrate the complexity of the design problem when multiple interactive considerations exist, remains far short of the complexity of the rocket motor design problem to be described later.

Continuing with the cylinder model used above, we now desire a two part, telescoping cylindrical container that provides 200 in^3 of internal volume when opened, and no greater than 150 in^3 when collapsed. The smaller cylinder must fit entirely into the larger cylinder when the two are collapsed, as shown below:

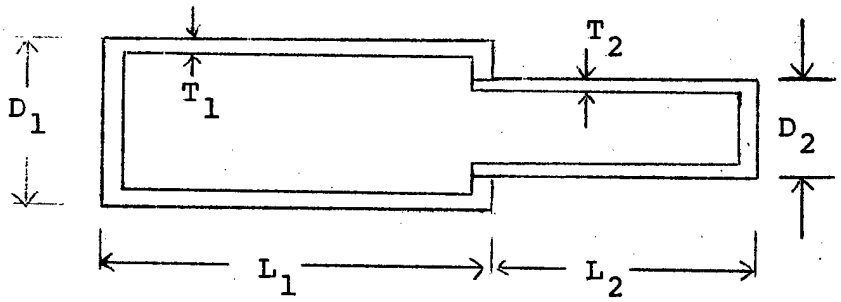

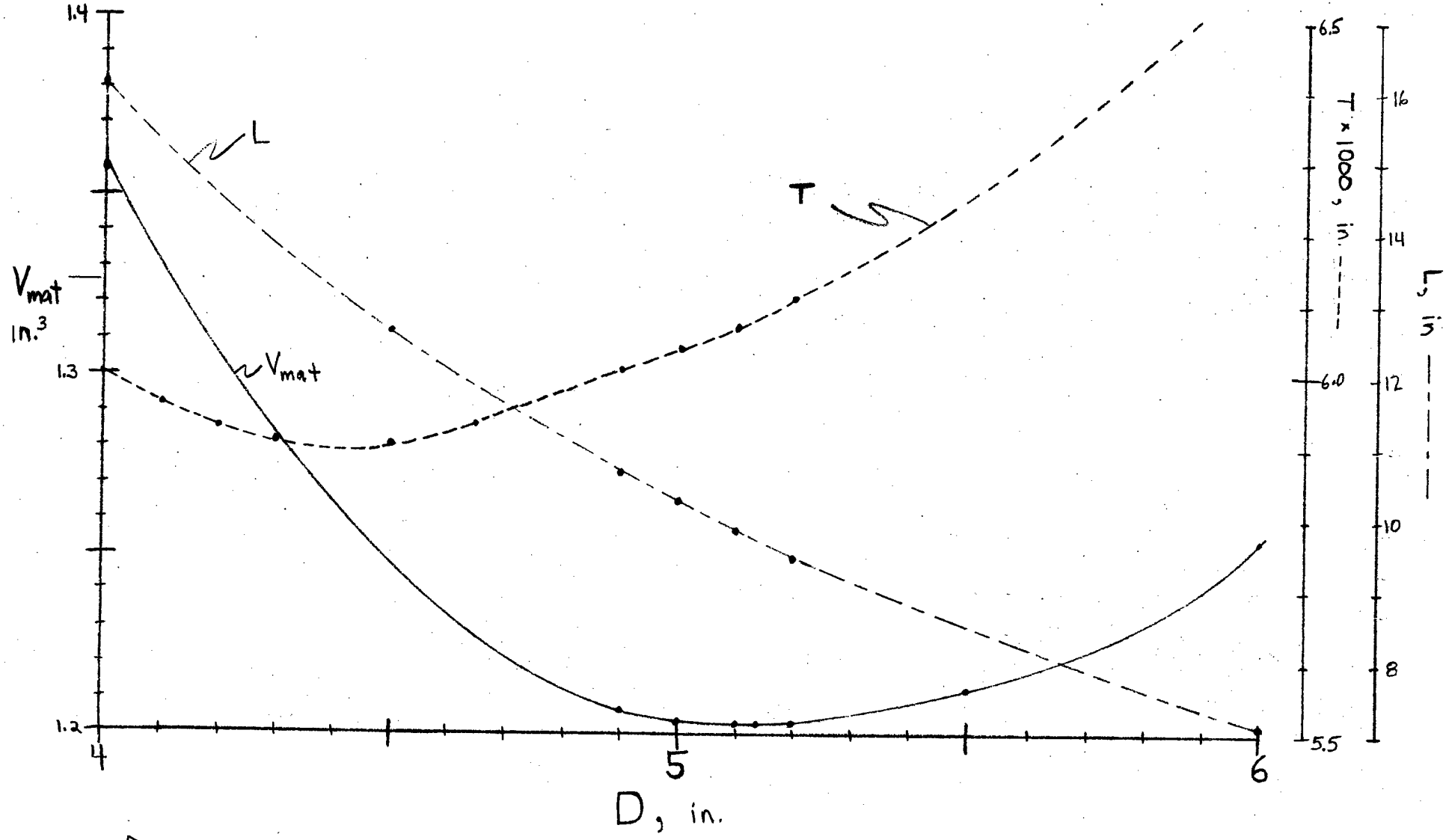

FIGURE 1: SINGLE CYLINDER WEIGHT MINIMIZATION

Thus, we have a design constraint: $L_2 + T_1 \leq L_1 - T_1$ or $L_2 \leq L_1 - 2T_1$. We further require that $\frac{L_2}{D_2} = \frac{L_1}{D_1}$, and our design goal is again to minimize weight (and hence material volume). Our model consists of the equations:

$$T_1 = \frac{D_1}{1000} + \frac{L_1/D_1}{2000}$$

$$T_2 = \frac{D_2}{1000} + \frac{L_2/D_2}{2000}$$

$$V_{inside_1} = \frac{\pi (D_1 - 2T_1)^2}{4} (L_1 - 2T_1)$$

$$V_{inside_2} = \frac{\pi (D_2 - 2T_2)^2}{4} (L_2 - T_2 + T_1)$$

$$V_{mat_1} = \frac{\pi D_1^2}{4} T_1 + \pi \left(\frac{D_1^2 - (D_1 - 2T_1)^2}{4}\right) (L_1 - 2T_1) + \pi \frac{(D_1^2 - D_2^2)}{4} T_1$$

$$= \frac{\pi T_1}{4} [2D_1^2 - D_2^2 + 4(D_1 - T_1)(L_1 - 2T_1)]$$

$$V_{mat_2} = \frac{\pi D_2^2}{4} T_2 + \pi \left(\frac{D_2^2 - D_2 - 2T_2)^2}{4}\right) (L_2 - T_2 + T_1)$$

$$= \frac{\pi}{4} T_2 [D_2^2 + 4(D_2 - T_2)(L_2 - T_2 + T_1)]$$

$$V_{outside} = \frac{\pi}{4} D_1^2 L_1 \ (\leq 150 \text{ in}^3).$$

Our approach is to pick values for L_1 and D_1, then solve for D_2 (and hence L_2 since $L_2/D_2 = L_1/D_1$) to achieve a total volume of 200 cu in. In order to evaluate various combinations of L_1 and D_1, we first fix L_1 and vary D_1 to find the minimum. We then change L_1 and repeat the process. The exercise generates the values shown in Figure 2. Note that the

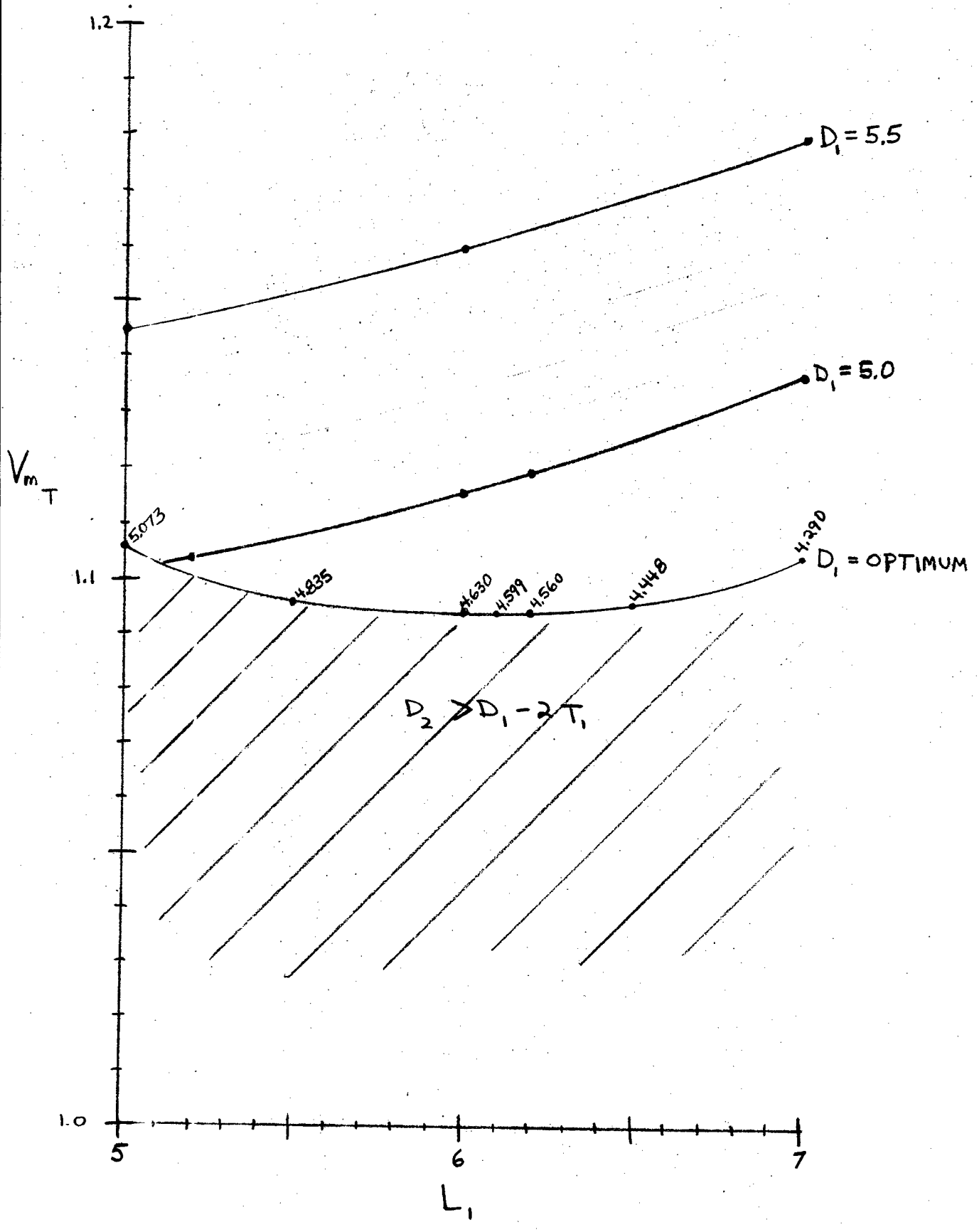

FIGURE 2: TELESCOPING CYLINDER MATERIAL VOLUME VERSUS LARGE CYLINDER LENGTH

optimum occurs near $L_1 = 6$, and that the optimum lies on a constraint boundary. The solution appears to be at a point where the two cylinders are as nearly identical as possible within the constraints. Note that the constraint that total outside volume of the collapsed cylinders not exceed 150 cu in was not approached.

This problem depicts several important trends in performing optimization. First, the solution lies on a constraint boundary (but is also far away from another constraint boundary). Second, along a line of constant diameter, the slope of the payoff (V_{M_T}) versus the parameter L_1 is not zero at the optimum. If D_1 had been fixed at 5, for example, the trend toward improved performance for $L_1 - 5.5$ would be in the direction of decreasing L_1, where in reality the trend is just the opposite if optimum values of D_1 are used. The problem here has been reduced to a two-dimensional search (L_1 and D_1) with a single two-dimensional constraint boundary. Imagine the difficulty (and incorrect performance trends) that can be encountered when 20 degrees of freedom and 50 or 60 possible constraints exist! The ratio $L_2/D_2 = L_1/D_1$ was arbitrarily held constant. We could release this ratio and add another design variable to the optimization. The increased complexity of the search that would result is obvious.

Given this insight into the optimization problem, we proceed to a description of the rocket motor design optimization which is the subject of this paper's title.

The Rocket Motor Design Problem

The solid rocket motor design problem consists of selecting the propellant grain configuration, inert component dimensions, propellant formulation, nozzle geometry, and igniter design that provide the required performance over the operating temperature extremes of the motor, with a design goal of minimum cost, minimum weight, maximum range, or some other characteristic to be maximized or minimized. In order to discuss the design optimization, we must first describe the rocket motor design variables, constraints, and performance requirements.

Figure 3 shows the model used for the rocket motor optimization program. The case is a thin-walled cylinder for which a variety of materials and manufacturing methods were examined. The total motor length is L_{MO}, the outside diameter is D_{MO}, and a nozzle/blast tube of reduced diameter is provided to allow packaging of aerodynamic controls at the aft end of the missile. At the head end of the motor, a combined forward closure/igniter is provided. L_{CLO} is the length from the end of the motor to the inside face of the closure. A fixed gap between the closure and the end of the propellant grain is provided to allow burning on the forward end of the grain. In the current model, a fixed weight was assumed for the igniter.

The forward end of the grain contains a number of "fins" or "slots" which provide added burning surface and under which an extra layer of insulation is required. The length of this forward insulation is L_{IF} and its thickness is T_{IFWD}. A short transition from the slotted region to the circular port (C.P.) region is used. The length of this region, L_{TRAN}, was a fixed input in the current work. The slots are described by: the radius from the motor centerline to the bottom of the slot, R_5; the angle on the side of the slot, α; the radius of curvature of the slot tip, R_4; and the center port radious, R_2. The program used the same center port radius in the slotted region and the circular port (C.P.) region (which is of length L_{CP}) with an increased radius at the end of an aft end cone. The internal ballistics model requires dividing the motor into a number of sections separated by planes perpendicular to the centerline. In the work described here, fourteen planes were used (hence R_{5_1}, R_{5_3}, R_{2_1}, $R_{2_{12}}$, and $R_{2_{14}}$ are radius values at planes 1, 3, 12 & 14). The length of the center port region is L_{CP}. The aft conical port is provided to reduce the Mach number within the motor to prevent erosive burning of the propellant

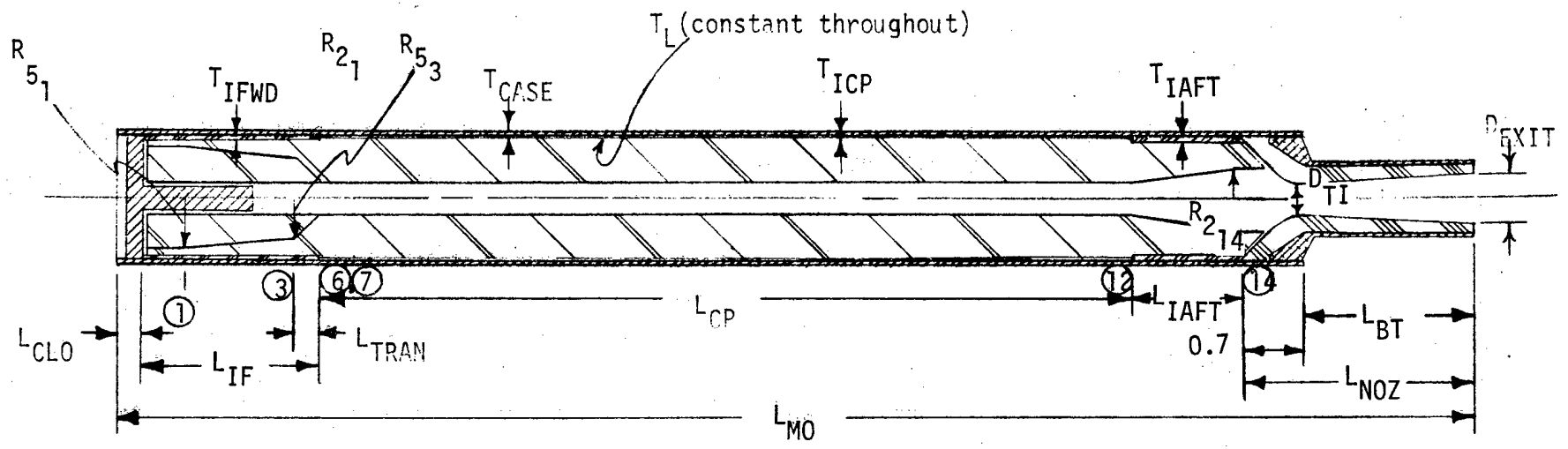

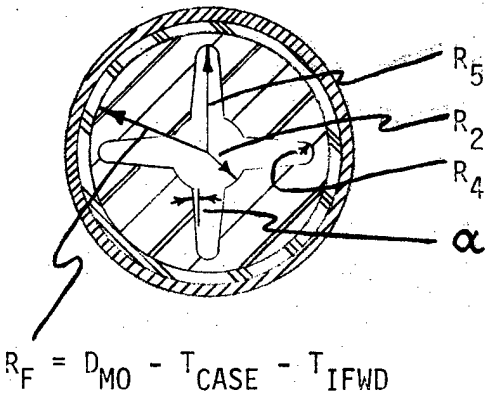

$R_F = D_{MO} - T_{CASE} - T_{IFWD}$

PROPELLANT FORMULATION PARAMETERS

TOTSOL (total solids)

FEO (iron oxide)

OX1 (large AP)

OX2 (medium AP)

OX3 (small AP)

FIGURE 3: ROCKET MOTOR DESIGN PARAMETERS

and for overall control of the thrust-time profile. This conical region also requires extra insulation, which has length L_{IAFT} and thickness T_{IAFT}. An insulation layer in the CP region can be used with thickness $T_{I_{cp}}$. A constant thickness (T_L) layer of liner material is used throughout the motor.

For the designs to be shown here, the nozzle/blast tube total length L_{NOZ}, the blast tube diameter D_{BT}, the inside diameter of the nozzle exit D_{EXIT}, and the 0.7 inch interface length between case and nozzle were all held constant. The initial nozzle throat diameter D_{T_I} was an optimized parameter, and the model accounted for erosion of the throat.

The propellant model used was for a family of reduced smoke composite propellants. The model consisted of a series of theoretical and empirical regressions, some of which are shown in Figure 4, which provided propellant burning rate, temperature sensitivity of burning rate, mechanical properties, energy level, density and combustion stability characteristics as functions of the propellant formulation. It should be noted that good analytical models for these characteristics do not exist, so that reliance on experimental data was heavy in this area. The program is currently limited to propellant formulations within this data base.

Cost was modeled in the form of ingredient costs for propellant, with other components modeled using the equations shown in Figure 5.

The optimization scheme employed is the Pattern Search (PATSH) subroutine developed by D. E. Whitney[5] at the Massachusetts Institute of Technology. This routine incorporates a modified Hooke and Jeeves[6] direct search nonlinear parameter optimization scheme. While this is one of the least elegant schemes around, it is extremely compact (about 75 lines of FORTRAN coding) and has compared quite well with other schemes in the literature.

PATSH performs an unconstrained optimization. That is, it simply varies the design parameters in order to minimize a single number called the objective function. This number must be constructed in a way that reflects both the payoff quantity to be minimized (such as cost), and the satisfaction of performance requirements and design constraints. This is performed using a penalty function approach, so that the objective function is of the form

$$OBJ = PAYOFF + \sum PENALTIES$$

Penalties are incurred for any violation of a constraint or any failure to meet performance requirements. All penalties are second order (i.e., proportioned to the square of the amount of violation). When the solution is reached, all penalties should be zero (or negligible) and the payoff should be minimized (for maximization, such as maximum range, we multiply by -1 so that we minimize - range).

The overall program flow is shown in Figure 6. After reading the inputs, the initial guess design is generated and evaluated, along with a detailed printout of its characteristics and performance. The optimization process then begins, with the printout suppressed. During the optimization, the Pattern Search subroutine repeatedly calls the design evaluation portion of the program, each time with a different set of values for the design parameters. A complete optimization generally requires 300-1000 such design evaluations. On the AFRPL CDC 6400 computer, these evaluations require an average of 10 seconds (CPU time) to compute, so that a total of 3000-10000 seconds (about 1-3 hours) of computer time are required per design. On a CDC 7600, this would reduce to about 150-500 seconds (about 2-5 minutes). Once the optimization has converged to a solution, the final design is run with the detailed printout of the design and its operating characteristics.

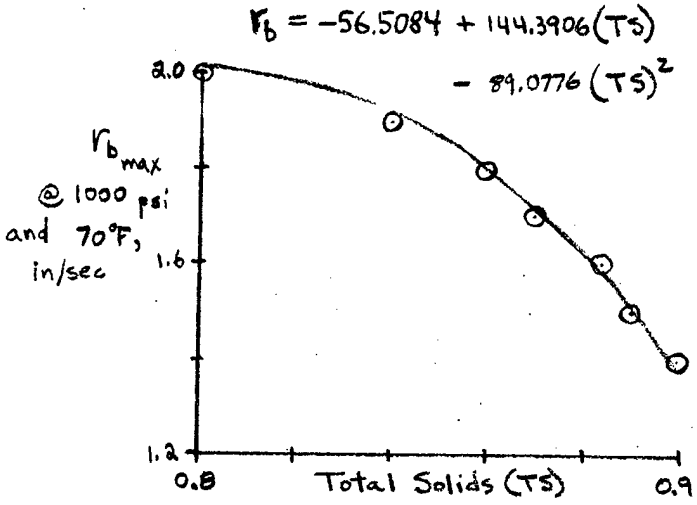

a. LIMITING MAXIMUM BURN RATE

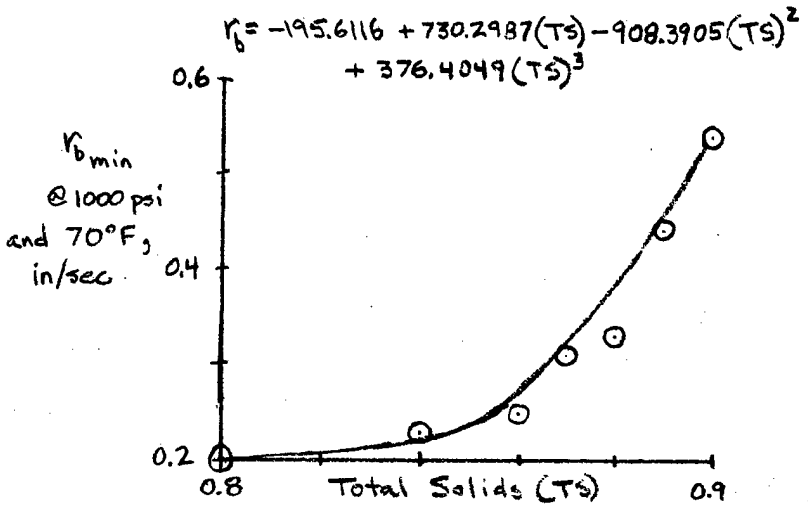

b. LIMITING MINIMUM BURN RATE

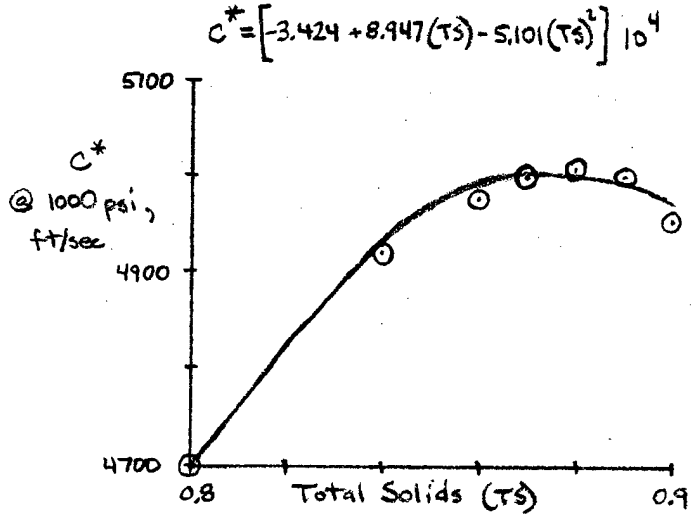

c. CHARACTERISTIC VELOCITY VS TOTAL SOLIDS

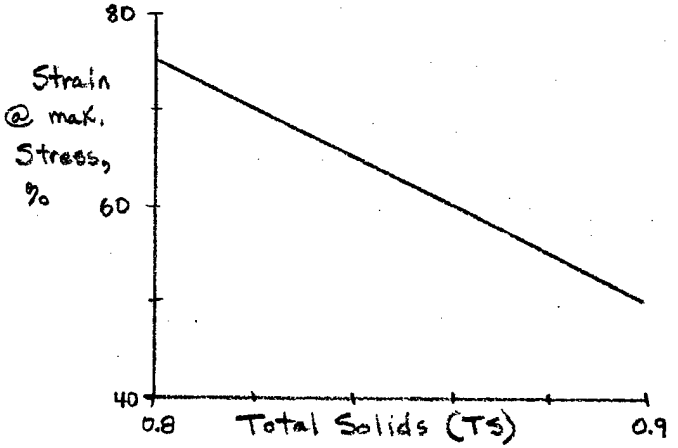

d. STRAIN FOR 400/200/50 MICRON AP COMBINATIONS

FIGURE 4: TYPICAL PROPELLANT PROPERTY MODELS

- Nozzle Cost = $4.5 + \text{Cost}_{\text{nozzle structure}} + (CN_1)$ (Volume of ablative)

- Propellant Cost Per Pound = C_{FEO} (FEO) + C_{OX1} (OX1) + C_{OX2} (OX2) + C_{OX3} (OX3) + C_{GRAF} (GRAF) + C_{ZR} (ZR) + C_{ZRC} (ZRC) + C_{POL} (POLY) + C_{CC} (CC) + C_{CA} (CA) + C_{PLA} (PLAS) + C_{BOND} (BOND) + C_{ANT} (ANTI)

  where

FEO	= iron oxide	CC	= cure catalyst
OX1, OX2, OX3	= AP particle size	CA	= curing agent
GRAF	= graphite	PLA	= plasticizer
ZR	= zirconium	BOND	= bonding agent
ZRC	= zirconium carbide	ANTI	= antioxidant
POLY	= polymer		

- Total Propellant Cost = cost/lb x weight of propellant
- Insulation Cost = $C_1 + C_2$ x weight of insulation
- Case Cost = $C_\phi + C_1$ x case thickness

FIGURE 5: COST EQUATIONS

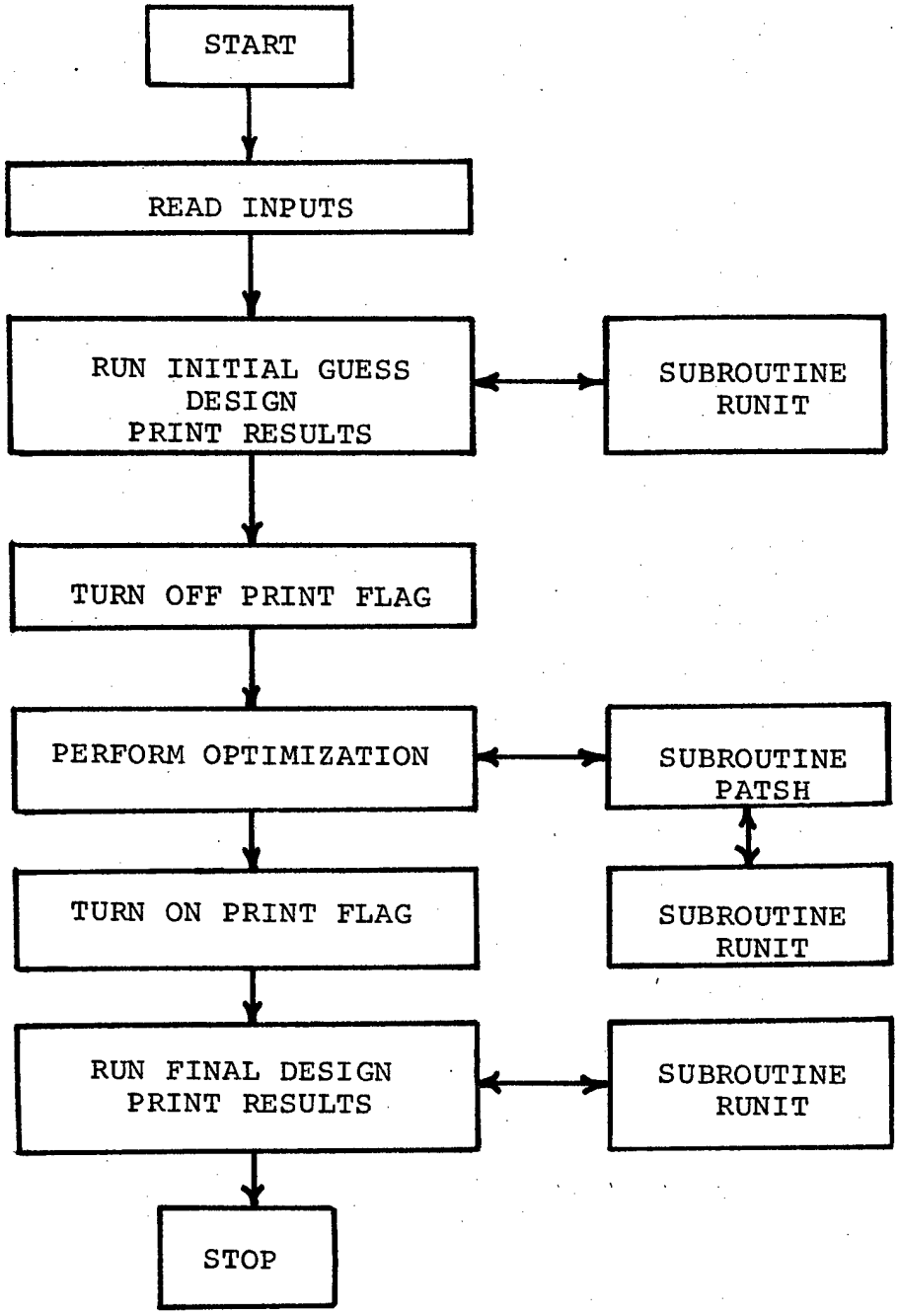

FIGURE 6. OVERALL PROGRAM FLOWCHART

Sample Design Optimization

The capability of the rocket motor design optimization code will now be illustrated by an actual motor design generated for an AFRPL contract. The design goal was minimum cost. Performance requirements were:

Minimum thrust @ $-65^{\circ}F$ = 1600 lbf
Maximum thrust @ $+145^{\circ}F$ = 2800 lbf
Minimum burn time @ $+145^{\circ}F$ = 1.5 sec
Maximum burn time @ $-65^{\circ}F$ = 4.5 sec
Maximum acceleration @ $-65^{\circ}F$ = 45 g's
Design safety factor = 1.4
Minimum total impulse @ $-65^{\circ}F$ = 6500 lbf-sec

The design variables that could be varied during the optimization process were (See Figure 3):

T_{CASE} - motor case thickness

D_{TI} - initial throat diameter

R_{2_1} - inside radius of circular port (CP) in propellant grain

α - angle on side of forward grain slots

L_{IF} - forward internal insulation length (hence slot length)

L_{MO} - total motor length

L_{IAFT} - aft internal insulation length (hence aft cone length)

$R_{2_{14}}$ - propellant bore radius at extreme aft end of grain

TOTSOL - total solids level of propellant formulation

FEO - iron oxide fraction in propellant

OX1 - weight fraction of large ammonium perchlorate (AP)

OX2 - weight fraction of medium size AP

OX3 - weight fraction of small AP

The design constraints imposed on the problem were:

Case thickness sufficient for maximum pressure plus safety factor

Propellant formulation within allowable limits:

$0.8 \leq$ TOTSOL ≤ 0.9
FEO ≤ 0.015
OX1 ≥ 0.0
OX2 ≥ 0.0
OX3 ≥ 0.0

Angle on side of slot ≥ 0.0 degrees

Forward insulation length $\geq$ transition length + web thickness (the thickness of the grain in the C.P. section)

Grain C.P. section length ≥ 0.0

Aft insulation length ≥ 0.0

Propellant thickness under slot tip = 0.25 in

Radius to bottom of slot $\geq$ bore radius + slot tip radius

Propellant web fraction (thickness in C.P. section divided by outside radius) ≤ 0.68

Radius at end of aft cone $\geq$ C.P. bore radius

Maximum pressure @ $-65^{\circ}F \leq 2000$ psi

Maximum port Mach number during burn ≤ 0.6

Total motor length ≤ 50.0 in

Nozzle ablative margin of safety ≥ 0.0

Propellant strain margin of safety ≥ 0.0 for both ignition pressurization and temperature extremes

Propellant combustion stability response function at first three motor longitudinal mode frequencies ≤ 5.0

Motor combustion stability decay coefficient with unity response function for first longitudinal mode $\leq -100.$

Total motor weight $\leq$ 48.0 lb

The complexity of the problem is clear. An initial guess for the design variables, based on previous "manual" design work done for the motor, was as follows:

T_{CASE} = 0.040 in

D_{TI} = 1.170 in

R_{2_1} = 0.665 in

α = 4.476 deg

L_{IF} = 4.728 in

L_{MO} = 50.0 in

L_{IAFT} = 3.571 in

$R_{2_{14}}$ = 0.889 in

TOTSOL = 0.858

FEO = 0.00518

OX1 = 0.5027

OX2 = 0.3178

(OX3 = 0.0173 determined by TOTSOL, FEO, OX1 AND OX2)

This design met all of the performance requirements, but violated two constraints: (1) case thickness was slightly lower than required, and (2) propellant web fraction exceeded the maximum allowable. The cost of the motor was $154.15 (processing is not included), but this cost has no meaning since the motor design was unacceptable.

After 4,095 seconds of CPU time on the AFRPL CDC 6400 computer, the following design was obtained:

T_{CASE} = 0.0505 in (up 26.25%)

D_{TI} = 1.0564 in (down 9.71%)

R_{2_1} = 0.7010 in (up 5.41%)

= 6.6201 degs (up 47.90%)

L_{IF} = 5.1738 in (up 9.43%)

L_{MO} = 50.0 in (no change - against maximum constraint)

L_{IAFT} = 4.7975 in (up 34.35%)

$R_{2_{14}}$ = 1.2459 in (up 40.15%)

TOTSOL = 0.858 (no change)

FEO = 0.00330 (down 36.29%)

OX1 = 0.5235 (up 4.14%)

OX2 = 0.3158 (down 0.63%)

OX3 = 0.00037 (down 97.84%)

This design meets all performance requirements, does not violate any constraints, and has a cost of $152.77. More striking than this result are the results obtained from the trade study for various case, nozzle ablative, and internal insulation materials. These trade studies, which consisted merely of inputting the appropriate material properties and rerunning the optimization, were completed in less than eight manhours. The motor design and propellant formulation were completely reoptimized for each change in motor materials. The same results, if obtainable at all, would have taken a number of manyears to generate without the automatic optimization process. One particular result is worthy of special note. A motor design using 1035 steel (cheap and not very strong compared to more conventional case materials) was investigated

just for academic interest. This design would not have been examined at all using conventional design methods because of the Project Engineer's intuition that "it wouldn't work anyway". The computer-generated design met all performance requirements and design constraints and was the lowest cost of all designs with a cost of $129.92! For a 240,000 motor production run envisioned for this type of motor, the net savings over the previous design would be $5,484,000 in material costs alone (not including G&A and profit)!

Summary and Conclusions

A computer program has been developed to perform detailed solid rocket motor design optimization for a limited class of air-to-ground rockets. This program generates designs with greatly improved cost-effectiveness than would usually be obtained using conventional design methods. In addition, the program enables rapid, accurate assessment of the payoff of new technologies for the applicable class of motors. Future improvements to the program will be oriented toward generalizing its capabilities and including missile performance (via trajectory simulation) in the design evaluation.

More important than the specific application discussed here is the fact that this methodology constitutes a new way of business. The program size and speed capabilities of computers are advancing at a very high rate. One recent assessment was that the computer capabilities that cost $500,000 in 1970 would cost $5,000 in 1980 and $50 in 1990. With this increased capability comes the ability to perform highly complex design integration/optimization automatically at low cost. What is required to exploit this ability is cooperative effort between the separate technology specialists to produce a single computer code that accounts for the important considerations in each area.

The use of these methods is not limited to any particular area. General Motors has begun to use such techniques in truck designs (reference the inside back cover of the July/August 1978 Aeronautics and Astronautics Magazine). Trajectory analysts have used such methods (and paid for much of the original development work) for problems such as space launch vehicle trajectory optimization. Structural optimization of aircraft control surfaces to minimize flutter has been performed. Perhaps the most dramatic use of these methods was reported in the Air Force Systems Command AFSC Newsreview for August 1978, wherein a computer-controlled wing has been developed by General Dynamics/Convair (under joint Air Force and Navy sponsorship) that changes its shape during a wind tunnel test to provide optimal performance!

One final note. What is described here is a tool. Nothing more. Just as the electronic calculator has enabled the designer to accomplish more in less time, the methods described here also are to assist him, not to replace him. Codes such as the rocket motor design code not only require the same technology specialists that we've always needed, but they also require (and facilitate) a team effort that makes each member more effective.

REFERENCES

1. Lyons, J. T., Woltosz, W. S., Abercrombie, G., and Gottlieb, R. G., "Rocket Ascent G-Limited Moment-Balanced Optimization Program - RAGMOP", NASA CR-129000, August 1972.

2. Woltosz, W. S., "The Application of Nonlinear Optimization Techniques to Solid Rocket Motor Design", unpublished Master's Thesis, Auburn University, March 1977.

3. Woltosz, W. S., Unpublished Preliminary Documentation for the AFRPL Missile Energy Management and Design Optimization Program - MEMDOP, March 1977.

4. Woltosz, W. S., Unpublished Preliminary Documentation for the AFRPL Ballistic Missile Optimization Program - BMOP, March 1977.

5. Whitney, D. E., private communication, Joint Mechanical and Civil Engineering Computing Facility, Massachusetts Institute of Technology, 77 Massachusetts Avenue, Cambridge, Massachusetts 02139.

6. Hooke, R., and Jeeves, T. A.,"'Direct Search' Solution of Numerical and Statistical Problems", Journal of the Association for Computing Machinery, Vol 8 No. 2, Pp 212-229.

Biographical Sketch

Walter Stanley Woltosz was born in Harrison, Arkansas, on November 19, 1945. After graduating from Greece Olympia High School in Rochester, New York, in June 1963, he entered the United States Air Force, serving in the Strategic Air Command for 35 months and in the Air Training Command for 25 months. He was discharged as Staff Sergeant on October 11, 1968. He received the degree of Bachelor of Aerospace Engineering from Auburn University in June 1969, entered graduate school at Auburn the same month, and remained until the completion of his Master's Degree course work in August 1970. He received a Master of Administrative Science Degree from the University of Alabama in Huntsville in August 1976, and completed the Master of Science in Aerospace Engineering from Auburn University in March 1977. Since 1970 he has held a variety of positions in government and industry, and is currently a Project Manager for the Tactical Air-Launched Missile Propulsion Section with the Air Force Rocket Propulsion Laboratory at Edwards Air Force Base, California.

QUANTIFICATION OF THE THERMAL ENVIRONMENT FOR AIR-LAUNCHED WEAPONS

BY

Howard C. Schafer

Ordnance Test & Evaluation Division

Naval Weapons Center
China Lake, California 93555

Quantification of the Thermal Environment for Air-Launched Weapons

Abstract

The design penalties paid because of a misunderstanding of the probable chance of occurrence of the "worst case extreme" for air-launched weapons and materiel in general have led to a review of the Department of Defense method of criteria assignment. These penalties include dollar cost, performance deterioration in the majority of use circumstance, time of development cost, and service life costs. The Naval Air Systems Command and Naval Weapons Center have derived a method by which the thermal design goals for any event of the stockpile-to-target sequence can be quantified. This method is based on a field measured data base in excess of 20 million data points derived from the thermally extreme locations worldwide over the last 1-1/2 decades. This method is in concert with the spirit of the guidance given in the Department of Defense Directive 5000 series, the current direction to tailor all specifications and standards, and MIL-STD-1670A. It will be shown that the present thermal design goals being used on the Department of Defense's present air-launched weapons may have a probable chance of occurrence of 10^{-4} to 10^{-6} while overall reliability goals are typically much less severe. A means will be given to return to the project manager the ability to, on a basis of fact and knowledge, assign thermal design goals, and judge the advisability of granting or rejecting waivers for thermal noncompliance.

Introduction

In concert with Department of Defense direction, an effort is being made to bring "real life" into the assignment of Environmental Criteria for military materiel development. The Naval Air Systems Command commissioned the Naval Weapons Center to take whatever steps necessary to convert the black art of environmental criteria determination into something approaching an area of technology much like stress analysis or machine design.

In 1965 the Naval Weapons Center initiated a program of worldwide data collection to describe in a technical format the thermal exposure of military materiel on a worldwide basis. This program, reached its data measurement peak in the late 1960's and early 1970's, and has so far yielded more than 50 million data points over a continuous measurement period of up to 8 years. The materiel used as measurement matrices ran the size gambit from small arms ammunition through air-launched ordnance and the aircraft themselves. The events of the stockpile-to-target sequence included transportation, storage, onboard ship or at the forward airfield and air carried excursions. The main thrust of the program was to find the extreme exposure locations worldwide to which free world ordnance can logically be expected to be exposed, and measure the thermal response under those conditions until an infinite amount of engineering data is available. This has essentially been done. But, as will be shown, missing data from the temporate zones of the world tend to bias the resulting "worldwide probable chance of occurrence" displays toward the extreme. Therefore, data from the continental United States and the European Theatre of operations is badly needed to balance out this effort. Even so, the data now in hand are useful in that it allows environmental criteria to be tailored to a given development program's needs, though the chosen values will tend toward the conservative.

Results and Discussion

It is easy to efficiently handle 50, 500, or 5000 data points for a single consideration or situation. A sum of 50 thousand to 20 million data points can force the issue somewhat and lead to data display problems. The NWC TP 5039 report series presents a more complete discussion of the particular data display matrices used herein. Parts 1, 2, and 3 of this report present the evolution of data display. The cumulative probable chance of occurrence, probability

density format has proven the most useful for the greatest amount of readers; this format, in the Gaussian context, is thus used exclusively in this paper.

The specific goal has been to provide the tools and techniques necessary to allow project engineering or management personnel to tailor the thermal environmental criteria to their programs' parochial needs. To do this it is necessary to combine the specific every hour thermal excursions of many different ordnance items into a generalization of events with a resulting probability of happening. In this way, the true risk that attends the choice of a set of thermal design values is revealed to the person who makes the choice and ultimately to the program manager who is fully responsible for the design criteria.

The job of placing the vast quantity of field measured thermal data into a single display was simplified by the discovery that nature tends toward moderation even in the more extreme climatic zones of the earth. Being a water based planet, it should be no surprise that the 50 percentile point of any statistically infinite number of thermal measurements is about 70°F. Fig. 1 was derived from over 10 million data points taken over an 8 year period of continuous half-hourly sampling of 200 channels of temperature information. The measured ordnance ranged from .30 caliber carbine ammunition of WW II fame through iron bombs and Howitzer projectiles to air-launched rockets and guided missiles. Notice in Fig. 1 that the various data sources overlay into a very compact mass for easy display. Also notice that, even in a pure hot-dry desert, the 50% region is displayed in the temperature range of 60°F to 90°F even for low mass, high surface area thin-walled shipping container surface skins. When ordnance alone is considered the band of temperatures narrows to from 60°F to 80°F. In fact, the chance of any dump stored ordnance surface skin experiencing a temperature greater than 125°F is commensurate with a less than 10% probability. It is, of course, understood that the internals of the ordnance will, at the same time, be subjected to temperature extremes less severe than the surface. (For more discussion of the derivation and ramifications of Fig. 1, refer to NWC TP 5039, Part 3.)

The display of Fig. 1 does suffer from two shortcomings. First, very few, if any, weapons are designed only for desert use. Therefore, the display of desert exposure is somewhat misleading. Using only these data it could be said that a weapon would have less than a 10% chance of experiencing a

temperature as low as +25°F. This could mislead many users. Therefore, the Department of Defense apparent philosophy of design must be consulted and the data fit to the apparent need. It is customary for any project to be designed for "worldwide use". This term is itself very prone to misconceptions. It must be realized that "worldwide" for the ship-launched missile is different from the infantryman's 5.56 MM small arm cartridge. A ship-launched missile need only work off a ship sailing in a liquid state ocean. The 5.56 MM round must work wherever an infantryman can walk on the surface of the earth. Thermally there is a profound difference in the real meaning of the phrase "worldwide" for these two ordnance items. A fuller understanding of these differences can and should lead to reductions in cost and enhancement of positive performance of future weapons.

The second fault with Fig. 1 is the "end point trap". The unwary or unthinking historically reason that, if they can find the extreme temperatures and somehow design to them, then the entire enveloped temperature regime will take care of itself. Though this is the subject of a whole discussion unto itself, let it suffice to say that this logic is demonstratively not valid and has lead to the degradation of necessary 50 percentile performance in the past.

To sidestep the above two major problems and bring this effort in line with DOD Instructions 5000 and 4120 series, the displays of Fig. 2-7 are presented. These 6 graphs show that the thermal data is in concert with the major requirements of MIL-STD-1670 use and related efforts.

This paper can only summarize the effort to date. A detailed description of only the first half of this effort has filled over 40 NWC TP reports and more than 15 open literature articles. The following discussion is built on these publications (a list of which is available from the author).

The following figures show only the thermal information necessary to delineate the data needed to detail the factory-to-target sequence. The similarity of exposure of some of the events of the factory-to-target sequence makes it easy to group the data of more than one event on a single data display. For example, notice that the events truck and rail transportation are handled by Fig. 2; onboard ship and sea transport by Fig. 3; and igloo and covered storage by Fig. 5.

A few of the mitigating circumstances for the use of Fig. 2-7 is in order. The main point is that all 6 graphs should not be given the same weight in any design scenerio. It is my opinion that the weights or weighing scale should be nearly as follows:

Navy

Fig.	Title	Weight
2	Truck & Rail Transport	2%
3	Onboard Ship/Sea Transport	45%
4	Dump Storage	Less than 1%
5	Igloo & Covered Storage	45%
6	Airfield Use	5%

Air Force

Fig.	Title	Weight
2	Truck & Rail Transport	2%
3	Sea Transport	10%
4	Dump Storage	Less than 1%
5	Igloo & Covered Storage	70%
6	Airfield Use	10%

Ammunition record cards and field observation indicate that the preponderence of weapon lifetime is in storage of one type or another.

Some assumptions are made that may have introduced small errors in the graphical displays of Fig. 2-6. The temperature distributions for Fig. 2, 5, and 6 are not, with the present data, strictly Gaussian though they are so depicted. The true distribution would be better approximated by a Weibull distribution. However, since designers are historically more interested in the 3 sigma plus and minus portion of the curve, not much demand is evident for the data between 99.85% hot to

temperature as low as +25°F. This could mislead many users. Therefore, the Department of Defense apparent philosophy of design must be consulted and the data fit to the apparent need. It is customary for any project to be designed for "worldwide use". This term is itself very prone to misconceptions. It must be realized that "worldwide" for the ship-launched missile is different from the infantryman's 5.56 MM small arm cartridge. A ship-launched missile need only work off a ship sailing in a liquid state ocean. The 5.56 MM round must work wherever an infantryman can walk on the surface of the earth. Thermally there is a profound difference in the real meaning of the phrase "worldwide" for these two ordnance items. A fuller understanding of these differences can and should lead to reductions in cost and enhancement of positive performance of future weapons.

The second fault with Fig. 1 is the "end point trap". The unwary or unthinking historically reason that, if they can find the extreme temperatures and somehow design to them, then the entire enveloped temperature regime will take care of itself. Though this is the subject of a whole discussion unto itself, let it suffice to say that this logic is demonstratively not valid and has lead to the degradation of necessary 50 percentile performance in the past.

To sidestep the above two major problems and bring this effort in line with DOD Instructions 5000 and 4120 series, the displays of Fig. 2-7 are presented. These 6 graphs show that the thermal data is in concert with the major requirements of MIL-STD-1670 use and related efforts.

This paper can only summarize the effort to date. A detailed description of only the first half of this effort has filled over 40 NWC TP reports and more than 15 open literature articles. The following discussion is built on these publications (a list of which is available from the author).

The following figures show only the thermal information necessary to delineate the data needed to detail the factory-to-target sequence. The similarity of exposure of some of the events of the factory-to-target sequence makes it easy to group the data of more than one event on a single data display. For example, notice that the events truck and rail transportation are handled by Fig. 2; onboard ship and sea transport by Fig. 3; and igloo and covered storage by Fig. 5.

A few of the mitigating circumstances for the use of Fig. 2-7 is in order. The main point is that all 6 graphs should not be given the same weight in any design scenerio. It is my opinion that the weights or weighing scale should be nearly as follows:

Navy

Fig.	Title	Weight
2	Truck & Rail Transport	2%
3	Onboard Ship/Sea Transport	45%
4	Dump Storage	Less than 1%
5	Igloo & Covered Storage	45%
6	Airfield Use	5%

Air Force

Fig.	Title	Weight
2	Truck & Rail Transport	2%
3	Sea Transport	10%
4	Dump Storage	Less than 1%
5	Igloo & Covered Storage	70%
6	Airfield Use	10%

Ammunition record cards and field observation indicate that the preponderence of weapon lifetime is in storage of one type or another.

Some assumptions are made that may have introduced small errors in the graphical displays of Fig. 2-6. The temperature distributions for Fig. 2, 5, and 6 are not, with the present data, strictly Gaussian though they are so depicted. The true distribution would be better approximated by a Weibull distribution. However, since designers are historically more interested in the 3 sigma plus and minus portion of the curve, not much demand is evident for the data between 99.85% hot to

temperature as low as +25°F. This could mislead many users. Therefore, the Department of Defense apparent philosophy of design must be consulted and the data fit to the apparent need. It is customary for any project to be designed for "worldwide use". This term is itself very prone to misconceptions. It must be realized that "worldwide" for the ship-launched missile is different from the infantryman's 5.56 MM small arm cartridge. A ship-launched missile need only work off a ship sailing in a liquid state ocean. The 5.56 MM round must work wherever an infantryman can walk on the surface of the earth. Thermally there is a profound difference in the real meaning of the phrase "worldwide" for these two ordnance items. A fuller understanding of these differences can and should lead to reductions in cost and enhancement of positive performance of future weapons.

The second fault with Fig. 1 is the "end point trap". The unwary or unthinking historically reason that, if they can find the extreme temperatures and somehow design to them, then the entire enveloped temperature regime will take care of itself. Though this is the subject of a whole discussion unto itself, let it suffice to say that this logic is demonstratively not valid and has lead to the degradation of necessary 50 percentile performance in the past.

To sidestep the above two major problems and bring this effort in line with DOD Instructions 5000 and 4120 series, the displays of Fig. 2-7 are presented. These 6 graphs show that the thermal data is in concert with the major requirements of MIL-STD-1670 use and related efforts.

This paper can only summarize the effort to date. A detailed description of only the first half of this effort has filled over 40 NWC TP reports and more than 15 open literature articles. The following discussion is built on these publications (a list of which is available from the author).

The following figures show only the thermal information necessary to delineate the data needed to detail the factory-to-target sequence. The similarity of exposure of some of the events of the factory-to-target sequence makes it easy to group the data of more than one event on a single data display. For example, notice that the events truck and rail transportation are handled by Fig. 2; onboard ship and sea transport by Fig. 3; and igloo and covered storage by Fig. 5.

A few of the mitigating circumstances for the use of Fig. 2-7 is in order. The main point is that all 6 graphs should not be given the same weight in any design scenerio. It is my opinion that the weights or weighing scale should be nearly as follows:

Navy

Fig.	Title	Weight
2	Truck & Rail Transport	2%
3	Onboard Ship/Sea Transport	45%
4	Dump Storage	Less than 1%
5	Igloo & Covered Storage	45%
6	Airfield Use	5%

Air Force

Fig.	Title	Weight
2	Truck & Rail Transport	2%
3	Sea Transport	10%
4	Dump Storage	Less than 1%
5	Igloo & Covered Storage	70%
6	Airfield Use	10%

Ammunition record cards and field observation indicate that the preponderence of weapon lifetime is in storage of one type or another.

Some assumptions are made that may have introduced small errors in the graphical displays of Fig. 2-6. The temperature distributions for Fig. 2, 5, and 6 are not, with the present data, strictly Gaussian though they are so depicted. The true distribution would be better approximated by a Weibull distribution. However, since designers are historically more interested in the 3 sigma plus and minus portion of the curve, not much demand is evident for the data between 99.85% hot to

99.85% cold. Accuracy in the center portion of the curve therefore was not considered as important as putting the "extreme" information in familiar format. The data in Fig. 3 and 6 were very close to Gaussian with an error of not more than 3°F even at the center points, which is well within engineering error. It must also be stated that the quest for the "extreme" data in the NWC field measurements would preclude a "worldwide" display that would be necessarily Gaussian. Recognizing this, NWC has expanded the field measurement work to include the more temporate continental United States and European exposures.

The last figure of the series suggests how the other Gaussian figures can be statistically added to provide the true DOD defined "worldwide" probable temperature exposure quantification for a Naval air-launched weapon. The basis for this display is the ratio of percent of life of 2:45: 1:45:5 of the factory-to-target sequence figures. The method of combination was to use the mean, plus 3 sigma and minus 3 sigma temperatures of each statistical figure weighed as above. These values were added and divided by 100 to reveal the combined Gaussian representation of the five figures. It is realized that the addition of Gaussian distributions are not necessarily conducive to a resultant Gaussian distribution, even if the mean values are the same, which in this case they are not. However, in our case the three points do lay on a straight line and therefore the approximation should be reasonably good. It is suggested that the risk value assigned by the program authorities can be converted into overall "worldwide" design limits for the "survive, but need not function" portion of a Naval air-arm used missile.

At this point I would like to present a walk-through of this concept. Notice that the data display of Fig. 2 shows a 3 sigma high temperature value of about 115°F and a 3 sigma low temperature value of about -10°F. In other words 99.85% of the time during transportation, the air-launched weapon will experience no more extreme temperatures than -10°F to 115°F. The corresponding temperature for the other events of the factory-to-target sequence are as follows:

Event	% of Lifetime	Range	
Truck & Rail	2	-10°F	+115°F
A/C Carrier/Ship	45	+25°F	+100°F
Field Storage	Less than 1	-10°F	+130°F
Igloo & Covered	45	+20°F	+ 95°F
Airfield Use	5	-10°F	+120°F

Notice in Fig. 7 that the statistical addition of all the events shows a high and low temperature 3 sigma excursion for Naval air-launched ordnance of 40°F to 100°F. It must be emphatically stated that the much abused design values of -65°F and 160°F are not even approached. These values are directly readable in a Gaussian data display at the commensurate risk value. However, the presented figures are terminated at scale values of 99.99%. What non-nuclear, non-man rated ordnance has ever been designed to the 99.99% risk or reliability point with field use that verified this? It seems time that we treat environmental criteria determination as we do the other technology areas and stop blindly assigning 10^{-4}, 10^{-5}, 10^{-6}, etc. probable chance of occurrence design values out of habit.

Conclusions and Recommendations

The data on which to base the rational thermal design goals required by the DOD 5000 series of instructions and MIL-STD-1670 may be available.

The traditional practice of blindly assigning -65°F to 165°F or more extreme values for all development programs can stop, based on measured, quantified fact.

The risk taken by a program when assigning any set of design temperatures can be quantified.

The thermal exposure risk of a waiver to the design specification can be evaluated on a scientific basis.

The thermal exposure risk can be weighed against the gain in performance of semi-risky design concepts.

Efforts should now concentrate on developing a DOD handbook of event versus temperature displays for Army, Navy, and Air Force use covering ship-launched, air-launched, infantry, and helicopter assault missions. This effort will require considerable support to assure a speedy and accurate publication.

In addition, all air-launched weapons program thermal criteria should be reevaluated against the existing event-temperature data.

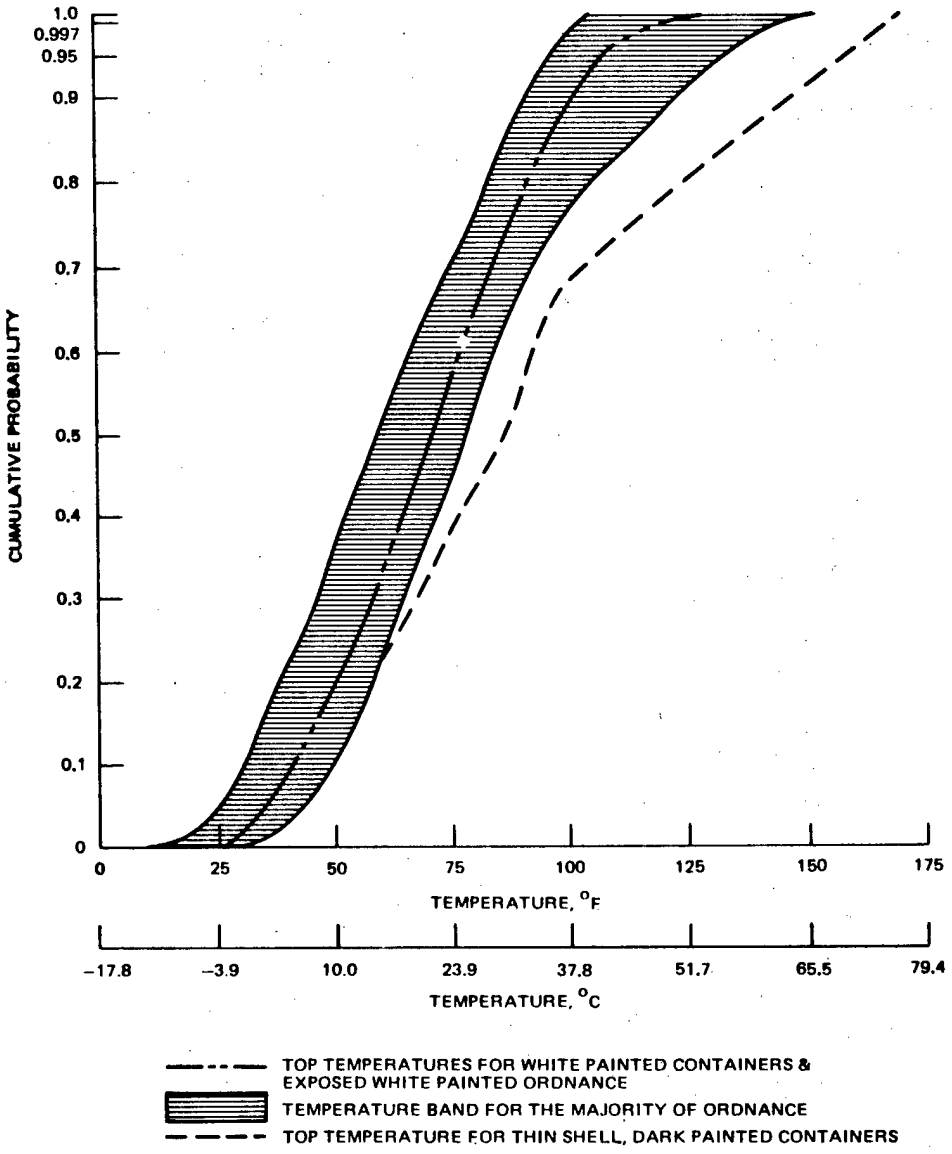

(U) FIGURE 1. Composite of All Exposed Dumpstored Ordnance (1970-1975, China Lake, Calif.). (U)

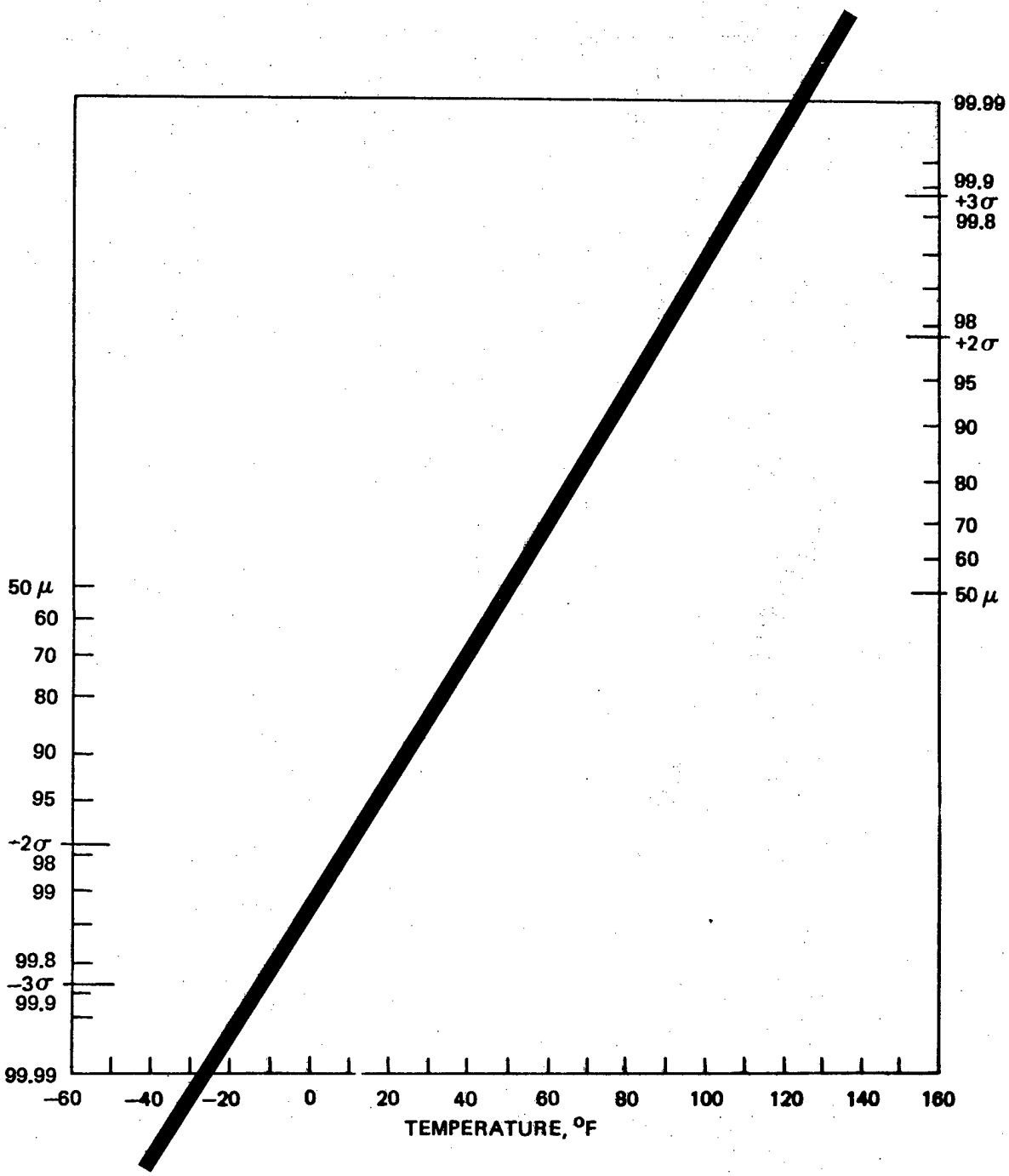

FIG. 2. Transportation, Truck and Rail.

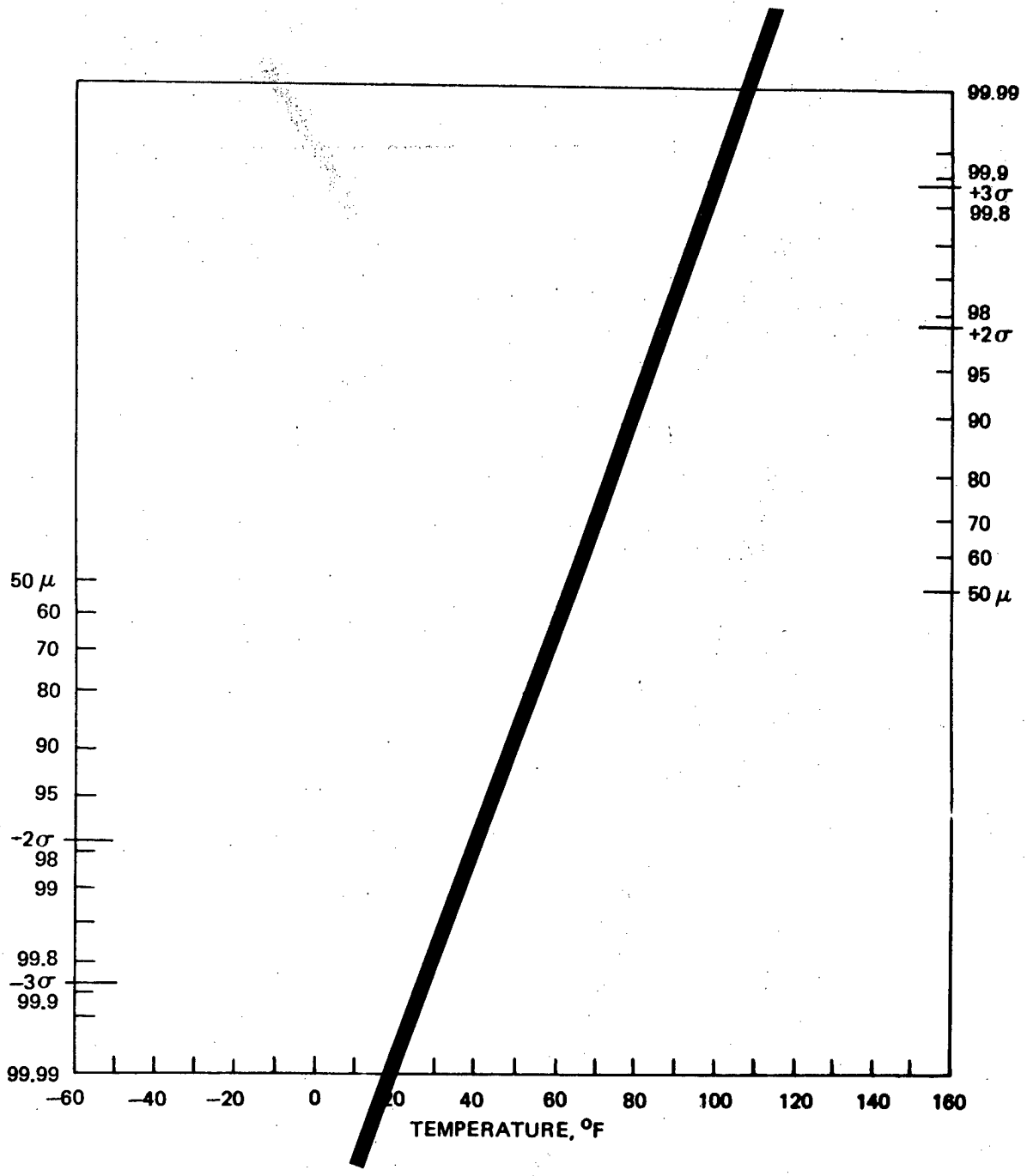

FIG. 3. Ship Transport and Aircraft Carrier Flight Deck.

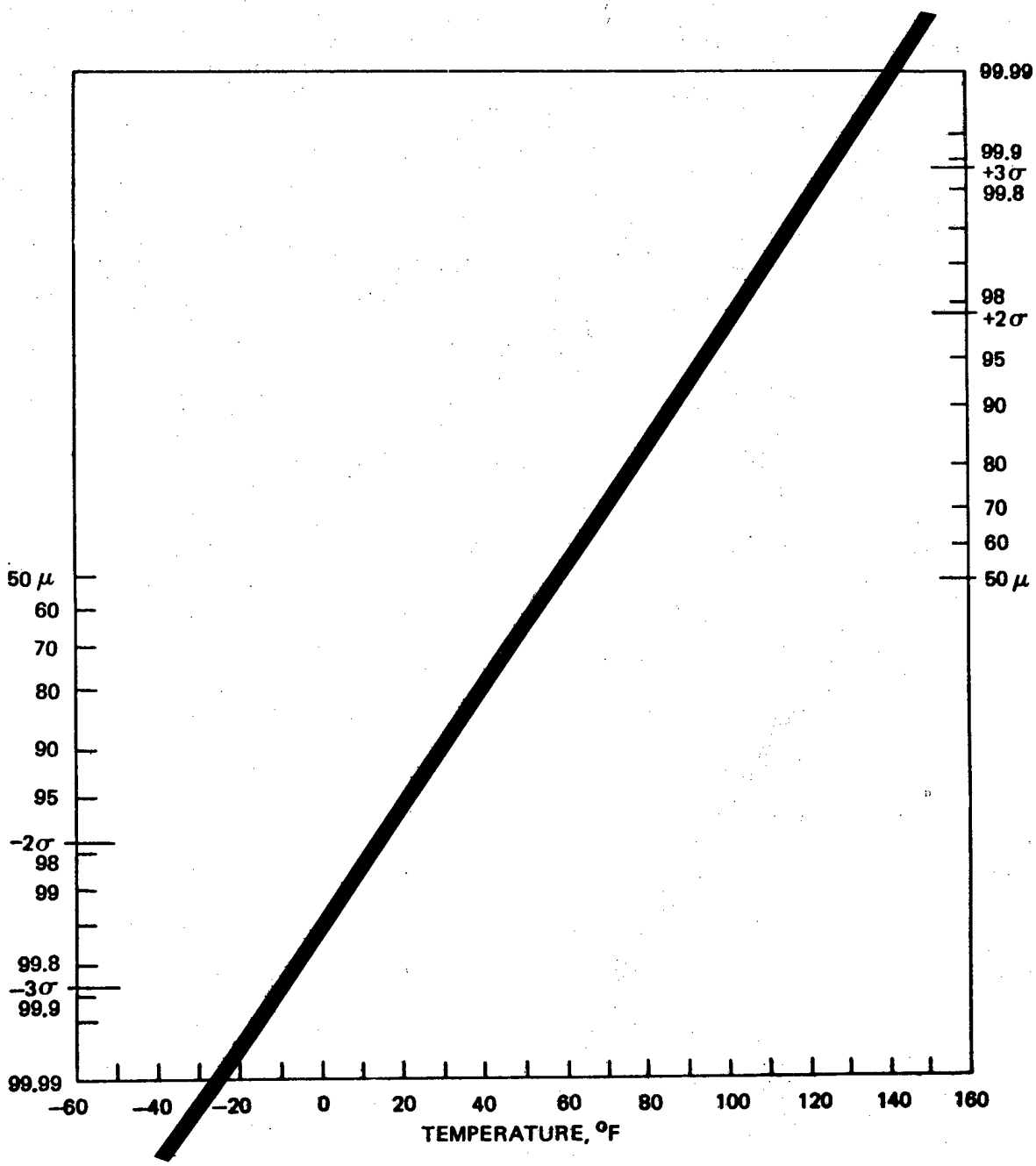

FIG. 4. Navy and Air Force Open Field (Dump) Storage.

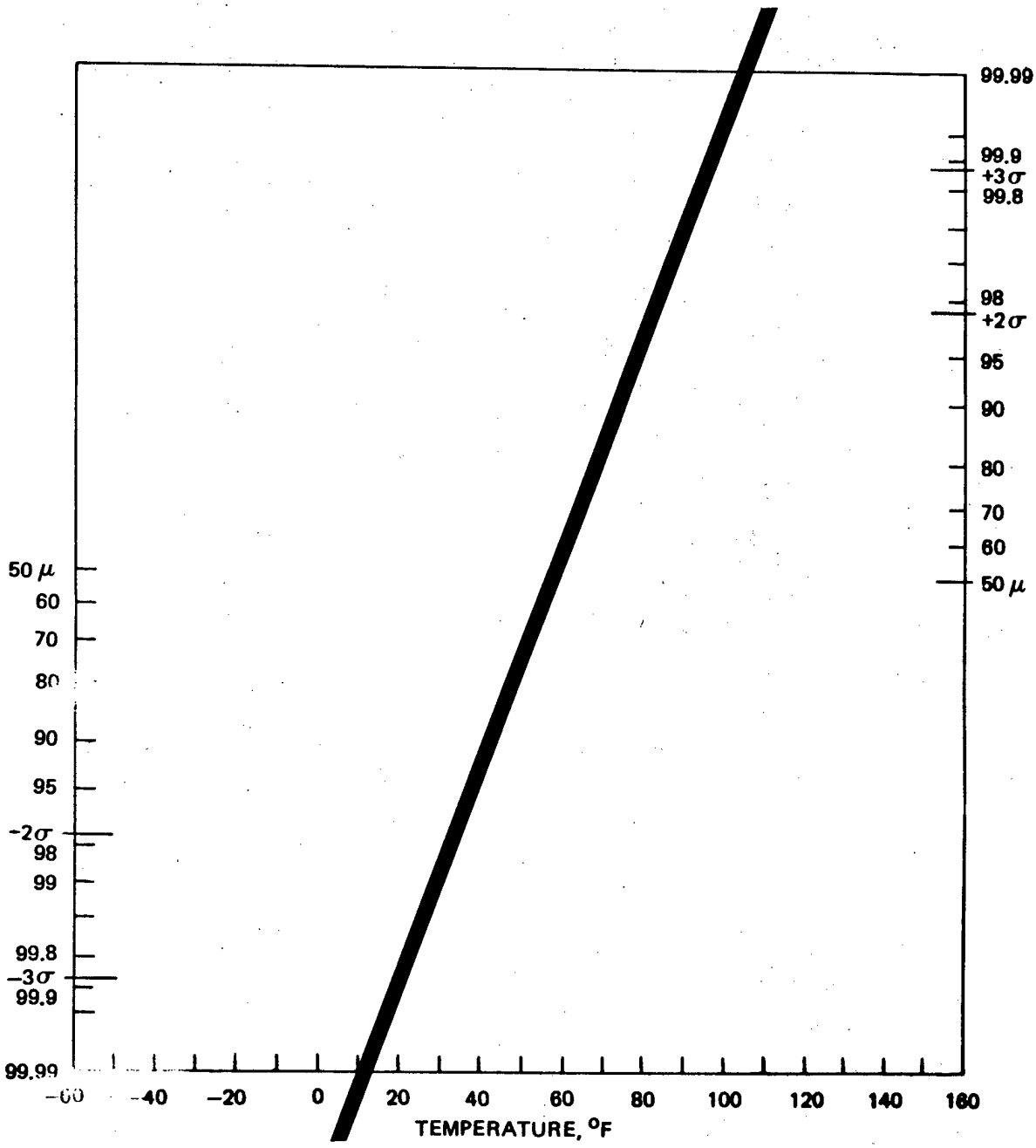

FIG. 5. Covered and Depot (Igloo) Storage.

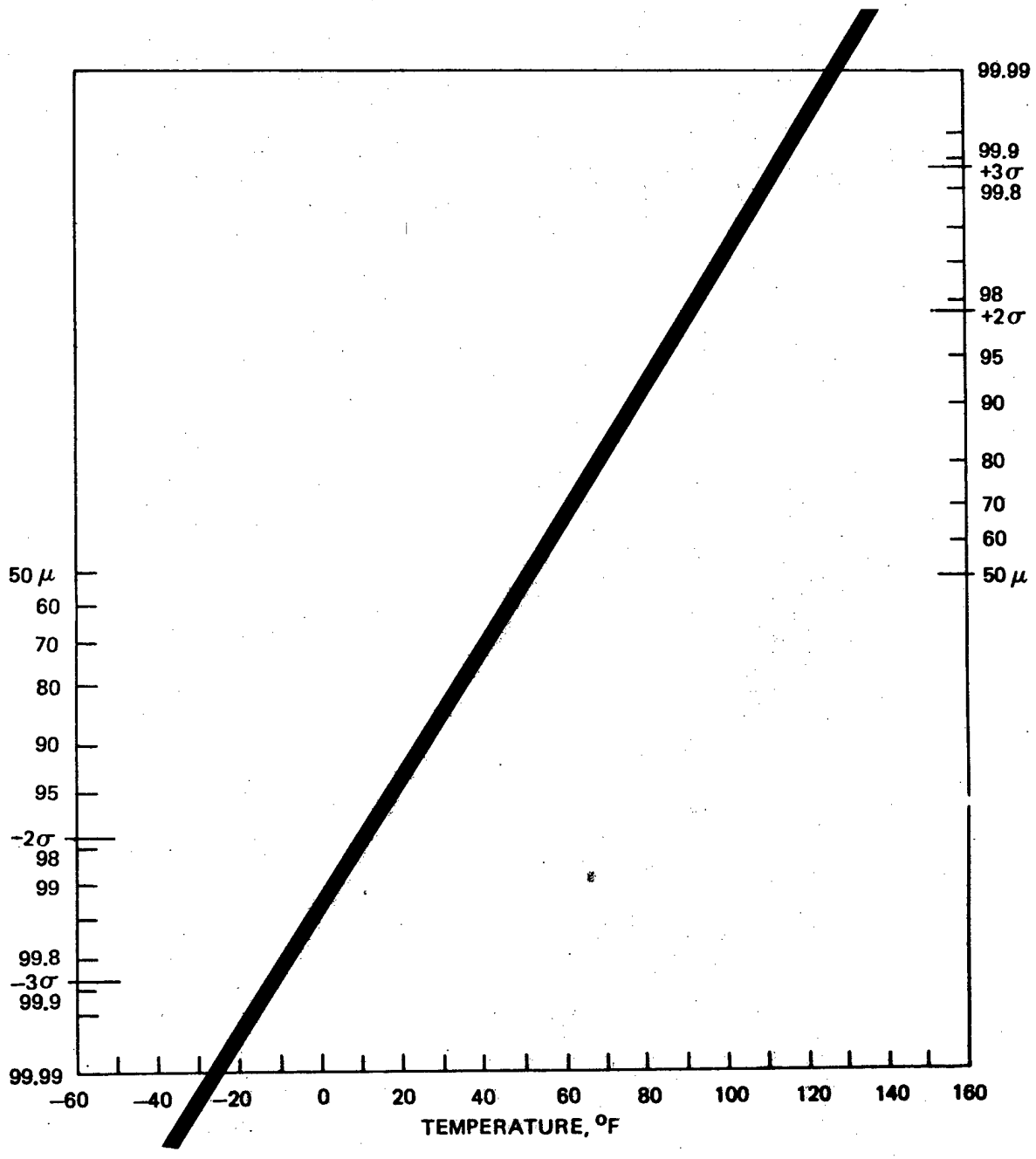

FIG. 6. Marine and Air Force Airfield.

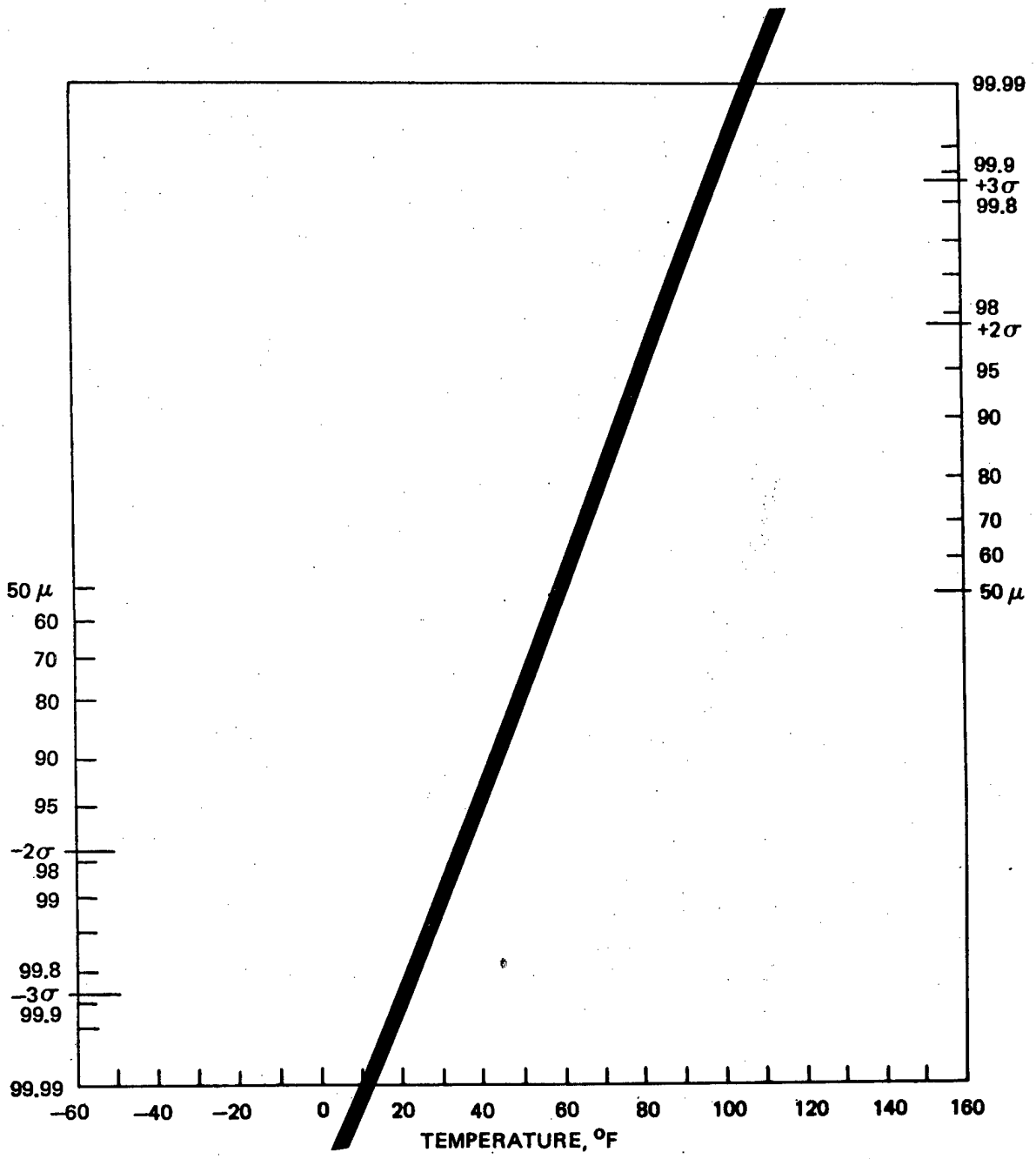

FIG. 7. Overall Probable Chance of Air-Launched Weapon Temperature (2:45:1:45:5).

Biographical Sketch

Mr. Howard C. Schafer received his AA Degree in Engineering from Los Angeles City College in 1955 and his BSME from California State College, Los Angeles, in 1959. He followed a career as a mechanical designer in heavy industry, light industry, and petrochemical research until 1959, when he entered Civil Service. While in government service assigned to a pilot escape-rocket program (RAPEC) in 1960, the need for real world environmental criteria became apparent. The lack of needed environmental information with which to design led to an assignment to measure thermal criteria. He has been in the environmental criteria measurement and determination field ever since, and has travelled extensively worldwide in search of "environmental reality". These efforts led to the receipt of the NWC Technical Director's Award and also the DOD Superior Civilian Service Medal. At the Naval Weapons Center he is also responsible for cooperative environmental criteria determination programs with the five power agreement countries, and has active liaison with other free world nations. He has authored 53 open literature papers and official documents devoted exclusively to the environment and is the U. S. Navy engineering representative for MIL-STD-210B.

(U) A STUDY OF ROCKET-PROPELLED STAND-OFF MISSILES

BY

1Lt. L. K. S. Slimak, USAF

Propulsion Analysis Division
Air Force Rocket Propulsion Laboratory
Edwards AFB, CA

A STUDY OF ROCKET-PROPELLED STAND-OFF MISSILES*

Abstract

This paper presents the results of an investigation of solid rocket-powered Stand-Off Missiles (SOMs) conducted at the Air Force Rocket Propulsion Laboratory, Edwards Air Force Base, California. The study examined the interaction of SOM trajectory and design via computer-aided missile synthesis and trajectory simulation.

Results indicate that non-ballistic, lifting trajectories roughly double semi-ballistic ranges for missiles designed with the same constraints, launch conditions and payloads. Based upon these results, the solid rocket appears to be a viable SOM propulsion candidate.

Introduction

Rising costs of manned aircraft and the increasing size and sophistication of the Soviet Air Defense Arsenal have led to greater interest in weapon systems other than manned aircraft for use in high Anti-Aircraft Armament (AAA) threat environments. One candidate weapon system is the Stand-Off Missile (SOM) which, in this study, is considered to be an air-to-surface weapon of sufficient range and accuracy to allow the launching aircraft to strike at or beyond a defended area from outside the range of the defenses. While this definition could include missiles ranging in size from Maverick and SRAM (Short Range Attack Missile) to ALCM (Air Launch Cruise Missile) and Tomahawk, the emphasis of this effort was confined to conventional SOMs employing warheads weighing 750-2000 pounds and satisfying typical launch vehicle constraints for tactical aircraft. The concepts investigated were envisioned to be useful for primary strike missions against high value, heavily defended, relatively immobile targets, such as counterair (e.g., airfields) and interdiction (e.g., communication and traffic bottlenecks).

* The author wishes to acknowledge the support provided both by Lockheed Missiles & Space Co., Inc. (Sunnyvale) and by co-workers, particularly Capt. L. W. Matuszak, Mr. M. C. Dieckhoff, and Mr. W. S. Woltosz, at the Air Force Rocket Propulsion Laboratory

Objectives of this study were primarily: (1) to assess the ability of solid rocket-powered SOMs to satisfy the mission goals currently being discussed in USAF, (2) to determine the rocket technologies required by conventional SOMs and the payoffs of more advanced (and generally more expensive) rocket technologies, and (3) to provide preliminary payload/range data to those who are in the process of defining SOM. The approach taken, results obtained, and conclusions drawn from the study are described below.

Approach

The study consisted of a four-phase effort covering a period of approximately eight months. Phase I involved data collection. Phase II was an investigation of semi-ballistic trajectory SOMs; lifting trajectories were examined in Phase III. Phase IV consisted of sensitivity and advanced technology studies.

Phase I data collection included the decision to limit the study to tactical missions. Two candidate launch aircraft were selected -- the F-4 and C-130 -- to establish typical diameter, length and weight constraints. The F-4 appeared to be the most constraining aircraft, so it was used to define constraints for two designs: a 3200 lb gross weight vehicle for the F-4 inboard wing station and a 5000 lb gross weight missile for the F-4 centerline station. Though F-4 and C-130 appeared to be the most likely launchers at the start of the study, increasing interest in F-16 launch and decreasing interest in the F-4 became apparent as the study progressed. As a result, when Phase III started, F-16 cases (3500 lb gross weight for F-16 centerline or inboard wing station) were substituted for the 3200 lb designs.

The study SOM was configured as a single stage, single booster, boost-glide, solid-rocket powered missile. Code limitations, plus the lack of contrary SOM requirement definition, led to the use of an all boost thrust profile. A boost-glide trajectory was selected as that believed most likely to maximize the range of a rocket SOM.

Warhead weights used in the study are intended to cover the range of tactical warheads of interest rather than representing specific warheads; weights ranged from 750 to 2000 lbs. Other non-propulsive weight and volume estimates were based largely on data provided by Lockheed Missiles and Space Company (Sunnyvale). Some alterations were made to this data both to allow for differences between the subject design details and to allow for motor growth as design payload was varied. However, throughout the study, when extrapolations and estimates were involved, an attempt was made to insure that all resulting numbers were conservative.

Aerodynamic data used (i.e., CN and CA vs Mach number) was generated by Hughes Aircraft Corporation for the Hughes 12-7 configuration 1/2 SEV (SRAM Equivalent Volume) conceptual Short Range Bomber Defense Missile (SRBDM). This data was the best and most readily available at AFRPL at the start of the study; its use was continued as a further conservatism compared to the aerodynamics of a winged SOM. This SRBDM concept is a relatively clean, ogive-nosed, tail controlled missile with strakes; it is depicted in Figure 1.

Because the SOM is designed to enable the launch aircraft to operate outside the range of enemy defenses and because motor burnout was expected outside of visual range of the target, no requirement for reduced observables (i.e., reduced or minimum smoke propellants) was enforced. This allowed selection of an 88% total solids/ 18% aluminum HTPB propellant as the baseline. This type of propellant is considered state-of-the-art. Also, while no prohibition against Class 1.1 (formerly Class 7) propellants exists, this Class 1.3 (formerly Class 2) was considered more appropriate because of its reduced operational limitations.

SOM launch is envisioned being made well behind the FEBA (Forward Edge of Battle Area), an area where the launch aircraft is not subject to enemy action. In this situation, it was assumed the launch aircraft would, to the extent it was able, perform a pitch-up maneuver to put the SOM velocity vector at launch on a flight path angle resulting in maximum range. This maneuver is

employed at times by fighter aircraft under similar conditions to extend the range of GBU-15.

All designs for Phases II-IV were generated using the AFRPL Ballistic Missile Optimization Program (BMOP) which performs constrained optimization of motor and trajectory control parameters using a direct search parameter optimization routine. Motor design parameters varied by the program included average chamber pressure (pc), motor cylindrical length (Lc), motor diameter (Dmot), nozzle throat area (At), nozzle expansion ratio (ε), and nozzle exit half angle (α). Trajectory parameters optimized included the initial flight path angle (γ_i), time at initial constant inertial attitude (Δt_1), inertial pitch rate ($\dot{\chi}_p$) and duration of pitch (Δt_2), command angle-of-attack (α_c), time to command angle of attack (t_3), and time to end angle of attack and return to zero angle of attack (t_4).

This methodology in Phases II-IV was to fix missile gross launch weight and then size an individual missile for each warhead weight/volume (the motor weight and volume maximums being the weight/space remaining after accounting for warhead, guidance, etc.). All non-propulsive weights except warhead were held constant throughout the study, so as warhead weight/size increased, motor weight/size decreased (and vice versa).

Phase II consisted of an investigation of SOM designs employing semi-ballistic trajectories. This semi-ballistic trajectory consisted of launch at an initial flight path angle (γ_i) which was then a time (Δt_1); the missile then pitched over at constant inertial pitch rate ($\dot{\chi}_p$) for time (Δt_2). After this pitch phase, missile inertial attitude was held constant until the velocity vector aligned itself with the body axis (i.e., angle of attack (α) equals zero); zero α was then held to impact. This trajectory is depicted in Figure 2.

Initially, the Phase III lifting trajectory model was the same as the ballistic except that the final phase became a glide at a commanded non-zero angle of attack (for lift). Further range was achieved by flying ballistic to apogee before commanding lift; finally, both the command angle of attack and time of its initiation were made optimized parameters. This led to trajectories

with extremely low terminal velocities. The code was further modified to optimize a time at which command angle of attack is again set to zero in order to meet an input terminal velocity requirement.

A brief examination was made of a pulse motor for SOM, using part of its impulse to attain a high altitude for cruise and the remainder of its impulse to sustain. Little range extension appeared available with this approach so effort was concentrated on the single pulse boost-glide rocket.

During Phase III, new optimized designs and trajectory controls were generated employing boost-glide lifting trajectories. Optimized parameters included those used in Phase II plus three additional parameters: time to begin command angle-of-attack (t_3), command angle-of-attack (αc), and time to end command angle-of-attack and return to zero angle-of-attack (t_4). (Figure 3). Range-payload curves were again generated for the previously discussed launch conditions and missile gross weights.

Two Phase III designs were selected as baselines for examination in Phase IV. Sensitivity to specific design inputs was examined by fixing the parameter of interest at a different value and re-optimizing the design for maximum range. Change in maximum range from the baseline was used as the determinant of sensitivity.

Assessment of Models and Assumptions

BMOP is a preliminary design tool. Motor design detail is at the relatively simple level appropriate to preliminary design. No propellant grain design is attempted; although certain input parameters (notably volumetric loading efficiency and web fraction) are included to account for gross grain geometry effects, a real design could well be different. Constraints are enforced on overall motor characteristics that must be satisfied by the grain design; however, these constraints are not sufficient to guarantee that the specified motor can be built.

The basic premise of the BMOP code is that the complex interrelation between motor and trajectory variables demands simultaneous and equal consideration of each. At the same time, a code the size of BMOP cannot address all of the interactions of motor and trajectory variables with other sub-system parameters (or between non-propulsive parameters), some of which could have impact of the same order of magnitude as those relations handled in the code. This is one of the difficulties of the approach taken in BMOP.

As stated in the introduction, this study was propulsion oriented. While an attempt was made to account for non-propulsive considerations impacting propulsion design and missile performance, much work remains for future efforts.

Contact with other government and private organizations has led to the belief that a guidance set could be built for a missile such as the lifting SOM discussed here. Although such a set may not be available today, the range from this trajectory shaping, if nothing else, offers an indication of the benefit of developing a suitable guidance system.

While the pitch-up angles called for in the study may not be beyond the capability of the F-16 at the altitudes discussed, they are well beyond that of the C-130. Lower launch angles have been examined but launch angle/velocity/range trades need to be further investigated. Use of other methods to pitch-up the missile velocity vector at motor ignition should also be examined.

Another area of uncertainty deals with the aerodynamic stability of a boost-glide SOM at the relatively high altitudes encountered at and near apogee. An assessment of stability was beyond the scope of this study; however, should tumbling/instability prove a problem, a possible solution is the use of a reaction control system.

Non-propulsion considerations could alter the designs presented here. Actuator packaging and ejection bending loads could, for example, force an increase in chamber wall thickness to meet these loads; then, having the thicker case, "optimum" pressure should be that

matching the case thickness. Similarly, ejection loads could eliminate composite cases from consideration. Aerodynamic heating could affect the results either by impacting the guidance set or by dictating the selection of case materials with better high temperature properties. However, lacking data, these considerations were not addressed.

For certain aircraft, particularly the F-4, position of the missile center of gravity (CG), rather than weight or volume, will be the driving constraint. Since determination of CG position would involve further extrapolation of available data, no accounting was made in the study of or for CG position. Such an accounting could alter the designs significantly.

Another area for future consideration is SOM aerodynamics. While the data used was the best available, aerodynamic data representative of a real SOM might differ. For example, the nose/radome might be incompatible with the guidance used, or terminal maneuverability considerations might force a different configuration.

Some tradeoff between winged (higher lift) and unwinged (lower drag during boost) SOMs should be performed, as it is not obvious which configuration is best for a boost-glide missile using trajectory shaping. Deployable wings, offering the advantages of both clean and winged missiles, are a possible alternative; however, such a system was beyond the scope of this effort.

A detailed, authoritative analysis of the penetration capability of the SOMs presented herein was also beyond the scope of this effort. The survivability of the ballistic SOM should be excellent because of its high terminal velocity. A minimum terminal Mach number of 1.2 was enforced on the lifting SOMs to enhance their survivability. Further examination of SOM radar and infrared signature plus consideration of the capability of enemy defenses is needed to define penetration requirements.

Results

Results of the ballistic phase of the study are presented in Figure 4 (Ballistic SOM range-payload curves) and Table 1 (Ballistic SOM Design summary). Each point in Figure 4 represents an independent, optimized missile design with Table 1 giving further detail on each design and trajectory. Each of the Figure 4 curves is roughly exponential, as anticipated from the basic rocket equation: $R \propto \Delta V \ln \frac{mi}{mf}$

where R = range

ΔV = velocity change from ignition to burnout of the stage

m_i = rocket mass at stage ignition

m_f = rocket mass at stage burnout

As the warhead weight of a weight limited missile increases, range decreases.

However, several anomalies are apparent in Table 1. The two designs with average chamber pressure of 3000 psi clearly stand out against the trend to lower chamber pressures (and greater ranges); it is believed that a lower pressure solution, more in accordance with the trend, would yield higher range. (The BMOP optimization scheme, like many others, often finds locally, not globally, optimal designs). Chamber pressures on the order of 300 psi, shown in some cases, are at least partially the result of a flaw, since corrected, in the code.

After a brief examination of these results, the decision was made to go on to lifting trajectories immediately because the ballistic SOM ranges were approximately half those desired with the payloads of interest. No further effort was expended on ballistic SOM. Consequently, this data should be viewed only as an indication of ballistic SOM potential. It is presented primarily to offer a guage of the payoff for trajectory shaping.

Figure 5 (Lifting SOM Range-Payload curves) and Table 2 (Lifting SOM Design Summary) present the results of the "lifting" phase of AFRPL's effort. Again, each point represents a different, optimized missile design. Each point was also more thoroughly exercised than its ballistic companion, leading to both smoother curves and greater confidence that these designs are closer to the best possible within the imposed limits and assumptions. As before, the curves are roughly exponential.

Several generalizations can be made about these lifting designs. Average chamber pressures are lower than those common in other high-performance air-launched missiles. Designs to date have been weight, not volume constrained; i.e., the designs are at the maximum weight limits imposed while remaining well within the length and diameter bounds used. Lifting is commanded just before or at apogee.

For the purpose of this study, the most significant generalization that can be drawn is that use of the lifting trajectory approximately doubles SOM range for a given weight and launch condition. Another interesting generality is that with the warhead weights considered (750, 1000, 1200, 1500, and 2000 lbs) the C-130 SOM offers approximately the same range as the F-16 SOM with the next lightest warhead.

Two designs were selected as baselines for the advanced technology and sensitivity investigations of Phase IV: F-16 launch with 1500 lb warhead and C-130 launch with 2000 lb warhead. They were selected because each met the nominal 200 NM range goal with relatively large warheads and because each represents a different weight class of missile. These designs are depicted in Figures 6 and 7 while their trajectories are shown in Figure 8.

Since no one warhead has been specified for SOM, an assumption was made that the design will accept a variety of warhead modules, allowing the selection of the most appropriate warhead for a given mission. Figure 9 presents the results of varying the warheads of the baseline designs; trajectory parameters were optimized in each case.

Results of the sensitivity analyses are presented in Figures 10 and 11. Sensitivity was evaluated by varying a parameter from the baseline and fixing it; the design was then re-optimized with this fixed value and the change in range taken as the sensitivity. Motor parameters included in sensitivity examination included average chamber pressure (PC), cylindrical case length (LC) and motor diameter (DMOT).

Other parameters varied for sensitivity analysis were: WMISC (input value of non-propulsive, non-payload inert weight), ISPR (the table of reference values of motor specific impulse vs. chamber pressure; used by BMOP as part of the motor performance calculation), FWEB (motor web fraction; a BMOP input parameter used to calculate propellant burn rate), RB1000 (propellant burn rate at 1000 psia chamber pressure), NRATE (propellant burn rate exponent), and VEND (impact velocity).

The magnitude of the changes made to examine sensitivity was not intended to be uniform. Instead, the intent was that the changes shown would be of uniform difficulty to bring about in reality. Thus, while chamber pressure was examined, at $\pm$ 100 psi, specific impulse was varied $\pm$ 1%. Case cylindrical length was varied $\pm$ 1 in, as was motor diameter; non-propulsive inert weight was varied from 200 lbs baseline $\pm$ 100 lbs.

Web fraction was varied from its baseline value of 0.72; burn rates at 1000 psi were 0.25 for both the F-16 and C-130 baselines. Baseline burn rate exponent was 0.2. Terminal velocities of 1674 (M 1.5) and 1800 (M 1.6) fps were examined for several reasons: higher terminal velocity generally enhances survivability and some SOM warhead candidates require higher terminal velocities to function.

Changes of less than three percent in range are regarded as being within the modeling accuracy of the BMOP code. Any sensitivity greater than this three percent is believed significant.

As can be seen, both the F-16 and C-130 SOM designs are quite sensitive to inert weight, the F-16 showing greater change because the $\pm$ 100 lb used is a larger

fraction of the F-16 SOM gross weight than of the C-130 SOM. Both designs show similar sensitivity to terminal velocity, range naturally decreasing as demanded terminal velocity is increased.

The most surprising of the sensitivities was that of the F-16 SOM design to a decrease in motor diameter. Considerable effort had been made in attempting to get the F-16 baseline to optimize to a lower diameter in Phase II. Failure of these efforts had mistakenly led to the conclusion that the larger diameter was preferred; however, sensitivity results indicate otherwise. As BMOP does not handle detail grain design factors, the BMOP optimum design is likely to be that minimizing diameter (because diameter being used to generate reference area, minimizes drag) while meeting the maximum weight and not violating length constraints.

Sensitivity to a 1% change in specific impulse is the last of the sensitivities considered to be of significance. While the 1% change in sensitivity lies within modeling error, a larger change in specific impulse, possible through the use of more advanced propellants, would most likely offer a more significant payoff.

Conclusions

Based upon the work presented here, within the limits of the assumptions, the solid rocket has been shown to be a viable candidate for SOM propulsion. Furthermore, the rocket propulsion herein proposed for SOM is not technology driven. It need not entail more advanced propulsion technologies, although advanced technologies can be used to improve performance.

Too much work remains in SOM mission definition and system trades to identify any preferred SOM propulsion option. However, the solid rocket belongs among the candidates deserving further investigation.

STAND-OFF MISSILE MOTOR DESIGN

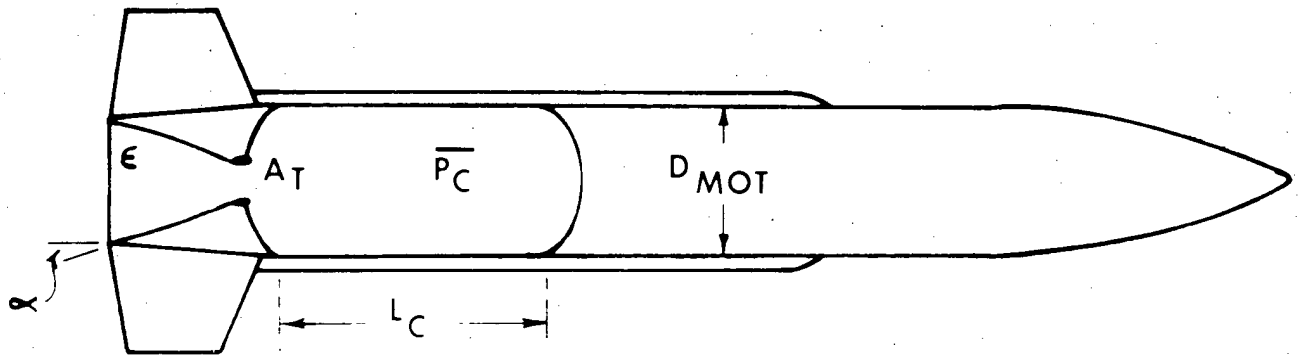

CONSTRAINED PARAMETERS:

- MAXIMUM DIAMETER
- MIN EXPANSION RATIO
- MAX NOZZLE EXIT DIAMETER
- MAX, MIN PROPELLANT BURN RATE
- MAX TOTAL MOTOR LENGTH
- MAX, MIN CHAMBER PRESSURE
- MAX TOTAL WEIGHT
- MAX, MIN NOZZLE SUBMERGENCE
- MIN BURN TIME
- MIN "PORT TO THROAT" AREA RATIO

FIGURE 1. STAND-OFF MISSILE MOTOR DESIGN

STAND-OFF MISSILE TRAJECTORY BALLISTIC

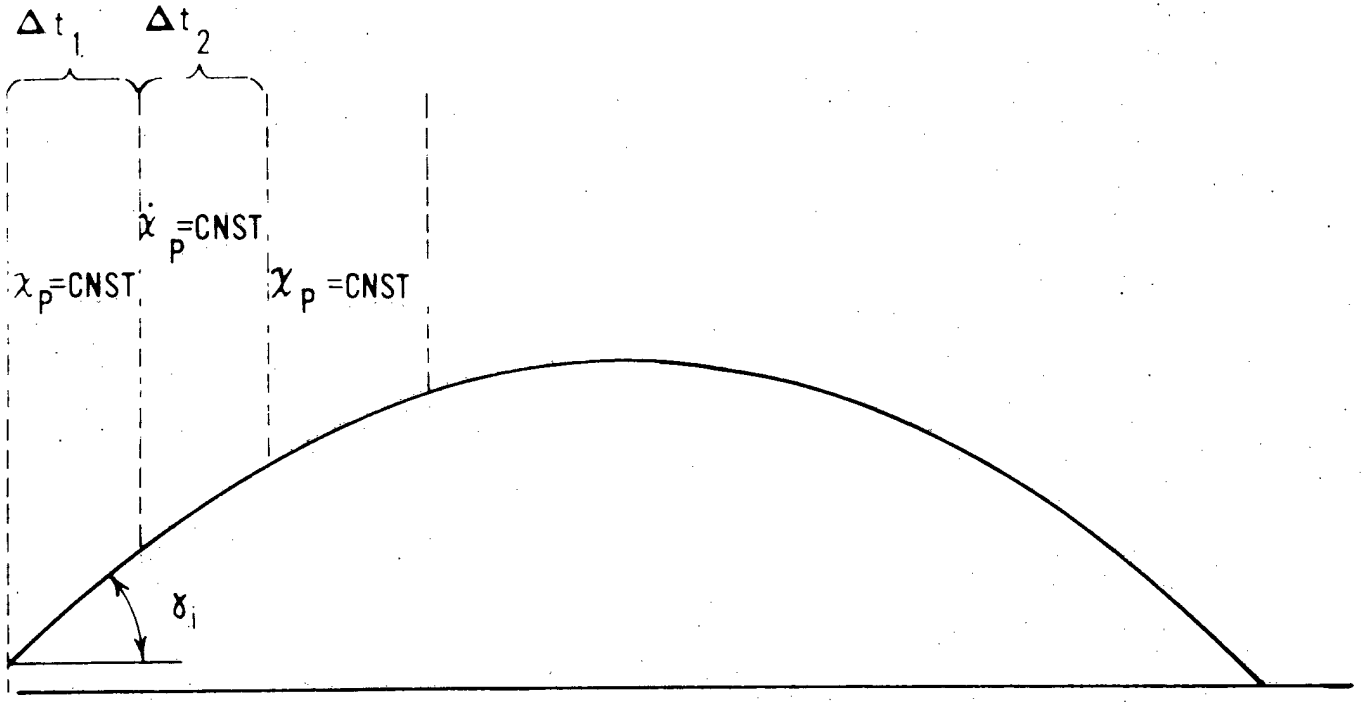

CONSTRAINED PARAMETERS

—AXIAL/NORMAL ACCELERATION

—PITCH RATE

—α

FIGURE 2. STAND-OFF MISSILE BALLISTIC TRAJECTORY

STAND-OFF MISSILE TRAJECTORY LIFTING

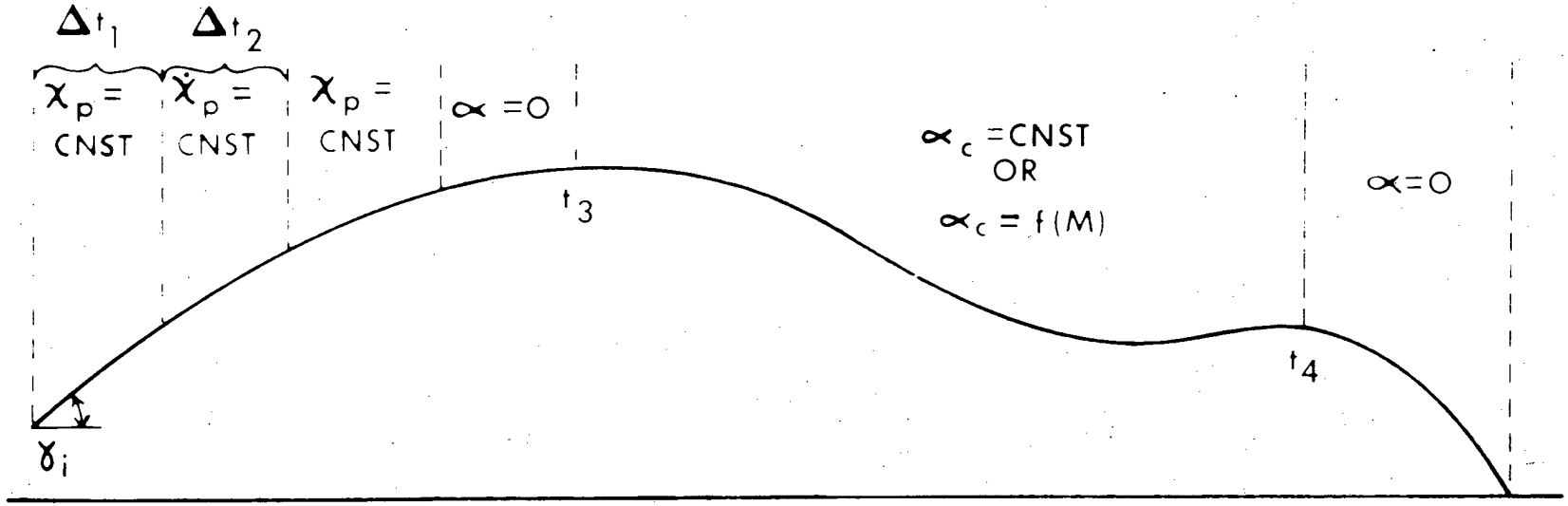

CONSTRAINED PARAMETERS

- —AXIAL/NORMAL ACCELERATION
- —PITCH RATE
- —α
- —TERMINAL VELOCITY

FIGURE 3. STAND-OFF MISSILE LIFTING TRAJECTORY

BALLISTIC SOMS

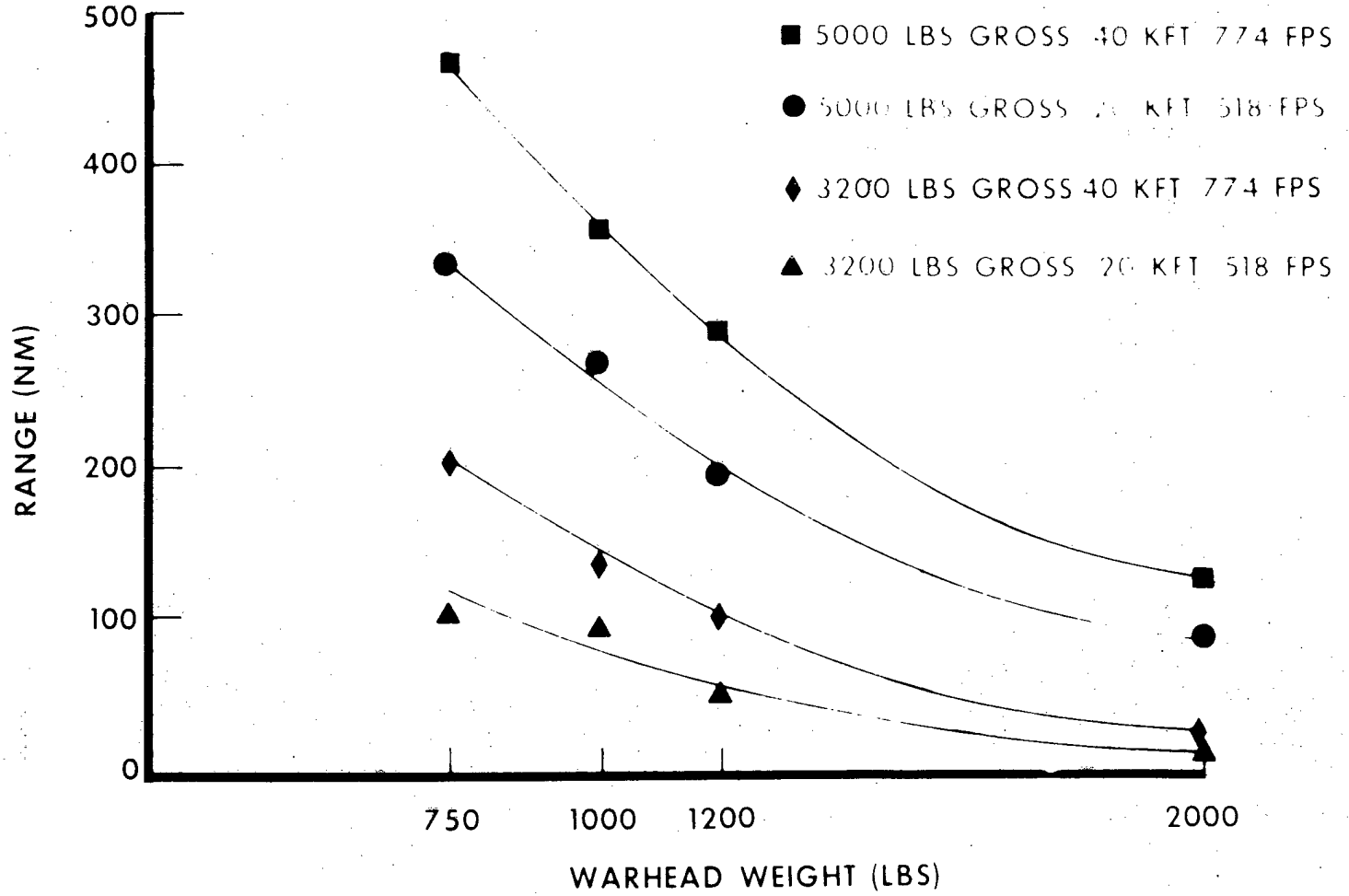

FIGURE 4. BALLISTIC SOM RANGE vs. PAYLOAD CURVES

LIFTING TRAJECTORY SOMS

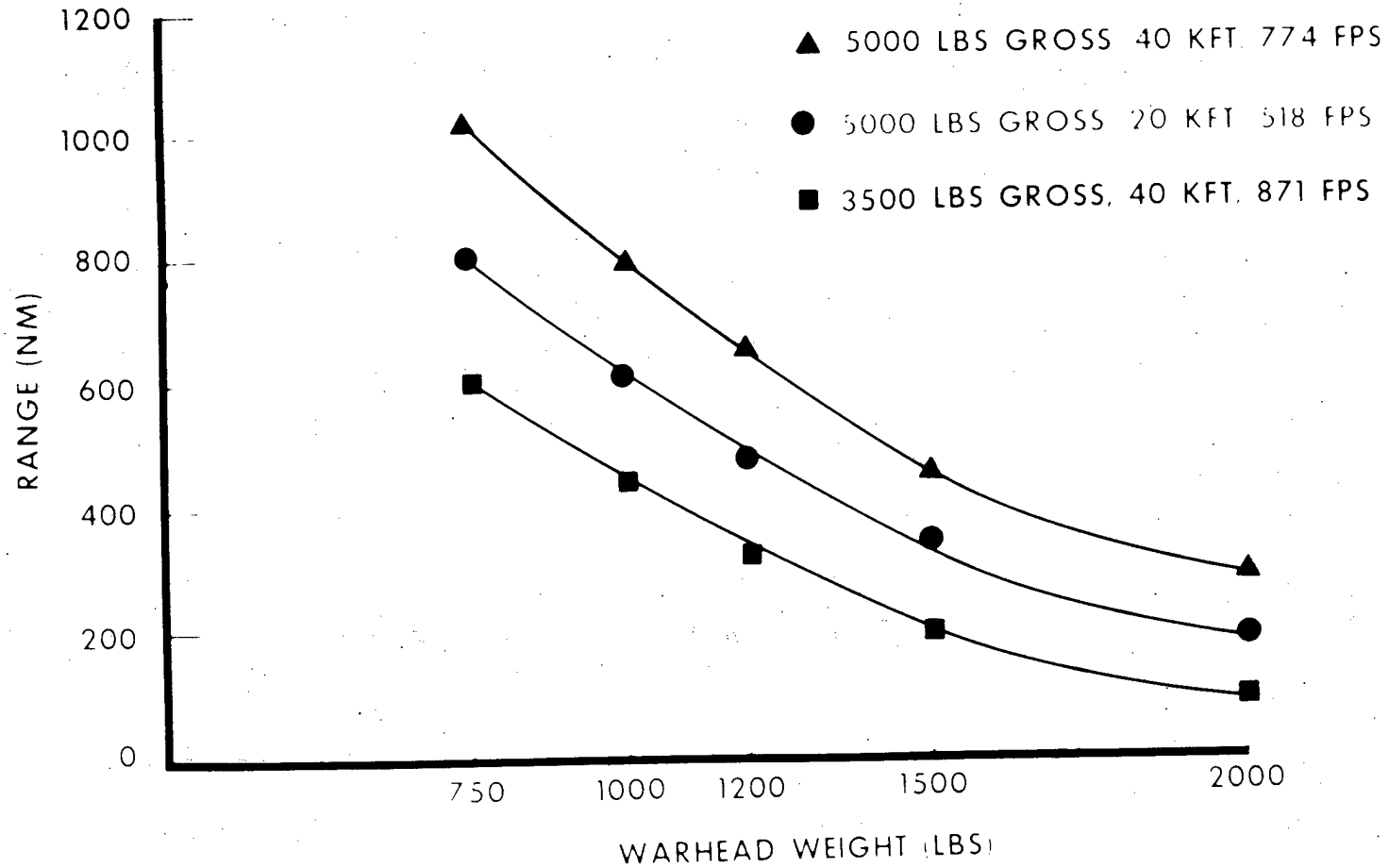

FIGURE 5. LIFTING SOM RANGE vs. PAYLOAD CURVES

F 16 SOM 1500 LB WARHEAD 3500 LB GROSS

194 NM RANGE
22 NM APOGEE

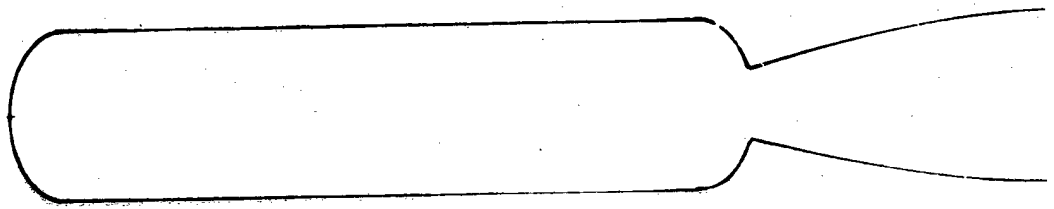

P_C =576 PSI

L_{TOTAL} =111 IN

D_{MOT}=22.69 IN

A_T=9.97 IN^2

ϵ =34.79

$I_{SP_{VAC}}$ =279 SEC

T_{VAC} =10,273 LBS

$I_{T_{VAC}}$ =400.685 LB_F SEC

W_{PROP} =1435 LBS

MR 588

FIGURE 6. F-16 BASELINE SOM

C 130 SOM 2000 LB WARHEAD 5000 LB GROSS

196 NM RANGE

26 NM APOGEE

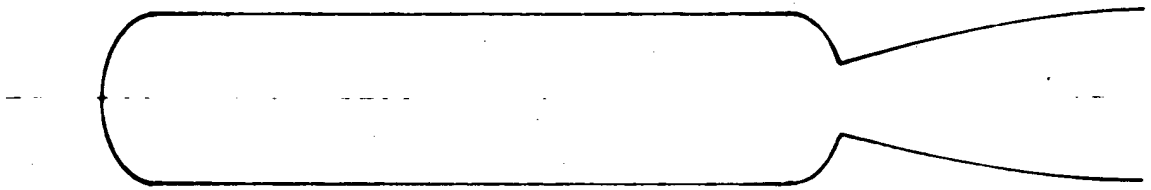

P_C =737 PSI

L_{TOTAL} =150.0 IN

D_{MOT} =21.7 IN

A_t =14.65 IN^2

ϵ =19.81

$I_{SP_{VAC}}$ =271 SEC

T_{VAC} =18,692 LBS

$I_{T_{VAC}}$ =622,429 LB_F SEC

W_{PROP} =2299 LBS

MR =.539

FIGURE 7. C-130 BASELINE SOM

F 16 SOM LIFTING TRAJECTORY 1500 LB WARHEAD, 3500 LB GROSS

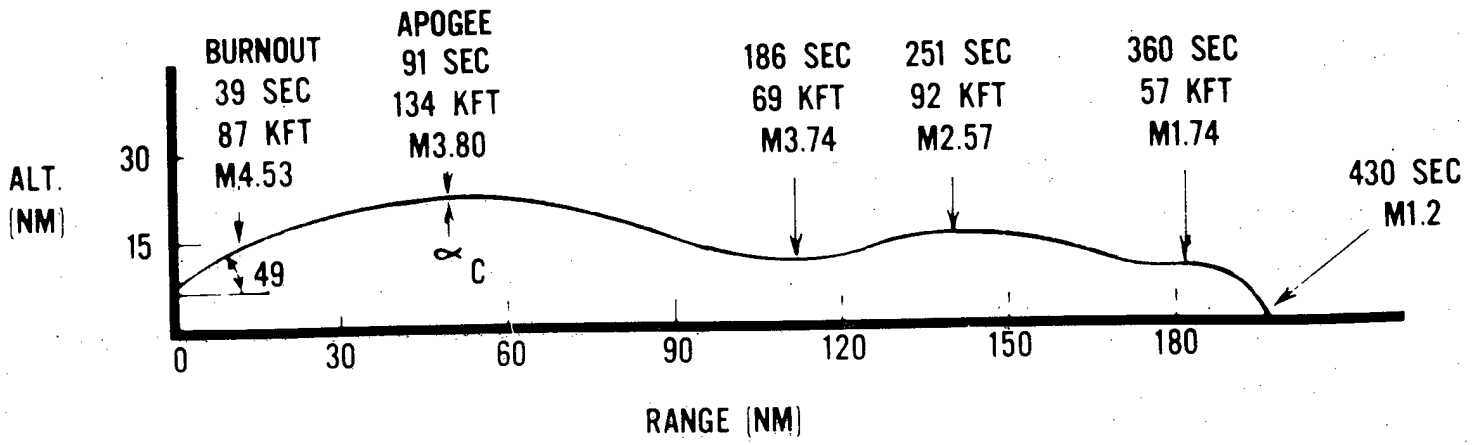

C 130 SOM LIFTING TRAJECTORY 2000 LB WARHEAD, 5000 LB GROSS

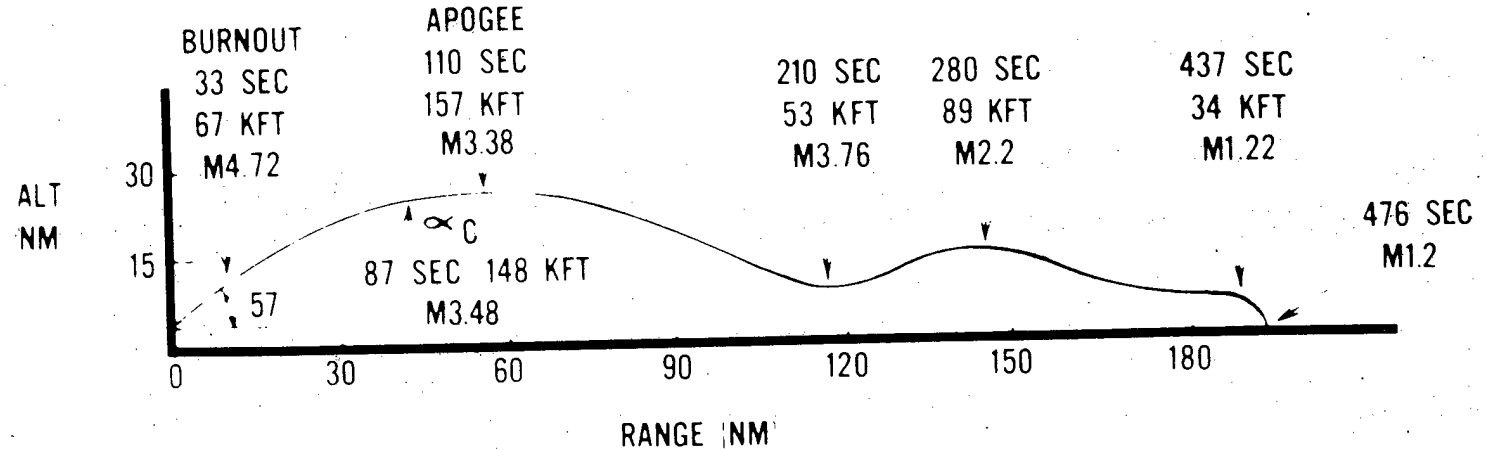

FIGURE 3. BASELINE SOM TRAJECTORIES

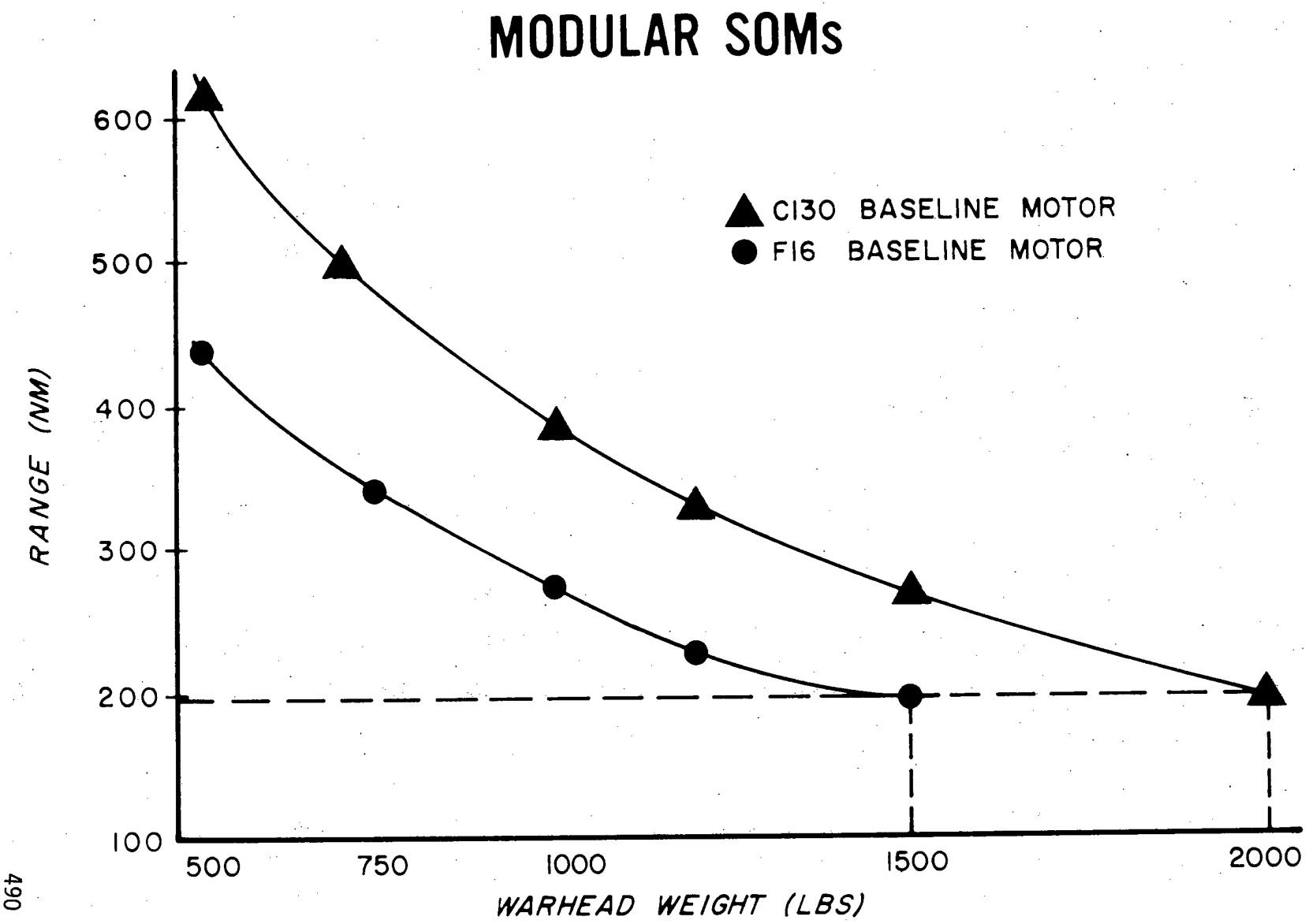

FIGURE 9 - SOMS WITH MODULAR WARHEAD

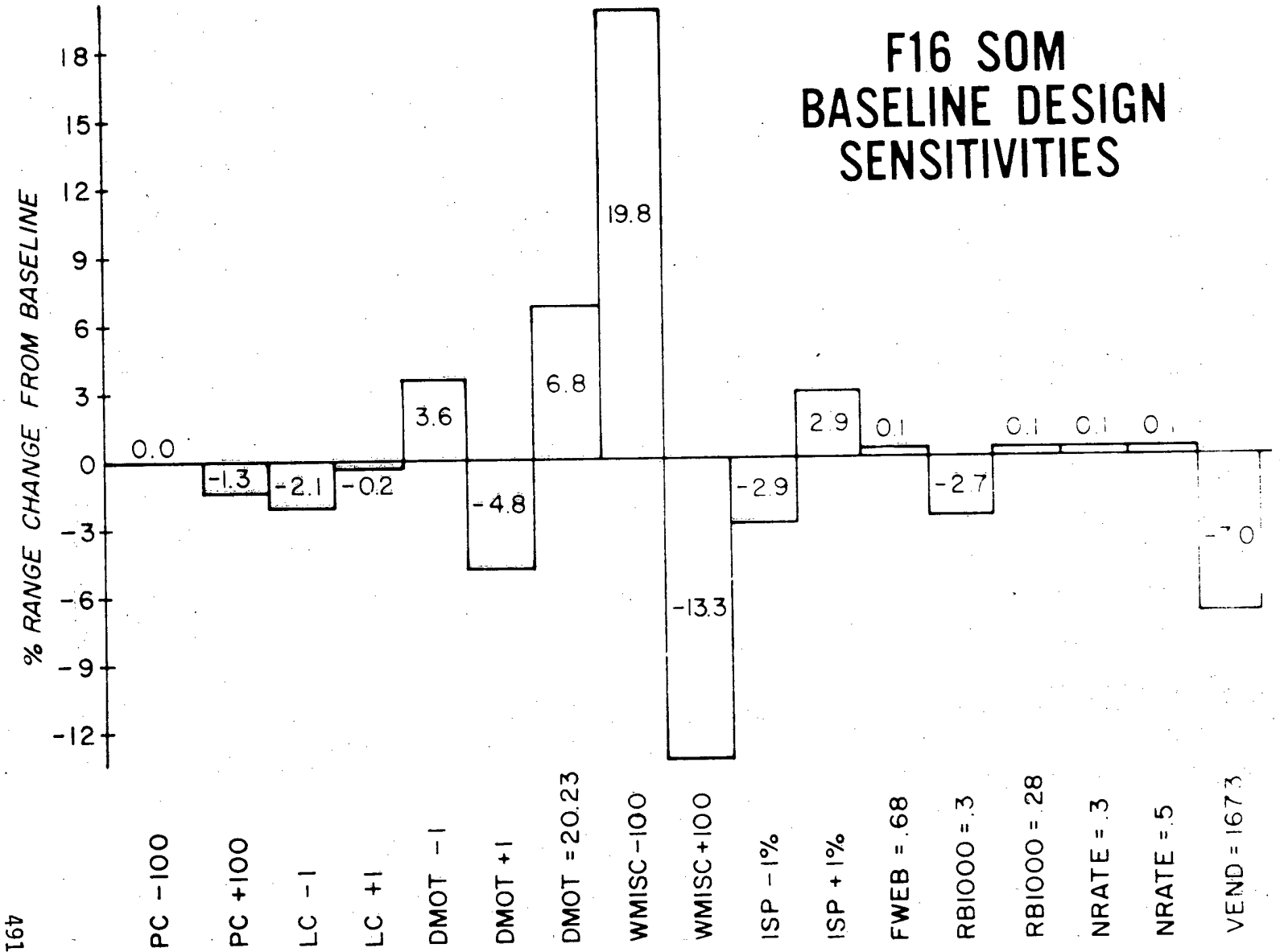

FIGURE 10 - F-16 SOM BASELINE DESIGN SENSITIVITY

C130 SOM BASELINE DESIGN SENSITIVITIES

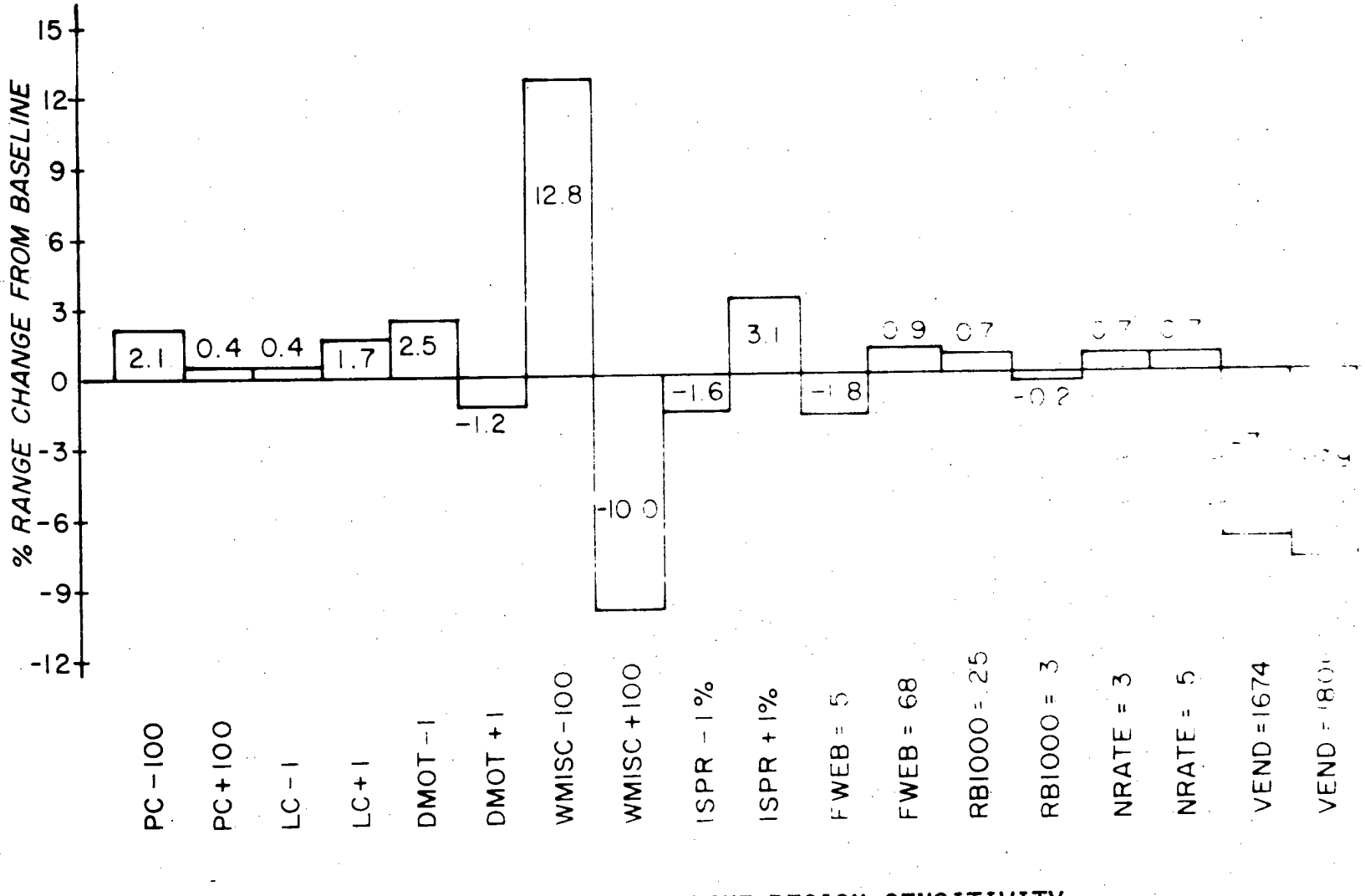

FIGURE 11 - C-130 SOM BASELINE DESIGN SENSITIVITY

TABLE I. BALLISTIC SOM DESIGN SUMMARY

WARHEAD WEIGHT (LBS)	GROSS WEIGHT (LBS)	PROPELLANT WEIGHT (LBS)	LAUNCH ALTITUDE (KFT)	FLIGHT PATH ANGLE AT LAUNCH (DEG)	LAUNCH VELOCITY (FPS)	VACUUM DELIVERED THRUST (LBF)	VACUUM DELIVERED SPECIFIC IMPULSE (SEC)	NOZZLE THROAT AREA (IN^2)	AVERAGE CHAMBER PRESSURE (PSI)	NOZZLE EXPANSION RATIO	MOTOR LENGTH (IN)	MOTOR DIAMETER (IN)	MACH NUMBER AT IMPACT	FLIGHT TIME (SEC)	APOGEE (NM)	RANGE (NM)
2000	5000	2046	40	43	774	17209	282.4	19.2	507	17.2	117.6	24.6	2.97	246	36.4	128.4
2000	5000	2274	20	45	518	19550	285.5	13.0	842	20.2	139.3	22.3	3.18	259	38.1	131.9
2000	3200	506	40	35	774	4898	289.8	4.4	616	22.1	61.0	23.3	1.35	120	10.2	23.7
2000	3200	542	20	22	518	3127	267.5	5.4	347	7.9	59.0	22.4	1.10	97	3.8	15.7
1200	5000	2867	40	44	774	14832	278.1	25.0	342	15.1	131.6	26.2	4.18	372	74.0	293.1
1200	5000	2703	20	45	518	16459	283.9	12.4	754	17.8	106.0	30.0	2.56	322	54.8	191.7
1200	3200	1182	40	58	774	11701	283.8	11.5	573	18.0	101.2	20.3	2.66	221	30.4	103.5
1200	3200	838	20	58	518	25179	287.1	3.5	3000	70.7	62.4	27.1	1.42	176	19.4	49.45
1000	5000	3048	40	44	774	15399	278.3	26.5	333	14.6	141.9	26.2	4.92	412	89.5	359.8
1000	5000	3048	20	45	518	15574	275.5	25.3	356	12.3	141.0	26.2	3.62	379	74.4	276.5
1000	3200	1373	40	61	774	10733	286.5	11.9	506	21.3	78.7	27.8	1.78	261	39.2	134.4
1000	3200	1357	20	50	518	11763	280.9	10.5	637	14.9	109.9	20.3	2.60	246	34.5	97.7
750	5000	3308	40	43	774	14977	276.8	28.8	300	13.6	124.7	30.0	5.70	472	113.9	463.8
750	5000	3310	20	45	518	14167	275.7	25.6	321	12.5	123.9	30.0	3.60	438	96.0	355.4
750	3200	1629	40	63	774	10579	284.2	15.6	381	19.5	86.4	27.9	2.01	318	56.0	205.8
750	3200	1103	20	56	518	35048	275.7	5.1	3000	56.0	75.6	24.9	2.14	230	33.1	100.1

TABLE II. LIFTING SOM DESIGN SUMMARY

WARHEAD WEIGHT (LBS)	GROSS WEIGHT (LBS)	PROPELLANT WEIGHT (LBS)	LAUNCH VELOCITY (FPS)	FLIGHT PATH ANGLE AT LAUNCH (DEG)	LAUNCH ALTITUDE (KFT)	VACUUM DELIVERED THRUST (LBS)	VACUUM SPECIFIC IMPULSE (SEC)	AVERAGE CHAMBER PRESSURE (PSI)	NOZZLE THROAT AREA (IN^2)	NOZZLE EXPANSION RATIO	MOTOR LENGTH (IN)	MOTOR DIAMETER (IN)	MAXIMUM DYNAMIC PRESSURE (PSF)	FLIGHT TIME (SEC)	APOGEE (NM)	RANGE (NM)
2000	5000	2375	774	57	40	12783	269.2	392	18.8	18.8	123.5	25.7	2132	528	26.8	262.4
2000	5000	2299	518	57	20	18692	270.8	737	14.6	19.8	150.0	21.7	2132	476	25.8	196.2
2000	3500	956	871	46	40	13785	275.1	752	10.4	28.5	95.8	20.3	2133	300	16.8	91.89
1500	5000	2766	774	53	40	18813	276.2	647	16.4	29.0	156.0	24.6	3485	678	44.0	457.6
1500	5000	2796	518	57	20	18886	269.6	571	19.1	18.8	160.3	23.1	3146	616	38.2	343.0
1500	3500	1435	871	49	40	10273	279.2	576	10.0	34.8	110.9	22.7	2117	430	22.1	194.3
1200	5000	3056	774	45	40	20278	273.8	594	19.5	23.7	167.2	24.2	3450	834	47.4	649.4
1200	5000	3069	518	42	20	19031	268.6	574	19.3	18.5	152.0	25.1	4328	688	52.4	444.0
1200	3500	1719	871	51	40	12691	272.9	512	14.2	23.5	134.7	20.6	2423	585	21.8	326.0
1000	5000	3250	774	39	40	21443	271.1	562	21.9	20.	178.1	23.6	4573	925	60.4	792.0
1000	5000	3238	518	59	20	22819	267.2	596	22.4	16.9	189.0	22.3	4322	840	32.8	614.9
1000	3500	1916	871	41	40	12303	273.9	448	15.6	25.6	132.4	22.6	2530	633	39.3	423.6
750	5000	3491	774	44	40	23290	265.1	527	26.0	15.0	199.7	22.3	4739	1011	67.1	1022.7
750	5000	3510	518	50	20	23315	259.7	496	28.2	11.0	207.4	21.4	6010	979	73.0	831.6
750	3500	2127	871	54	40	14217	274.4	514	15.7	26.0	140.2	22.9	3598	739.	57.8	602.0

BIOGRAPHICAL SKETCH

Lieutenant L. Kevin S. Slimak was born in Kingston, Pennsylvania on 26 June 1952. He graduated from the Massachusetts Institute of Technology in 1974, receiving an S. B. degree in Aeronautical and Aerospace Engineering. He was commissioned in the Air Force through the AFROTC program in 1974 and was granted a delay from extended active duty in order to pursue graduate studies at the Massachusetts Institute of Technology.

In August 1976, he entered active duty and was assigned to the Air Force Rocket Propulsion Laboratory. He has since served as a Propulsion Analyst in both the Rocket Lab's Solid Rocket and Propulsion Analysis Divisions. He has published one other paper on tactical stand-off missiles.

PREDICTION OF ROCKET MOTOR EXHAUST PLUME EFFECTS ON TACTICAL MISSILE EFFECTIVENESS

by

Andrew C. Victor, Physicist

Ordnance Systems Department
Naval Weapons Center
China Lake, California

ABSTRACT

The exhaust plumes of modern rocket motors can reduce battle effectiveness of missiles and associated equipment by a variety of means. Exhaust plume blast, impingement and contamination are a threat to equipment and human safety. Plume signature effects can degrade detection, guidance, tracking and homing effectiveness. As a result, performance of our own missiles may be degraded, while that of threat missiles may actually be enhanced. This paper describes and discusses these exhaust plume effects and methods for predicting and controlling them.

The purpose of this paper is threefold:

1. To introduce to this symposium some systems implications of exhaust plume technology.
2. To briefly describe the aspects of exhaust plume technology which have such implications.
3. To advocate levels of inter-disciplinary, inter-service and intra-service cooperation which will reduce the risks and costs of plume related problems in military operations.

INTRODUCTION

Theoretical predictions of plume phenomena must be made when insufficient information is available from direct measurements. In order to make such predictions, one must know the relationships which exist between the propulsion system, the environment, the plume physics and chemistry, and the plume phenomena being predicted. For reasons of expediency, it is also helpful to know the relative importance of the detailed factors so that unimportant effects can be ignored.

The necessary calculational models may be considered in two separate categories: plume gas dynamic models and plume effect models. The technology for both types of calculations is currently being documented in a JANNAF handbook (Ref. 1).*

Plume gas dynamic models predict the chemical and physical properties of the flow field which comprises the plume. Some of the more sophisticated new models predict turbulent fluctuations of properties as well as steady state values (average values). The fluctuating values are necessary for predicting radar cross section, laser beam wander and spreading and RF (radio frequency) signal modulation, and for estimating fluctuations in a number of observables such as temperature, pressure, and emitted radiation. The results of plume gas dynamic models directly provide the information needed for many impingement problems. Other problems require subsequent use of plume effect models.

Plume effects models are applied to the results of the gas dynamic models to predict the specific plume effects of concern. Thus, there are a large number of plume effect models (Ref. 1). Most of these are actualized as computer codes, although some crude calculations can be performed *by hand*. Among the plume effect models currently in existence are:

1. RF attenuation (including absorption, refraction, diffraction, pulse distortion)
2. RF modulation (a scattering/attenuation effect)
3. Radar cross section
4. Primary smoke
5. Secondary smoke
6. Smoke visibility (i.e., optical scattering)
7. Laser attenuation (both by smoke and clear plume turbulence)
8. Infrared (IR) emissions
9. Visible emissions
10. Ultraviolet (UV) emissions

* The JANNAF (Joint Army Navy NASA Air Force) Plume Technology Handbook is intended to provide an introduction and useful text and tool at all working and management levels. Although it does not document the most sophisticated techniques, it provides references to original sources for them. When complete, the Handbook will comprise over 1,000 pages.

Although plume effect predictions have been made for a number of years, such predictions are generally performed in isolation from the operation situation in which they are important. In the past, for example, it seemed sufficient to predict RF attenuation effects and, as a consequence, modify the rocket motor propellant to achieve acceptable levels as defined by specifications. We are coming to realize, increasingly, that many other operational variables, both deterministic and statistical, may have to be included to obtain realistic estimates of the magnitudes of operational plume effects.

Before acceptable plume signature levels can be defined, it is necessary to quantify the effects of plumes on operational scenarios. This is now being done, for the first time, in studies at the Naval Weapons Center. By trying to include plume effects in the "big picture" we ask such questions as: How many ships do we lose in a particular scenario because of plume effects, compared to standard analyses which ignore such effects? or How many more defensive missiles must be launched in a fleet defense scenario, because of plume effects, in order to maintain the same level of defense?

Current studies involve two portions of the fleet scenario: (1) *shipboard plume effects during defense against cruise missiles* and (2) *plume effects on the terminal effectiveness of anti-aircraft missiles* (i.e., reduced kill probability due to detectability of anti-aircraft missile plumes). The first of these studies is documented in a preliminary report (Ref. 2).

Continuing work will complete the study of these two scenario elements and, on that basis, lead to recommendations for acceptable levels of plume signature and design specifications for appropriate rocket motors. In addition, theoretical and experimental studies of rocket and ramjet engine exhausts are being pursued by the three military services to provide necessary information for modern propulsion designs and anti-missile weapon designs.

The three military services and NASA cooperate continuously in plume technology. Through JANNAF and various ad hoc groups, tri-service program plans now exist in the areas of plume UV and IR signature and plume smoke. Jointly funded programs include contract development of standardized computer codes for predicting low altitude plume gas dynamics and for IR signature.

Studies of aircraft turbine engine IR signatures have contributed significantly to current IR models and measurement techniques for missile exhaust signatures.

Finally, although it is not the subject of this paper, high altitude plumes of space engines and military strategic missiles have received even more study than the low altitude plumes of tactical missiles. Where appropriate, the knowledge gained in Air Force and NASA studies of these plumes is applied to tactical missile plumes.

BACKGROUND

One result of the current demands for effective, accurate, lightweight, low cost, safe, high efficiency tactical missiles is that increasing attention must be paid to the motor exhaust. For example, accuracy requires minimal exhaust interference with guidance or tracking signals and effectiveness necessitates low vulnerability to enemy detection and countermeasures. Because these considerations arise at the interface between propulsion system and guidance system design and development, there has been some tendency for exhaust effects to be overlooked in both phases, sometimes with unfortunate consequences.

Three main objectives of the work on exhaust plume technology are:

1. To provide information on the exhaust properties of threat missiles for application in areas of
   a. Detection of enemy missiles
   b. Identification of enemy missiles
   c. Intelligence gathering on enemy missiles
   d. Homing on enemy missiles

2. To provide information on exhaust properties of U.S. and NATO missiles for application in areas of
   a. Guidance, tracking and range safety
   b. Blast, impingement and contamination effects
   c. Countermeasure avoidance
   d. Interference with concurrent military operations

3. To generate new ideas for future missile systems including development of lower-signature propulsion systems which are difficult to detect or which cause less interference with our own forces.

To illustrate the various contexts in which problems associated with propulsion system exhausts may arise, the following questions are typical of those frequently asked:

What are the spectral and spatial structures in the infrared, visible and ultraviolet of plume emissions from threat missiles? What are the implications of these signatures for defensive detection and guidance system designs? How can these signatures be simulated in target drones for testing U.S. and NATO detection and homing systems?

What levels of radio wave attenuation occur in rocket motor plumes? How do these vary with propellant and other motor characteristics and with missile trajectory variables? Can viable RF beam rider or semi-active guidance systems be designed to operate with these motors? What are the effects of alternative propellant compositions?

What levels of plume temperature, blast and particle flow impinge various aircraft, ship and ground launchers as a result of missile firings?

What are the spectral and spatial structures in the infrared, visible and ultraviolet of plume emissions from U.S. and NATO missiles? What are the implications of these signatures for enemy detection and countermeasures? How can these signatures be reduced to acceptable levels? At what cost in dollars and other performance parameters? What are acceptable levels of signature?

Are the primary and secondary smoke* trails from various propulsion systems likely to provide an enemy with a means of detection? Under what meteorological conditions do smoke trails, formed from the efflux of different motors, cause significant degradation of optical guidance (laser) signals?

What levels of radar cross section (RCS) are caused by the exhausts of different propulsion systems? What sorts of problems are likely to arise from plume RCS as missile RCS is otherwise reduced by new designs and materials?

The field of plume technology attempts to answer these and similar questions by a program which deals both with experimental and analytical research at the technology base level and with plume-related phenomena in current developmental and operational systems.

TECHNICAL DISCUSSION

The technical discussion is divided into three categories: (1) causes of plume phenomena, which includes a brief review of rocket exhaust science, (2) scenario assumptions, which describe some scenarios currently being studied for sensitivity to plume effects, and (3) plume effect modeling, which includes some simplifications that can be applied to plume modeling and the results of some past modeling studies.

Causes of Plume Phenomena

In a typical missile power plant, combustion of fuel and oxidizer occurs in a combustion chamber in which the combustion products are moving toward the chamber exit at subsonic speed. Constriction of the chamber cross-sectional area into a nozzle throat near the exit accelerates the gas flow to sonic velocity. The flow, expanding and accelerating downstream of this nozzle throat, remains supersonic and the static temperature of the gas decreases while the velocity increases. The flow

* "Primary smoke" is composed of the solid effluent from propulsion systems. "Secondary smoke" is a contrail generally formed by condensation of plume and atmospheric water on the microscopic particulate efflux.

becomes a free jet or exhaust plume when it leaves the confines of the nozzle. This usually happens at the nozzle exit (downstream end of the nozzle). However, it can occur within the nozzle, due to flow separation (detachment of the flow boundary layer from the nozzle walls), if the external ambient pressure exceeds the jet static pressure by a factor of between 2.5 and 3.5 (depending on nozzle shape, nozzle size and chamber pressure).

The supersonic free jet flow adjusts to ambient pressure by a series of shocks (Figure 1). The shocks are the result of "nature's feedback." Pressure information from the outer jet boundary is fed at sonic speed to the jet. However, since the jet flow is supersonic, the internal jet pressure tends to overshoot the ambient pressure, and the shocks, which are temperature, pressure and density discontinuities, result from the buildup of pressure difference between the jet and its environment.

While this is occuring near the centerline of the plume, other effects occur near the outer jet boundaries. There may be flow separation, mixing and recirculation at the missile base which leads to additional shocks and to a relatively low pressure, stagnated region (indicated as region 7 in Figure 1). There will always be a mixing of jet material with the surrounding air, indicated by regions 5 and 6 in Figure 1. This mixing region spreads both toward and away from the plume centerline with increasing distance from the nozzle. The jet material in the mixing region becomes increasingly diluted with distance from the centerline and from the nozzle.

Combustion of the jet material ("afterburning" or "secondary combustion") may occur in the mixing region if the local temperature and chemical species permit. Afterburning can raise the static temperature of portions of rocket plumes to above 2,500 K.

In order for afterburning to occur, there must be present unburned fuel species (usually CO and H_2 and sometimes carbon soot), a relatively high temperature for ignition (usually greater than 1,000 K) and a sufficient concentration of free radical species (H, O and OH) to propagate the combustion chain reactions. In rocket motor exhausts sufficient temperature to initiate afterburning is often available in the mixing region itself, however, in some cooler exhausts, afterburning can only be initiated by the elevated temperature and/or production of free radicals behind a strong shock or in a base stagnation region.

In general, the combustion products of ramjet propulsion systems contain more air than the stoichiometric proportion needed for complete combustion of all fuel species. Although afterburning is thus unlikely to occur in the plumes of ramjet engines, it can occur if incomplete or irregular combustion of fuel species results in the expulsion of these species into the jet or in those cases where insufficient air is introduced into the combustor.

Optical emissions from plumes are caused by atomic and molecular spectral emissions from the hot gaseous species and by thermal radiations from hot particles. These same mechanisms act in reverse in cooler regions of the plume to absorb some plume emissions and thus to attenuate, to some degree, the plume optical signature as a function of viewing angle (see Figure 5).

In the ultraviolet spectral region, thermal radiation from hot particles may be the major source of emission. There is also some evidence to suggest that continuum producing exothermic reactions may be the cause. Additional molecular continuum radiation (blue flame continuum) comes from the chemiluminescent reaction: $CO + O \rightarrow CO_2 + h\nu$. Minor spectral band radiation may also come from thermally excited electronic states of NO and OH molecules.

In the infrared spectral region, the primary sources of radiation are thermal radiation from particles and molecular (vibrational) emissions from CO_2, H_2O, CO and any other species, such as HCl and HF, which may be present.

RF (radio frequency) radiation interacts with charged species in plumes. Generally these are free electrons and ions; however, the ion contribution is not believed to be important at RF frequencies above 500 MHz. These charged species are usually present in significant quantities only in the presence of afterburning, behind strong shocks, or very close to the nozzle. The presence of a few parts per million of alkali metals or other substances with low ionization potentials increases the free electron concentration to many times the value obtained from chemi-ionization alone.

Blast and impingement effects depend upon the specific details of surfaces behind the motor or engine nozzle. The stagnation temperature and the dynamic pressure of the plume flow field are determined in the flow field calculational models. Particle impingement effects may be calculated if the plume model includes coupled gas-particle flow.

Optical (including laser beam) power losses and scattering are usually due to smoke (i.e., particles) in the plume. In the absence of particles, density gradients in the plume will cause measurable power losses and forward scattering. However, particle scattering and absorption of optical radiation are by far the more important effects since they are responsible for most of the problems involving optical guidance and detection systems and plume visibility. The plume smoke particles have been classified into two major categories:

Primary smoke particles are formed in the chamber combustion or nozzle expansion processes. These are usually particles of metal oxides or soot (hydrocarbon smoke). These are the same particles responsible for the thermal emission and particle impingement effects described in previous paragraphs. In concentrations typical of high energy composite propellant exhausts, primary smoke particles of Al_2O_3 may cause plumes to be visible even beyond the "meteorological" range or so-called "visual

range" of atmospheric transmission. This visibility is caused by scattering of solar radiation (Ref. 3).

Secondary smoke is the name given to droplets of water and water solutions which may form and grow in cooler regions of the plume. An obvious minimum requirement for secondary smoke formation is a local relative humidity, or saturation ratio of the condensing species greater than unity. Secondary smoke forms on condensation nuclei which may come from the atmosphere as well as from primary smoke particles. The water vapor in the plume and in the ambient atmosphere both contribute to condensation. The presence of water soluble compounds (such as HCl, HF, NaCl, NaOH, etc.) will promote the growth of secondary smoke (Ref. 4). Jet aircraft contrails are an example of plume secondary smoke.

Scenario Assumptions

Plume effects on scenarios cannot be evaluated until numerical values for the plume effects are obtained. To obtain values for these effects, it is necessary to abstract portions of the scenarios which describe the situations surrrounding plumes and then to calculate the magnitude of plume effects in these situations. The results of these calculations are later used in the scenario calculations whenever a plume is created as the result of a rocket firing.

Shipboard Plume Effects. It is instructive to consider the view from shipboard. The ship travels in a "tunnel" of signature or radiation. The view in any direction can be described by a time varying broadband spectrum. The launch of a missile by the ship contributes to this "tunnel" of signature (i.e, a tunnel of "fire and smoke"). The problem of defining shipboard signature effects comes down to one of describing this "tunnel" at the electromagnetic wavelengths of interest. The wavelengths of interest are determined by the on-board sensor characteristics. Obviously, the sky, the sun, clouds, the sea, other ships, aircraft, missiles–all of these–as well as missiles launched by the ship, and the effect of the intervening atmosphere, must be considered.

An example of the scenario abstraction is indicated in Figure 2. The fleet deployment and threat axes are indicated in Figure 2a. Computer simulation of the ensuing engagement results in a complete description of all events–target detections, combatant trajectories, ship losses, own misssile launch history and destruction of threats–which influence the outcome of the battle. For the study of plume effects on shipboard operations, we have determined that the missile launch histories are the most important data. If we know the complete history of missile launches, including types and trajectories, we have established when, where and what plumes are generated on shipboard. Figure 2b shows typical missile launch histories for five ships and three missile types. These lead to the "signature tunnel" shown symbolically in Figure 2c and, by analysis, to a typical time history of signature level for one ship in one direction shown in Figure 2d.

Since in a typical battle, dozens of missiles will be launched, even the abstraction described above becomes horrendous. The analysis can be greatly simplified if the missile launch histories can be reduced to statistics which give the probability of each type of missile being launched from a ship at any time in the battle. Since the scenario calculations use a Monte Carlo technique, these statistics are readily generated. Figure 2e shows typical missile launch statistics. The statistics of threats being in detectable positions are also developed from the Monte Carlo scenario simulations. Add to these two sets of statistics the effects of plume signatures on sensor detection probability, and all the elements needed to calculate plume sensor degradation are available.

Plume Effects on Terminal Effectiveness. A much simpler abstraction has been devised to determine the kill probability due to detection of our SAM and AAM missiles by their intended aircraft targets. The premise of the abstraction is this: If the SAM missile is spotted early enough, the target can maneuver or use other countermeasures to evade the missile. If the missile is spotted too late, the target cannot escape.

If we assume that the missile is spotted because of its plume signature, this will be a function of the plume (which derives from the motor, propellant, missile dynamics and environment) and also of the sensor, the effect of the environment on propagation, and the geometry of the missile-target encounter. Thus we can define a plume detection envelope (PDE) surrounding the missile. One-on-one missile/target encounter simulations can be run with parametric variations of encounter geometry and target countermeasures to define a "no escape envelope" about the target (TNEE - "target no escape envelope"). If the PDE is smaller than the TNEE, detection of the missile does not provide useful information to the target. Thus, in the framework of this abstraction, the analysis reduces to comparison of PDE and TNEE for each encounter.

Trajectory simulations for this problem were performed during FY 1978 at the Pacific Missile Test Center (PMTC), Point Mugu, California, for different guidance maneuvers for a number of different targets and anti-air missiles. During FY 1979 and 1980 the results of these simulations will be combined with plume signature calculations and projections of future enemy airborne sensors (Ref. 5) to complete the analysis of this problem at the Naval Weapons Center.

Plume Effect Modeling

The modeling of the different plume effects can generally be done separately. That is, for example, signature modeling need only be done for the bandpass of the sensor being studied. Thus, for an IR sensor in the 4.3 μm band, only the plume emissions, self-absorption and scattering, and ambient path attenuation and background

in that band need be considered. For the accuracy required, it is not necessary to include radiation transfer calculations in the flow field model itself.

The first two columns of Table 1 summarize the equipment and plume effects of importance to operational scenarios. The last two columns summarize the plume flow field and plume effect models which are needed to make predictions. The fourth column of Table 1 lists those plume effects which must be determined for the mission analyses. As indicated earlier, not all signatures have to be analyzed, only those which correspond to the pertinent equipment in the first column of Table 1. Techniques for predicting all of these plume effects have been documented extensively in Ref. 1.

It is sometimes possible to simplify the models under special conditions. For example, as summarized from Ref. 1:

1. ***RF guidance and range safety.*** For plumes with high electron density, RF diffraction will dominate "attenuation" effects and over-dense surface scattering will dominate the RF noise (modulation) effects.
2. ***Radar cross section.*** For plumes with high electron density, over-dense surface scattering will dominate, although in general the missile skin return will totally dominate the radar cross section (RCS) except for Doppler Radar systems and reduced RCS missiles.
3. ***Laser guidance.*** Effects in particle free plumes are limited to beam fluctuations and spreading due to turbulent density fluctuations, an effect not likely to cause more than 5 dB signal loss under the worst conditions.
4. ***IR and visible sensors.*** For strongly afterburning plumes, plume shock effects are relatively unimportant to the total plume signature. Particle emission and absorption are both very important.
5. ***UV sensors.*** Particle emission and continuum radiation behind strong shocks and in the afterburning region are the major source of radiation.
6. ***Optical sensors in general.*** Plume smoke from nearby ship-launched missiles may be the major source of plume interference.

Plumes are not expected to interfere in any serious way with RF detection systems (radar). Although some plumes will be detectable at close range, the missile body RCS will usually be much larger. Range or velocity gating will discriminate against these as interfering radar targets.

The degradation of RF guidance signals by rocket exhaust plumes, on the other hand, has long been known as a serious source of missile guidance failure. Because of extensive past study of this effect (Ref. 6), it is not being emphasized in the current studies. Its effects must be compensated for or corrected before one gets to the full fleet operational scenario analysis, otherwise it must be treated in the scenario analysis as a stochastic failure mode.

Plume toxicity can be determined by calculating or measuring the concentration of toxic species (such as HCl, HCN, HF, etc.) at various locations in the plume flow field. This kind of information is a direct output of all plume flow field calculations.

Plume blast effects are obtained by calculating or measuring the temperature, dynamic pressure and particle impingement effects of the plume flow field on intruding surfaces.

When measured data for these various effects are not available, they must be calculated. Even when available, such data are usually at conditions somewhat different than those needed in the mission analysis; then analytical techniques must be used to translate the measured results to the mission conditions. In either case, the calculations must be based on good flow field and plume effect models.

Although the technologies of plume flow field and plume effect modeling have been vigorously pursued for almost 15 years, only in the past year or so have sufficiently reliable models come to the horizon. Previously developed models, which were reasonably accurate in a number of cases, frequently failed for other cases because no way was known to incorporate phenomena which, in retrospect, are sometimes important. This should be corrected in the new JANNAF Plume Model Standardization effort (Ref. 11). This model will incorporate the important modeling improvements of the past decade including combined shock structure/mixing effects and gas-particle interactions in the flow field.

The reliability goal for the models depends on the particular plume effect being modeled. For example, a factor of two in station radiation is considered sufficient for most optical emission calculations. A similar reliability (which corresponds to 3 dB) is sufficient for most RF interference or RCS effects. Reasonable reliability goals for plume smoke effect prediction are 10% for light transmission and 20% for visible range predictions. These goals appear to be attainable for many cases in the next few years. Current tri-service measurement programs will evaluate the reliability of existing and developmental models.

One area long overlooked in U.S. analytical and experimental plume studies concerns non-axisymmetric or three-dimensional plume flow fields. Such flow fields occur whenever a missile is flying at a non-zero angle of attack. Plans to study this problem will await success in the simpler axisymmetric case.

I prefer to refer to these as reliability goals rather than accuracy goals because the failure mode in model predictions is usually due to omission rather than inaccuracy in the model formulation. These omissions are due to lack of knowledge of the basic processes or to the inability to incorporate all known processes in a model which can be run in reasonable times, even on the fastest digital computers. Thus, prediction failures occur when the problem falls outside the limits of the model assumptions.

Hopefully, it will not be necessary to model all plume effects for every operational situation. For example, in the shipboard situation, it is possible to design IR sensor logic which discriminates against broad targets, such as the sun, clouds and close-in missile plumes. Sensor logic can also be designed to discriminate against receding targets. Even these sensors, which do not suffer interference from missile launch self-emissions, can fail in their detection role if missile exhaust smoke lies on the line-of-sight between sensor and target and severely attenuates the target signal. Smoke scattering of ambient light at the sensor bandpass can introduce noise which reduces the target detection probability even if attenuation does not reduce the detectable target signal below the detector threshold.

Plume interference with optical sensors can take several forms: (1) plume smoke can attenuate and reduce the target signal below the sensor detection threshold, (2) plume smoke scattering of ambient radiation can introduce enough noise between the target and detector to reduce the signal-to-noise (S/N) below the level of sensor discrimination, (3) plume emission in the detector bandpass can dominate reception, again reducing the target S/N below discrimination levels. The first two of these effects can be long-lived since plume smoke can remain fairly concentrated for minutes. The third effect is of shorter duration; the very large launch emission signature rapidly diminishes as the missile leaves the ship and soon becomes a "point source". Even the large initial signature is not likely to be in the same detector resolution cells as are the targets since the detectors will be mounted on the ship superstructure. Thenceforth the chance of emission interfering with target detection is at most the same as the probability of the missile plume and target being in the same resolution cell of the detector.

Since models for predicting the formation, spatial distribution, and visibility of plume smoke were not available when the operational analysis was started, their development was pursued for the following situations: (1) smoke trails from rocket motors fired statically or at constant flight velocity (Ref. 2 and 3); (2) exhaust smoke clouds of missiles launched from slowly moving platforms (Ref. 2 and 7); and (3) smoke from static motor firings in limited volume controlled temperature and humidity test chambers (Ref. 4). The models, based on very simple flow field assumptions, include both primary and secondary smoke formation. Visibility and attenuation are calculated by combining the results of the smoke formation models with Mie scattering calculations, brightness contrast and atmospheric attenuation models. The model of secondary smoke formation includes the effects of HCl and HF on the saturation vapor pressure of water and the effects of soluble as well as insoluble condensation nuclei.

The missile launch cloud has been modeled separately since a free jet model is inadequate to describe it. Using the launch cloud model (Ref. 2 or 7), the position, size, shape, dilution and temperature of the launch cloud can be calculated as a function of time after launch and prevailing environmental conditions.

Results. In the shipboard defense problem (Ref. 2), all the plume effects in Table 1 were considered. Preliminary calculations for a typical multi-threat, multi-ship fleet engagement have indicated that there is about a 10-20% probability that a single smoky launch plume cloud from current ship-launched anti-air missiles will interfere with electro-optical (EO) detection of incoming low flying missiles or aircraft on random threat axes. When such interference occurs, it may reduce detection ranges against even large IR targets to as little as 4-10 km. When folded back into the scenario analysis, this results in a possible doubling of the number of penetrating threat missiles if the detection band is the 4-5 μm infrared. No other effect than launch plume smoke was calculated to have such devastating potential.

The main cause of this degraded sensor performance is the scattering of ambient radiation (mainly solar) by the smoke surrounding a ship from previous missile launches. While this effect will not degrade detection of the initial threat wave by EO sensors, it will seriously degrade subsequent detections, to the extent that use of EO surveillance is required to avoid RF radar jamming and sea clutter effects. Alternatives which will be studied in FY 1979 include examination of other surveillance bands, special ship maneuver tactics and the effects of varying the sensor field of view.

Other interesting operationally relevant results which have been derived in analytical plume studies are shown in Figures 3, 4 and 5. Figure 3 is a nomograph for sea level static line-of-sight X-band attenuation calculations, done some years ago, of aluminized composite propellants. To use the nomograph, one connects, with a straight line, the percent Al (line 1) with percent ammonium perchlorate (line 2). The intercept on line 3 is connected by straight line to the motor thrust level on line 4. The projection of that straight line to line 5, and thence from line 5 through the appropriate aspect angle on line 6, will give predicted diagonal attenuation on line 7. Curve 6 would have to be modified for other antenna positions. The nomograph is set up only for an antenna located three exit radii from the nozzle centerline. Although antenna location has a major effect on calculated line-of-sight attenuation, for attenuation values greater than about 10 dB, diffraction (or scattering) effects will predominate and greatly reduce the actual signal loss (Ref. 1). Those cases are less sensitive to the antenna location and Figure 3 provides usable input for diffraction calculations.

Figure 4 combines the various factors involved in predicting the visibility of primary smoke due to aluminum containing composite solid propellants. This figure corresponds to the plume of a 18 kN thrust motor flying at sea level, Mach 2, and viewed broadside about 100 meters behind the missile. Liminal contrast curves for two atmospheric conditions are included: σ = 0.1, corresponding to a very clear day, and σ = 0.03, corresponding to an exceptionally clear day. A clear sky background is assumed. To use Figure 4, the intrinsic contrast is located as a function of $\emptyset$ on the straight line corresponding to the appropriate sunlight-plume-observer scattering angle. One then moves horizontally to intersect the appropriate curve for liminal contrast and vertically upward to read the detection range for 50% detection probability on the

upper abscissa. For highly aluminum loaded propellants, the calculated contrast may exceed that shown for Lambert scattering on the right-hand ordinate of the figure. In such cases, the Lambert scattering values should be used.

Figure 4 can be applied to plumes of different size since the intrinsic plume contrast increases in direct proportion to increasing diameter and the liminal contrast decreases roughly in inverse proportion to changing plume diameter. Therefore, since doubling of the plume diameter is calculated to cause a fourfold increase in visibility, all other things being equal, the visibility is predicted to vary directly as the rocket motor thrust level.

Figure 5 shows the predicted source spectral radiant intensity from a particular booster rocket motor over the entire wavelength range (UV-visible-IR) of potential interest. Calculated values are shown at near nose on (10 degrees), broadside (90 degrees) and near tail-on (178 degrees) (see Ref. 2). Were it not for plume self-absorption, these curves would overlap completely since missile body effects are ignored.

These several examples represent a sort of "grab bag" of plume problems. They show the kind of operationally relevant results which can be obtained with predictive plume technology. Although the nomographic techniques can be used to obtain estimates of the magnitude of plume effects, it is always better to use the latest technology to make detailed estimates, especially in cases where error might be costly. No attempt has been made to turn the readers into plume technologists, since experience has demonstrated that there are considerable hazards in "do it yourself" plume technology.

CONCLUSIONS

Although plume technology may seem to be an esoteric specialty, it deals with a subject which has serious implications for modern warfare involving self-propelled missiles. Some past plume-related problems could be adequately treated by suboptimizing the operational environment and concentrating on the plume interaction with specific system elements. Examples include plume interference with RF guidance, communications and range safety, with satellite surveillance and blast effects. New problems involving low altitude optical surveillance and guidance introduce additional operational and environmental relationships which require that related plume effects be treated in the context of the complete scenario. This is necessary to assure that all warfare elements (propulsion, surveillance, guidance, communications, launch vehicle design, tactics, etc.) are compatible.

Although the Army, Navy and Air Force each faces somewhat different plume-related problems, these problems all fall into the categories discussed in this paper; at the technology level the problems are often identical. Close tri-service

cooperation in plume technology has existed for at least a decade. At the present time every area of common interest is worked cooperatively, and in several areas (plume gas dynamics, optical signatures and plume smoke), the ongoing work has been organized into multi-service joint programs to avoid duplication and to optimize progress (Ref. 12). The value of this cooperation will be fully realized only if equally good cooperation is developed between plume technology and the weapons development areas with which it interacts.

The Air Force has taken a major step in this direction by centralizing all its rocket exhaust plume technology work at the Air Force Rocket Propulsion Laboratory and providing technology base as well as weapon program funding. Because the Army and Navy have not centralized their plume technology work, I believe they are more susceptible to the problems which can arise when potential plume problems are overlooked early in weapons development. Of course, complete centralization carries the risk of parochialism which can result in overlooking or prematurely cancelling valid competitive approaches to problem solution. However, with good tri-service cooperation and communication, chances are good that any such errors will be caught by one or more of the services.

RECOMMENDATIONS

My recommendations were previewed in the previous section:

1. Inter-service cooperation in plume technology should continue at current levels.

2. Navy and Army intra-service coordination in plume technology should be improved.

3. Inter-disciplinary coordination between plume technology and weapons development should be improved at all levels of the acquisition process.

4. Some level of technology base funding in plume technology is important for maintenance of capability in those areas which are not currently supporting development programs but which may be needed again.

These statements are intended to be more than just "motherhood." Inter-service cooperation through the JANNAF Plume Technology Subcommittee is excellent, to the extent that new information is exchanged even as the work is going on.

However, within the services themselves, we often find much longer delays on information exhange than between the services. In many cases these delays occur because people with plume problems don't know whom to contact for information.

Another result of this lack of information exchange is the appearance of local plume "technology" groups to solve particular plume-related weapon system problems. Unfortunately these groups tend to function years behind the current state of the art.

If I can leave you with one thought, I would like it to be this: If you are faced with a plume-related weapon system problem and don't know whom to call, get in touch with the JANNAF Plume Technology Subcommittee, either through me or through the Chemical Propulsion Information Agency, Johns Hopkins University/ Applied Physics Laboratory, Laurel, Maryland.

ACKNOWLEDGMENT

Support for this work is provided by the Naval Sea Systems Command (J. Murrin and R. Cassel), Plume Low Signature Requirements for Point/Area Defense Solid Propellant Motors; Program Manager, Mr. George Buckle, Naval Ordnance Station, Indian Head, MD; and the Naval Air Systems Command, Advanced Reliable Solid Propulsion Design, Propulsion Administrators, Mr. Robert Heitkotter, NAVAIR, and Dr. Charles Thelen, NWC.

REFERENCES

1. Chemical Propulsion Information Agency. "JANNAF Handbook, Rocket Exhaust Plume Technology." CPIA Publication 263.
   Chapter 1. Introduction, to be done
   Chapter 2. Gas Dynamic Flow Models, May 1975
   Chapter 3. Plume Radiation, in final review
   Chapter 4. Plume-Electromagnetic Interactions, April 1977
   Chapter 5. Base Flow, in progress
   Chapter 6. Plume Impingement and Contamination, to be done
   Chapter 7. Plume Measurement Techniques, to be done

2. Naval Weapons Center. "Rocket Exhaust Plume Effects on Shipboard Operations (U)," by A. C. Victor and G. A. Buckle. China Lake, Calif., NWC, April 1978 (NWC TM 3462)
   Volume 1. Analysis (U) (Publication CONFIDENTIAL.)
   Volume 2. Background (Appendicies) (U) (Publication SECRET.)

3. A. C. Victor and S. H. Breil. "A Simple Method of Predicting Rocket Exhaust Smoke Visibility," *J. Spacecraft and Rockets*, Vol. 14, No. 9 (September 1977), pp. 526-533.

4. A. C. Victor. "Prediction of Rocket Exhaust Secondary Smoke Formation in Free Jets and Smoke Chambers," presented at the *1978 JANNAF Propulsion Meeting*, 14-16 February 1978. (CPIA Publication 293, publication CONFIDENTIAL.) For more detail and computer programs, see Naval Weapons Center report, same title. China Lake, Calif., NWC, February 1978 (NWC TM 3361, publication UNCLASSIFIED.)

5. Pacific Missile Test Center. "Predicted Threat Airborne Electromagnetic Sensors (U)," March 1978, Document 00-66432, enclosure to ltr Ser S128 of 21 April 1978 (SECRET) and "Predicted Soviet Threat Warning Receiver Technology," May 1978, enclosure to ltr Ser S201 of 12 June 1978 (SECRET).

6. Naval Weapons Center. "Plume Signal Interference," by A. C. Victor. China Lake, Calif., NWC. (NWC TP 5319, publication UNCLASSIFIED.)
   Part 1. Radar Attenuation, June 1975
   Part 2. Plume Induced Noise, May 1972

7. ———. "Prediction of Growth and Dispersion of Rocket Exhaust Clouds from Surface Launched Missiles," by A. C. Victor. China Lake, Calif., NWC, July 1977. (NWC TM 3200, publication UNCLASSIFIED.)

8. ———. "An Analytical Approach to the Turbulent Mixing of Coaxial Jets," by A. C. Victor and R. W. Buecher. China Lake, Calif., NWC, October 1966. (NWC TP 4070, publication UNCLASSIFIED.)

9. R. R. Mikatarian, C. J. Kan and H. S. Pergament. "A Fast Computer Program for Non-equilibrium Rocket Plume Predictions. Air Force Rocket Propulsion Laboratory, AeroChem Research Laboratories, August 1972. (AFRPL-TL-72-94.)

10. D. E. Jensen, D. B. Spalding, D. G. Tatchell and A. S. Wilson. "Computation of Structures of Plumes with Recirculating Flow and Radial Pressure Gradients." (To be published in *Combustion and Flame.*)

11. *JANNAF Plume Model Standardization*, Contract No. DAAK-78-C-0124, Aeronautical Research Associates of Princeton. (Scheduled for completion in 1981.)

12. *JANNAF Exhaust Plume Technology Subcommittee Report.* Prepared for JANNAF Executive Committee, 5 October 1978.

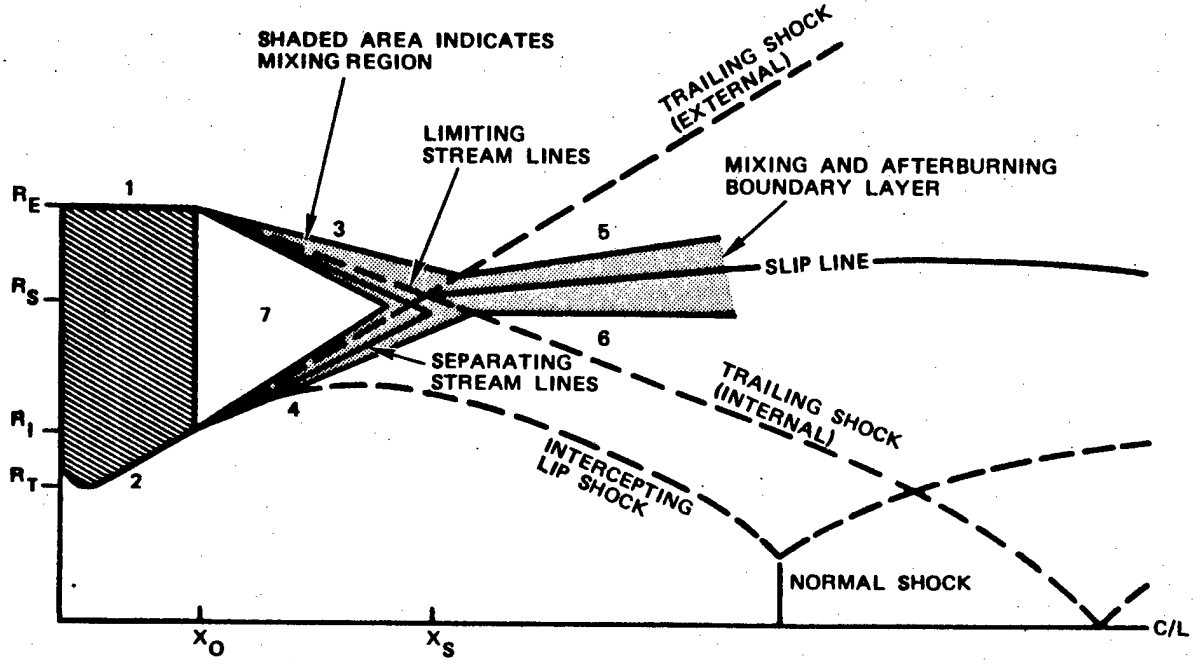

FIGURE 1. Schematic Drawing of Plume Including Base Effects. Regions shown are (1) external freestream flow, (2) internal nozzle flow, (3) external base region flow, (4) internal base region flow, (5) external exhaust plume flow, (6) internal exhaust plume flow, and (7) base recirculation flow.

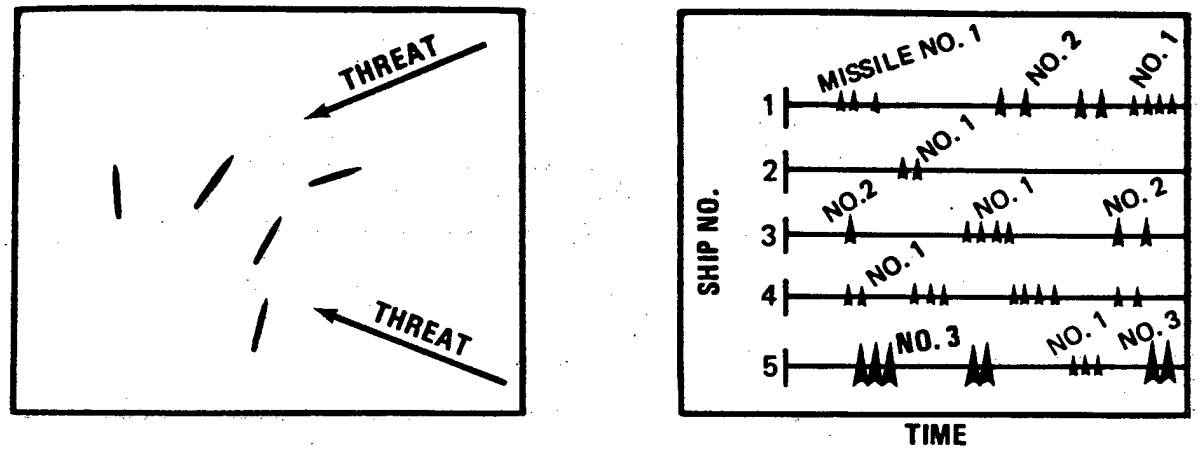

a. SCENARIO 1

b. MISSILE LAUNCH HISTORY

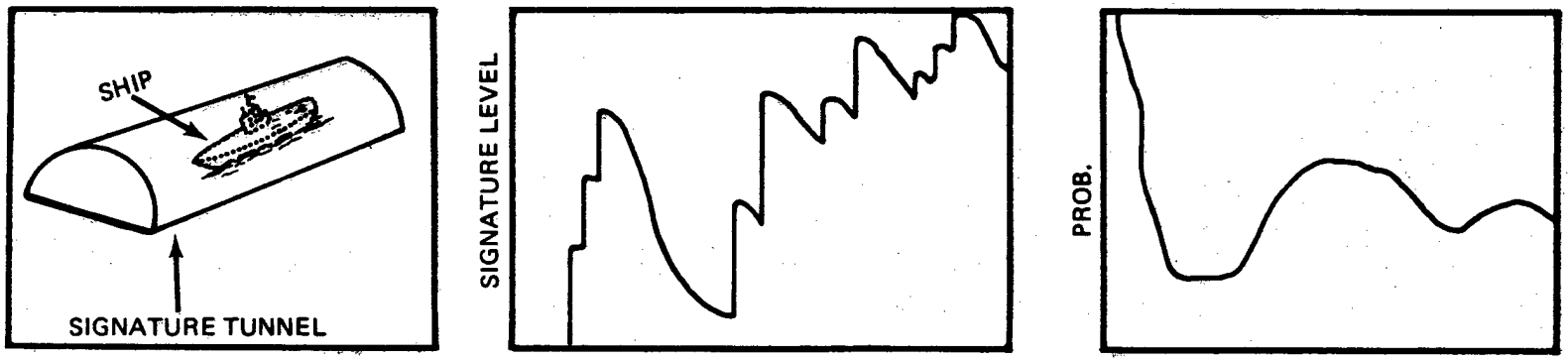

c. "ESSENCE"

d. ONE CASE HISTORY, SHIP NO. 1

e. PROBABILITY OF MISSILE LAUNCH IN 5 SECOND TIME PERIOD

FIGURE 2. Essence of the Shipboard Plume Signature Problem.

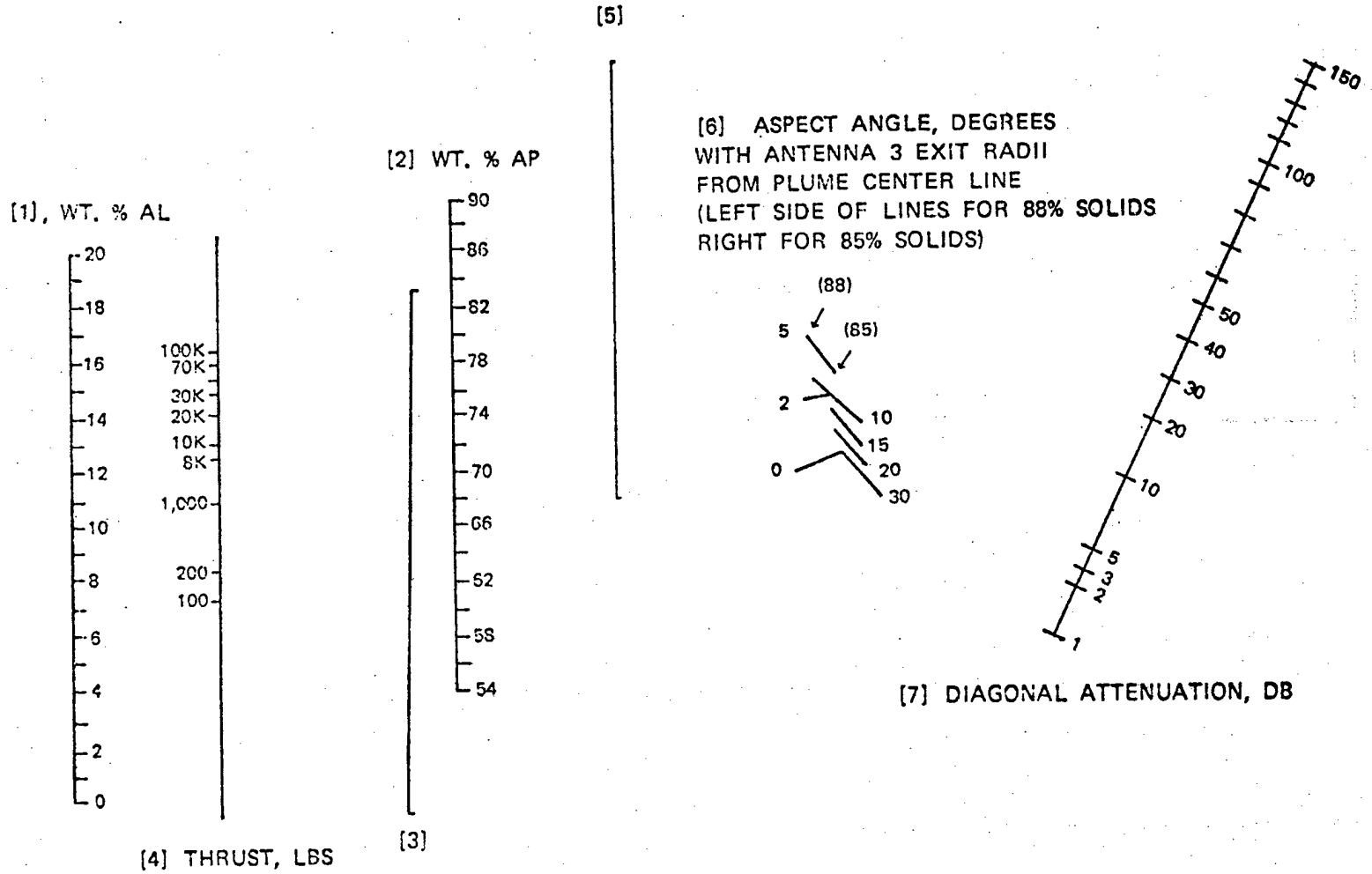

FIGURE 3. Line-of-Sight X-Band Attenuation Nomograph for Composite Propellants.

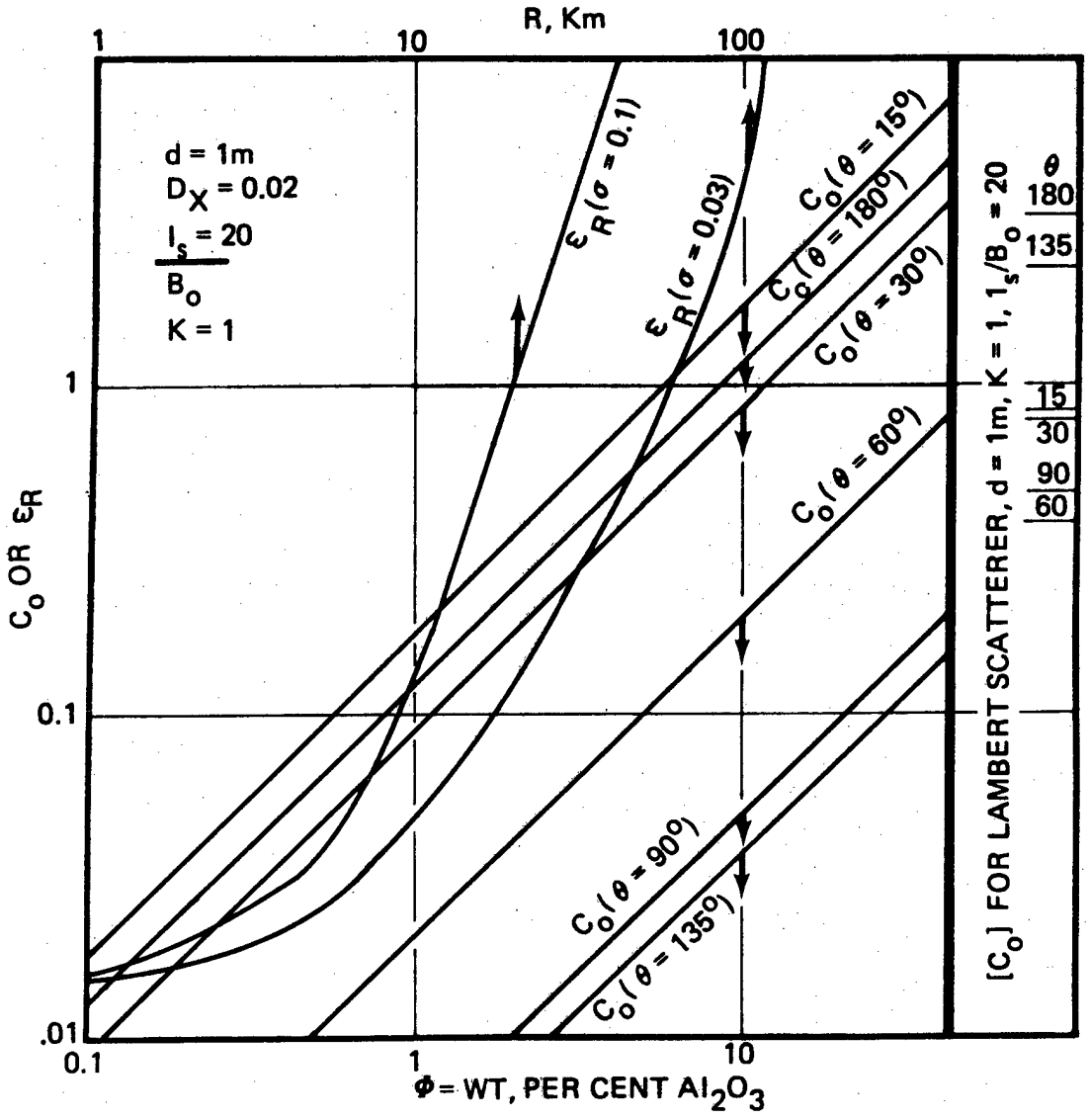

FIGURE 4. Plume Contrast and Liminal Contrast as Function of Al_2O_3 Concentration and Range. Nomograph for calculating plume visible range. θ_1 corresponds to the excluded sun-plume-observer scattering angle.

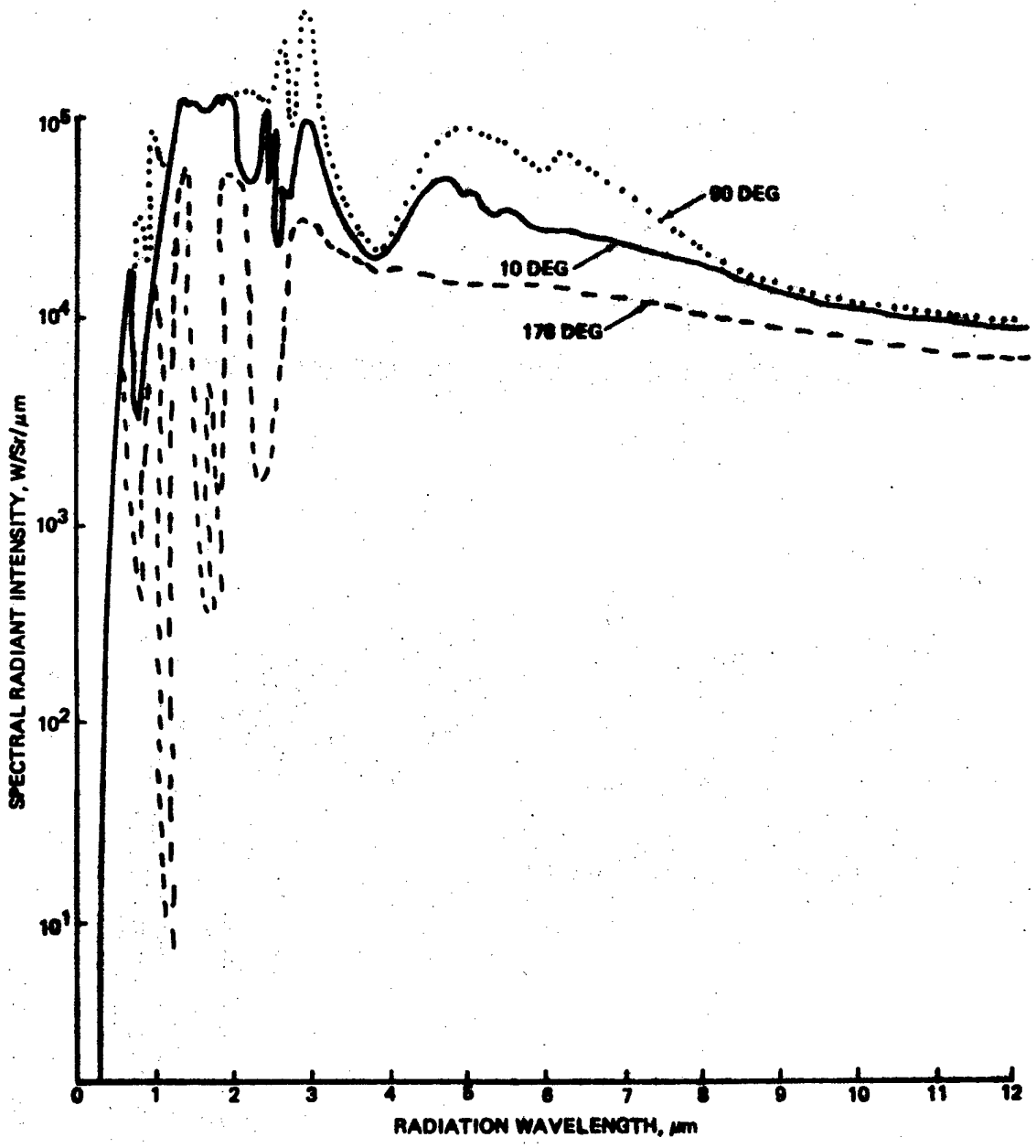

FIGURE 5. Calculated Source Spectral Radiant Intensity for a Large Rocket Booster Plume at Three Viewing Angles.

TABLE 1. Plume Models Needed to Predict Effects on Various Equipment.

Equipment	Effect	Adequate plume[a] flow model	Plume effect models
RF guidance RF communications Range safety	Attenuation/noise	2	Charged gaseous species, RF absorption, scattering, refraction, diffraction.
Radar	Radar cross section	2	Same as above.
Laser guidance	Attenuation/beam spreading	2	Gas optical absorption, scattering refraction; Mie scattering by particles.
IR sensors	IR emission absorption	3 (1)[b]	IR band and line by line and gray body continuum; gas and particle effects include smoke scattering of ambient radiation.
Visible light sensors	Plume visibility	3 (1)[b]	Gray body continuum, excited atomic states; smoke scattering.
UV sensors	UV emission, absorption	3 (1)[b]	Gray body continuum, minor effect of OH and NO; smoke scattering.
Humans	Toxicity	2	Toxic gas.
Humans and mechanical equipment	Blast	2	Temperature, pressure and particle impingement.

[a] Three levels of plume flow models are generally considered:
1. Equilibrium chemistry, constant pressure plume (Z.B. Ref. 8 and 3).
2. Kinetic rate chemistry without detailed shock structure (Z.B. Ref. 9)
3. Kinetic rate chemistry with detailed shock structure (Z.B. Ref. 10 and 11).

[b] The author believes that only very simple plume flow field models are needed to make adequate plume smoke predictions (Ref. 3 and 4).

BIOGRAPHY

The author has been active in the field of plume technology at the Naval Weapons Center for 14 years. Previous and interspersed technical and management activities have included research in thermochemistry, operational analysis, propulsion systems mission analysis, propulsion systems cost analysis and standards laboratory and computer software management. Mr. Victor has published about 60 technical papers and reports of which 36 are in areas of plume technology. He is currently chairman of the JANNAF Plume Technology Subcommittee and has been U.S. leader of the TTCP Plume Technology Action Group since 1968. BA, Chemistry, Swarthmore College, 1956. MS, Physics, University of Maryland, 1961. Mr. Victor is an associate follow of the American Association of Aeronautics and Astronautics and a member of Sigma Xi and of the American Defense Preparedness Association.